Improving the bioavailability of collagen-derived peptides: studies in cell culture models

by

Mengmeng Feng

A thesis submitted in partial fulfillment of the requirements for the degree of

Doctor of Philosophy

in

Food Science and Technology

Department of Agricultural, Food and Nutritional Science

University of Alberta

ABSTRACT

Collagen hydrolysates (CH) are emerging health supplements associated with a growing body of evidence indicating that they may positively influence skin conditions, promote joint and bone health, and even ameliorate hypertension and type 2 diabetes. The biological effects of CH, however, are limited by their low bioavailability. This thesis was committed to improving the bioavailability of CH and collagen-derived peptides, and, interested in elucidating the effects they have on the human dermal fibroblast. The strategy of the first part of the thesis focused on facilitating the absorption of CH by reducing the molecular weight (MW) through enzymatic hydrolysis, as documented in study 1. A practical and efficient method was developed to extract collagen from extremely tough and highly cross-linked bovine hide. This was achieved by a pretreatment with alkaline conditioning, and an extraction process using acetic acid and pepsin. The final product was highly pure and pepsin-acetic acid soluble collagen. The combination of two commercial enzymes, Alcalase and Flavourzyme, was determined to be the best treatment to hydrolyze the collagen generating over 80% of peptides with MW lower than 2 kDa. The *in vitro* absorption experiment using a human intestinal Caco-2 cell model revealed the positive correlation between a lower MW and a higher transepithelial transport of CH.

In addition to the first part which was in an effort to increase the effective proportion of CH that can be absorbed, the second part of the thesis focused on introducing other absorption pathways through chemical modification of collagen-derived peptides, which is summarized in study 2 and study 3. A novel glycopeptide was synthesized from a model collagen peptide Pro-Hyp by conjugating with an amino sugar glucosamine (GlcN). After purification and MW identification, the glycopeptide was clarified to be an amide derivative by nuclear magnetic resonance spectroscopy, i.e. Pro-Hyp-CONH-GlcN. Later, the glycopeptide was subjected to

simulated gastrointestinal digestion and Caco-2 cell transport. It showed a desirable enzymatic stability (~90% remaining) with superior permeability compared to its parent peptide Pro-Hyp (P_{app} 2.82 ×10^{-6} cm/s vs. 1.45 ×10^{-6} cm/s). The improvement was achieved by introducing the activity of an extra transport pathway - GLUTs; GlcN moiety in the glycopeptide molecule was structurally comparable to the free GlcN, which makes the glycopetide transported similarly as GlcN. Study 3 investigated effects of the glycopeptide on human dermal fibroblasts, the primary resident cells that account for skin function, and cells mainly affected by health benefits of CH. Interestingly, the glycopeptide activated the proliferation of fibroblasts to 1.5-fold of untreated control. This activity was similar with its parent collagen peptide, so was the performance in stimulating the hyaluronic acid (HA) biosynthesis. The effective concentration of both the collagen peptide and the glycopeptide for the stimulation was revealed to be 200 nmol/ml, representing a physiologicall evel observed in animal studies. The underlying mechanisms were linked to their ability in arresting more cells in the DNA synthesis phase for the cell growth stimulation, and in up-regulating the transcription of hyaluronan synthase genes that encode HA synthesis. This doctoral project provides strategies and a foundation for future research to improve the bioavailability of collagen protein hydrolysates by reducing MW through enzymatic hydrolysis. Also, the chemical modification by glycosylation represents a novel approach to facilitate intestinal absorption of collagen-derived bioactive peptides.

PREFACE

This thesis is an original work of Mengmeng Feng. It is presented in a manuscript format composed of six chapters.

Chapter 1 is an introduction chapter that briefly introduces the background, hypothesis and objectives of this project.

Chapter 2 is a relatively comprehensive literature review in this field. It describes the basics of collagen, the collagen and gelatin production, bioavailability and beneficial biological effects of collagen products, and finally addressed the potential of collagen products as nutricosmetics.

Chapters 3 to 5 describe the major results of this thesis.

Chapter 3 was partially published as "Feng, M.; Betti, M. Transepithelial transport efficiency of bovine collagen hydrolysates in a human Caco-2 cell line model. *Food Chem.* **2017**, *224,* 242– 250."

Chapter 4 was published as "Feng, M.; Betti, M. Both PepT1 and GLUT intestinal transporters are utilized by a novel glycopeptide Pro-Hyp-CONH-GlcN. *J. Agric. Food Chem.* **2017**, *65* (16), 3295–3304."

Chapter 5 is based on the manuscript of "Feng, M.; Betti, M. A Novel collagen-derived glycopeptide, Pro-Hyp-CONH-GlcN, stimulates cell proliferation and hyaluronan production in cultured human dermal fibroblasts". The manuscript was submitted for publication.

Chapter 6 is a conclusion chapter that summarizes the main findings of this project. It also discussed the implications and applications, and the promising directions for future research.

I was responsible for all the related work for this thesis, including the experimental design, data collection and analysis, and manuscript preparation. Dr. Mirko Betti was the supervisory author who provided overall guidance and advices for concept formation, project progress, and manuscript preparation.

Dedication

to my beloved parents,

my sisters,

and my friends.

In the memory of my benign grandmother.

致

我的家人和朋友

一路有你们

真好

--- 心于心上

ACKNOWLEDGEMENNTS

I would like to foremost voice the appreciation to my academic supervisor, Dr. Mirko Betti, who was there enlightening me to accomplish this doctoral project in the last a few years. He was the one who conveyed encouragements, supports, and valuable solutions to get through those tough times when I was frustrated by the experiments. His enthusiasm and inspiration also deeply infect my PhD experience.

I would like to express my sincere gratitude to my committee members, Dr. Linyun Chen and Dr. Zbigniew (Zeb) Pietrasik for their patience, suggestions, challenges and evaluations during the committee meetings. It made me think of my experimental approaches and concepts more comprehensively, and helped me grow to be a more mature and professional scientist.

Thank you to Dr. Afsaneh Lavasanifar and Dr. Rotimi Aluko for spending time on reviewing my thesis and presenting in the PhD final exam.

I would like to thank the senior people in our lab, Dr. Zied Khiari, Dr. Abhishek Bhattacherjee, Dr. Hrynets Yuliya, and Dr. Maurice Ndagijimana for their advices, trainings, and guidance to qualify myself to be skilled in my field.

Thank you to Jack Moore from Institute of Biomolecular Design for his patience to explain and analyze mass spectrometry results.

I am also grateful to Xuejun Sun, Mark Miskolzie, Urmila Basu, Gary Sedgwick, and Lisa Nikolai for their technical support.

I would like to thank Henan Wang, Pui Khoon Hong, and all my other lab mates for working together and help each other in my academic life.

A special appreciation should give to Lihui Du, a supportive friend who also provided valuable advices for life and lab work during the last a few years.

Another special appreciation I would like to say to my close friends here Xinyao Lu, Dan Zhang, Yuan Shi, and some others back to home. Thank you all for accompanying me in those good and bad times.

Thank you Jie Wang for being helpful and considerate these years, thank you for being around when needed.

Importantly, I would like to acknowledge the China Scholarship Council to provide four years financial support for me to pursue this PhD.

I cannot be more grateful to my dear parents and family members. Thank you for making me, me. And thank you for being supportive all the time, and being a forever harbor for me.

Finally, thank you. You, my dear, are still you, never leaves, never gives me up……

TABLE OF CONTENTS

LIST OF TABLES

LIST OF FIGURES

ABBREVIATIONS

A -- Alcalase

ACE -- angiotensin I-converting enzyme

ACN – acetonitrile

ADAM -- amantadine hydrochloride

ADAMTS -- A disintegrin and a metalloproteinase with thrombospondin repeats

AF -- a dual enzyme treatment by Alcalase/Flavourzyme

AFT -- a cocktail enzyme treatment by Alcalase/Flavourzyme/trypsin

AGE -- advanced glycation end products

ANOVA -- analysis of variance

AH -- collagen hydrolysates from Alcalase hydrolysis

AFH -- collagen hydrolysates from Alcalase/Flavourzyme hydrolysis

AFTH -- collagen hydrolysates from Alcalase/Flavourzyme/trypsin hydrolysis

AT -- a dual enzyme treatment by Alcalase/trypsin

ATH -- collagen hydrolysates from Alcalase/trypsin hydrolysis

bFGF -- basic fibroblast growth factor

BMP1 -- bone morphogenetic protein 1

BOP -- Benzotriazol-l-yl-N-oxy-tris-(dimethylamino) phosphonium hexafluorophosphate

BSA -- bovine serum albumin

CH -- Collagen hydrolysates

DAPI -- *2*-(*4*-Amidinophenyl)-6-indolecarbamidine dihydrochloride

DCM – Dichloromethane

DH -- Degree of hydrolysis

DMEM -- Dulbecco's Modified Eagle Medium

DMF – Dimethylformamide

DMSO -- dimethyl sulfoxide

DPP-IV -- dipeptidyl-peptidase IV

ECM -- extracellular matrix

Edu -- 5-Ethynyl-2'-deoxyuridine

ER -- endoplasmic reticulum

F -- Flavourzyme

FACIT -- fibril-associated collagen with interrupted triple helices

FBS -- fetal bovine serum

FH -- collagen hydrolysates from Flavourzyme hydrolysis

FTH -- collagen hydrolysates from Flavourzyme/trypsin hydrolysis

FPLC -- fast protein liquid chromatography

FT -- a dual enzyme treatment by Flavourzyme/trypsin

GAG -- glycosaminoglycans

GI – gastrointestinal

GlcN – glucosamine

HA -- hyaluronic acid

HAS -- hyaluronan synthase genes

HBSS -- Hank's balanced salt solution

HDF -- human dermal fibroblast

HEPES -- N-2-hydroxyethylpiperazine-N-2-ethane sulfonic acid

HOBt -- 1-Hydroxybenzotriazole

HPLC -- high-performance liquid chromatograph

Hyp -- hydroxyproline

MES -- Morpholineethanesulfonic acid

M phase -- mitosis phase

MMP -- matrix metalloproteinase

MTT -- Methylthiazolyldiphenyl-tetrazolium bromide

MW – molecular weight

NCE -- normalized collision energy

NMM -- N-Methylmorpholine

NMR -- nuclear magnetic resonance spectroscopy

SHR -- spontaneously hypertensive rats

OA -- osteoarthritis

P_{app} -- permeability coefficient

PBS -- phosphate buffered saline

PE -- permeation enhancers

PEG -- polyethylene glycol

PO -- Pro-Hyp

POGlcN – the collagen-derived glycopeptide Pro-Hyp-CONH-GlcN

POT -- proton-coupled oligopeptide transporters

qRT-PCR -- quantitative reverse transcription polymerase chain reaction

RNS -- reactive nitrogen species

ROS -- reactive oxygen species and nitrogen species

SEC -- size exclusion chromatograph

T -- trypsin

TCA -- trichloroacetic acid

TEA – trimethylamine

TEER -- transepithelial electrical resistance

TH -- collagen hydrolysates from trypsin hydrolysis

Trp -- tryptophan

UHPLC -- ultra-high pressure liquid chromatography

UV – ultraviolet

CHAPTER 1.

General Introduction

Collagen hydrolysates (CH) have been widely used in the food industry due to the intriguing functional properties, such as emulsifying and water-binding properties. But what makes CH extraordinary is that they can provide various health benefits. For example, oral ingestion of CH helps to improve joint and bone health, and refine the appearance and texture of skin (Moskowitz, 2000; Adam et al., 1996). This qualifies the incorporation CH into nutricosmetics - ingestible products that can enhance skin health and afford beauty benefits (Tabor and Blair, 2009; Machado et al., 2017). CH are composed of various bioactive collagen-derived peptides that are either formed by pre-digestion hydrolysis or created by *in vivo* digestion system. To be biologically active at specific organs or tissues, CH first need to be intestinally absorbed, like other proteins and peptides, primarily in the form of free amino acids and/or small oligopeptides (e.g. di- and tripeptides) (Ganapathy et al., 2006). Generally, a low MW is believed to favour the bioavailability of CH, since materials with lower MW have a higher chance for solubilization, and have a greater proportion of small collagen fragments that may be absorbed better. An effective hydrolysis process before oral ingestion, therefore, can facilitate the absorption of CH and improve the ultimate proteolysis of CH. Native collagen is not digestible in the gut. Gelatin - a partially hydrolyzed collagen product- and some commercial CH possessing both a high average molecular weight (MW) and a broad MW range, can only be degraded to a certain extent after being orally taken (Schrieber and Gareis, 2007; Moskowitz, 2000).

Enzymatic hydrolysis is often used to produce low MW peptides. Numerous enzymes can generate CH, including endoproteases such as pepsin, trypsin, papain, Alcalase, etc. and exoproteases such as Corolase® and Flavourzyme (Mendis et al., 2005; Baehaki et al., 2015;

Alemán et al., 2011; Dolphin and Russell, 2011). The efficiency of using enzymes to hydrolyze collagen depends on the source and extraction method of collagen, the conditions applied during hydrolysis, and the specific enzymes selected. Most studies focus on isolating and identifying bioactive collagen peptides, yet information is limited about how these enzymes affect the MW distribution of CH generated, and if the low MW correlates with subsequent CH bioavailability. The novelty of the first part of the project was therefore to bridge this gap, and investigate the potential of reducing MW of CH to increase their intestinal absorption.

In contrast to pre-digestion hydrolysis, peptide intestinal delivery can be enhanced by physical formulation strategies such as the use of permeation enhancers and carrier systems, and with chemical modifications. The co-administration of permeation enhancers, e.g. bile salts, can cause toxicity since they may damage the intestinal barrier after long-term usage (Maher et al., 2016). Chemical modification, especially by conjugation with naturally penetrating molecules, has achieved promising benefits including enhanced transporter mediated transport with less chances of antigenicity and toxicity. In synthetic chemistry, chemical modification of proteins/peptides through covalent attachment of glycosyl units falls into the broad category of glycosylation (Solá and Griebenow, 2010; Moradi et al., 2016). Synthetic glycosylation of proteins/peptides targeting glucose transporters, for example, the structural modification of albumin with glucose, and the conjugation of α-melanocyte-stimulating hormone octapeptide with galactose, have both been successful to improve the uptake of the parent peptide (Adessi and Soto, 2002; Bapst et al., 2009). A previous study in our lab indicated that glucosamine (GlcN) is an active glycating agent at mild conditions (Hrynets et al., 2015). GlcN is a naturally occurring amino sugar that can be absorbed via the glucose transporters - GLUTs (Uldry et al., 2002). It is interesting to investigate the potential of glycosylation of collagen-derived peptide with GlcN to improve its intestinal

permeability. Moreover, many clinical trials showed that orally administrated CH can improve skin hydration, elasticity and smoothness, and counteract UV-induced skin damage (Matsumoto et al., 2006; Proksch et al., 2014; Schwartz et al., 2012; Tanaka et al., 2009). The underlying mechanisms include an enhanced production of matrix components such as collagen and hyaluronan, the suppression of expression of matrix degradation enzymes, and the activation of skin fibroblasts to proliferate (Zague et al., 2011; Tokudome et al., 2012). Some contributing collagen-derived peptides have been identified, such as the Pro-Hyp and Hyp-Gly (Ohara et al., 2010b; Shigemura et al., 2011). The influence of the chemical modification of collagen-derived peptides on its efficacy in triggering matrix-related changes, and cell responses is still obscure and needs critical research.

Firstly, this thesis was aimed to improve the bioavailability of CH by using a series of different enzyme combinations. To understand the problem better, a more complete picture was visualized, starting from the raw materials, gaining better control in making CH with various structural profiles, and finally, to understand the intestinal permeation of CH produced. Key in this research was to address the causal influence of the enzymatic hydrolysis. In the second part, the major focus was on demonstrating the potential of a new glycosylation approach to improve the intestinal absorption using a model collagen peptide. This part also addressed two immediate questions that 1). How would glycosylation alter the transport of the parent peptide? 2). How would glycosylation guide the behaviour of human dermal fibroblasts? To meet the main objectives and to answer these specific questions, three studies were conducted as described below.

Chapter 3 "*Transepithelial transport efficiency of bovine collagen hydrolysates in a human Caco-2 cell model*" uses a whole bloody bovine hide as starting material, which represents a low-quality by-product of the bovine meat industry. To add value to the bovine hide, it was first bio-

converted into very low MW (<2 kDa) peptides through enzymatic hydrolysis, and then the effects of hydrolysis on subsequent gastrointestinal digestion and transepithelial transport of CH were studied. Alcalase, Flavourzyme, and trypsin were used as either a single enzyme treatment, a combination of two enzymes, or a cocktail of the three together. It was hypothesized that 1). The combination usage of multiple enzymes can exhibit a broader specificity to generate CH with lower molecular weight; 2). a lower molecular weight of CH correlates with a higher transepithelial transport. The specific objectives of this study were:

1). to develop a simple and efficient bench method for the extraction of collagen from a raw bovine hide;

2). to maximize the production of very low MW (< 2kDa) collagen peptides via different enzymatic hydrolysis;

3). to evaluate the effects of the enzymatic hydrolysis on the subsequent gastrointestinal digestion of CH;

4). to determine the transepithelial transport of CH from different enzymatic treatments using a human intestinal Caco-2 cell model.

Chapter 4 "*Both PepT1 and GLUT intestinal transporters are utilized by a novel glycopeptide Pro-Hyp-CONH-GlcN*" was a study that modified the structure of Pro-Hyp with GlcN to form a novel glycopeptide, and examined its intestinal permeability. To validate the feasibility of chemical modification to improve intestinal absorption of CH, Pro-Hyp was selected as a model peptide since it is the most abundant collagen-derived peptide found in plasma and skin after CH ingestion. It was hypothesized that the conjugation of GlcN may facilitate the transport of Pro-Hyp by the incorporation of GLUTs pathway. This study specifically aimed:

1). to establish a feasible method for the conjugation of GlcN with Pro-Hyp;

2). to evaluate the stability of the synthesized glycopeptide under *in vitro* gastrointestinal digestion;

3). to estimate the intestinal permeation of the glycopeptide using the Caco-2 cell model;

4). to clarify the transepithelial transport mechanism of the glycopeptide in comparison with its parent peptide.

Chapter 5 "*A novel collagen-derived glycopeptide, Pro-Hyp-CONH-GlcN, stimulates cell proliferation and hyaluronan production in cultured human dermal fibroblasts*" investigated the cellular response of dermal fibroblasts to the glycopeptide. Pro-Hyp is a stimulus for the proliferation of skin fibroblasts and the biosynthesis of matrix hyaluronic acid (HA). GlcN can also enhance the production of HA by some other cell lines. It was hypothesized that the glycopeptide may exhibit equal promoting effects on the growth of fibroblasts and their ability to produce extracellular ingredients compared to Pro-Hyp; or in a better scenario, a greater efficacy is introduced due to the incorporation of GlcN. Therefore, this study was designed in comparison with the parent peptide:

1). To evaluate effects of the glycopeptide on the proliferation of dermal firbroblasts;

2). To study effects of the glycopeptide on the biosynthesis of matrix components, i.e. HA and collagen;

3). To understand the underlying mechanism of the glycopeptide in influencing fibroblast cell cycle;

4). To explore the regulatory role of the glycopeptide on gene expression of the fibroblast.

CHAPTER 2.

Literature review

2.1. Collagen and collagen hydrolysates

2.1.1 Collagen structure and biosynthesis

Collagen as the most abundant animal protein accounts for about 30% of total body protein. It functions as a structural protein in extracellular matrix (ECM) to maintain the mechanical integrity of tissues and organs. Nowadays, at least 29 types of collagen have been described (McCormick, 2009), the molecules of which share similar right-handed triple helical structure that is composed of three homogeneous or heterogeneous alpha-chains. Generally, one or more regions of the alpha chain are occupied by repeating occurrence of Gly-X-Y triplets, where X and Y sites can be any amino acid with the preference of Pro and hydroxyproline (Hyp), respectively. The amino acid composition of different collagens may vary, while they are typically absent of tryptophan, and have very little methionine, cysteine, tyrosine, and histidine, etc. (Johnston-Banks, 1990). More than forty discovered alpha chains endow the structural and functional diversity of collagen, based on which they are classified into fibrillar, fibril-associated collagen with interrupted triple helices (FACIT), basement membrane collagen, etc. (Table 2.1) (Mouw et al., 2014). The collagen is assembled in different manners among various organs to meet tissue-specific mechanical requirements. For example, collagen fibres in skin are relatively random orientated, whereas in tendons are highly ordered in a parallel fashion, in bone are assembled concentrically, and in the cornea are precisely arranged with very defined angles (Bailey et al., 1998).

Table 2.1. Primary types of collagen and their generic diversity (Mouw et al., 2014). Reprinted by permission from Macmillan Publishers Ltd: [Nat. Rev. Mol. Cell Biol.], copyright (2014).

Classes	Type	Genes encoding collagen chains	Description
Fibrillar	I	COL1A1 and COL1A2	Quarter-stagger packed fibrils that are primarily found in fibrous stromal matrices, such as skin, bone, tendons and ligaments
	II	COL2A1	
	III	COL3A1	
	V	COL5A1, COL5A2 and COL5A3	
	XI	COL11A1, COL11A2 and COL11A3	
	XXIV	COL24A1	
	XXVII	COL27A1	
FACIT	IX	COL9A1, COL9A2 and COL9A3	Fibril-associated molecular bridges that are associated with fibrillar collagen
	XII	COL12A1	
	XIV	COL14A1	
	XVI	COL16A1	
	XIX	COL19A1	
	XX	COL20A1	
	XXI	COL21A1	
	XXII	COL22A1	
Basement membrane	IV	COL4A1, COL4A2, COL4A3, COL4A4, COL4A5 and COL4A6	Network structure composed of laminins and basement membrane proteins

Collagen production in ECM is the result of the biosynthesis from related genes. Numerous genes have been identified and cloned corresponding to each alpha chain in specific collagen types as shown in Table 2.1. The expression of collagen genes is regulated by some transcription factors such as CCAAT binding factors and nuclear factor-1, cytokines, such as tumor necrosis factor alpha. Collagen gene expression is also regulated by interferons, and growth factors, such as

transforming growth factor-beta and its positive/negative modulators, basic fibroblast growth factor (bFGF), and insulin-like growth factor (Ghosh, 2002). Resident cells in ECM, like skin fibroblasts, may also respond to several other external stimuli for collagen accumulation. For example, both collagen hydrolysates (Zague et al., 2011) and ascorbic acid (Kishimoto et al., 2013) are reported to stimulate the synthesis of type I and type IV collagen. In addition, regulatory regions in collagen genes also control their expression. COL1A1 and COL1A2 gene expression is regulated by the upstream promoter, e.g. -376 to +58 bp region of COL1A2 and -174 to -84 bp region of COL1A1. Since most collagen genes show complex exon and intron patterns, the resultant transcripts vary among different organs due to transcription initiated from different sites.

Generally, after transcription and translation, the alpha chains are transported to the endoplasmic reticulum (ER) for procollagen synthesis, and to the Golgi apparatus for modification and packaging before secretion. Finally, various intra-and inter-molecular crosslinks are formed to stabilize the structure. Fibrillar collagen is the most representative class found mainly in skin, bone and tendons, and its structure and biosynthetic route are relatively well established. In the ER, three pro-alpha chains are synthesized with two large propeptide sequences at the C-terminal and N-terminal side of each chain (Figure 2.1), respectively. In the presence of signal recognition site, propeptide regions of the chain is imported to ER where the lysine and proline residues are hydroxylated by lysyl and prolyl hydroxylase enzymes (mainly prolyl 4-hydroxylase), respectively (Mouw et al., 2014). The hydroxylation level of proline and lysine, however, are different. The former one is relatively consistent (~50%) among different types in various tissues, while the latter
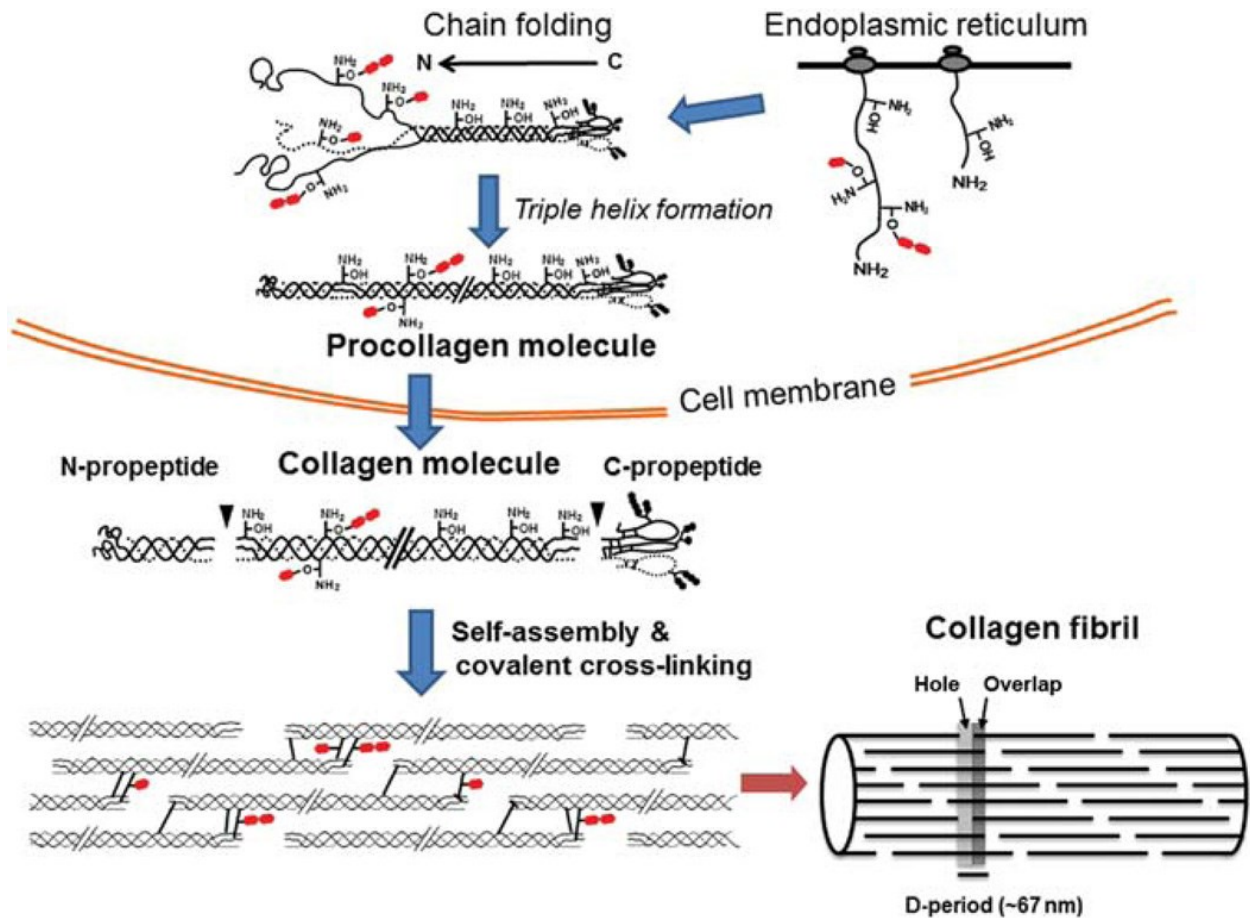
Figure 2.1. Biosynthetic route of type I collagen molecule. The red molecules denote galactose or glucose-galactose attachment (Yamauchi and Sricholpech, 2012). Republished with the permission of Biochemical Society.

one can differ largely from 15% to 90% depending on the sources of collagen and the physiological condition of the tissues (Miller, 1984; Uzawa et al., 2003). Some of the hydroxylysines are then glycosylated with glucose and/or galactose contributing to the stabilization of the triple helical structure. This glycosylation occurs more often in randomly organized collagen, like type IV than that is seen in fibrillar collagens, like type I, II, or III (Shinkai et al., 1979). Following the mono/di-saccharide decoration, procollagen molecules are formed from the trimerization of three pro-alpha chains, initiation and correction of which are controlled by the recognition sequence at the C-terminal propeptide region (Figure 2.2) (Bourhis et al., 2012). Other proteins like prolyl

hydroxylase and glucose-regulated proteins are also involved in the assembly of alpha chains. Hyp

formed in the Y- position stabilizes the helical structure mainly by the steroelectronic effect, and

provides a thermodynamic advantage by the formation of hydrogen bonds. From the C-terminal

towards N-terminal, a tight triple helix is generated resulting in rigid steric constraints for every

third amino acid position where only a glycine can fit in without trimming. This explains the

repeating occurrence of Gly-X-Y triplets and the stability of this structure (Mouw et al., 2014).
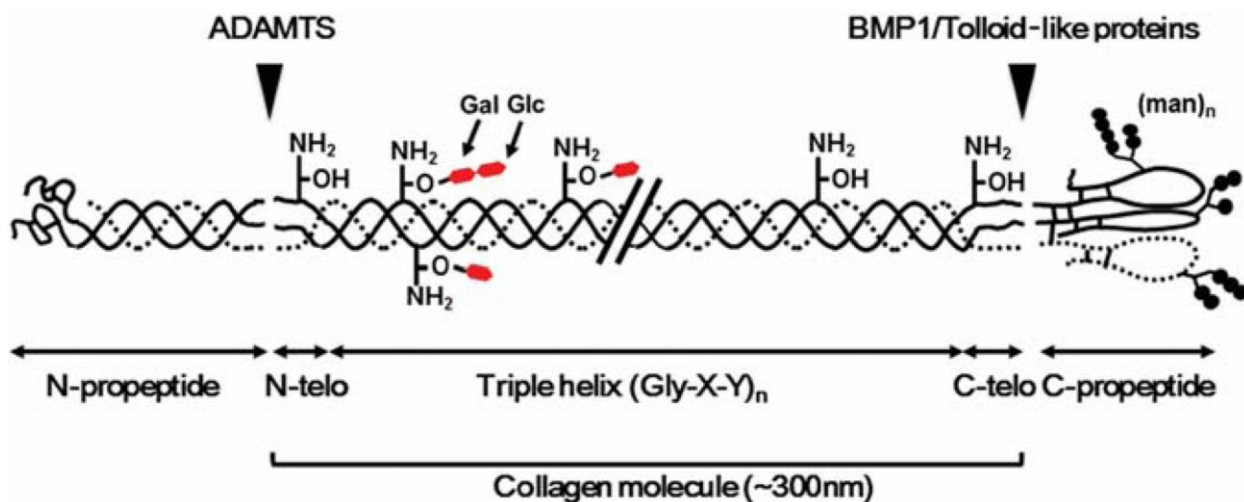
Figure 2.2. The structure of type I procollagen molecule. The procollagen is cleaved at specific sites as indicated by the arrows. Gal denotes galactose unit, Glc denotes glucose unit (Yamauchi and Sricholpech, 2012). Republished with the permission of Biochemical Society.

In the next step, the procollagen molecule is packed into the Golgi apparatus where the

formation of collagen bundles is initiated, following which they are transported to cell membrane,

recognized by fibripositors, and secreted via exocytosis. Following or during the transportation

and secretion process, the propeptide regions of the procollagen molecule are cleaved by

metalloproteinases, i.e. the "a disintegrin and a metalloproteinase with thrombospondin repeats"

(ADAMTS), bone morphogenetic protein 1 (BMP1)/Tolloid-like families, and the furin-like

proprotein convertases (Hulmes, 2008). The mature collagen molecule generated after cleavage

still maintains a short non-helical telopeptide region at both C-terminal and N-terminal of the backbone giving a final total molecular size of ~300 nm (Figure 2.2). These collagen molecules then spontaneously assemble to generate cross-striated and quarter staggered microfibrils with an axial repeat distance of ~67 nm, called the D period. This is the result of an overlap and the hole zones formed alternately as the collagen molecules axially associate (Figure 2.1). These microfibrils further merge to form mature fibrils, length and diameter of which are affected by the extent of propeptides' removal (Hulmes, 2002) and the collagen interactions with small leucine-rich proteoglycans (McEwan et al., 2006). Other collagen molecules such as Type V collagen and FACIT collagen also fuse into the fibrils, and thus change the surface properties as well as the interactions with additional ECM macromolecules and cell surface receptors to finally influence the fibrillogenesis. In the final step, the strength and stability of mature fibrils are achieved by covalently cross-linking within and between collagen molecules. The lysine and hydroxylysine in the telopeptide regions are deaminated by copper-dependent lysyl oxidase forming corresponding aldehydes which can react with another telopeptidyl aldehyde or unoxidized lysine/hydroxylysine that is in telopeptide or in backbone helices. The cross-links can be further complicated by a condensation reaction with histidine residue that has the correct proximity (Yamauchi et al., 2012). Non-enzymatic cross-linking, the glycation with glucose and other glyoxal aldehydes also facilitates the maturation of collagen fibrils during aging (Avery et al., 2008). Overall, collagen synthesis, as a cell-driven process that is also regulated by interactions with other surrounding macromolecules, affords its tissue- and age- specific structure to fulfill the various biological roles.

2.1.2 Collagen and gelatin production

In the meat industry, gelatin is conventionally produced from mammalian animals like pig and cattle, especially from pig skin, bovine hide, and their bones. Gelatin products have been

widely used as food sources, food processing ingredients and pharmaceuticals for a long time. However, the traditional bovine and/or pig source may introduce health risks considering the occurrence of bovine spongiform encephalopathy. Also, must be considered are practicalities regarding religiously acceptable slaughtering process for people of Jewish and Muslim faiths (Regenstein et al., 2003). Gelatin production from fish (scales, bones, fins, and swim bladders) and poultry (skin, feet, bones, and even meat residues) are promising alternative sources (Hanani, 2016). In general, gelatin processing includes trimming and cleaning, pretreatment conditioning, extraction, filtration and clarification, concentration, sterilization, drying, and standard packaging. The produced gelatin is classified as either type A (acid pretreated) or type B (alkaline pretreated) according to the conditioning process. Depending on the nature of the raw material, processing procedures vary accordingly. For example, considering the large mineral content, bone is subjected to maceration with dilute hydrochloric acid followed by a precipitation step with lime to remove phosphate and calcium carbonate. A defatting step maybe incorporated in the processing of pig skin due to their relatively large fat content (~30% of raw material). Despite the pretreatment conditioning is intensively long (up to a few months in lime) and acute with respect to the high degree of cross-links in the mature collagen fibrils, bovine hide represents a relatively pure collagen form with a large collagen content. The corium layer of the bovine hide is composed of practically pure collagen (Schrieber and Gareis, 2007). The extended long liming treatment breaks down most of the crosslinks as well as removes non-collagenous proteins such as albumin and globulin, and non-protein components like glycosaminoglycans.

Unlike the processing of gelatin, which usually requires a series of heating steps with gradually increasing temperature from 50 to 100°C to solubilize the conditioned material, most of collagen extraction processes after conditioning is carried out at a controlled low temperature (2-

8°C) to avoid the degradation of collagen molecules. The solubilization of collagen can be achieved by diluted acid such as hydrochloric acid, citric acid and acetic acid (Silva et al., 2014). Acetic acid at a concentration of 0.5 M was reported to efficiently extract collagen from bovine hide, turkey heads, and flatfish (Khiari et al., 2014; Heu et al., 2010). The extraction yield can be improved by the addition of enzymes such as pepsin and papain to cleave the telopeptide regions, and thus facilitate the removal of telopeptide-associated cross-links and improve collagen solubility (Hong et al., 2017). The product is then recovered by salt precipitation (> 2 M NaCl), dialysis or ultrafiltration to minimize the salt content, and freeze dried to obtain a final acid- and pepsin- soluble pure collagen.

2.1.3 From collagen to collagen hydrolysates

Collagen hydrolysates (CH) are produced from collagen or gelatin by chemical and/or enzymatic hydrolysis, during which the alpha chains unfold, and some peptide bonds are cleaved. The hydrolysis not only affords the release of numerous bioactive peptides which may be inactive in the parent polypeptide chain, but also creates specific functional properties including emulsifying ability, water-binding capacity, forming ability, etc. In contrast to gelatin and collagen products, CH have superior solubility in cold water, and do not form gel even at greater concentrations; CH are termed as "non-gelling edible gelatine" in European Food Regulations. CH are widely applied in the food industry due to their intriguing functional properties. For example, they can serve as an emulsifier and stabilizer in low-fat cheese, are used to increase the solubility/dispersion of other additives in some beverages, and increase the amount of binding water in meat. Moreover, since very few bitter peptides are generated in CH, they also function as a taste-neutral protein ingredient (Schrieber and Gareis, 2007).

Although chemical acid/alkaline hydrolysis is cost effective with simple operation, the mild biological approach by enzymes is more popular to obtain CH with relatively controllable and consistent molecular weight (MW). Numerous enzymes have been described to effectively produce CH in the literature, including endoproteases such as animal-originated pepsin, trypsin, chymotrypsin (Mendis et al., 2005), plant-based papain (Baehaki et al., 2015), and microorganism-originated Alcalase® and Neutrase® (Alemán et al., 2011), or exoprotease such as Corolase® and Flavourzyme (Dolphin and Russell, 2011). The combination of both endo- and exoprotease provides broad specificity resulting in a greater cleavage efficiency and smaller peptides fractions (Khiari et al., 2014; Dolphin and Russell, 2011). For each collagen of specific origin and type, the selection of enzymes and hydrolysis conditions (i.e. pH, temperature, enzyme/substrate ratio, reaction time, etc.) has to be optimized through necessary and time-consuming primary experiments. The MW of the final hydrolysates product is one of the most important factors to determine the functional properties, bioactivities, and bioavailability. The mean molecular size of CH varies widely from 2,000 to 20,000 Da (Schrieber and Gareis, 2007) due to variation in collagen sources, hydrolysis methods and conditions. Generally, CH with lower MW exhibit greater solubility and less viscosity. More intensive hydrolysis process facilitates to release greater amount of bioactive collagen peptides, as well as expose greater amount of accessible cleavage sites for the later gastrointestinal (GI) digestion. This contributes to improving the overall proteolysis and absorption of CH, and thus increasing their bioavailability.

2.2. Bioavailability of collagen hydrolysates and collagen-derived peptides

2.2.1. Absorption and distribution of collagen hydrolysates (CH)

Bioavailability generally refers to the relative amount of ingested compounds that are absorbed intestinally, transported and distributed by blood circulation system, and finally serve to

maintain the metabolic effect or storage function in the body (Richelle et al., 2006). Figure 2.3 indicates the brief digestion route of oral ingested compounds (Lindley et al., 2011). The current understanding of proteins and peptides absorption is relatively well established that they are primarily hydrolyzed in GI tract by both extra- and intracellular proteases and peptidases to a mixture of free amino acids and small oligopeptides (mainly di- and tripeptides), which are then absorbed and used as building blocks for the synthesis of necessary body proteins (Lindley et al., 2011). Further degradation may occur since the oligopeptides entering in circulation system are subjected to enzymatic cleavage by plasma peptidases and esterase during the distribution. The GI tract is lined by a thin layer of epithelial cells that are joined by tight junction complexes to form a selective and polarized barrier. This establishes two functionally different membrane surfaces; one apical lumen-facing surface and a basolateral blood-facing surface. It also creates two separate compartments that protect the body from harmful xenobiotics. The absorption of peptides is facilitated by the large surface area especially created by folding of villi and microvilli in small intestine (Lindley et al., 2011). Figure 2.4 is an oversimplified summary figure showing intestinal membrane structure and pathways for nutrients absorption (Balimane and Chong, 2005). In general, permeation across intestinal membrane is achieved paracellularly or transcellularly. Paracellular transport is a passive pathway controlled by the resistance of the tight junction, through which the net permeation largely depends on the size and charge of the applied peptides and amino acids, and the porosity of the tight junction itself. Transcellular transport of peptides and amino acids involves several mechanisms including passive transcellular diffusion, active carrier-mediated pathway, and transcytosis. Most of amino acids are absorbed through a class of specialized transporters (e.g. Na^+-dependent or Na^+-independent), while peptides are mediated by proton-coupled oligopeptide transporters (POT). PepT1 is the major isoform of POT accounting for GI

absorption of peptides and peptide-like therapeutic agents. Other POT isoforms do not play an important role or yet to be discovered in this respect. For example, PepT2 has not been found in GI tract *in vivo*, and PHT2 expressed intracellularly does not significantly alter peptides' absorption (Sakata et al., 2001; Herrera-Ruiz and Knipp, 2003). In contrast, lipophilic peptides can rapidly merge with cellular membrane through transcellular diffusion depending on their hydrogen-bonding capacity, hydrophobicity, etc. However, the permeation of peptides may be counteracted by the action of some ATP-binding cassette transporters, such as the most characterized efflux pump P-gp, through excluding them out of cytoplasm (Sharom et al., 1995). Overall, the transport of peptides and amino acids can be very complex process considering the mechanism involved, which is determined by the physicochemical structure of the nutrients, the interaction with the intestinal membrane, as well as the interaction with the food matrix.
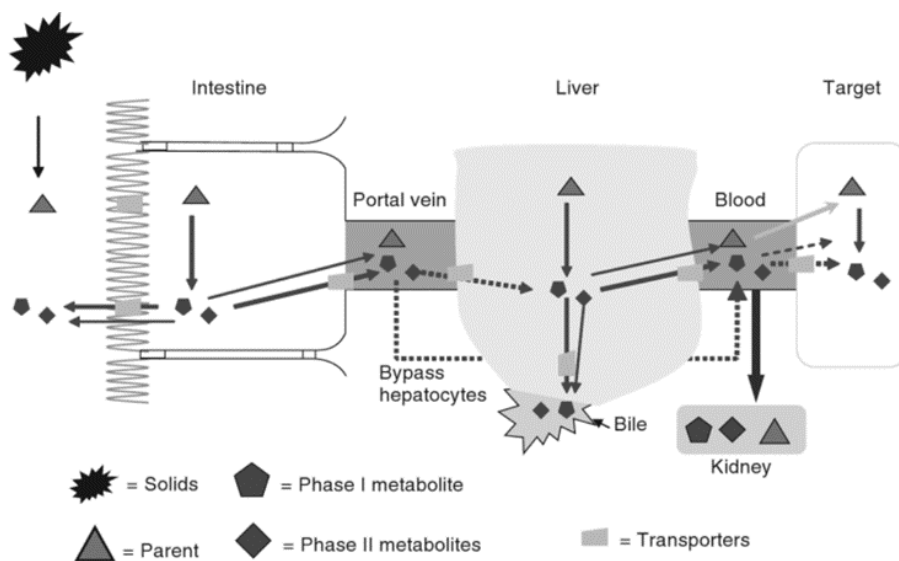
Figure 2.3. Organ bioavailability barriers to orally administrated compounds. These processes include the dissociation of solid compounds, the digestion and transport, and metabolism in major digestive organs in human body (Lindley et al., 2011). Copyright © 2011 John Wiley & Sons, Inc. Reproduced with the permission of John Wiley & Sons.
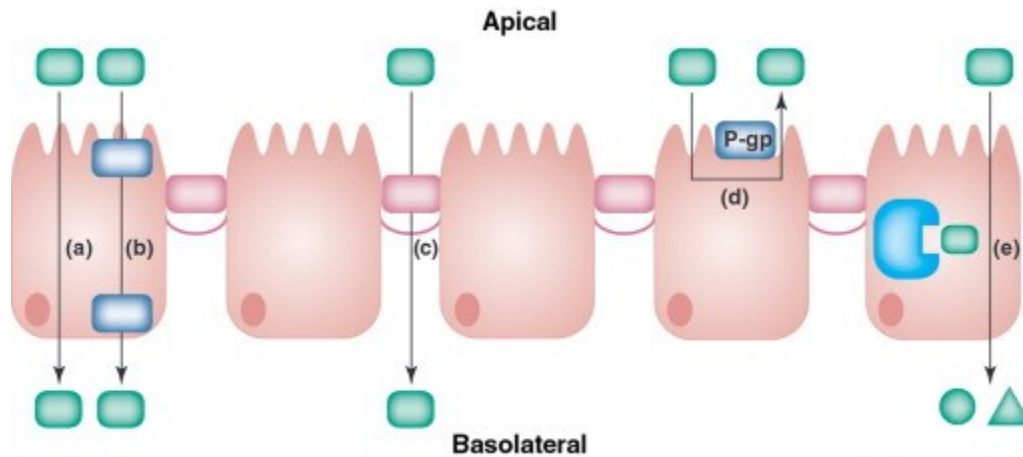
Figure 2.4. Intestinal membrane, and the potential pathways for absorption of applied compounds. (a) transcellular passive permeability; (b) carrier-mediated transport; (c) paracellular passive permeability; (d) efflux by P-gp; and (e) cellular metabolism. Reprinted from Balimane and Chong (2005), Copyright (2005), with permission from Elsevier.

In contrast to the digestive resistance of native collagen, gelatin (a denatured collagen product) and collagen hydrolysates can be easily digested and absorbed to a certain extent yet do still possess some relatively high MW fractions. The final intestinal absorption is around 10% (Moskowitz, 2000), which may vary depending on the source of CH and the experimental model used. Previous studies indicated that the oral ingestion of CH results in its wide distribution among various tissues in rats including the liver, kidney, cartilage, brain, muscle, skin, etc. The peak values were obtained after a few hours but mostly disappeared after 14 days in those tissues, except for skin, where up to 70% of the maximal amount remained. This suggests that skin is the preferential long-lasting accumulation site for collagen peptides (Watanabe-Kamiyama et al., 2010). There are also studies that found cartilage is another long-lasting accumulation site of CH (Oesser et al., 1999).

2.2.2. Identification of collagen-derived peptides in plasma

Like other proteins and peptides, it is currently elucidated that orally taken CH can be digested to small oligopeptides and amino acids that are then absorbed. Hyp as the signature amino acid of collagen, is absorbed mainly in the free amino acid form, while less so in the peptide form (~30%) (Ohara et al., 2007; Shigemura et al., 2014). Previous *in vivo* studies identified a series of Hyp-containing small peptides in plasma, such as Pro-Hyp, Pro-Hyp-Gly, Ala-Hyp-Gly, Leu-Hyp, etc. Although the concentration of each peptide may vary significantly among different studies, Pro-Hyp was observed to be the major type accounting for up to 95% of total Hyp-containing peptides (Ichikawa et al., 2010; Iwai et al., 2005; Ohara et al., 2007). Recently, another new major collagen-derived peptide Hyp-Gly is identified in human plasma with the ratio to Pro-Hyp from 0.0 – 5.0 among different subjects after oral ingestion of fish scale CH (Shigemura et al., 2011). This discovery is probably the result of the recent use of precolumn derivatization by a phenyl isothiocyanate method that facilitates the resolution of peptide separation by reversed phase liquid chromatography. Only minor amount of these two collagen-derived peptides degraded after 3 hours at 37°C in human serum, i.e. 5.5% of Pro-Hyp, 0.5% of Hyp-Gly (Shigemura et al., 2011). Around 75% of synthetic Pro-Hyp survived even after exposure to plasma for 24 h (Iwai et al., 2005). In addition, a recent study reported a greater enrichment of tripeptide Gly-Pro-Hyp than Pro-Hyp in plasma using both the mice model and human trial after the administration of CH containing a large proportion of tripeptides. Meanwhile another 15 types of collagen-derived peptides were confirmed including some Pro-containing peptides, such as Pro-Ala, Pro-Ser, Gly-Pro, etc. (Yazaki et al., 2017). The Gly-Pro-Hyp is also seen to persist (more than 90%) in plasma after 2 hours incubation at 37°C (Sontakke et al., 2016), even though it may be further degraded to Pro-Hyp when reaching the skin (Yazaki et al., 2017). These different findings suggest that the type and amount of collagen-derived peptides distributed in plasma and diverse tissues are

dependent on the CH source and the preparation method, the experimental subjects and their digestion/absorption ability. The elevated level of Hyp- and/or Pro-containing collagen-derived peptides in plasma and specific tissues after CH oral ingestion reveals the large resistance of these peptides to human body digestion system. Some of these peptides, such as Pro-Hyp, are even excreted as an intact peptide form in the urine (Weiss and Klein, 1969).

Most of collagen-derived peptides found in plasma are small di- and tripeptides, which are substrates for the oligopeptide transporters especially true for PepT1. PepT1 has been demonstrated to have wide specificity in mediating di- and tripeptides from any combination of the 20 naturally occurring L-α-amino acids (Herrera-Ruiz and Knipp, 2003). When Gly-Pro-Hyp was applied to porcine brush border membrane vesicles, as proposed by Aito-Inoue et al. (2007), it was partially cleaved to generate free Gly and Pro-Hyp by the brush border membrane enzymes. The induced Pro-Hyp was then in part transported across the membrane by the PepT1 transporter, since its permeability is inhibited in the presence of Gly-Pro - an established competitive PepT1 substrate. Other transporters such as amino acid transporter PAT1 and peptide transporter PepT2 may also contribute to CH (intestinal and non-intestinal) absorption, since they exhibit selectivity on proline, proline derivatives (e.g. Hyp), and/or proline-containing dipeptides (Brandsch, 2006). Despite most of the previous studies claimed that CH are finally absorbed in small fractions (i.e. free amino acid, di- and tripeptides), bigger peptides have also been detected at the serosa side of intestine in other studies. Oesser et al. (1999) found that CH can be absorbed in a wide MW range from 1 to 10 kDa using gut-sac model from mouse small intestine. This suggests that except for amino acid and peptide specific transporters, larger fractions of CH may be absorbed through other pathways as mentioned above via transcellular diffusion which requires favorable lipophilicity, or

transcytosis which is a relatively rare case. The absorption mechanism of the high MW CH remains to be explored in detail.

2.2.3. Approaches to improve the bioavailability of collagen peptides

Collagen hydrolysates (CH) have been used as food supplements and pharmaceuticals because of its versatile beneficial biological functions (section 2.3 and 2.4). Their bioavailability, however, is barely satisfactory. This limitation likely is associated with solubility issues, MW, and physicochemical structures, which affect their subsequent dissociation, GI digestion, and interactions with the intestinal membrane for absorption, respectively. The MW is probably the most important limiting factor, since to some extent it determines the solubility and physicochemical properties of CH. Generally, CH with high MW which may retain some extent of helical structure of collagen showing a low solubility. Chi et al. (2014) and Jridi et al. (2014) revealed that CH fractions with lower MW correlated with greater solubility probably because smaller peptides liberation leads to more polar groups to be exposed that can assist water solubilization. Effects of MW on the interaction of CH with the intestinal membrane depend on their hydrophilic/hydrophobic properties. Hydrophilic collagen peptides are expected to transport across intestinal membrane either paracellularly through tight junctions or transcellularly through a transporter-mediated pathway, both of which favors molecules with small size (Artursson et al., 2012). Therefore, numerous studies have focused on producing CH with a low MW distribution. Enzymatic hydrolysis is the most popular approach to generate CH, of which the MW is determined by the starting collagen material and the performance of enzymes. Pepsin treatment for extraction of collagen can improve the production of low MW collagen peptides from spent hen since it hydrolyzed collagen telopeptide regions where most of cross-links occur (Hong et al., 2017). Ultrasound assistance for the extraction of collagen, which may damage the covalent cross-

links and triple helical structure, also facilitate its hydrolysis efficiency to generate collagen peptides with low MW (Zhang et al., 2017). For the subsequent hydrolysis of collagen, instead of selecting a single enzyme, sequential hydrolysis by various enzymes with distinct specificities is effective to reduce the average MW of final CH product. For example, Dolphin and Russell (2011) used serial hydrolysis by endopeptidase (e.g. papain, bromelain and Corolase®7089) and exopeptidase (e.g. Validase® FPII and Corolase® LAP) to produce bovine CH with MW from 100 Da to 2,000 Da, of which MW is lower than commercial available ones (mean MW >2,000 Da) (Schrieber and Gareis, 2007). Hydrolysis by a cocktail of enzymes that function at similar condition (pH and temperature) is an efficient strategy to save time. In this scenario, the screening of enzymes should be careful to achieve optimized performance without compromising efficiency of each component. Successful example is the microorganism-origin crude protease extract which contains multiple enzymes (Nasri et al., 2013). Other techniques, such as fermentation and ultrasound, coordinate with the hydrolysis to facilitate the efficiency of corresponding enzymes. Overall, the pre-digestion hydrolysis of collagen can help to release small bioactive peptides to a certain extent, but more research is needed to improve the intestinal absorption after oral administration.

In contrast to the ingestion of the CH mixture, collagen or gelatin, the bioavailability of any specific health benefitting peptide after being released or directly administrated, relies on its metabolic stability and the ability to cross body's physical and biochemical membrane barriers such as the intestinal barrier. An ideal peptide delivery system, therefore, should be designed to improve both the stability and permeability. Peptides targeting specific sites must survive from not only the large pool of endogenous peptidases (e.g. pepsin, trypsin, chymotrypsin, elastase, carboxypeptidase, etc.), but also the dynamic pH condition among various organs, from harsh

acidic environment of the stomach (pH 1-3) to mild basic condition of the blood (7.35-7.45). Using enzyme inhibitors has proven to be effective to reduce the degradation of therapeutic peptides. Frequently, inhibitors are used to suppress the performance of trypsin and chymotrypsin, the two primary digestion enzymes in GI tract, including classical ones such as aprotinin and soybean trypsin inhibitors (Yamamoto et al., 1994; Tozaki et al., 1997), and new ones like chicken and duck ovomucoids (Agarwal et al., 2000). These enzyme inhibitors, the majority of which are highly toxic, may negatively interfere with the digestion and absorption of other dietary peptides after long time performance, as well as trigger the development of hypertrophy and hyperplasia of the pancreas (Bernkop-Schnurch, 1998). Alternatively, to increase the stability of proteins and peptides in the harsh gastric environment and maintain their sustained release, carrier systems such as emulsions, microspheres, and liposomes (e.g. calcitonin) can be used. The major concern here arises from the physicochemical stability of each system. Improvements have been made by the development of nanoemulsions with greater surface area than normal macroemulsions (Shah et al., 2010; Rao et al., 2008). The stability of liposomes can be improved by surface modification with polyethylene glycol (PEG) (Iwanaga et al., 1999). Recently, a multilayered liposome has been developed to encapsulate collagen peptides by thin film hydration and ultrasonication techniques which employ charged lipids to reduce size (Chun et al., 2017). This small liposome (<100 nm) was physically stable, and thus promising for the oral delivery of collagen peptide. Other encapsulation strategies using hydrophilic mucoadhesive polymers, such as chitosan and thiolated polymers (Bernkop-Schnurch and Krajicek, 1998), are also effective to protect peptides from degradation as well as improve absorption by interacting with intestinal mucus to generate a steeper concentration gradient. Novel carrier system using nanoparticles is promising since, like other mucoadhesive reagents, they easily attach to the mucous membrane, and thus increase the

residence time of peptide moiety and slow down the clearance (Chan et al., 2010; Carvalho et al., 2010).

Penetration through intestinal barrier is a greater obstacle for the absorption of bioactive peptides. As mentioned before, two main mechanisms, paracellular and transcellular pathways, account for the translocation of peptides. Since the paracellular pathway is gated by tight junctions, the adherent belt between enterocytes, co-administration of permeation enhancers (PE) with target peptides is a common way to increase this pathway-specific transport. Generally, PE are applied at maximum non-toxic concentration to reversibly open up tight junctions; thus, small hydrophilic peptides can pass the tight junction easily. Typical PE include chitosan, Zonula occludens toxin, lectins, etc. (Bruno et al., 2013), which improve the transport of macromolecules non-specifically. For example, chitosan was also reported to enhance the absorption of glucosamine up to 4-fold in a Caco-2 cell model (Qian et al., 2013). Surfactants as one type of PE can affect barrier function of tight junctions by interacting with cell lipid bilayer membrane (Edward et al., 1997), which is reflected by the action of bile salts (sodium cholate and deoxycholate) and sodium dodecyl sulfate (Davis and Illum, 2003). Long-term usage of PE may introduce damage to the intestinal membrane and affect its barrier function. However, this point of view is debated in the literature since prolonged exposure to high concentrations of PE is unlikely considering the short and dynamic transit *in vivo* within the GI environment (Maher et al., 2016).

In addition to a physical strategy by co-administration of target peptide with enzymatic inhibitors or PE, chemical modification of peptide structure may induce multiple benefits including the improvement of (lipid or aqueous) solubility, digestion resistance, and/or absorption rate. A representative example is the PEGylation of protein or peptides. The incorporation of PEG, an amphiphilic molecule, helps to improve the effects of bovine lactoferrin (an anticanacer

glycoprotein) (Nojima et al., 2008) and insulin (Calceti et al., 2004) by increasing their digestion stability and oral absorption. Direct modification of peptides aims to increase the transcellular diffusion is usually achieved by conjugating with a more hydrophobic group via cyclization, methylation, lipidization, esterification, acetylation, etc. This strategy helps to reduce the hydrophilicity of the target peptide or protein, and thus favoring its interaction with the cell membrane. Examples are, Cycloporine, an immune system modulator, and cyclized somatostatin that has growth-hormone release-inhibiting activity, both of which show improved bioavailability due to the cyclization. It appears that cyclization decreases the flexibility and hydrogen bonding capacity of their parent peptides (Craik et al., 2013; Biron et al., 2008). Also, lipidization of a protein or peptide with fatty acid can be reversible (like a prodrug), such as palmitoyl-salmon calcitonin (Wang et al., 2003) or triglyceride incorporated deltorphin II (Patel et al., 1997). Chemical modification that aimed to improve the receptor/transporter mediated transport of peptides is primarily the result of conjugation with a naturally penetrated molecule without concern about antigenicity. Peptides glycosylation with glucose, as in the case of albumin (Adessi and Soto, 2002), can endow their ability to be recognized by GLUT transporters. Similarly, the incorporation of receptor detectable proteins such as insulin fragments (Fukuta et al., 1994), and ligands such as vitamin B12 (Chalasani et al., 2007), into a target peptide or protein can also enhance their absorption by introducing an extra receptor-mediated pathway. Recently, a novel CH mixture with improved efficiency of blood distribution in mice was developed by the cyclization of its enriched X-Hyp-Gly tripeptide components, e.g. Ala-Hyp-Gly to clyco(Ala-Hyp). This conversion was carefully carried out through heating of the CH for 3 h at 85°C with pH of 4.8 (Taga et al., 2017). The superior absorption of cyclic collagen peptides such as cyclo(Ala-Hyp) and cyclo(Leu-Hyp)

compared to collagen oligopeptides such as Pro-Hyp suggests that chemical modification by cyclization is a promising way that may improve the collagen peptide bioavailability.

2.3. Beneficial biological effects of collagen-derived peptides

2.3.1. Role in joint and bone health

Collagen hydrolysates and collagen-derived peptides are becoming intriguing sources of nutraceuticals to meet society's increasing demands for nutritional supplements and foods that can provide health benefits. One of the best-known health benefits of CH is their chondroprotective role to prevent and treat joint and bone related diseases such as osteoarthritis (OA) and osteoporosis. OA is a chronic disease resulting from continuous degeneration of cartilage in joints, the subsequent abnormal remodeling of adjacent bones and joint space narrowing. OA is accompanied with symptoms like joint pain, stiffness, and reduced joint mobility (Rahmati et al., 2017). Figure 2.5 shows the typical structural changes in osteoarthritic joint. Clinical studies have demonstrated the effectiveness of CH ingestion to relieve OA symptoms. For example, a randomized, double-blind trial showed that the daily ingestion of 10 g CH for 60 days reduced OA-associated knee and hip pain of patients and led to increased mobility (Moskowitz, 2000). This was confirmed by Benito-Ruiz et al. (2009) who observed a significant greater visual analogical scale score (less pain) in the CH treated group than that in the placebo group. With a lower dosage (1.2 g/day) for 6 months, the proportion of clinical responders (>20% improvement compared to control) was also higher than that in the placebo group (Bruyere et al., 2012). Despite positive results from these short-term experiments, further research to study long-term efficacy are pending to better determine the therapeutic effects of CH on OA (Bello and Oesser, 2006).
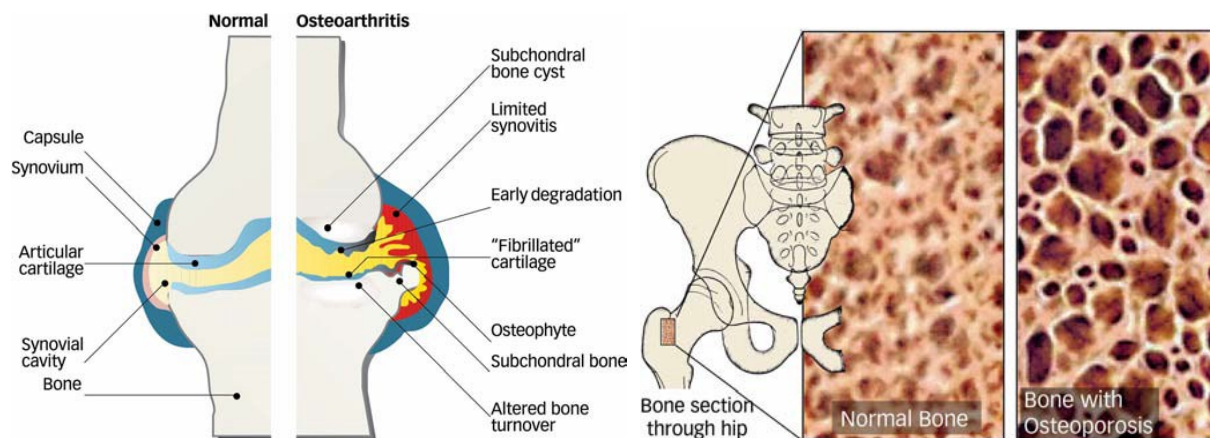
Figure 2.5. Features of osteoarthritis (left) and osteoporosis (right) in comparison with normal joint and bone, respectively. Schrieber, R.; Gareis, H. *Gelatine handbook: Theory and industrial practice.* Page 302-306. **2007**. Copyright Wiley-VCH Verlag GmbH & Co. KGaA. Reproduced with permission.

The biological and physical functions of articular cartilage are conferred by the ECM. The components of ECM such as collagen and proteoglycan are synthesized by chondrocytes that also maintain their homeostasis. Conventionally, it is believed that the continuous loss of ECM in OA cartilage cannot be controlled, and OA cannot be cured; thus, OA treatments have been mainly aimed to relieve symptoms via analgesics (e.g. acetaminophen) and non-steroidal anti-inflammatory drugs whilst introducing significant side effects. In contrast, CH are proposed to work through both preventative and curing effects. Oesser et al. (2007) revealed that CH ingestion for 3 months could decrease and retard the degeneration and destruction of cartilage in the knee joint of mice with OA. In contrast, active performance of CH was reported to stimulate the synthesis of type II collagen by cultured chondrocytes in a dose-dependent manner (Figure 2.6) (Oesser and Seifert, 2003). In a human trial, CH significantly benefited the deposition of proteoglycans in medial and lateral regions of the cartilage, but the benefit was not significant for other regions of interest due to the small sample size (McAlindon et al., 2011). But an *in vivo* study using guinea pigs suggested the improvements realized therapeutically by CH was correlated to

proteoglycans deposition in the epiphyses (Ohara et al., 2010a). In addition, both CH and its major peptide component, Pro-Hyp, can suppress the loss of chondrocytes as well as the thinning of mouse articular cartilage layer. In the *in vitro* experiment, they can enhance the production of glycosaminoglycans (2-fold by CH and 3-fold by Pro-Hyp) by cultured chondrocytes (Nakatani et al., 2009). Pro-Hyp also promotes hyaluronic acid (HA) secretion by cultured synovium cells (Ohara et al., 2010a). The cartilage stimulation responses to CH validate the regenerative potential underlying their therapeutic effects and give merit to use CH to restore the homeostasis of cartilage mass components, e.g. HA, collagen, proteoglycans, etc.
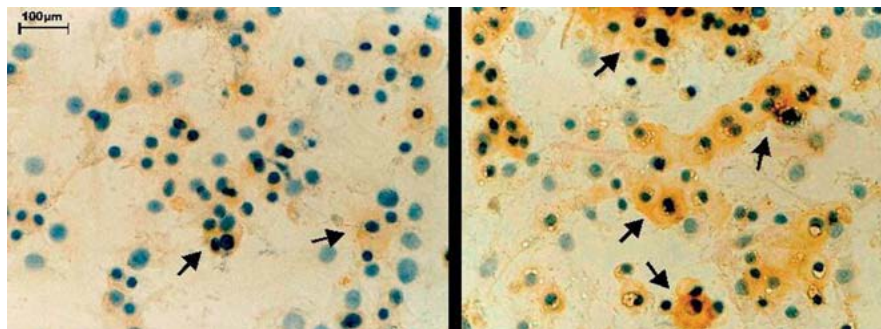
Figure 2.6. Stimulation of collagen hydrolysates on the deposition of collagen (right), in comparison with non-treated group (left). Arrow indicates the collagen accumulation (brown color) around chondrocytes. Cell Tissue Res. Stimulation of type II collagen biosynthesis and secretion in bovine chondrocytes cultured with degraded collagen. 311 (3), 2003, 393–399. Oesser, S.; Seifert, J., © Springer-Verlag 2003. With permission of Springer.

Similar with OA, osteoporosis is the result of the ongoing deterioration of bone substance. Osteoporosis is featured by low bone mineral density, a porous bone structure and bone fragility (Kanis et al., 2008) (Figure 2.5). The loss of bone matrix is manifested in the urinary excretion of pyridinoline crosslinks (found in mature collagen) and deoxypyridinoline crosslinks (specific in bone collagen, not in cartilage), which can be used as biomarkers for the diagnosis of osteoporosis (McLaren et al., 1992; Miyamoto et al., 1994). Compared to OA treatment, the effects of CH on

osteoporosis are less studied, especially in clinical trials, so far. An earlier study by Adam et al. (1996) revealed that CH had an additive effect with calcitonin, a naturally produced hormone used to treat osteoporosis, to attenuate bone loss. After a 24-week intervention, the reduction of collagen crosslinks' excretion in urine was significantly greater in osteoporosis patients treated with calcitonin and CH combination than the group of calcitonin treatment alone. However, a later clinical trial investigating postmenopausal women with low mineral density did not find any significant effects for CH administration (10 g/day) on either bone resorption or formation after 24-weeks treatment (Cúneo et al., 2010). Contradictory results were also observed in some *in vivo* assays. For example, CH did not change the bone mineral content or density in the femur of normal mice when a large total protein diet (14%) were ingested, but was effective with a lower total protein diet (10%) (Koyama et al., 2001). Using ovariectomized rats (Nomura et al., 2005) or mice (Guillerminet et al., 2009), however, the therapeutic effects of CH was shown with respect to improvement in bone mineral density and bone strength due to the enhanced deposition of type I collagen, glycosaminoglycans. The conflicting results indicates that CH may exhibit better performance in subjects that encounter more severe bone loss such as women with osteoporosis and the ovariectomized animal models with estrogen deficiency-induced bone loss. *In vitro* studies indicate that CH with a low mean MW of 2 kDa can stimulate the osteogenesis ability and reduce the resorption activity of osteoblasts (Guillerminet et al., 2010). Both CH and Pro-Hyp are reported to up-regulate the expression of bone related genes such as COL1A1 and Runx2 by osteoblastic cells (Kimira et al., 2014; Liu et al., 2014; Kim et al., 2013). Studies of the effects of CH on osteoporosis are still in the first stage, and more comprehensive clinical studies are needed to confirm the therapeutic role of CH, their effective dosage, and optimal time of ingestion. Although to date there is no perfect animal models to mirror all the physiological features of humans with

osteoporosis, ovariectomized rodent models which share similarities with post-menopausal women in bone loss, could play a crucial role in preclinical trials before costly and time-consuming clinical human trials are funded (Banu, 2011).

2.3.2. Antihypertensive properties

Primary hypertension is a common problem that occurs worldwide. It results from a cardiovascular physiological response, elevating blood pressure due to factors that regulate renin-angiotensin system and autonomic nervous system (Setters and Holmes, 2017). The antihypertensive properties of CH are manifested by its inhibitory effects on the activity of angiotensin I-converting enzyme (ACE). ACE, as an important contributor to the performance of the renin-angiotensin system, can convert the inactive angiotensin I peptide to its active form, angiotensin II. Angiotensin II subsequently causes an increase in blood pressure through vasoconstrictor effects, and through increased sodium and fluid reabsorption to boost the blood circulation volume. ACE inhibitors such as captopril and ramipril, therefore, have been clinically used to treat hypertension (Perazella et al., 2003). CH from various sources including porcine, bovine, pacific cod, shark, squid, etc., are found to suppress ACE-activity, and some contributing peptides have been identified. O'Keeffe et al. (2017) used a microorganism-originated prolyl endoproteinase to generate gelatin hydrolysates which significantly reduced the systolic, diastolic and arterial blood pressure, and heart rate of spontaneously hypertensive rats (SHR) compared to saline treated subjects. This antihypertensive activity was proposed to be accounted for by some Gly-Pro- containing small peptides among which the ACE-inhibitory potency ranked as follows: tripeptides > tetrapeptides > Gly-Pro dipeptide. Met-Gly-Pro was identified as the most effective. A study from Herregods et al. (2011) suggested that a low MW of CH favors the antihypertensive property, since high MW hydrolysates could not attenuate blood pressure of SHR until being

hydrolyzed by thermolysin which then induced a shift to lower molecular mass. It was also confirmed by *in vitro* assays that indicated greater ACE inhibitory activity of simulated GI digested or ultrafiltrated (3 kDa) CH. Several small peptides were identified, including the Gly-Pro containing ones (i.e. Ala-Gly-Pro and Val-Gly-Pro), and a potential collagen specific Hyp-containing dipeptide Hyp-Tyr. A similar implication was indicated by Lin et al. (2012) who found the *in vitro* ACE suppression was inversely proportional to the MW of the squid skin gelatin hydrolysates fractions (Figure 2.7). Other studies, however, identified some larger ACE inhibitory peptides, such as LGPLGHQ, MVGSAPGVL, GRGSVPAHypGP, GASSGMPG, etc. (Ngo et al., 2015; Alemán et al., 2013; Ngo et al., 2016), which probably cannot survive the human body GI digestion, and thus will be further cleaved into small di- and tripeptides. Whether or not these GI digestion -generated small peptides maintain their antihypertensive properties remain to be investigated. Unfortunately, very few of those identified ACE-inhibitory peptides (no matter small or big) from prepared CH contain typical abundant and bioavailable collagen sequences, such as Pro-Hyp, Gly-Pro-Hyp, and Hyp-Gly, or even contain Hyp, the signature amino acid of collagen. Therefore, we should be skeptical about the contributing effect and the origin of those non-typical peptides and verify whether they are derived from collagen or from contamination proteins. If from collagen, then are the amounts large enough to show any significant contribution to overall ACE inhibition of corresponding CH mixtures?
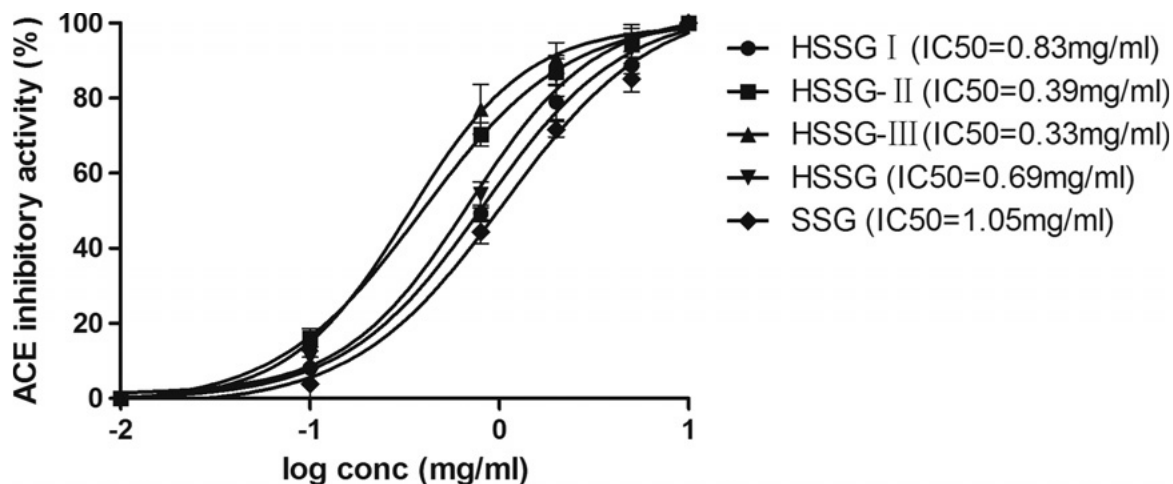
Figure 2.7. ACE inhibitory activity and molecular weight of gelatin hydrolysates: does-response curves of fractions after ultrafiltration. HSSG-I, -II, and -III represents fractions of squid skin gelatin hydrolysates with molecular weight range 6~10 kDa, 2~6 kDa, and <2 kDa, respectively Reprinted from Lin et al. (2012), Copyright (2012), with the permission from Elsevier.
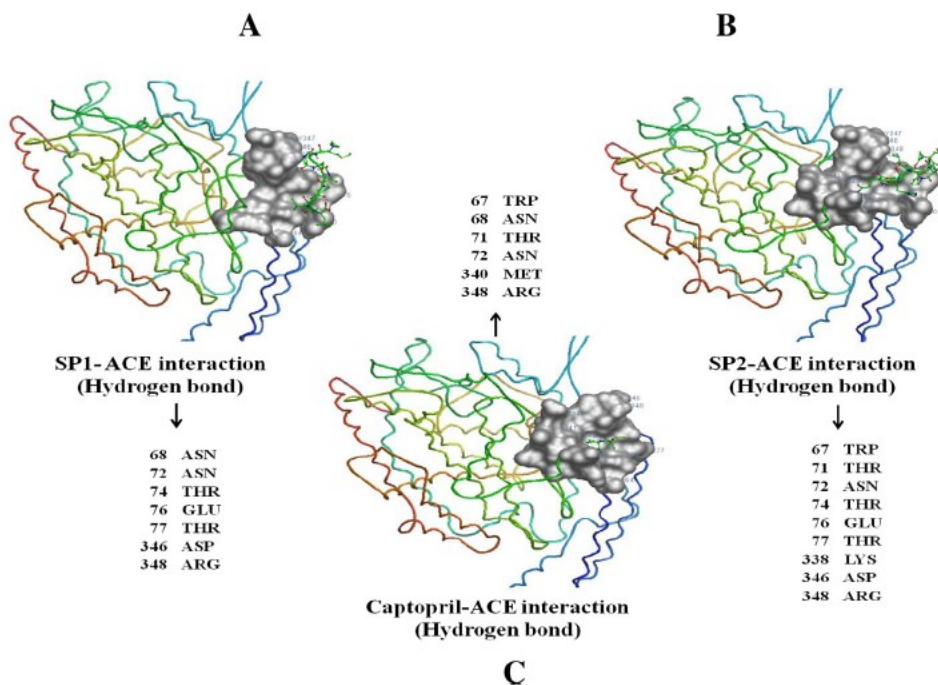
Figure 2.8. Docking images of the interacting of the purified peptides. SP1: MVGSAPGVL (A), SP2: LGPLGHQ (B), and captopril (C) with angiotensin I-converting enzyme (ACE). Reprinted from Ngo et al. (2015), Copyright (2015), with permission from Elsevier.

To identify the molecular mechanism of the ACE inhibitory effects, recent studies conducted computational docking simulations of some identified collagen peptides. It revealed a common docking site for GASSGMPG, LAYA and the ACE inhibitor captopril at the Asn72 residue of ACE. Hydrogen bonds, polar and hydrophobic interactions are involved in the peptides-ACE binding (Ngo et al., 2016). This docking site is also recognized by the other two identified collagen peptides (Figure 2.8, Ngo et al., 2015). Docking sites of peptides from other proteins vary significantly (Ko et al., 2017). Real X-ray crystallography may be needed to confirm the ACE domain selectivity of different collagen peptides and clarify their potential similarity. Ngo et al. (2015) monitored expression level changes of several hypertension-related genes, and proposed that the mechanism of the antihypertension property of skate gelatin hydrolysates involves the inhibition of PKC/ERK pathway, the stimulation of PPAR-γ signaling pathway, and the inhibition of pro-inflammatory cytokines secretion. To date, no human clinical trials have validated the therapeutic effects of CH on hypertension.

2.3.3. Effects on muscle repair

It is a relatively new concept that CH can benefit muscle repair and recovery. The connective tissue within skeletal muscle, especially the collagen enriched ECM, provides structural support, and influences muscle force transmission, maintenance, and repair. Various types of collagen are expressed in muscle ECM, including the fibrillar collagen like type I and III, fibril-associated collagen like type XII and XIV, and basement membrane collagen such as type IV and VI. By decoration on type I collagen fibrils, type XII collagen increases the elasticity of collagen fibrils to absorb the shear stress from mechanical loading and to protect muscle integrity (Chiquet et al., 2014). Meanwhile, type XII and XIV are related to muscle fiber and muscle fat metabolisms (Listrat et al., 2016). Type VI collagen deficiency can result in related muscular

dystrophy (Noguchi et al., 2017; Tagliavini et al., 2014). The primary type I and III collagen are found in endo-, peri, and epimysium (Gillies and Leiber, 2011). Since collagen is the major component in ECM, it not only serves as scaffold to muscle fibers (Figure 2.9), but also interacts with muscle myoblasts during the development and maturation of muscle fibers. This interaction through the binding molecules, laminin and fibronectin, further influences the differentiation of myoblasts, and orientation and arrangement of muscle fibers (Kjaer, 2004; Lawson and Purslow, 2000; Chaturvedi et al., 2015). Physical training and activity accelerate collagen turnover in muscle ECM, and to some extent also increase the net production of collagen; thus, altering the mechanical properties of muscle and making it more load resistant (Kjaer, 2004). A recent double-blind placebo controlled clinical trial revealed that supplementation with collagen peptides (mean MW around 3 kDa) increased muscle strength of elderly men with sarcopenia (degenerative loss of muscle mass) (Zdzieblik et al., 2015). Accompanied with guided exercise resistance training, the subjects were randomly treated with either collagen peptides (26 men) or silica (27 men). After 12-weeks of intervention, muscle strength and sensory motor control increased significantly in both groups refer to the baseline of elderly men before treatment, indicating the effectiveness of exercise. Moreover, oral administration of collagen peptides further significantly improved muscle strength compared to the silica placebo group. The combination effects can be explained by the stimulatory effect of resistance training on muscle protein synthesis (Evas, 2004), which is enhanced by post-exercise protein supplementation (Paddon-Jones et al., 2008; Beelen et al., 2008). This theory is confirmed with other protein sources, such as soy protein (Deibert et al., 2011). The muscle recovery effects of collagen peptides supplementation have not been proven until recently by Zdzieblik et al. (2015). Other studies found a simultaneous stimulation of mechanical loading from exercise on muscle protein and collagen synthesis with similar time course increase, however

whether sharing common signaling pathways are debatable (Miller et al., 2005; Cuthbertson et al., 2006). Other factors, such as the short post-exercise interval (peptides taken within 60 min after the training), and the low MW of ingested collagen peptides (greater bioavailability) may have specific influence. However, research to elucidate any collagen specific mechanisms is very limited. When investigating skin health promoting effects of CH, Shimizu et al. (2015) unexpectedly found that the two typical collagen peptides, Pro-Hyp and Hyp-Gly, up-regulated the expression of some muscle-related genes encoding myofibril, contractile fiber, and sarcomere. Considering the abundance of Pro-Hyp and Hyp-Gly in collagen molecule and their high presence in plasma after oral ingestion, these findings may imply the underlying mechanisms of the muscle recovery property of collagen peptides. Further researches are needed to verify this intriguing property on other populations (e.g. younger exercisers), and to determine a suitable dosage, and the mechanism of action.
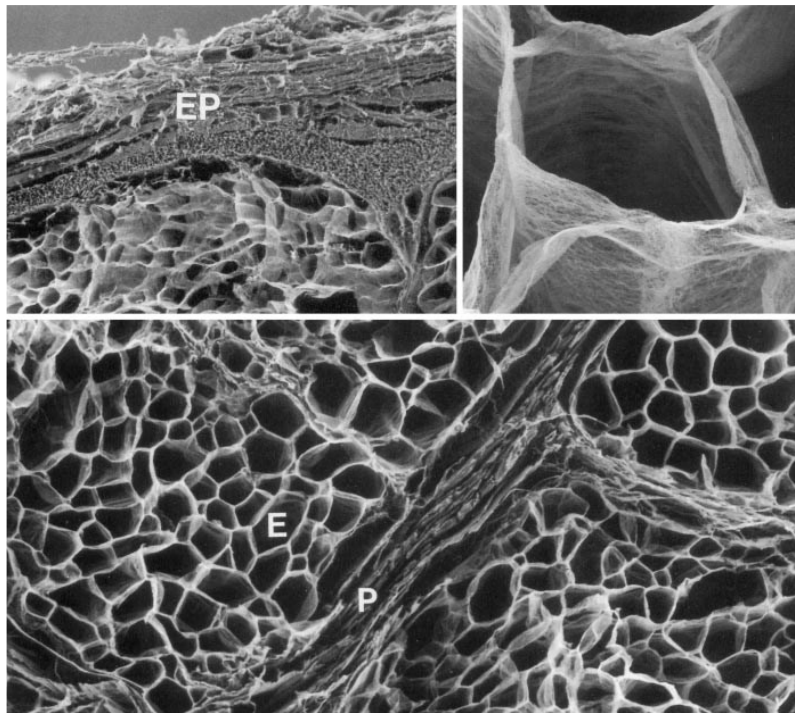
Figure 2.9. Structure of intramuscular connective tissue, image captured by scanning electron microscope from bovine skeletal muscle. EP: epimysium; P: perimysium; E: endomysium (Kjaer, 2004). Copyright ©2004, Karger Publishers, Basel, Switzerland.

Except oral supplementation of CH, intact collagen could also be used in clinical surgery to treat muscle tearing. In a follow-up of 24 months, the securement of collagen in the surgery significantly reduced the pain level of muscle tearing and the proportion of patients with severe limp, while it increased the gluteus muscle force of these patients. Similarly, Rao et al. (2012) used the human acellular dermal matrix that is rich in collagen in the transosseous surgery to augment gluteus muscles, and to a similar extent alleviate the symptoms of hip tearing after about 22 months. However, detailed mechanisms of this newly developed technique are still unknown. The role of collagen in improving the performance of surgery in repairing muscle complexes remains to be established.

2.3.4. Other properties

In addition to all the above-mentioned health benefits, CH is claimed to also show anticholesteremic activity, dipeptidyl-peptidase IV (DPP-IV) inhibition activity, and antioxidant activity, amongst others. An *in vivo* study by Zhang et al. (2010) revealed that chicken CH containing (10%) diet for mice reduced the total plasma and hepatic cholesterol, and the hepatic triacylglycerides concentration. Apart from the lipid- and cholesterol-lowering activity, the preventive effect on atherogenesis resulted from suppression of proinflammatory cytokines expression, since inflammation is part of atherosclerosis etiology. This effect may also be closely related to the ACE-inhibitory activity of CH (Stoll and Bendszus, 2006). Moreover, CH generated from turkey heads were reported to bind with cholic acids and deoxycholic acids (Khiari et al., 2014), both of which are dominant products of cholesterol catabolism. Binding of bile acids retards

intestinal reabsorption which facilitates their excretion, thus reducing plasma cholesterol concentration via stimulating cholesterol catabolism (Fukuda et al., 2013; Iwami et al., 1986). Type 2 diabetes mellitus is the most common type of chronic hyperglycemia and is characterized by enhanced hepatic glucose content but a reduced peripheral glucose uptake due to insulin deficiency or dysfunction (Upadhyay et al., 2018). The antidiabetic effects of CH are mainly reflected by its DPP-IV inhibitory activity. Generally, DPP-IV inhibitors decrease the degradation of incretin hormones, the substrates of DPP-IV, which can stimulate insulin secretion (Gupta et al., 2016). The antihyperglycaemic potential of CH from various sources has been confirmed *in vitro* and *in vivo*. Skin gelatin hydrolysates from both warm-water fish (tilapia) and cold-water fish (halibut) were reported to improve the glycaemic control of diabetic rats after 30 days of diet supplementation. Meanwhile the *in vitro* DPP-IV inhibitory activity of these fish gelatin hydrolysates was observed (Wang et al., 2015). DPP-IV inhibition of CH from other sources, such as deer skin, salmon skin, porcine skin, etc. has also been described in previous research works. The isolated and identified peptide sequences includes Gly-Pro-Val-Ala, Pro-Pro, Gly-Phe, GPVGHypAGPPGK, etc., some of which are multifunctional having both ACE and DPP-IV inhibitory activities (Huang et al., 2014; Neves et al., 2017; Jin et al., 2015). In addition, the antioxidant activity of CH has been extensively studied with respect to its free radical scavenging and metal ion chelating capacities (Liu et al., 2015). All these health benefits induced by CH and collagen-derived peptides confer their potential of being functional food ingredients and nutraceuticals.

2.4. Beauty from within: collagen products as nutricosmetics?

2.4.1. Skin ECM and fibroblasts

Skin, the largest organ of human body, serves as mechanical and chemical barrier to protect our internal organisms from environmental impacts, as well as maintain both body temperature and osmotic pressure. The skin produces melanin pigment to protect it from further UV damage. More advanced barrier functions of skin lie in its being a biological shield against microorganisms like fungi, bacteria, and viruses. This anti-infection function is firstly conducted by stratum corneum, the outermost layer, which is composed of densely arranged dead keratinocytes. Secondly, other components of the integument-related innate immune system would respond to produce anti-infectious agents by various immune cells located in skin, such as conventional T cells, NK-T cells, and Langerhans cells. Being an anatomical interface, skin is also an important sensory organ which is innervated with nerves and receptors to communicate with various internal organs to trigger specific biological responses. Therefore, skin is appreciated to have an integral role to modulate the homeostasis of the entire body through interconnections with the endocrine, immune and nervous system (Chuong et al., 2002).

Fibroblasts are the most representative resident cells found in skin especially the dermis layer to confer its biological functions and physical appearance. Generally, they are responsible for the homeostasis and maintenance of skin ECM in its normal condition as well as in activated/pathological conditions such as wound healing, fibrosis and skin cancer. Heterogenicity of skin fibroblasts occurs among different parts of body with respect to their embryonic origins. For example, fibroblasts in facial skin are differentiated from the neural crest while those in skin of back are from the dermatomyotome. On the other hand, even at a specific tissue like dermis, the fibroblasts from the same origin are diversely differentiated with distinct morphologies and functions depending on the anatomical locations. Dermal fibroblasts are primarily differentiated into two phenotypes, the papillary fibroblasts and reticular fibroblasts. The former lies in the

immediate thin layer underneath epidermis, while the later one in the middle dermis layer (Figure 2.10; Driskell and Watt, 2015). Except the morphological differences, these fibroblasts also vary physiologically, and differ in the ability to control ECM pattern which may in return alter the behaviour of corresponding resident cells. The differences are shown in the ECM of papillary dermis and reticular dermis, which display relatively randomly packed collagen fibers and well-oriented collagen fibers, respectively (Sorrell and Caplan, 2004). The ability to synthesize ECM macromolecules is also differentiable. Cultured papillary dermal fibroblasts can produce more decorin and type I collagen, but less versican compared to reticular fibroblasts (Schönherr et al., 1993; Tajima et al., 1981). Other differences lie in the secretion of growth factors such as keratinocyte growth factor, and cytokines such as interleukin-6 (Sorrell et al., 2004). Moreover, cell sub-populations associated with the hair follicles are dermal sheath fibroblasts and dermal papilla fibroblasts (Sriram et al., 2015; Driskell and Watt, 2015). In contrast, these subsets of dermal fibroblasts function as regulators for hair growth and hair cycle (Schneider et al., 2009).
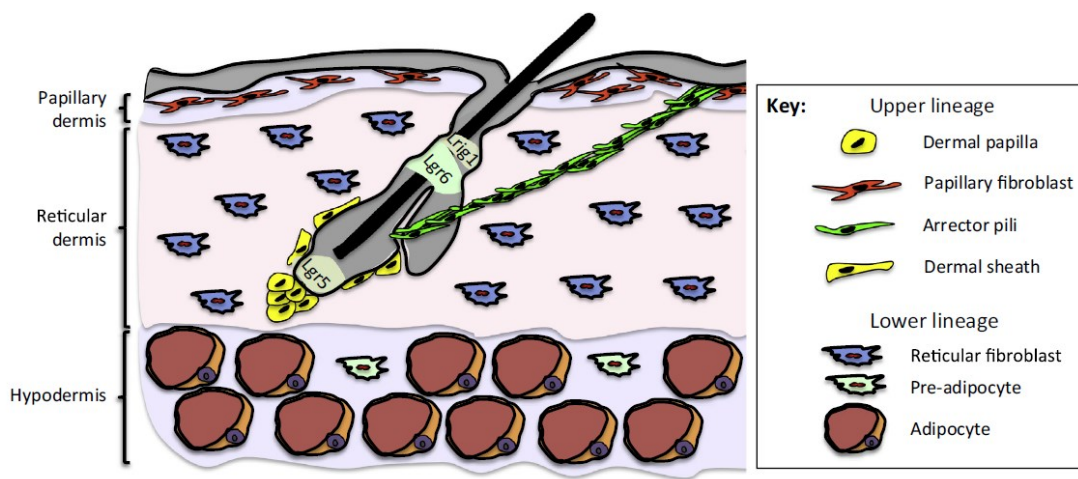
Figure 2.10. Heterogenicity of fibroblasts in skin dermis. Three layers of skin are indicated, the epidermis (thin grey layer on the top), dermis (including papillary and reticular dermis), and hypodermis (adipose tissue). Reprinted from Driskell and Watt (2015), Copyright (2015), with permission from Elsevier.
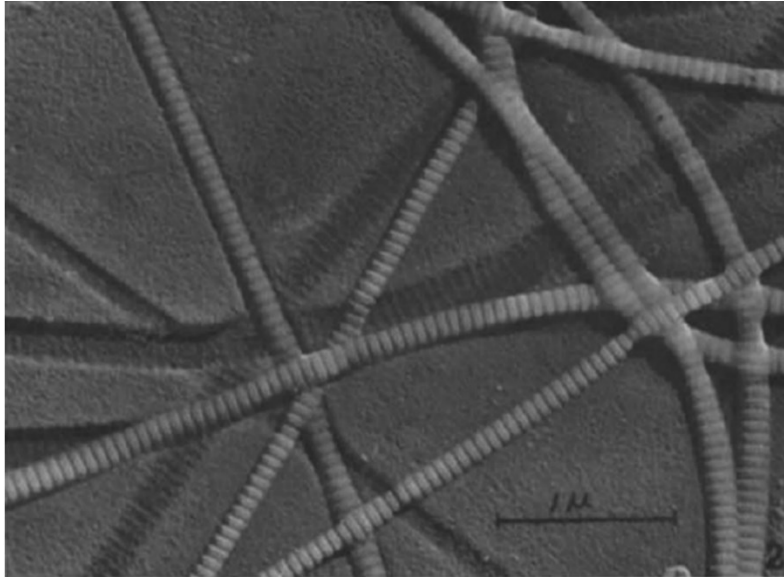
Figure 2.11. Typical collagen fiber network in human skin. (©Gross and Schmitt. Originally published in J. Exp. Med. 1948, 88(5), 555-568).

Dermal ECM is a complex network occupied with macromolecules including fibrillar proteins, proteoglycans, glycosaminoglycans (GAG), growth factors, cytokines, etc., all of which are primarily synthesized by fibroblasts (Stern et al., 2008). Fibrillar proteins in skin are mainly collagen with minor amount of elastin, which provides the strength and elasticity of ECM, respectively (Huertas et al., 2016). Unlike the highly paralleled collagen fibers bundles in tendon, those in the dermis are intertwined to generate a scaffold to exert their biomechanical properties and avoid severe stress and stretch damage (Gibson et al., 1965). Figure 2.11 shows a typical collagen fiber orientation in human skin obtained by transmission electron microscopy (Gross and Schmitt, 1948). Collagen is the most abundant component in ECM of skin, with mainly type I (85-90%) and III (10-15%), and minor proportion of type IV and VII (Tobin, 2017). Proteoglycans (e.g. versican, decorin) and GAG (e.g. hyaluronan, dermatan sulfate) are present in the ground substance surrounding fibrils and cells. Proteoglycans, as the name implies, are products of core proteins covalently linked with GAG, which are highly negatively charged polysaccharides

composed of repeating disaccharide units. GAG, especially hyaluronic acid (HA), together with proteoglycans (having GAG in the molecule), confer the hydrodynamic characteristics of ECM due to the large water-binding capacity of GAG, which exhibit desirable hydrophilicity. This helps to maintain the ECM space and provide compressive resistance. A higher order of the ECM structure is reinforced by the interaction among collagen fibrils, proteoglycans, GAG and other component molecules through connector proteins (e.g. laminin, fibronectin) (Timpl and Brown, 1994; Singh et al., 2010), which in turn guides cellular behaviors.

2.4.2. Skin aging
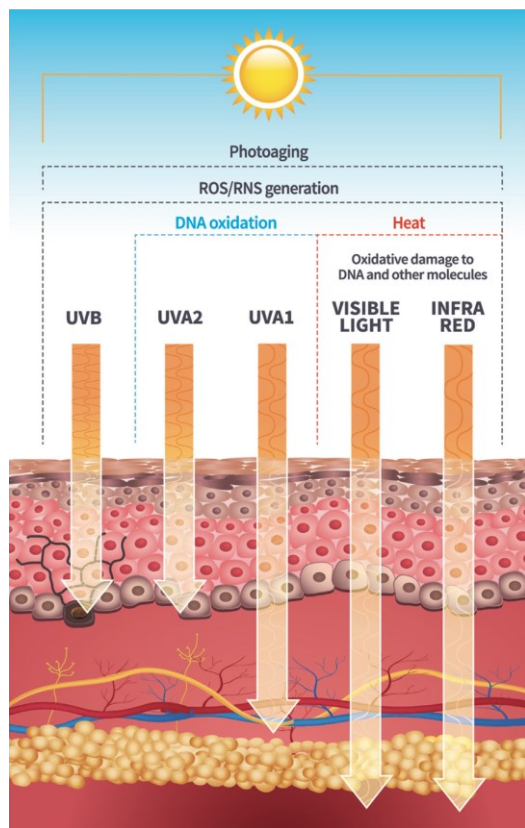
Figure 2.12. Sunlight with longer wavelengths, lower energy, reaches deeper layers of skin. Overlapping effects may be observed ROS: reactive oxygen species, RNS: reactive nitrogen species. (Krutmann et al., 2017). (open access:

https://doi.org/10.1016/j.jdermsci.2016.09.015, with CC BY NC ND license)

Skin aging is a complex and progressive biological process leading to decreased elasticity and hydration of skin with the appearance of wrinkles, drier and rougher skin surface, and impaired regeneration and wound healing capacity. It is initiated from chronic intrinsic changes while accelerated and exacerbated by extrinsic factors and interactions between them. It is summarized to be the result of skin aging "exposome" which includes the totality of those factors and corresponding body responses that trigger biological and clinical signs of skin

aging (Krutmann et al., 2017). Intrinsic aging is mainly derived from gradually decline of fibroblasts and their ability to regenerate. Extrinsic factors represent a wide range of factors, including sun exposure, air pollution, diet, smoking, etc. Solar radiation is probably the most well studied external risk of skin aging, the effect of which is also called photoaging. Sunlight with different wavelengths has specific (and overlapping) photoaging effects as they can reach different layers of skin depending on the energy values (Figure 2.12) (Dupont et al., 2013; Krutmann et al., 2017). Yet they share the common property of activating the generation of harmful reactive oxygen (ROS) and nitrogen species (RNS) as absorbed by skin chromophores such as melanin. Although only consisting around 5% of total sunlight, ultraviolet (UV) radiation causes huge impact on skin, of which UVA (315-400 nm) and UVB (280-315 nm) contribute the most effects. UVB mainly causes sunburn and abnormal generation of DNA dimer, triggering cell mutations and further inducing risk of skin cancer (Svobodová et al., 2012). Except the oxidative damage and cancer risk, UVA has extra tanning effect comparing to UVB, while its protective action against future sun exposure is arguable since the melanin synthesis may not be stimulated (Miyamura et al., 2011). The impacts of visible and infrared light on skin aging have been underestimated for a long time. Besides the known heat sensation induced by infrared, only until recently visible and infrared light were revealed to be closely linked to the production of matrix metalloproteinase (MMP), such as MMP1 and MMP9, and thus accelerate the degradation of collagen (Yoon et al., 2012; Schroeder et al., 2008; Liebel et al., 2012). It is interesting to note that part of the up-regulation on expression of MMP1 is solely attributed to sun exposure-induced heat when sunlight is blocked (Cho et al., 2008). In addition, traffic-related air pollution exacerbates aging skin appearance mainly because of incorporated chemicals (e.g. NO2, ozone) bringing about the formation of wrinkles and pigment spots (Hüls et al., 2016; Hüls et al., 2015). Skin aging may also correlate

with our lifestyle, for example, years of smoking, chronic emotional stress and deprivation of sleep, and improper selection and use of cosmetics. For a detailed review of this respect one can refer to Krutmann et al. (2017).

The undesirable appearance and atrophy of skin during aging is essentially the overall reflection of numerous changes underneath, including in skin resident cells, the ECM structure and composition, the interaction among different layers of skin, and even the biological response to aging of other internal organs. From an endogenous point of view, like the aging of other organs, skin aging can be partially explained by the emerging and accumulation of senescent cells. The cell senescence occurs in the dominant fibroblasts, as well as in other key supporting cells like keratinocytes (epidermal cells), melanocytes (melanin secretion), sebocytes (sebum secretion) and skin stem cells, which exhaust their proliferation capacities and reduce the synthetic abilities (Toutfaire et al., 2017). Other senescent-induced changes such as decreased DNA repair ability and shortening of telomeres are inevitable (Makrantonaki and Zouboulis, 2007). To look at skin aging at the molecular level, changes in ECM components are the main culprit. As skin ages, the homeostasis of collagen leans to the degradation side because of reduced biosynthesis and increased deterioration of collagen. Matrix metalloproteinases (MMP) such as MMP1 are up-regulated to facilitate fragmentation of dermal collagen through the activation of ROS during both intrinsic mechanisms and photoaging (Fligiel et al., 2003; Rittie and Fisher, 2002). As mentioned before, the cross-link level of collagen increases as skin ages, which results in increased density of collagen bundles but with less elasticity and being less ordered. In addition, glycation cross-links of collagen with sugars such as glucose and fructose make it incapable of easy repair (Danby, 2010) and susceptible to mechanical stimuli due to inferior flexibility (Avery and Bailey, 2006). This structural modification of collagen suppresses its being degraded by MMP, and thus impairs

its functional turnover (Panwar et al., 2017). What makes the scenario worse is the formation of advanced glycation end products (AGE) which can be recognized by AGE-receptor on the surface of skin fibroblasts to impair their proliferation but also accelerate apoptosis (Alikhani et al., 2005). Chronic exposure to UV radiation should boost this case by stimulating AGE formation (Farrar, 2016). Obviously, glycation also occurs to other extracellular proteins, such as elastin and fibronectin as well as some intracellular proteins, further leading to skin dysfunction (Gkogkolou and Böhm, 2012). Changes to another most abundant ECM component, HA, have been reported as well, despite some contradictory results. More recent studies suggest that total content of HA does not change in the dermis but decreases in the epidermis (Oh et al., 2011). A higher level of interaction of HA with tissue structure and proteins is assumed in aged skin, which explains its lower extractability, less exposure of HA molecule, and a diminished water binding capacity (Meyer and Stern, 1994; Stern and Maibach, 2008). In addition to changes in the ECM, a notable flattening and protein diminution of dermal-epidermal junction is observed. This is the joint between the epidermal and dermal compartments, its structural change and protein reduction may impair the integrity of skin or skin's resistance to shear forces, and promote the formation of wrinkles (Langton et al., 2016; Grove, 1989; Sudel et al., 2005). Overall, the skin aging is a multifactorial process; many internal changes can trigger a series of biological responses, which accumulate and result in skin damage, and finally are manifested in its undesirable appearance and dysfunction.

2.4.3. Physiological function on improving skin conditions: CH as nutricosmetics?

The new term "nutricosmetics" is derived from terms of "nutraceuticals" and "cosmetics" to emphasize the dual function of these products. Nutricosmetics, therefore, refer to orally ingestible products that can both enhance skin health and provide beauty benefits (Tabor and Blair,

2009; Machado et al., 2017). Nowadays, natural ingredients that have claimed to be nutricosmetics in the market or used in dermatology are mainly antioxidants such as beta-carotene, isoflavone soy beans, vitamin C, etc. Other ingredients that are proposed to maintain skin hydration, are, for example, rice ceramides and tocotrienols. Collagen hydrolysates (CH) have been used in food supplements and pharmaceuticals for a long time given their beneficial effects to improve skin health and appearance. In this regard, many clinical studies have been performed to clarify the efficacy of CH, as well as some CH containing food products on skin. One representative study by Prosksch et al. (2014) who applied specific porcine CH (mean MW~2 kDa) from GELITA to women between 35-55 years old for 8 weeks showed that CH induced an improvement on skin elasticity, an effect that started to appear after 4 weeks of ingestion with a dosage of 2.5g/day or 5.0g/day. Other parameters such as skin moisture and skin evaporation did not differ between the CH group and placebo group, while an improvement was still observed in the subgroup of women over 50 years old. The long-lasting efficacy of CH was observed, since the significance continued till even after 4-weeks following the last intake, especially for elderly subjects (>50). The race and complexion of subjects in this study, however, were not specified. In another study, a longer treatment (12 weeks) of a specific tripeptide enriched (15%) CH on Korean volunteers (30-48 years old) was conducted. Besides elasticity, the increase in skin hydration and decline in transepidermal water loss were observed compared to placebo cohort at a dosage of 3 g/day (Choi et al., 2014). The difference in results may come from variance in subjects, length of treatment, and CH ingested. Similarly, the improvement in skin hydration was confirmed within a Japanese cohort (Asserin et al., 2015), where a greater dosage at 10 g/day was used. Moreover, in the same article, Asserin et al. (2015) also reported another study conducted in France with Caucasian women (40-65 years old). With a much larger sample size (106 subjects), this study parallels the

previous *in vivo* results (Matsuda et al., 2006). It found that dermal collagen density was significantly enhanced from 4 weeks consumption of a specific fish CH in the form of a powdered drink. The fragmentation of collagen fibers, quantified from confocal images, was attenuated upon the ingestion of CH for 4 weeks. Both effects were accumulated, and became more pronounced as the treatment was prolonged to 12 weeks. The anti-aging effects of CH on skin as fortified in other food and beverage product, for example, BioCell Collagen®, Pure Gold Collagen and other similar products, were also reported somewhere else (Schwartz and Park, 2012; Borumand and Sibilla, 2014; Borumand and Sibilla, 2015).

Oral administration of CH also protects the skin against UV radiation induced damage in animal models. Since UVA has long time been regarded as inoffensive (Dupont et al., 2013), earlier studies mainly focused on attenuating skin injury from UVB radiation. Tanaka et al. (2009) used CH (0.2 g/kg/day) from fish scales (*Tilapia Zillii*, freshwater fish) to feed UVB exposed (repeatedly) hairless mice for 6 weeks. Daily ingestion of CH ameliorated UVB-induced hydration loss after 3 weeks and continued to increase mice skin hydration to be greater than that of mice which were not exposed to UVB. The thickening of epidermis caused by UVB radiation was also suppressed at the end of study. Similar effects were observed with the ingestion of CH from scales of marine fish (Fujii et al., 2013). Overall, oral ingestion of CH from various sources with specific dosage and frequencies can ameliorate the skin aging signs caused by the chronically accumulated damage from both intrinsic and/or extrinsic factors. The efficacy of CH should not be compromised by the race of subjects (e.g. Asian or Caucasian), or by the taken form (e.g. CH itself accompanied with a regular diet, or fortified within food products), which qualifies the candidacy of CH being developed as nutricosmetics or food supplements.

2.4.4 Potential mechanisms of the effects on skin

The supplementation of CH and other collagen-derived products, which share similar composition with endogenous collagen, may provide the building blocks for the biosynthesis of skin collagen. As mentioned in previous sections, ingested CH (radiolabeled) can reach the plasma circulation, accumulate in skin, and even stay there for 14 days (Watanabe-Kamiyama et al., 2010). Upon hydrolysis of the skin tissue, the corresponding autoradiograph shown on thin layer chromatography indicated the presence of CH-derived Pro and Hyp. This implies that ECM components could be used for the anabolism of skin ECM. Gradual collagen deterioration inevitably accompanies skin aging. Indeed, the stimulatory effects of CH on collagen production and their suppression on degradation enzymes likely contribute to its anti-aging benefits through restoring collagen homeostasis and maintaining skin biomechanical properties. Earlier studies that tested on pigs with the oral ingestion of porcine CH-containing diet (Matsuda et al., 2006) found that CH facilitated the collagenesis as implied from the enhanced diameter and density of collagen fibrils in pig skin. This was also illustrated by the findings from another *in vivo* study which revealed an increased accumulation of collagen types I and IV, and decreased activity of MMP2 in rat skin after 4 weeks of CH intake (Zague et al., 2011). MMP2 is a multifunctional matrix degradation enzyme that can digest collagen types I and III, both of which are dominant collagen that support the skin ECM structure. It cleaves the basement membrane type IV collagen that partially regulates the formation of wrinkles (Contet-Audonneau et al., 1999), and elastin that complements the elasticity of collagen fibers (Doren, 2015). Similar effects were found in some *in vitro* studies, CH treatment can stimulate the dermal fibroblast expression of COL1A1 (encodes type I collagen biosynthesis) but suppress that of MMP1 (collagenase) (Tokudome et al., 2012). In skin damaged by UV radiation, the destruction of collagen can be alleviated by CH ingestion (Tanaka et al., 2009; Sun et al., 2013) which also retards the abnormal up-regulation of MMP1

(interstitial collagenase) and MMP9 (gelatinase) transcription (Chen and Hou, 2016). The action

of CH against aging likely also work through the alternation of GAG production. In the case of

photoaging, CH ingestion may calm irate skin by suppressing the potential immediate elevation of

total GAG (Sun et al., 2013). However, in cultured normal dermal fibroblasts, the collagen-derived

Pro-Hyp was found to stimulate the production of HA in both polysaccharide level and mRNA

level (Ohara et al., 2010b), suggesting that action of CH and collagen-derived peptides maybe

dependent on the status of skin cells. CH administration may not alter the ratio of HA to dermatan

sulfate (Matsuda et al., 2006), while physiological responses regarding the HA secretion in normal

aged skin are still unknown. As for the proteoglycans, supplementation of CH can stimulate their

expression by cultured fibroblasts (Proksch et al., 2014); yet *in vivo* the information in this respect

is very limited.

Besides the alterations in matrix molecules, the beneficial effects of CH and collagen-

derived peptides in skin are inseparable from their contribution toward positive cellular responses.

Ohara et al. (2010b) tested a series of previously identified bioavailable collagen-derived peptides

on human dermal fibroblasts culture. Only three of them, Pro-Hyp, Ala-Hyp, and Ala-Hyp-Gly,

were found to be growth stimuli for fibroblasts at the dosage of 200 nmol/ml. Among those

peptides, Pro-Hyp was the most effective and increased the cell proliferation to 1.5-fold compared

to the non-treated control. The efficacy of Pro-Hyp was also reported by Haratake et al. (2015).

Later, Hyp-Gly was identified, and it enhanced the proliferation of mouse primary fibroblasts more

than Pro-Hyp (Shigemura et al., 2011). These results suggest that CH and other collagen products

could counteract the aging-induced reduction of the abundance of fibroblasts and skin thickness

by improving the cell proliferative capacity. The action of liberated small peptide stimuli upon

body digestion would accelerate the accumulation of matrix components. However, as biological

messengers, the cell signaling pathways and cell surface receptors involved to stimulate the growth of fibroblasts are still obscure. Moreover, as more collagen peptides have been identified in plasma and skin as described recently (Yazaki et al., 2017), more stimulus peptide may be discovered, and many synergistic effects among them are also possible. The antiphotoaging effects of CH are likely due to their antioxidant activity that attenuates the oxidative stress generated from UV radiation-induced ROS. CH ingestion can help to recover the cellular antioxidant defense system by preventing pathological damage of some enzymatic scavengers such as superoxide dismutase, catalase and glutathione peroxidase (Sun et al., 2013; Hou et al., 2009). CH alleviates the decrease of type I collagen in photoaged skin by stimulating the expression of receptor for transforming growth factor-beta 1 that favours the biosynthesis of collagen (Chen and Hou, 2016). In summary, the amelioration of skin aging by CH and collagen-derived products involves the alteration in both ECM and cellular responses, the mechanisms of which may be different for the chronic aged normal skin versus photo-aged pathological skin.

CHAPTER 3.

Transepithelial transport efficiency of bovine collagen hydrolysates in a human Caco-2 cell model

Abstract

Collagen was extracted from raw bovine hide and hydrolyzed by one of three enzymes - Alcalase, Flavourzyme, or trypsin - or by using a combination of two or three of these enzymes. The Alcalase-containing enzymatic hydrolysis treatments generated a greater proportion of hydrolysates with molecular weight (MW) < 2kDa (79.8% to 82.7%). Flavourzyme-containing hydrolysis treatments exhibited the greatest proportion of free amino acids (686 nmols/mg to 740 nmols/mg). The hydrolysates were then subjected to a simulated gastrointestinal (GI) digestion, and transport studies were conducted using a Caco-2 cell model. Due to the lower MW, the hydrolyzed collagen showed greater resistance to GI digestion and greater transport efficiency than the unhydrolyzed collagen control. Hydrolysates from a dual enzyme mixture - the Alcalase/Flavourzyme combination - generated the greatest transport efficiency across Caco-2 cell monolayers (21.4%), two-fold more than that of the collagen control.

3.1. Introduction

As a by-product of the meat industry, bovine hide is the major source of collagen for gelatin production. Collagen is made up of three helical polypeptide chains with non-helical telopeptide zones at the end. With biological aging, collagen covalently forms intra- or intermolecular crosslinks creating a more stable and insoluble molecule (Johnston-Banks, 1990). Native insoluble collagen cannot be hydrolyzed by most enzymes, except some specific collagenases from bacteria. However, a long treatment with alkali can breakdown the crosslinks to make bovine collagen soluble in acidic media, as well as to allow it to be then purified by removing non-collagenous proteins and other components. As the collagen crosslinks breakdown however, the telopeptide region can then be attacked by some common enzymes such as pepsin, chymotrypsin, and pronase, thus facilitating further removal of intra- and intermolecular crosslinks. This then makes the collagen further accessible by many other enzymes to produce collagen hydrolysates (CH) (Ballian & Bowes, 1977).

CH are widely used in food industry due to their excellent functional properties, such as the good solubility and emulsifying capacity. Also, collagen-derived peptides possess beneficial bioactive properties, such as anti-aging, antioxidative, and antihypertensive activities (Alemán & Martínez-Alvarez, 2013). Interestingly, some collagen peptides, such as Pro-Hyp and Hyp-Gly, are able to stimulate the growth of fibroblasts and the regeneration of collagen, improving both the hydration and elasticity of skin (Shigemura et al., 2009 & 2011; Sibilla et al., 2015). In addition, CH can benefit the health of bones and joints, by improving the bone collagen metabolism and mineral density, and by inhibiting the loss of chondrocytes and the decreasing of articular cartilage volume, respectively (Wu et al., 2004; Nakatani et al., 2009). Further studies by Kimira et al. (2014) and Nakatani et al. (2009) confirmed that Pro-Hyp can promote the differentiation of osteoblastic

cells and chondrocytes. These many health benefits explain why CH have become increasingly popular ingredients among food, pharmaceutical, and cosmetics industries.

Orally ingested collagen undergoes degradation by gastric and pancreatic proteases into small peptides and free amino acids, which are then absorbed and transported by the intestine mainly in the form of free amino acids and di- and tripeptides (Ganopathy et al., 2006). However, in the digestive system collagen can only be degraded to a certain degree, with some high MW fragments remaining, leading to poor absorption (Moskowitz, 2000). By contrast, to improve the bioavailability of collagen, pre-digestion with specific enzymes can help to release bioactive peptides, as well as to expose more accessible cleavage sites. This translates to an improved gastrointestinal (GI) digestion and the creation of an even lower MW including more free amino acids, di- and tripeptides. Most commercial CH are relatively large and have an inconsistent MW range, from 2,000 to 20,000 Da (Schrieber & Gareis, 2007). Therefore, a better approach is needed to produce bovine CH with lower MW (< 2,000 Da) and thus more bioavailable, since these would then be more commercially marketable. Kim et al. (2001a) prepared low MW (<1,000 Da) bovine skin hydrolysates by continuous enzymatic hydrolysis with different conditions and complicated ultrafiltration steps, and introduced the use of collagenase. Similarly, to produce CH from limed hide gelatin with a low MW (about 100 Da to 2,000 Da), Dolphin and Russell (2011) proposed a serial hydrolysis by endopeptidase (i.e. papain, bromelain and Corolase® 7089) and exopeptidase (i.e. Validase® FPII and Corolase® LAP). However, these processes either used costly enzymes or included a series of complicated hydrolytic steps, which limited their application in industry.

To evaluate the bioavailability of CH we used an *in vitro* approach since it is more economical and less labor intensive than *in vivo* animal studies. The Caco-2 cell model is the most well established intestinal *in vitro* model currently and widely used to evaluate the transepithelial

transport of chemicals and drugs. In this model, Caco-2 cells are able to differentiate into monolayers with polarized tight junctions, apical microvilli and basolateral surface (Turco & Angelis, 2011). Therefore, the objective of the present study was to produce CH with MW lower than 2,000 Da from bovine hide collagen using an efficient enzymatic hydrolysis protocol. Next, the effects of these CH on *in vitro* GI digestion and transepithelial transport across Caco-2 cell monolayer were studied. Bovine hide collagen was hydrolyzed by commercially available enzymes (Alcalase, Flavouzyme, or trypsin) either alone, or in combination as a dual enzyme mixture (Alcalase/Flavourzyme, Alcalase/trypsin, or Flavourzyme/trypsin), or as three enzymes together (Alcalase/Flavourzyme/trypsin). The CH were characterized by measuring the MW distribution and free amino acid content. The GI digestion was simulated by digesting the CH with an *in vitro* pepsin-pancreatin model, and transport studies were conducted using a Caco-2 cell model.

3.2. Materials and methods

3.2.1 Materials

Fresh bovine hides were supplied by Canadian Premium Meats inc. (AB, Canada) (Figure 3.1) and stored at -20°C before use. Pepsin (EC 3.4.23.1), Alcalase (EC 3.4.21.62), Flavourzyme (EC 3.4.11.1), trypsin (EC 3.4.21.4), pancreatin, protein and peptide markers used in Size Exclusion Chromatography (SEC), and amino acid standards used in SEC were purchased from Sigma-Aldrich (St. Louis, MO, USA). The synthesized peptide 1(GNNRPVUIPRPPHPRL), peptide 2 (PRGDGETGE) and peptide 3 (Pro-Hyp-Gly) used in SEC were obtained from GenScript (Piscataway, NJ, USA). AccQ-Tag Ultra Derivatization Kit was supplied by Waters (Milford, MA, USA).

Caco-2 cells (HTB-37) and MTT (3-(4,5-dimethylthiazolyl-2)-2) Cell Proliferation Assay Kit were purchased from American Type Culture Collection (Manassas, VA, USA). Dulbecco's Modified Eagle Medium (DMEM), 0.25% (w/v) Trypsin-0.91 mM EDTA, Hank's balanced salt solution (HBSS), N-2-hydroxyethylpiperazine-N-2-ethane sulfonic acid (HEPES), fetal bovine serum, and penicillin were all obtained from Gibco (Life Technologies Inc., ON, CA).

3.2.2 Methods

3.2.2.1 Extraction of collagen

Collagen was extracted according to the pre-treatment method described by Daniel (1973) and purified according to Khiari et al. (2014) with some modifications. The extraction scheme is shown in Figure 3.2. Frozen bovine hide was thawed under room temperature and cut into 2-3 cm square small sections before being washed with water to remove excess impurities. The bovine hide was then washed with 10 volumes (v/w) of 0.5 M NaCl for 2h and then thoroughly with water. Cleaned bovine hide was pre-treated with lime suspension (Cacium hydroxide 40 g/L) at a ratio of 1:10 (w/v) for 4 d at room temperature. After liming pre-treatment, the swollen bovine hide was dehaired (Figure 3.1). The internal flesh layer and external grain layer were cut off, while the central corium layer was further pretreated with 2% NaOH (1:10, w/v) for 5 more days at room temperature. All the pre-treatment processes were under regularly stirring by a stirrer (Eurostar Power-b, IKA®-Werke GmbH & Co. KG, Staufen, Germany). The alkali pre-treatment removed the excess soluble non-collagenous protein and other impurities, which made the conditioned central layer to be almost pure collagen. To avoid the denaturation, all the later purification experiments were performed in a 4°C cold room. The pretreated central layer was ground and thoroughly washed with water until the pH was stable at about 7.0. The cleaned hide pieces were

blended using a heavy-duty blender (Waring Laboratory, Torrington, CT, USA) with 0.5 M acetic acid at a ratio of 1:100 (w/v)

Figure 3.1. Raw and de-haired bovine hides
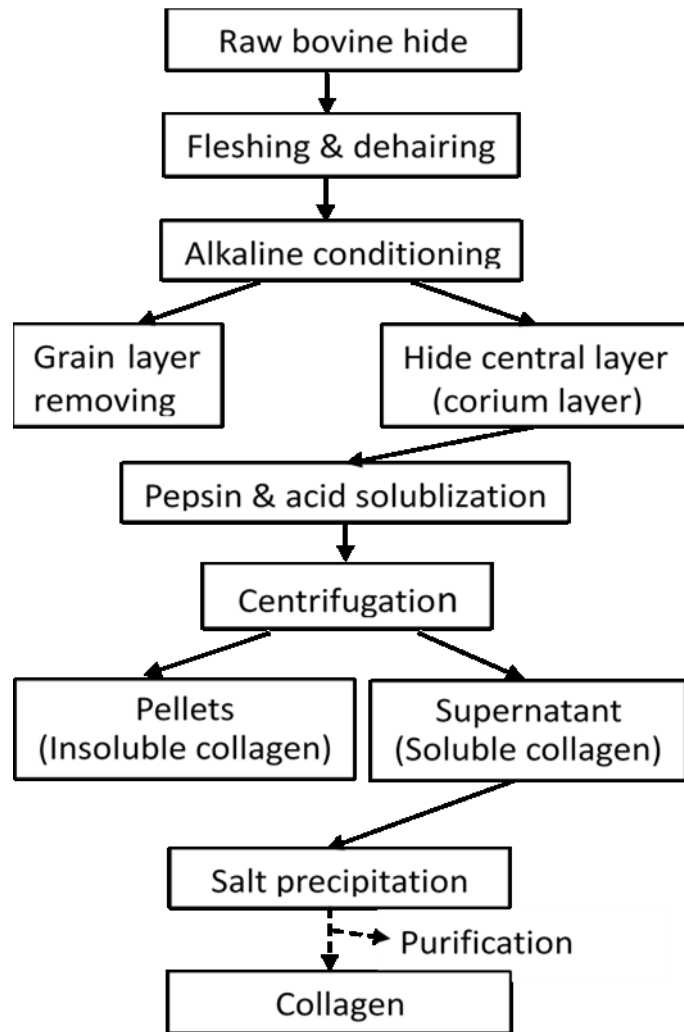
Figure 3.2. Collagen extraction scheme

for 2-3 min to form a viscous suspension. Pepsin was added at an enzyme/substrate ratio of 1:20 (w/w) to solubilize the suspension for 2 d with continuous stirring. Then the suspension was centrifuged (Avanti® J-E, Beckman Coulter Inc., Palo Alto, CA, USA) at 20,000×g for 20 min at 4°C. The supernatant was collected and precipitated for 6 h in the presence of 2M NaCl. After centrifugation of the mixture at 20,000×g for 15 min at 4°C, the precipitated collagen was recovered, and dialyzed (14 kDa MW cut-off cellulose membrane dialysis tubing, Sigma-Aldrich) against deionized water for 4 more days to remove superfluous ions. Then the dialyzed collagen was freeze-dried and stored at -20°C.

3.2.2.2 Quality characteristics of collagen

Hydroxyproline determination

As collagen is the major source of hydroxyproline (Hyp) in animal protein, the Hyp content can be used to indicate the collagen level. The Hyp content (dry weight basis) of raw hide, the conditioned central layer, and extracted collagen were determined following the method of Edwards and O'Brien (1980).

Protein profile

The protein profile of extracted collagen was determined by SDS-PAGE according to the method of Du et al. (2013).

Tryptophan determination

As collagen is absent of tryptophan (Trp) (Schrieber&Gareis, 2007), the Trp content of prepared collagen may indicate its level of contamination. The Typ content of prepared collagen sample was determined according to the method 988.15 in AOAC International (2000). Briefly, the sample was hydrolyzed with 4.2 M NaOH under vacuum condition for 20 h at 110°C. The

hydrolyzed sample was then analyzed using reverse phase liquid chromatography with UV detection at 280 nm.

3.2.2.3 Enzymatic hydrolysis of collagen

Freeze-dried collagen was mixed with deionized water and homogenized for 1-2 min at a ratio of 1:80 (w/v). The mixture was heated at 90°C for 10 min to inactivate the pre-containing enzymes, and cooled down to 50°C before the pH was adjusted to 8. The ratio was made up to 1:100 (w/v) by adding deionized water with pH at 8. The hydrolysis was carried out with seven different treatments: a single enzyme treatment by Alcalase (A), Flavourzyme (F), or trypsin (T); a dual enzyme treatment by Alcalase/Flavourzyme (AF), Alcalase/trypsin (AT), or Flavourzyme/trypsin (FT); and a cocktail enzyme treatment by Alcalase/Flavourzyme/trypsin (AFT). For all the treatments, the enzyme/substrate ratio was kept at 1:50 (w/w) for each enzyme. The hydrolysis went through 24 h at 50°C and pH 8 under continuous stirring in a pH-stat titrator with automatic control of pH and temperature (Titrando 842, Metrohm, Herisau, Switzerland). After the hydrolysis was terminated by heating at 90°C for 10 min and cooled down to room temperature, the mixtures were then centrifuged at 20,000 ×g for 10 min at 4 °C to precipitate the insoluble collagen hydrolysates. The supernatant was collected as soluble collagen peptides which were freeze-dried and stored under -20°C for later experiments. Stability of the enzymes was monitored by measuring the primary amino groups released using o-phthaldialdehyde according to Church et al. (1983) and no significant degradation was observed. The experimental design is shown in Figure 3.3.

3.2.2.4 Degree of hydrolysis (DH)

The DH of collagen was calculated following the pH-stat method described by Adler-Nissen (1986). The DH (%) was calculated from the amount of alkali used during the hydrolysis to keep the pH constant.
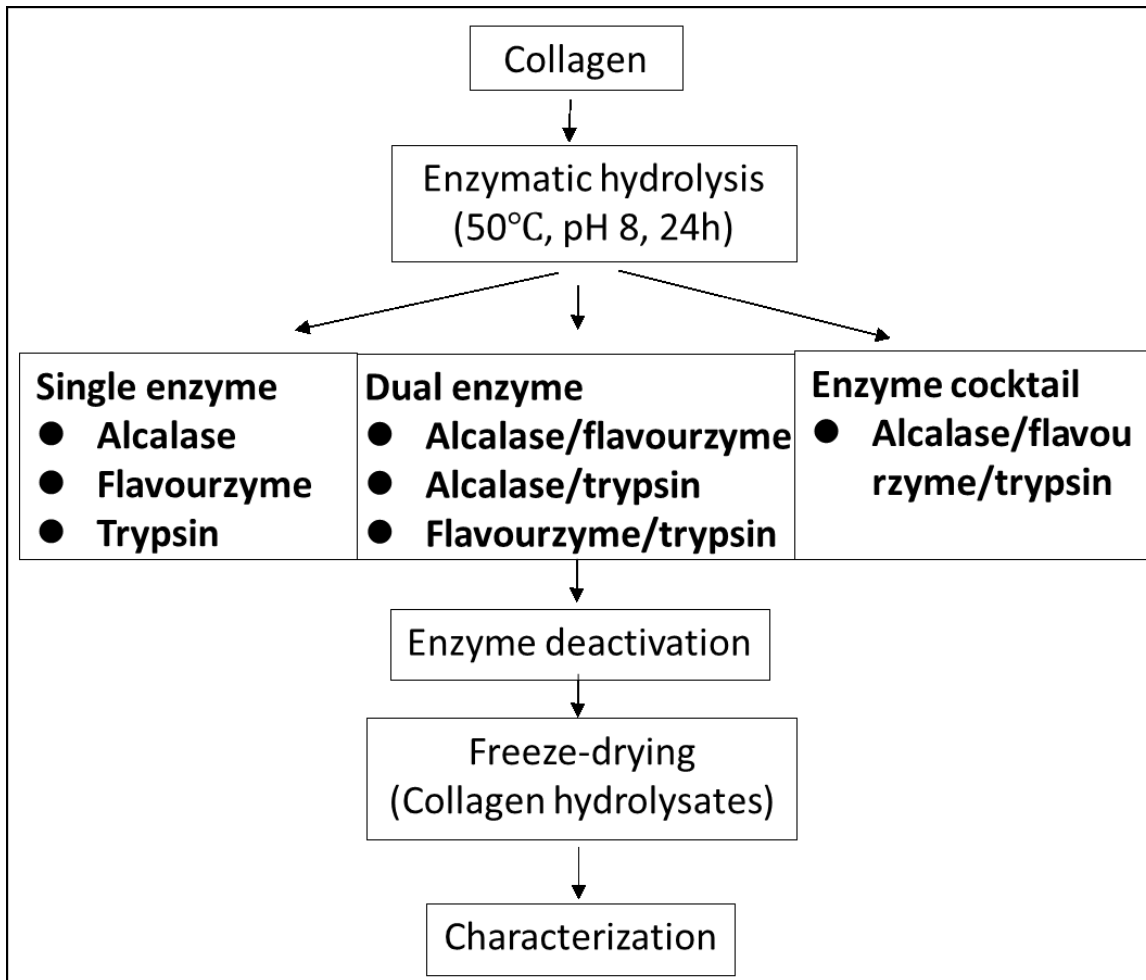
Figure 3.3. Collagen hydrolysis scheme

3.2.2.5 Characterization of collagen hydrolysates

Determination of MW by size exclusion chromatograph (SEC)

The MW distributions of collagen and CH were firstly estimated by a fast protein liquid chromatography (FPLC) system (GE Healthcare Life Sciences, Baie-D'urfe, QC, Canada) with a HiLoad 16/600 Superdex 200 pg column (L × I.D. 60 cm × 16 mm, GE Healthcare Life Sciences).

Each sample (500 μL at 1mg/mL) was injected and isocratically eluted out using 50 mM sodium phosphate buffer (pH7.4) containing 150 mM NaCl at a flow rate 1 mL/min. The MW distribution of CH was compared using MW markers containing thyroglobulin (669 kDa) and cytochrome C (12,384 Da). The absorbance of samples was detected at 280 nm and 215 nm. To further determine the MW distribution of prepared collagen hydrolysates, they were subjected to a high-performance liquid chromatograph (HPLC) system (Agilent 1100 Series, Agilent Technologies Inc., CA, USA) using a Superdex Peptide 10/300 GL column (L × I.D. 30 cm × 10 mm, GE Healthcare Life Sciences). Sample was injected (30ul of 5mg/mL) and eluted out at a flow rate of 0.45 mL/min by 50 mM phosphate buffer (pH 7.0) containing 50 mM NaCl. The absorbance was monitored at 214 nm. The peptide MW markers contain cytochrome C (12384 Da), aprotinin (6512 Da), synthesized peptide 1 (2108.46 Da), synthesized peptide 2 (916.89 Da), and synthesized peptide 3 (285.3 Da). The representative chromatographs of these peptide markers were shown in Appendix B. The MW of peptide markers were related to the elution volume (Ve) by the following equation: $Log (MW) = - 0.2361(Ve) + 6.4935$; ($R^2 = 0.9756$). The area of sample chromatograph was integrated at the level of 500 Da, 1 kDa, 2 kDa, and 10 kDa. The proportion of each range of peptides in the whole mixture were expressed as the percentage of area of corresponding MW range in the total chromatograph peaks' area.

Free amino acid analysis

The free amino acid composition of collagen hydrolysates was obtained by a HPLC system (Agilent 1200 Series) using AccQ-Tag C18 column (3.9 × 150 mm, Waters, Milford, MA). The samples were derivatized with 6-aminoquinolyl-N-hydroxysuccinimidyl carbamate according to the manufacturer protocol (AccQ-Tag Ultra Derivatization Kit, Waters), and detected by UV

detector at absorbance of 254 nm. The analysis was conducted at the Alberta Proteomics and Mass Spectrometry Facility (University of Alberta, Edmonton, Canada).

3.2.2.6 *In vitro* simulated GI digestion

To study the effect of enzymatic hydrolysis of collagen on its GI digestion, a simulated GI digestion model was used according to the method of Cinq-Mars et al. (2008) with some modifications. Hydrolysates were redissolved in deionized water (2%, w/v) by adjusting to pH 2.0 with 2 M HCl. The sample was firstly digested by pepsin at a ratio 1:35 (E/S, w/w) for 60 min, which was then inhibited by adjusting to pH 5.3 with 0.9 M $NaHCO_3$, and further to pH 7.5 with 2M NaOH. Further digestion was performed with pancreatin (1:25, E/S, w/w) at this pH for 120 min. The whole *in vitro* GI digestion process was carried out at 37°C with continuous shaking at 200 rpm (New Brunswick Scientific Co 126 incubator shaker series, Edison, US). The enzymes were finally inactivated in a 90°C water bath for 10 min. After cooling down to room temperature, the sample was centrifuged at 20,000 ×g for 20 min. The supernatant was then freeze-dried and stored at -20°C. The freeze-dried collagen digests were subjected to a HPLC system to determinate the MW distribution according to the method described in section 2.2.5.

Determination of primary amino groups

Aliquots of GI digests were removed while the digestion mixture was supplemented with an equal volume solution at the same pH, for monitoring the digestion process by measuring the release of primary amines following the method described by Church et al (1983). The assay was dependant on the reaction of primary amino groups with o-phthaldialdehyde at the presence of β-mercaptoethanol. L-leucine was used as a standard for the estimation of primary amine content, which was expressed as leucine amino equivalents.

3.2.2.7 Caco-2 cell culture

The Caco-2 cells were cultured in DMEM supplemented with 10% fetal bovine serum, 25 mM HEPES, 1% penicillin at 37°C in a constant humidified atmosphere containing 5% CO_2. The cells reached about 80% confluence were passaged by 0.25% (w/v) Trypsin-0.91 mM EDTA. For transport studies, the cells were seeded in 12- well transwell inserts (12 mm diameter, 0.4 μm pore size, Corning, NY, USA) at a density of 1×10^5 cells/cm^2 for differentiation around 21 days. During the incubation, the culture medium was changed every 2 d. The integrity of Caco-2 cell monolayers was monitored by measuring transepithelial electrical resistance (TEER) with EVOM2, Epithelial Voltohmmeter (World Precision Instrument, Sarasota, FL, USA). The transport studies were conducted on cell monolayers with TEER values greater than 350 Ω•cm^2. All cells used in this study were between passage 33 and 40. The cytotoxicity of samples on cell viability was performed using the MTT assay according to the manufacturer's instructions (ATCC, MTT cell proliferation assay).

3.2.2.8 Transport studies

The transepithelial transport of *in vitro* GI digested CH was simulated using Caco-2 cell monolayers following the method described by Ding et al. (2014) with minor modifications. The cell monolayers were firstly rinsed twice with HBSS to remove the remaining culture medium, and incubated with HBSS for 30 min to stabilize prior to the transport studies. Samples (0.5 mL) in HBSS at a non-toxic concentration (6 mg/mL) were then added on the apical side, while 1.2 mL fresh HBSS was added at the basolateral side of the monolayers. After 2 h incubation at 37°C in 5% CO_2 atmosphere, samples from the basolateral side were collected to estimate the transported amount using reverse phase HPLC. The transport experiments were conducted on three different passages of cells with duplicates for each passage.

Determination of transport amount

The transport amount of CH after *in vitro* GI digestion in Caco-2 monolayers was estimated by measuring the total amino acid content of samples at the apical side before the transport study (sum of total amino acid applied), and that of samples at the basolateral side after transport study (sum of total amino acid transported). The samples were hydrolyzed under vacuum by 6 M HCl with 0.1% phenol at 110ºC for 24 h. The hydrolyzed samples were then analyzed using reverse phase HPLC as described in section 2.2.5. The transport amount was expressed as

$$\% = \frac{sum\ of\ total\ amino\ acid\ transported}{sum\ of\ total\ amino\ acid\ applied} \times 100$$
.

3.2.2.9 Statistical analysis

Data were analyzed using one-way or two-way analysis of variance (ANOVA). The transport experimental design was completely randomized block design. Pre-digestion enzymatic treatments were analyzed as a fixed effect, while passage of cells was considered as a block and analyzed as a random effect. All the statistical analyses were performed using SAS 9.4 (Cary, NC, USA). Multiple comparisons of means were done by Tukey's test using 5% as the significant level.

3.3. Results and discussion

3.3.1 Quality characteristics of the extracted bovine collagen

Since collagen is the major source of hydroxyproline (Hyp) in animal proteins, the Hyp content can be used to indicate the collagen level in the starting materials and in the subsequent extraction steps. The Hyp content increased from 8.6% in raw hide to 9.7% in the conditioned central layer, indicating the effectiveness of the alkaline conditioning process to dissolve out the impurities such as the non-collagenous proteins (e.g. albumin and globulin, etc.) and non-protein components (fat, mucopolysaccharides, etc.) (Schrieber and Gareis, 2007). The Hyp content was further improved by purification with a large concentration of salt to precipitate the collagen, and with dialysis to exchange out the salt ions. The approximate Hyp content increased to 11.9% for

extracted collagen, which is comparable to the typical Hyp content for bovine skin collagen reported by Rose (1987).

The collagen extracted was both pepsin and acid soluble. The protein profile of collagen is presented in Figure 3.4. Bovine hide collagen is mainly composed of type I collagen which has two identical α_1 chains and one α_2 chains (Voet and Voet, 1995). Figure 3.4 shows a typical composition of skin collagen with two α chains (α_1 is the upper band, and α_2 is the lower band), and two β chains (dimer of two α_1 chains, or dimer of one α_1 chain and one α_2 chain), which is consistent with the results from Du et al. (2013). There were a few faint bands shown between 25 kDa and 75 kDa, which could be due to the degradation of collagen molecules during the alkaline and acid treatments of the extraction processes, or influence of heating during the SDS-PAGE analysis procedure, or contamination by other flesh proteins left on the hide. However, the flesh protein contamination possibility is less likely because they should have been dissolved during the long alkali pre-treatment. The results agree with the study of Zhang et al. (2013), where a short boiling treatment (90 ºC for 15 min) and a long acidic treatment facilitated collagen degradation.

Since Trp is absent in collagen (Schrieber & Gareis, 2007), the presence of this amino acid indicates contamination from non-collagenous proteins. To confirm the purity of extracted collagen, Typ levels were determined. The Trp content, however, was too low to be detected and calculated (Appendix A), which confirmed that there was no obvious contamination from other proteins. Overall, the large Hyp content, the typical protein profile, and the absence of Trp in the extracted collagen indicated the effectiveness of the extraction and purification processes.

3.3.2 Determination of DH

Determining the degree to which the collagen has been hydrolyzed is the most direct way to evaluate the efficiency of an enzyme to break peptide bonds over time. The DH of collagen over

time is shown in Figure 3.5. For all the enzymatic treatments, the hydrolysis time had significant effects on the DH, which increased rapidly during the first hour, slowly thereafter, and became stable after around 20 h. Except treatment F, the DH of all other treatments reached more than half of the maximum level of DH after 2 h. The DH of the Alcalase hydrolysis increased to 8.5% after 1 h and 10.5% after 2 h, which are comparable to the results from Zhang et al. (2013) who reported about 12% DH of the bovine achilles tendon collagen after 2 h Alcalase hydrolysis. A
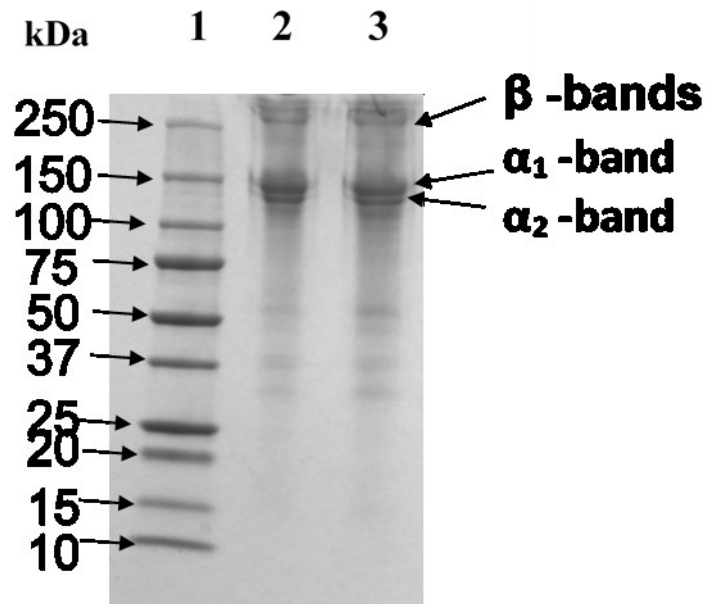
Figure 3.4. SDS-PAGE profile of extracted collagen. Lane 1: molecular weight markers; lane 2 and lane 3: extracted collagen.

different trend in DH was obtained by hydrolyzing with Flavourzyme, where the hydrolysis was slow at the beginning, followed by a rapid increase after 14 h. This indicated the rate of cleaving peptide bonds of extracted collagen by Alcalase and trypsin were greater than that of Flavourzyme over the hydrolysis process.

The final DH after 24 h hydrolysis implied that Alcalase contributed the most to hydrolyzing the collagen. Those treatments in the presence of Alcalase with DH values after 24 h

hydrolysis for treatment A (19.1%), AF (20.4%), AT (18.1%) and AFT (19.9%) were more than three times the DH of treatment F (5.8%) and T (6.6%), while almost two times of treatment FT (10.6%). Dong et al. (2008) also showed similar results indicating the superiority of Alcalase over Flavourzyme in hydrolyzing collagen. This may be from the broad specificity and high affinity of Alcalase toward food proteins. Flavourzyme, the protease from *Aspergillus oryzae*, contains both endoprotease and exopeptidase activities, while Alcalase and trypsin are in the family of serine endopeptidases. A mixture of enzymes may express broader specificity than a single enzyme indicating an additive effect (Cowieson & Adeola, 2005). However, in terms of DH, the additive effect only happened with treatment FT showing a significantly greater DH than that of both F and T. There was no additive effect of Flavourzyme on alcalase containing treatments, and also neither with trypsin on Alcalase treatments. Moreover, there was no significant difference among Alcalase containing treatments. The results in contrast to those reported by Khiari et al. (2014) who used Flavourzyme, and/or trypsin, and/or Alcalase on hydrolysis of turkey head collagen, indicating an additive effect with dual enzyme mixtures. The difference may come from variables in the raw materials as well as extraction processes. As Alcalase has a very broad specificity for peptide bonds, there may be competition among Alcalase, trypsin, and Flavourzyme when they are simultaneously used to hydrolyze collagen. The final highest DH (20.4%) in this study, however, was much greater than those reported by Khiari et al (2014) who obtained a maximum DH at 10.4%.
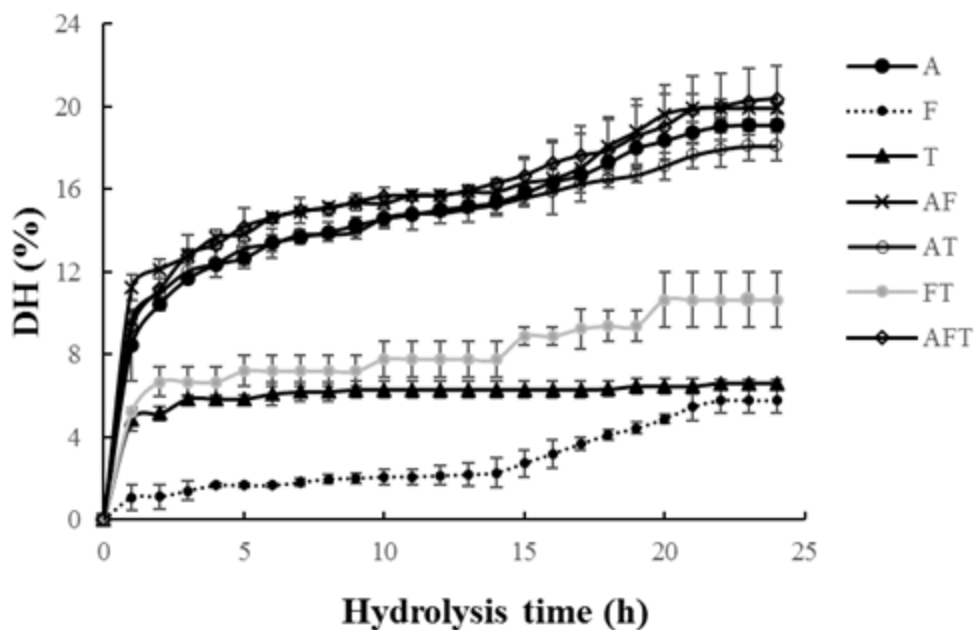
Figure 3.5. Degree of hydrolysis (DH) of extracted collagen with different enzymatic hydrolysis treatments: Alcalase (A), Flavourzyme (F), trypsin (T), Alcalase/Flavourzyme (AF), Alcalase/Trypsin (AT), Flavourzyme/trypsin (FT), and Alcalase/Flavourzyme/trypsin (AFT); n = 3.

3.3.3 Characterization of collagen hydrolysates

MW distribution of collagen and collagen hydrolysates by SEC

Figure 3.6A shows that the extracted collagen was presented at a MW higher than 669 kDa, while most of the CH presented at a MW less than 12384 Da. The data also indicated that all of the enzymatic treatments were able to digest the pepsin soluble collagen as the intensity of the peak at 669 kDa dramatically decreased as a function of treatment. However, to better distinguish the effect of different enzymatic treatments on the MW of the CH produced, they were further subjected to HPLC using a column which better separated peptides (Figure 3.6B). The vertical arrow of retention time for MWs 10 kDa, 2 kDa, 1 kDa, and 500 Da estimated from the calibration equation (shown in Section 3.2.2.5) were drawn. As highlighted in the introduction, the aim of this research was to increase the amounts of peptides with a MW less than 2 kDa.

As shown in Figure 3.6B, except for the hydrolysates (FH) from the Flavourzyme treatment which had a broad MW ranging from less than 285 Da to greater than 12kDa, all the SEC of CH from other treatments showed one major peak with a narrow MW range distribution. The MW of CH from different treatments is summarized in Figure 3.6C. Consistent with the DH results (Figure 3.5), CH from Alcalase-containing treatments (i.e. AH, AFH, ATH, and AFTH) had a significantly greater proportion of peptides with MW lower than 2 kDa (79.8 % -82.7 %) than that (25.2 % - 40.3 %) of hydrolysates from the other treatments (i.e. FH, TH, and FTH). Interestingly, in the Alcalase containing treatments less than 1% of the peptides had a MW higher than10 kDa, while in the rest of the treatments was between 9.6 - 44.3 %, indicating the effectiveness of Alcalase on breaking down the collagen into lower MW peptides. On the other hand, the amount of peptides with MW less than 500 Da in AFH, ATH, and AFTH were significantly greater than that of AH (28.3%), whichwas still much greater than the 15% reported by Dong et al. (2008). As proteins are mainly absorbed in the form of free amino acids and di- and tripeptides (Ganopathy et al., 2006) (MW < 500 Da), a treatment producing more peptides in this range would be more viable and competitive in terms of bioavailability. Therefore, with regard to the ability to produce low MW collagen peptides (<2 kDa and <500 Da), treatments AFH, ATH, AFTH were superior to others. In comparison to Kim et al. (2001b), who hydrolyzed bovine skin gelatin with Alcalase obtaining a major peak at 7 kDa and some shoulder peaks at around 2 kDa, CH produced in the present study from Alcalase-containing treatments were more uniform, with a major peak at lower MW around 500 Da -1 kDa.
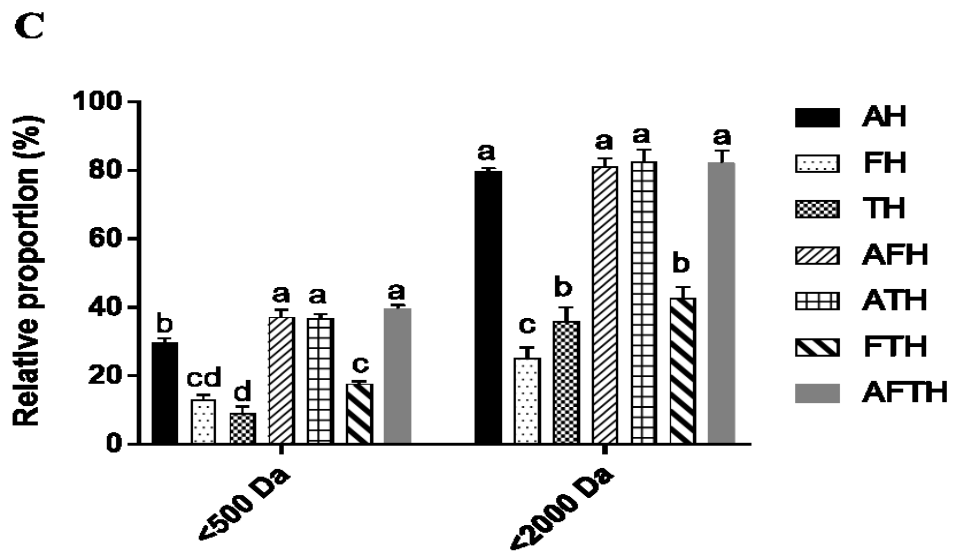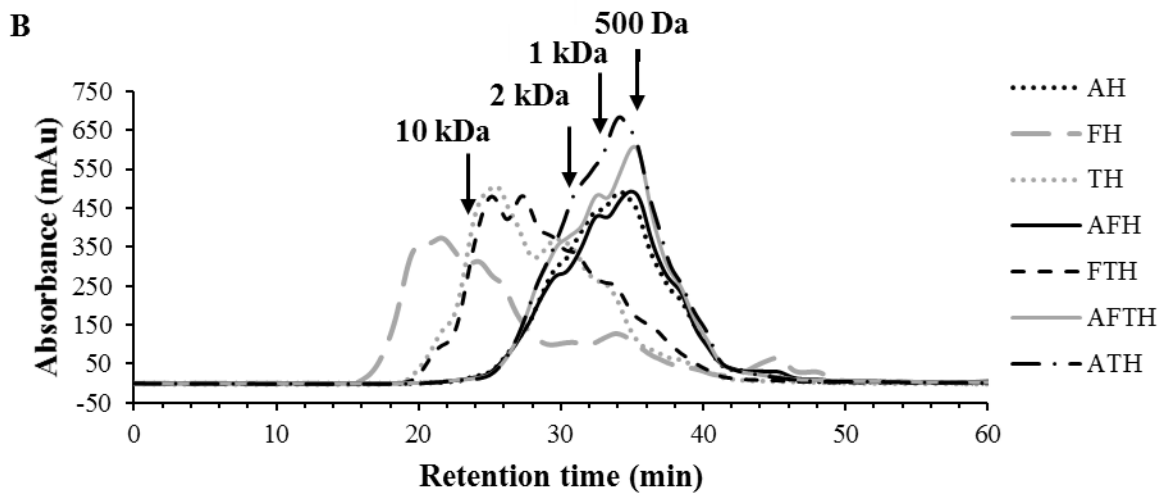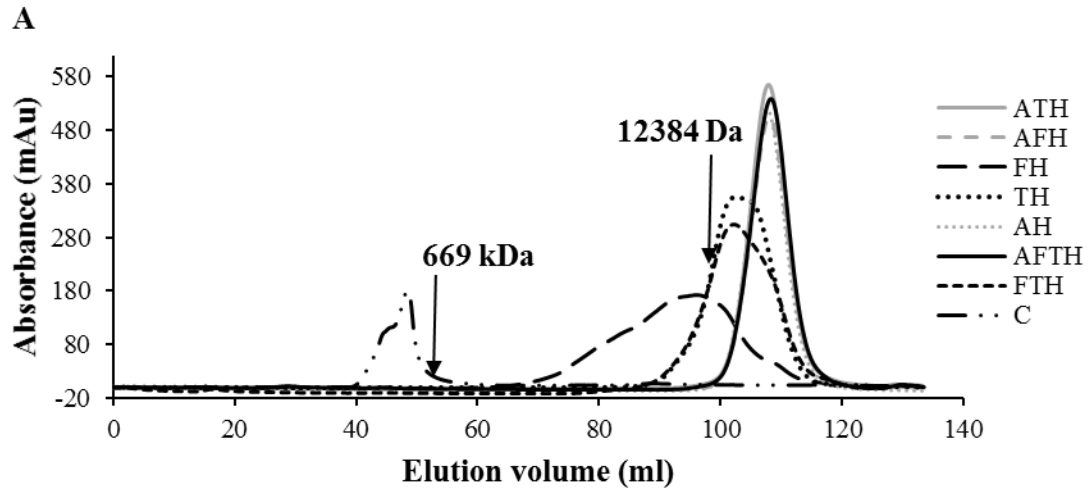
Figure 3.6. Molecular weight distribution of collagen and collagen hydrolysates. Size exclusion chromatography using FPLC system (A), and HPLC system (B), proportions of collagen hydrolysates at different molecular weight ranges (C) are shown. Statistical difference ($p < 0.05$) within each MW range among different treatments is denoted with letters[a-d]. AH: collagen hydrolysates from Alcalase hydrolysis; FH: collagen hydrolysates from Flavourzyme hydrolysis; TH: collagen hydrolysates from trypsin hydrolysis; AFH: collagen hydrolysates from Alcalase/Flavourzyme hydrolysis; ATH: collagen hydrolysates from Alcalase/trypsin hydrolysis; FTH: collagen hydrolysates from Flavourzyme/trypsin hydrolysis; AFTH: collagen hydrolysates from Alcalase/Flavourzyme/trypsin hydrolysis.

Free amino acid content

The level of free amino acids which results from and enzymatic hydrolysis can be an indicator to predict CH bioavailability. The free amino acid profile of CH for different treatments is summarized in Table 3.1. All the hydrolysates from different treatments had a relatively small proportion of serine, histidine, tyrosine and methionine, which are typically less in collagen. On the other hand, a relatively large proportion of valine, phenylalanine, isoleucine and leucine observed were all essential amino acids. The total sum of free amino acids in the hydrolysates (i.e. FH, AFH, FTH, and AFTH) from treatments containing Flavourzyme was almost eight times greater than that of other hydrolysates. The AF treatment generated the greatest amount of free amino acids (around $0.74 \times 10^{-3} \mu mol/\mu g$), comparable to that obtained by Dolphin and Russell (2011) who used a series of five different enzymes to hydrolyze gelatin. Flavourzyme is a mixture of endo- and exopeptidases, and likely its exopeptidase activity made it possible to cleave the collagen terminal peptide bonds and produce an appreciable amount of free amino acids.

Table 3.1. Free amino acid profile of prepared collagen peptides from different enzyme treatments

Amino acid (nmol/mg)	AH	FH	TH	AFH	ATH	FTH	AFTH
Hyp	ND[1]	114.56	ND	ND	ND	ND	ND
Asp	0.1	0.9	0.1	10.3	0.1	5.1	10.6
Glu	1.2	11.4	0.4	25.3	1.0	15.1	20.5
Asn	0.2	ND	0.3	ND	0.3	0.5	5.7
Ser	0.4	15.4	0.3	31.0	0.5	24.4	33.6
Gln	1.9	ND	3.8	ND	2.9	4.6	11.1
His	ND	13.4	0.6	12.4	4.8	11.1	4.6
Gly	22.3	161.9	2.1	250.8	23.1	215.5	223.1
Thr	1.3	51.6	0.4	20.2	ND	45.3	43.8
Arg	5.8	1.1	2.4	25.1	6.5	31.5	35.1
Ala	7.7	8.5	4.5	122.2	7.8	63.1	116.6
Tyr	3.6	25.1	1.6	9.6	2.5	12.5	8.2
Met	3.1	30.1	3.0	8.7	3.9	16.7	15.9
Val	4.3	54.1	4.4	58.6	4.9	56.6	56.3
Phe	8.3	58.7	13.1	26.6	10.2	36.5	22.3
Ile	14.2	37.7	17.6	47.9	13.3	59.2	43.3
Leu	9.7	107.9	18.2	41.4	8.1	68.8	38.0
Lys	2.5	15.6	2.3	50.0	2.0	19.0	27.6
Sum	86.7[b]	707.8[a]	75.0[b]	740.1[a]	91.9[b]	686.0[a]	716.6[a]

Values are presented as mean of three different trials (n = 3); Abbreviations are the same with those in Figure 3.6.

ND[1] means not detected; Proline content was not detected for all the collagen hydrolysates;

[a,b] Different letters within the raw means significant ($p < 0.05$) difference among the means.

    In general, peptides rich in proline and glutamic acid are resistant to enzymatic digestion (Yang & Russell, 1992; Hausch et al., 2002). This is also confirmed in the present study: free proline was non-detectable in CH from all the treatments. Only Flavourzyme hydrolysis generated some free Hyp. However, this activity was lost when Alcalase and/or trypsin were added. This

may be due to a competition between these enzymes. In addition, the free asparagine and glutamine content was also extremely small for all the treatments, likely due to the long alkaline hide pretreatment which may completely convert asparagine and glutamine into aspartic acid and glutamic acid, respectively.

The chains in collagen triple helix features a repeating Gly-X-Y sequence, in which X-position is preferably occupied by proline while Y- position by Hyp. Therefore, the glycine content in collagen is around 33%. Also, arginine favors the Y- position (Johnston-Banks, 1990). As shown in Table 3.1, except for free Gly in TH, all the other treatments generated a large proportion (over 22%) of Gly. Trypsin usually cleaves peptides on the C-terminal side of lysine and arginine (Keil-Dlouhá et al., 1971), releasing peptides which likely contain the enzymatically resistant tripeptide Gly-X-Y. This could explain why the free glycine content was small in this treatment. Note that free alanine content of AFH and AFTH was much greater than that of all other hydrolysates, indicating that the simultaneous use of Alcalase and Flavourzyme was more effective to release this amino acid. Alanine has important physiological functions in the glucose-alanine cycle in human body, hence a large amount of alanine in the CH are beneficial. Different from the pathways for peptides absorption, the free amino acids have their own specific efficient transporters in the intestinal epithelium. This means they are a crucial source of essential amino acids in protein synthesis and metabolic processes in human body (Bröer, 2008). In this respect the Flavourzyme-containing treatments were better than the others.

3.3.4 Simulated GI digestion of the selected hydrolysates

Contents of primary amino groups

Since the bioavailability of collagen hydrolysates is closely related to the MW and free amino acid content, the selected CH with three different levels of peptides with MW< 2 kDa but

with similar level of a large free amino acid content (i.e. FH, FTH, and AFH) were selected for the simulated *in vitro* GI digestion and subsequent transport studies. Extracted acid soluble collagen (C) was used as a control. Figure 3.7A shows the changes of primary amines content during the simulated GI digestion of CH. CH with a greater proportion of peptides with MW less than 2 kDa exhibited a greater free amino group content. For all the CH and soluble collagen, a significant amount of primary amino groups was released after the GI digestion. In general, during the digestion with pepsin, the increase of the primary amine groups was quite small in all treatments (14.8 - 26.1 mg/g increase), while during the subsequent pancreatin digestion a significantly greater increase was observed (46.9 -163.7 mg/g increase). This can be explained since all CH were derived from extracted pepsin soluble collagen which had no more cleavage sites left for further pepsin activity. In contrast, pancreatin is a mixture of trypsin, chymotrypsin and some other proteases, showed more hydrolysis specificity.

Overall, the amount of primary amino groups released during GI digestion was inversely proportional to the average MW of the CH. The hydrolysates with a greater proportion of compounds with MW < 2 kDa were associated with less release of primary amine groups. This is consistent with the research of Chen and Li (2012). The simulated digestion accounted for the least increase of primary amino groups (73.1 mg/g) for the AFH treatment, while the greatest increase (181.9 mg/g; $p < 0.05$) was observed for control C. This can be explained since CH can only be digested to a certain extent because the short peptides rich in proline and/or Hyp are quite resistant to further digestion (Sánchez-Rivera et al., 2014; Liu et al., 2015). It is also consistent with the large presence of Hyp-containing di-and tripeptides in human blood after gelatin hydrolysate ingestion (Iwai et al., 2005; Ichikawa et al., 2010). After digestion, however, the primary amino groups content of all the CH treatments were still significantly greater than that of control. In this

respect, the pre-digestion enzymatic hydrolysis still contributed to releasing more amount of free amino groups, corresponding to a greater degree of hydrolysis and lower MW.

Changes in MW of CH after digestion

As shown in Figure 3.7B, consistent with the results of primary amino group content, the GI digest of FH, FTH and AFH had significantly greater amounts of compounds with MW<2 kDa and MW<500 Da than that of the control collagen digest. However, the GI digestion reduced or eliminated the difference between FH and FTH, resulting in a non-significant difference in terms of the amounts of peptides with MW <2 kDa (59.3% vs. 58.8%) and MW<500 Da (22.8% vs. 24.3%). On the other hand, GI digestion further reduced the MW of all the samples when compared to the corresponding MW distribution before digestion (Figure 3.6C). All the digests of selected CH possessed significantly greater amounts of compounds in the range of both <500 Da and < 2000 Da. FH underwent the greatest increase, of 9.6% and 34.1% in the range of < 500 Da and < 2000 Da, respectively. This probably resulted from the action of protease in the pancreatin mixture. Digests from AFH contained up to 87.2% of compounds with a MW < 2000 Da, half of which had a MW < 500 Da (44.4%). In comparison to the control, these results confirmed the effectiveness of the pre-digestion enzymatic hydrolysis by F, FT, and especially AF.
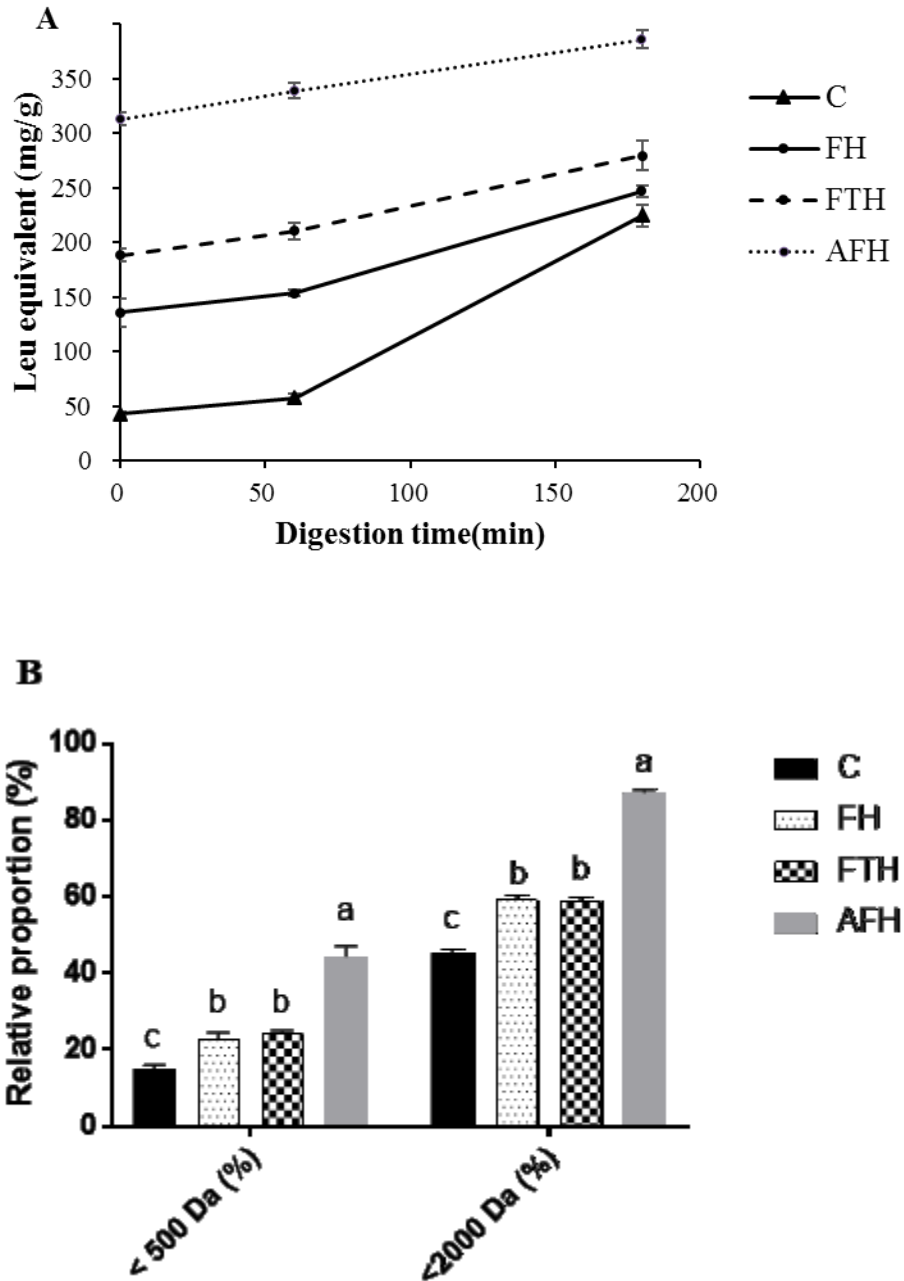
Figure 3.7. Changes during the simulated GI digestion of collagen and selected collagen hydrolysates (n = 3). Primary amine content changes (A) during *in vitro* GI digestion by pepsin (0-60 min) and pancreatin (60-180 min); molecular weight distribution of collagen hydrolysates after *in vitro* gastrointestinal digestion (B); the results were expressed as the relative proportion of total integration area of chromatograph (%). Statistical difference ($p < 0.05$) within each MW range among different treatments is denoted with letters[a-c]. C: collagen; FH: collagen hydrolysates from

Flavourzyme hydrolysis; FTH: collagen hydrolysates from Flavourzyme/trypsin hydrolysis; AFH: collagen hydrolysates from Alcalase/Flavourzyme hydrolysis.
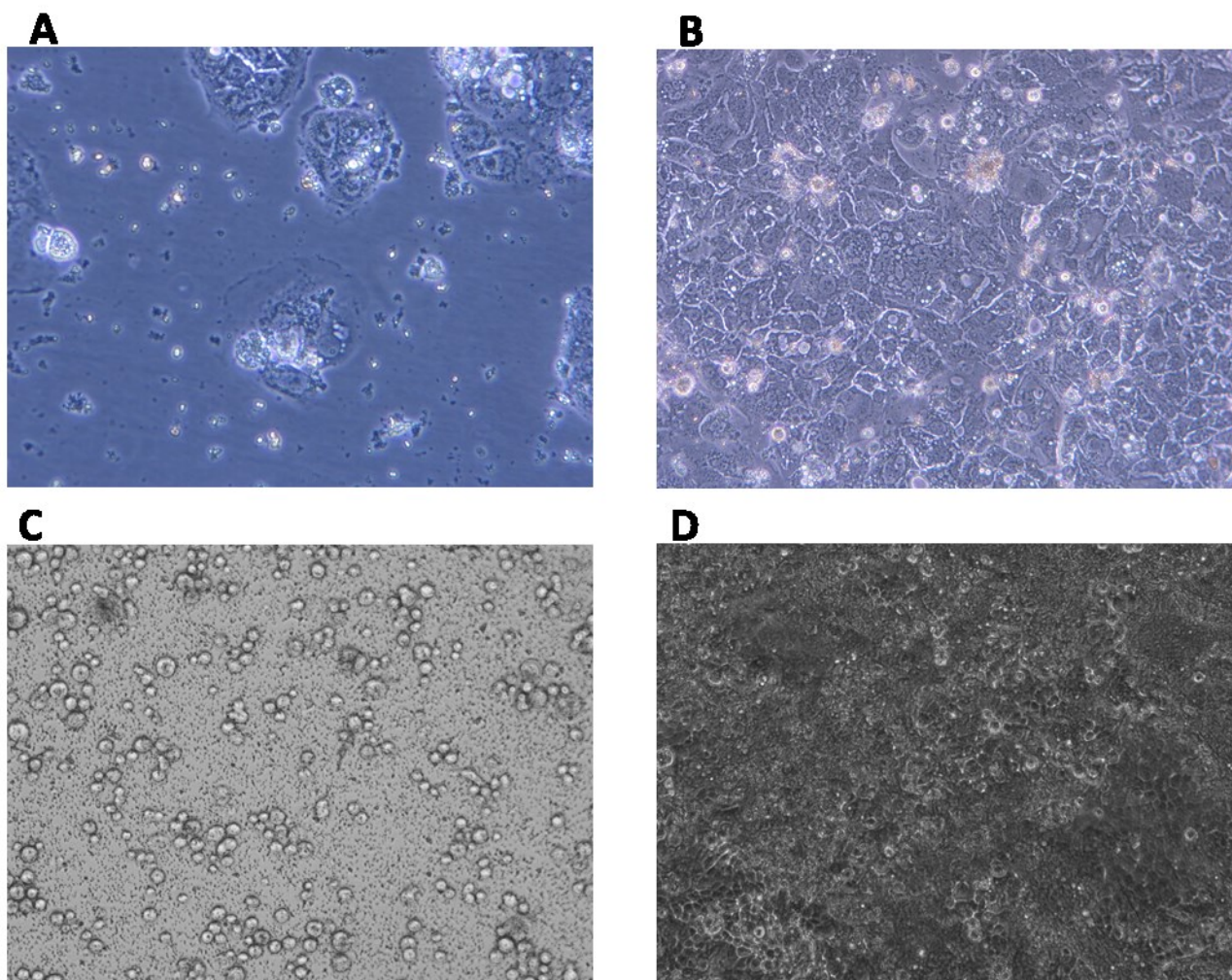
Figure 3.8. Caco-2 cell growth images. (A) Day 1 of Caco-2 cells (round-shaped) seeded on a plastic culturing flask; (B) Near to confluent cells after 5 days' culturing on the plastic flask; (C) Day 1 and (D) Day 21 of Caco-2 cells seeded on the transwell insert membrane

3.3.5 Effects of the enzymatic treatments on the transport efficiency in a Caco-2 cell model

The human colon carcinoma Caco-2 cell model, which has been used to reconstitute the differentiated human intestinal cell monolayer, is a well characterized approach to estimate the ability of food components to pass through the intestinal membrane (Figure 3.8). Figure 3.9 shows the transport amount of collagen-derived digest across Caco-2 cell monolayer. The digest of the

unhydrolyzed control collagen had an 8.9% uptake, which is comparable to the absorption amount of gelatin at 10% reported by Moskowitz (2000). Digests of collagen hydrolysates (i.e. FH, FTH, AFH) showed significantly greater transport amount than that of the control collagen digest, while there was no difference between the digest of FH and FTH. The greater transport amount can be partially accounted by the greater free amino acids content in the Flavourzyme hydrolyzed collagen and the greater primary amino group content after simulated digestion. However, the difference between the digest of FH and FTH in primary amino groups content was not strong enough to influence the final absorption. This is probably due to their similar MW distribution. The AFH digest which exhibited the highest proportion of compounds in MW<2 kDa, had the best transepithelial transport of 21.4%, more than two-fold of the digest of unhydrolyzed collagen. The transported AFH at the basolateral chamber of the transwell inserts was collected to monitor the MW by mass spectrometry (Appendix C). It shows that most of the fragments were below 600 Da, indicating that the higher transport efficiency of low MW compounds. However, the identification of transported peptides failed probably because of the sample complexity, and the difficulty of short peptide fragmentation during the tandom mass spectrometry.

Protein absorption is a complicated process involving a dynamic interaction between digestion and assimilation in the small intestine; ultimately, it is the free amino acids and small peptides such as di- and tripeptides that are absorbed (Ganopathy et al., 2006). In this respect, the MW of a protein plays an important role in its absorption. Results on the Caco-2 cell monolayer directly confirmed the impact of MW of CH on their transepithelial transport; for instance, the transport efficiency was proportional to the proportion of compounds with a MW less than 2000 Da. Interestingly, for each collagen-derived digest, there was no significant difference between the transport amount of total Hyp and that of the whole digest mixture (data not shown). Since Hyp is

the indicator amino acid for collagen, it is reasonable to indirectly evaluate the transepithelial transport of CH by determining the transport amount of total Hyp across the Caco-2 monolayer.

Even though the bioavailability of a compound is dependent on various processes such as liberation from the supplement, absorption from the intestine, distribution through the blood, and the metabolism in different tissues (Richelle et al., 2006), a large absorption rate in the intestine likely implicates good bioavailability. Therefore, the good transport of CH in the established *in vitro* intestinal Caco-2 cell model may correlate well with a relatively good bioavailability. As there has been evidence regarding beneficial biological effects of CH for skin, joint, and bone health, hydrolysates produced in the present study may have positive effects on enhancing their efficiency in these capacities.
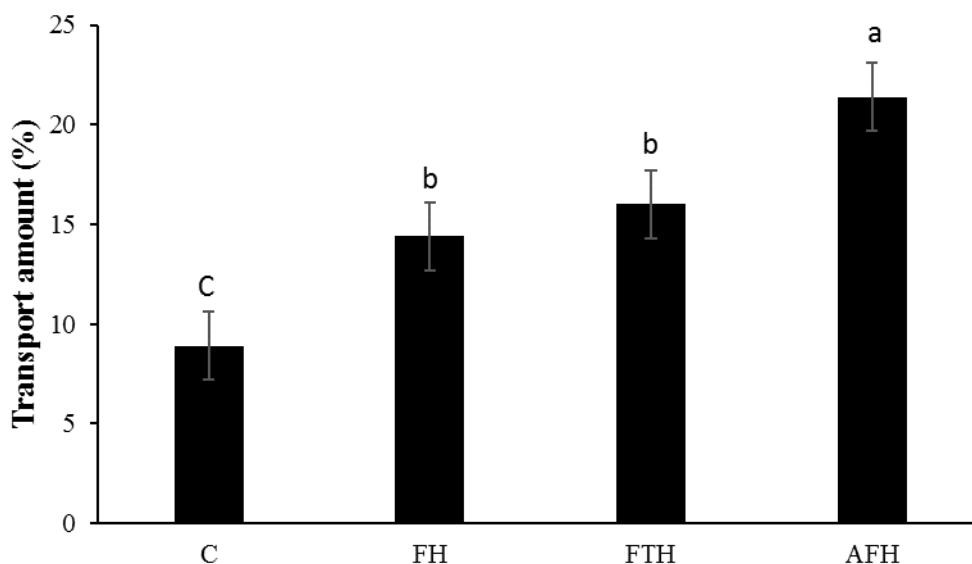
Figure 3.9. Transport amount of digest of collagen hydrolysates after *in vitro* GI digestion in a Caco-2 cell model; n = 6. Abbreviations are the same with those in Figure 3.7.

3.4. Conclusions

The present study successfully developed an efficient enzymatic hydrolysis method (hydrolysis by AF) to produce very low MW collagen hydrolysates that were efficiently transported across a Caco-2 cell monolayer. Alcalase contributed the best to hydrolyze acid-soluble collagen, while Flavourzyme was best at facilitating the release of free amino acids. The transepithelial study using a Caco-2 cell model showed that the greater transport efficiency of collagen hydrolysates was due to the lower MW (greater proportion with MW <2 kDa and MW < 500 Da). The most effective pre-digestion enzymatic hydrolysis, Alcalase and Flavourzyme combination (AF), increased the transepithelial transport by more than two-fold compared to the soluble collagen control. However, in previous studies, collagen peptides identified in blood were mostly Hyp-containing di- and tripeptides (Iwai et al., 2005; Ichikawa et al., 2010), implying the absorbed peptides may undergo further metabolism after intestinal absorption. To have a complete understanding of the bioavailability of collagen hydrolysates, further studies may need to focus on the absorption and metabolism *in vivo*.

CHAPTER 4.

Both PepT1 and GLUT intestinal transporters are utilized by a novel glycopeptide Pro-Hyp-CONH-GlcN

Abstract

Pro-Hyp (PO) accounts for many beneficial biological effects of collagen hydrolysates for skin and bone health. The objective of this study was to conjugate PO with glucosamine (GlcN) to create a novel glycopeptide Pro-Hyp-CONH-GlcN (POGlcN) and then to investigate the potential involvement of multiple transepithelial transport pathways for this glycopeptide. NMR results revealed the amide nature of this glycopeptide with α and β configuration derived from GlcN. This glycopeptide was very resistant to simulated gastrointestinal digestion. Also, it showed a superior transepithelial transport rate with permeability coefficient (P_{app}) of $(2.82 \pm 0.15) \times 10^{-6}$ cm/s) across the Caco-2 cell monolayer when compared to either the parental dipeptide PO or GlcN (P_{app} of $(1.45 \pm 0.17) \times 10^{-6}$ cm/s and $(1.87 \pm 0.15) \times 10^{-6}$, respectively). A transport mechanism experiment indicated that the improved transport efficiency of POGlcN can be attributed to the introduction of glucose transporters GLUTs.

Keywords: Glucosamine, Pro-Hyp, Glycopeptide, Pro-Hyp-CONH-GlcN, GLUT transporters

4.1. Introduction

When collagen is chemically or enzymatically hydrolyzed numerous collagen-derived peptides are released to impart beneficial bioactivities, such as anti-aging effects on skin conditions and growth-promoting effects on joints and bones. Some clinical trials have revealed the efficacy of collagen hydrolysates (CHs) to improve skin hydration, elasticity, and thereby reduce wrinkles due to the regeneration of skin collagen (Sibilla et al., 2015). Others have proposed an important role of CHs to improve bone mineral density and bone collagen metabolism (Koyama et al., 2001; Guillerminet et al., 2010). In addition, CHs may stimulate the synthesis of Type II collagen and inhibit the loss of cartilage mass, thus maintaining the structure and function of joint cartilage (Schrieber and Gareis, 2007). Some bioactive collagen peptides have also been identified. Ohara et al. (2010) and Shigemura et al. (2011) reported that Pro-Hyp (PO) and Hyp-Gly could stimulate the growth of fibroblasts, the cells responsible for the generation of skin collagen. Recently, PO and Hyp-Gly were demonstrated to alleviate a skin barrier dysfunction as well as modulate gene expression in skin (Shimizu et al., 2015). Moreover, the dipeptide PO promoted the activity of osteoblastic cells and the differentiation of chondrocytes (Nakatani et al. 2009; Kimira et al., 2014).

Unlike native collagen which is resistant to *in vivo* digestion, CHs are relatively easily digested and absorbed upon oral administration. Iwai et al. (2005) identified food-derived collagen peptides in human blood such as PO, Ala-Hyp, Pro-Hyp-Gly, and others, among which the dipeptide PO was the most prevalent peptide accounting for up to 95% of CHs in the blood after the ingestion of porcine type I collagen peptides. These findings were confirmed by Ohara et al. (2007) who also reported that CHs were absorbed mainly in Hyp-peptide form rather than free Hyp form due to the great enzymatic stability of Hyp-containing peptides. Although the dipeptide PO is more stable and bioavailable than other collagen peptides, its bioavailability is still limited

due to its low transepithelial permeability (Aito-Inoue et al., 2007). Therefore, in the present study, a representative collagen-derived bioactive dipeptide PO was selected to study the possibility of improving its transepithelial permeability.

The bioavailability of protein and peptides largely lies on their ability to cross the intestinal mucosa before reaching the systemic circulation; thus two major challenges in developing an effective peptide-delivery system are gastrointestinal instability and low intestinal permeability. The intestinal transport of peptide can be improved para- and transcellularly, by co-administrating with permeation enhancers and by using nano-carriers, respectively. However, the former strategy may introduce significant toxicity resulting from the perturbation of intestinal barrier, while the latter strategy may require large dose usage and be lack of control on peptide release (Renukuntla et al., 2016; Maher et al., 2013). Another promising approach is to conjugate with a specific molecule, such as glucose or chimeric vectors like insulin fragments, since these would be able to naturally penetrate the cell membrane via specific pathways (Adessi and Soto, 2002). Studies here offer encouraging results of enhanced permeability, stability and lower chances of toxicity.

Glucosamine (GlcN) is widely used as a natural dietary supplement to mitigate symptoms of osteoarthritis and improve joint function (Ibrahim et al., 2012). Previous research has demonstrated that the chemical conjugation of GlcN by amidation with etodolac can reduce the toxicity of etodolac (Pandey et al., 2013). Alternatively, esterification with Gly-Val can improve the intestinal permeation of GlcN itself (Kohan et al., 2015). Therefore, in the present study, the amino sugar GlcN, which is naturally transported by GLUT1, 2, and 4 (Uldry et al., 2002), was used to conjugate the target dipeptide PO. PO is primarily absorbed by the brush-border membrane through the di- and tripeptide transporter PepT1 (Aito-Inoue et al., 2007). We hypothesized that this conjugation may introduce multiple mechanisms of absorption to the synthesized glycopeptide,

including those devoted to GlcN transport (i.e. GLUTs) and the one specific for PO (i.e. PepT1). Our objective was to create an enzymatically stable PO glycopeptide with improved intestinal permeability, and to study its transepithelial transport mechanism using a Caco-2 cell model.

4.2. Materials and Methods

4.2.1 Chemicals

D-(+)-Glucosamine hydrochloride, dimethylformamide (DMF), triethylamine (TEA), *N*-methylmorpholine (NMM), Fmoc-Cl, dichloromethane (DCM), piperidine, amantadine hydrochloride (ADAM), acetonitrile (ACN), porcine pepsin (3,200-4,500 units/mg protein), porcine pancreatin (8×USP specifications), monobasic potassium phosphate, trichloroacetic acid (TCA), and ammonium formate were purchased from Sigma-Aldrich (St. Louis, MO, USA). Benzotriazol-l-yl-*N*-oxy-tris-(dimethylamino) phosphonium hexafluorophosphate (BOP) was from Novabiochem® products (EMD Millipore Corporation, Etobicoke, ON, CA). *1*-Hydroxybenzotriazole (HOBt) was provided by ApexBio Technology (Boston, MA, USA). The protected dipeptide Fmoc-Pro-Hyp (>98%) was purchased from Biomatik Corporation (Cambridge, ON, CA), dipeptide Pro-Hyp (>99%) from Bachem Americas, Inc. (Torrance, USA), and Pro-Hyp-Gly (>98%) from GenScript (Piscataway, NJ, USA).

Cell culture supplies such as Caco-2 cells (HTB-37) and methylthiazolyldiphenyl-tetrazolium bromide (MTT) Cell Proliferation Assay Kit were purchased from American Type Culture Collection (ATCC, Manassas, VA, USA). Morpholineethanesulfonic acid (MES), Lucifer yellow carbohydrazide lithium salt, cytochalasin D, wortmannin, Gly-Sar, phloretin, phloridzin dihydrate, quercetin, and dimethyl sulfoxide (DMSO) were the product from Sigma-Aldrich (St. Louis, MO, USA). Other cell supplies were obtained from Gibco (Life Technologies Inc., ON, CA), including Dulbecco's Modified Eagle Medium (DMEM), fetal bovine serum (FBS), Hank's

balanced salt solution (HBSS), penicillin, and *N*-2-hydroxyethylpiperazine-*N*-2-ethane sulfonic acid (HEPES).

4.2.2. Synthesis and Purification of Collagen-derived Glycopeptide Pro-Hyp-CONH-GlcN (POGlcN)

The collagen-derived glycopeptide POGlcN was synthesized by a stepwise solution phase synthesis according to Kohan et al. (2015) with some modifications. Firstly, GlcN (1eq) was dissolved in the mixture of DMF/TEA (5/1, v/v), and Fmoc-Pro-Hyp-OH (1eq) was dissolved in DMF. After Fmoc-Pro-Hyp-OH was pre-activated in DMF by BOP (1eq) in the presence of HOBt (1eq) and NMM (1eq), the GlcN mixture was added to react overnight with continuous shaking (200 rpm). In this step, the coupling reaction occurred between the activated carboxylate group of the dipeptide and the primary amine group of GlcN to form an amide derivative Fmoc-Pro-Hyp-CONH-GlcN. The temporary protective N-Fmoc group was then removed by adding piperidine to a final concentration of 20% (v/v), performed for 45 min to achieve a complete removal. The reaction mixture was then precipitated with 15-fold volume of cold diethyl ether for at least 4 hours at 4°C. The precipitate was rinsed two more times with diethyl ether and air-dried overnight to obtain the crude glycopeptide.

The crude product was then redissolved in distilled deionized water and purified according to its LC-MS profile. The samples were firstly separated by C18 column (Ascentis® Express, 2.7 μm, 15 cm × 4.6 mm) using an HPLC unit (Agilent 1100 series) with a binary pump. Briefly, the sample was separated by C18 column (Ascentis® Express, 2.7 μm, 15 cm × 4.6 mm) on a reverse phase HPLC unit (Agilent 1100 series). The crude product was eluted at a flow rate of 0.6 mL/min with a gradient of mobile phase A (0.1% acetic acid in water) and B (0.1% acetic acid in ACN): 0-25% B during 0-30 min, 25% -99% B during 30-42 min, 99% B during 42-47 min, 99%-

0% B during 47-50 min, and 0% B during 50-56 min. The signal was monitored at 214 nm by UV detector and the samples subjected to analysis using a triple quadrupole mass spectrometer, 4000 Q Trap LC/MS/MS System (Applied Biosystems/MDS Sciex) acquiring spectra in a positive ion mode. The parameters applied to the MS were: ion source temperature 500°C, capillary voltage 4500 V and the curtain gas at 20 psi. The corresponding peak with *m/z* 390 was collected as eluted out from LC. The collected solution was pooled and lyophilized to obtain the final POGlcN acetate. This lyophilisation process was repeated two more times to maximize the removal of excess acetic acid. The final product was stored at -20˚C.

4.2.3 Structural Characterization of the Collagen-derived Glycopeptide POGlcN by Tandem Mass Spectrometry (MS/MS$_n$) and Nuclear Magnetic Resonance Spectroscopy (NMR)

The identification of POGlcN was firstly confirmed by MS/MS$_n$ using a LTQ Orbitrap XL hybrid ion trap-orbitrap mass spectrometer (Thermo Scientific) calibrated with standard ion calibration solutions (Pierce LTQ, Thermo Scientific). Direct infusion of sample was performed at a flow rate of 5 µL/min using the on-board syringe pump. The mass spectrometer was operated using an electrospray ionization source in a positive mode with a source voltage of 4.0 kV and sheath gas flow rate of 10.0. The analyses were conducted at a resolving power of 60.000 full-width/half-maximum peak height and spectra were acquired over the range of *m/z* 100 - 500. The peaks at 390.19 and 391.19 *m/z* were isolated and fragmented at a normalized collision energy (NCE) of 27. Then the product ion with m/z at 372.18 was further isolated and a MS/MS/MS was performed at an NCE of 25. The data was acquired and reported by Tune Plus 2.7 software (Thermo Scientific).

To verify structure, purity and composition of the synthesized glycopeptide, the final product was dissolved in deuterium oxide and subjected to ^{1}H and ^{13}C NMR spectroscopy. The

data were acquired on a four channel 700 MHz Agilent VNMRS spectrometer using a HCN z-gradient pulsed field gradient cold probe. The data were processed with VNMRJ 4.2A software (Agilent Technologies).

4.2.4 Simulated Gastrointestinal (GI) Digestion of the Collagen-derived Glycopeptide POGlcN

To study the degradation in GI tract prior to the intestinal absorption, the glycopeptide POGlcN was subjected to a simulated GI digestion model. The simulated gastric and intestinal fluids were prepared as described in the United States Pharmacopeial Convention (Test Solutions, United States Pharmacopeia 35, NF 30, 2012). To prepare the gastric fluid, 50 mg sodium chloride was dissolved in 10 mL water, and 350 uL of 6 M HCl was added to adjust the pH. Eighty mg of pepsin was then gently mixed into the solution. Before diluting the test solution with water to 25 ml, aliquots of 0.2 M HCl/0.2 M NaOH were used to adjust to pH 1.2. The intestinal fluid was prepared by dissolving 68 mg monobasic potassium phosphate in 5 ml water, 770 μL 0.2 M NaOH then mixed before adding 100 mg pancreatin. Similarly, the test solution was gently mixed, and adjusted to pH 6.8. Sufficient water was added to make the final volume up to 10 mL. Both simulated fluids were freshly prepared immediately before use, at pH 1.2 and 6.8 for gastric fluid (0.32% w/v pepsin) and intestinal fluid (0.68% w/v pancreatin), respectively.

The digestion of POGlcN was investigated according to the method from Sontakke et al. (Sontakke et al., 2016) with some modifications. Briefly, 40 μM of POGlcN was incubated in the simulated gastric or intestinal fluid at 37°C for 2 h in a shaking incubator (200 rpm). The digestion was terminated and precipitated at 0, 15, 30, 60, 120 min with TCA containing Pro-Hyp-Gly as internal standard to make the final TCA concentration of 20% (w/v). Meanwhile, matrix blank without POGlcN was prepared. To facilitate the precipitation, the sample was then placed in an

ice bath for 10 min before centrifugation at 5000 × g for another 10 min at 4°C. Aliquot of the supernatant was collected, neutralized, and immediately analyzed to determine the remaining amount of intact POGlcN using UHPLC according to the method described below. Simultaneously, the chemical stability of the glycopeptide POGlcN was assessed by incubating with the enzyme-free gastric/intestinal fluid and determined the same way as described above for the experimental fluids. The results were calculated as follows:

$$\text{Remaining percentage (\%)} = \frac{remaining\ amount\ of\ intact\ POGlcN\ (\mu g)}{originally\ applied\ amount\ of\ intact\ POGlcN\ (\mu g)} \times 100\%$$

4.2.5. Caco-2 Cell Culture

The Caco-2 cells were grown in DMEM supplemented with 10% FBS, 25 mM HEPES, and 1% penicillin in a 37°C incubator which maintains a 90% humidified atmosphere and 5% carbon dioxide. Cells grown on a 25 cm^2/75 cm^2 cell culture flasks (Corning, NY, USA) were subcultured by 0.25% (w/v) trypsin-0.91 mM EDTA when around 80% confluence was reached. To ensure the cell monolayer integrity and differentiation, cells at a density of 2×10^5/cm^2 were seeded on polycarbonate membrane transwell inserts (12 well, 12 mm diameter, 0.4 μm pore size, Corning, NY, USA); and then gently shaken to obtain uniform cell distribution. During the incubation, cell growth media were carefully replaced every two days without damaging the monolayer. After 21-23 days' growth and differentiation, the integrity of the cell monolayers was assessed by measuring the transepithelial electrical resistance (TEER) and the permeability of Lucifer yellow. Only monolayers with TEER higher than 450 Ω•cm^2 were used for transport experiments. The cytotoxicity assay was performed using MTT assay as described in the instructions from ATCC (ATCC, MTT cell proliferation assay). The cells used were between passages 18 and 24.

4.2.6. Permeability Assay of Glycopeptide POGlcN, PO, and GlcN in the Caco-2 Cell Model

To verify the hypothesis that conjugation of the collagen-derived dipeptide PO with GlcN promotes its transport efficiency, permeability of the glycopeptide POGlcN, dipeptide PO, and GlcN were compared in the human intestinal epithelial Caco-2 cell model. According to Feng & Betti (2017a), the growth media were changed 12 to 24 h before the transport experiment to maintain the performance of the cell monolayer. To mimic the *in vivo* intestinal acid microclimate (Hubatsch et al., 2007), the transport experiments were conducted with a pH gradient, i.e. HBSS/MES buffer (pH 6.5, 10 mM MES in HBSS) in the apical chamber, and HBSS/HEPES buffer (pH 7.4, 10 mM HEPES in HBSS) in the basolateral chamber. On the day of transport, the cell monolayers were firstly rinsed twice with pre-warmed HBSS to wash out the remaining DMEM, and then equilibrated with 0.5 mL HBSS/MES (apical) and 1.5 mL HBSS/HEPES (basolateral) for 30 min. For the apical to basolateral transport (AB transport) experiment, 0.5 mL of the POGlcN, PO, and GlcN at a non-toxic concentration of 1 mM in HBSS/MES were applied to the apical side, and 1.5 mL HBSS/HEPES without test compounds were filled in the basolateral side. To measure the transport efficiency of each compound, 300 µL of each sample was withdrawn from the basolateral chamber at pre-determined time points of 0, 15, 30, 45, and 60 min. Meanwhile an equal volume (300 µL) of test compound-free and pre-warmed HBSS/HEPES media were supplemented. In addition, the bi-direction transport of POGlcN was carried out to better understand its transport efficiency. For the basolateral to apical transport (BA transport), similarly, the 1.5 mL of 1 mM POGlcN sample in HBSS/HEPES was loaded at basolateral side, while 0.5 mL compound-free HBSS/MES at apical side. Fifty microliters were withdrawn from the apical side and replaced with equal volume of HBSS/MES at the same time points mentioned above. Collected samples were subjected to analysis using UHPLC as described below. Moreover,

Lucifer yellow (1 mM) was used as paracellular marker during the experiment. The concentration of Lucifer yellow was determined using UHPLC with a fluorescent detector (excitation 428 nm, emission 536 nm). The transport efficiency of each compound was evaluated by apparent permeability coefficient (P_{app}) which was calculated with the following equation: $P_{app}(\text{cm/s}) = \frac{dQ}{dt} \times 1/(A \times C_0)$, where t is the incubation time (s), dQ/dt is the cumulative amount change of the intact test compound over time (pmol/s) at the receiver side, A is the surface area of the transwell insert (cm^2), C_0 is the initial concentration of the test compound at the donor side (pmol/cm^3). The resistance of PHG to degradation by the brush border enzymes and endocellular enzymes was assessed by measuring the presence of its digested and transported form-PH, GlcN, etc., at the basolateral side when it is applied apically.

4.2.7. Transport Experiment of POGlcN, PO and GlcN in the Presence of Various Transport Inhibitors/Interrupters

To investigate the transport mechanism of POGlcN across the Caco-2 cell monolayer, the effects of different transport inhibitors/interrupters on POGlcN were studied in comparison to that on GlcN and dipeptide PO. The experiment was performed according to Miguel et al. (2008) and Alzaid et al. (2013) with some modifications. Similar with the permeability assay, the cell monolayers were firstly gently rinsed with HBSS, and pre-incubated for 30 min with 0.5 µg/mL cytochalasin D (a tight junction interrupter), 500 nM wortmannin (a transcytosis inhibitor), 10 mM Gly-Sar (a competitive PepT1 substrate), 0.1 mM quercetin (a GLUT1 and 2 inhibitor), 0.1 mM phloretin (a GLUTs inhibitor), and 0.1 mM phloridzin (a SGLTs inhibitor), respectively. One millimolar of glycopeptide POGlcN, dipeptide PO, and GlcN were then applied apically on the monolayer in the presence of inhibitors/interrupters for 60 min, respectively. Gly-Sar was dissolved in HBSS/MES, while all other inhibitors were dissolved in DMSO and diluted with

HBSS/MES before adding on the monolayers (the final DMSO concentration was 0.044%). The control experiments were conducted by pre-incubating with 0.044% DMSO and HBSS/MES. Samples were then collected from the basolateral compartment and detected by UHPLC analysis as described below.

4.2.8. Analysis by UHPLC with Fluorescence Detection

Fmoc-Cl can react with the amino group to form a highly fluorescent compound. It has been used as an established derivatization reagent for the determination of amino acids, and was also extended to be used for the analysis of GlcN due to the amino group presence. In the present study, the determination of POGlcN, PO, and GlcN were performed with Fmoc-Cl pre-column derivatization using a UHPLC unit (Shimadzu, Columbia, MD, USA) according to Ibrahim and Jamali (2010) with some modifications. In brief, 100 µL of the sample was firstly mixed with 40 µL of 0.2 M borate buffer (pH 8.0) before being derivatized with 60 µL of 0.16 mM Fmoc-Cl (dissolved in ACN) for 30 min at 30°C. Fifty microliters of 6 mM ADAM (dissolved in 80% ACN (v/v)) was then added to consume the excess Fmoc-Cl and terminate the derivatization. Thirty microliters of the final derivatized sample was then injected into the UHPLC and separated by a Ascentis®Express HILIC column (10 cm × 4.6 mm I.D., 2.7 µm particles). The sample was eluted at 0.5 mL/min by mobile phase A: 13 mM ammonium formate in water and mobile phase B: 13 mM ammonium formate in 90% ACN with a 40-min gradient: 0-8 min with 100% B, 8-23 min from 100% to 55% B, then gradually increase to 100% B within 2 min, and finally maintain 100% B for 15 min. The column oven temperature was controlled at 35°C during the elution and the sample was finally detected by a fluorescent detector (excitation at 263 nm, emission at 315 nm). Standard curves for GlcN and POGlcN were linear quantifiable over the concentration range of

0.1 to 4 µg/mL ($R^2 \geq 0.99$), and for PO 0.05 to 4 µg/mL ($R^2 \geq 0.99$). All the analyses were repeated at least two times.

4.2.9. Statistical Analysis

All the data was analyzed using one-way analysis of variance by SAS 9.4 (Cary, NC, USA). Multiple comparisons of means were done by Tukey's test where $p \leq 0.05$ was considered significantly different.

4.3. Results and Discussion

4.3.1 Synthesis and Structure Characterization
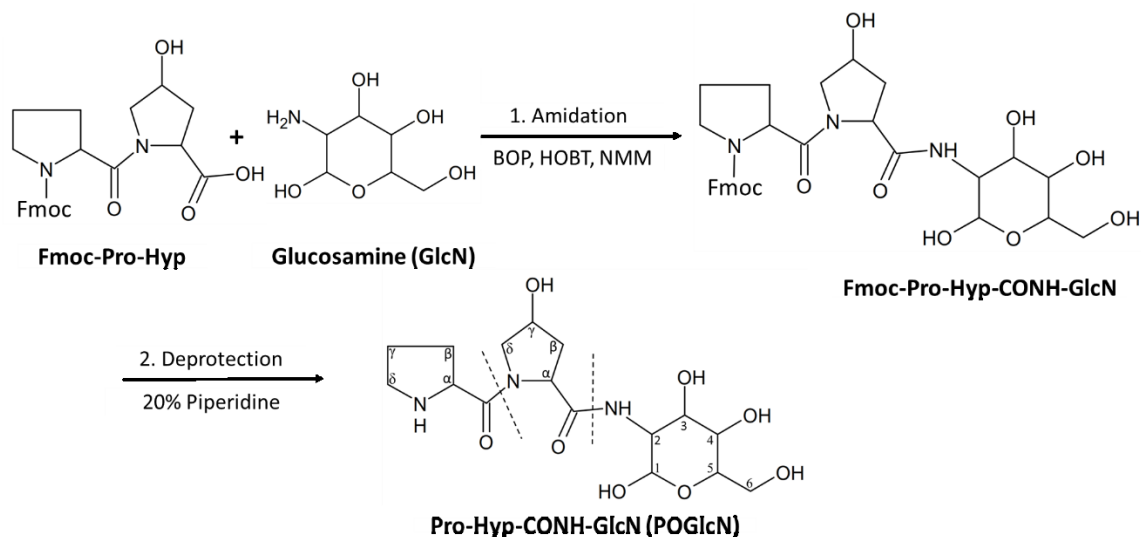
Figure 4.1. Synthetic scheme for the solution-phase synthesis of glycopeptide Pro-Hyp-CONH-GlcN (POGlcN)

Peptide synthesis in solution phase is an established conventional method utilized for the chemical synthesis of small peptides. As the name implied, the peptide is synthesized in organic solution such as DMF by coupling the amino and carboxyl groups of two amino acids to form an amide bond. GlcN could also be an appealing amine donor considering its reactive amino group similar with that of an amino acid. Typically, reagents like carbodiimides and phosphonium salts

are used to accelerate the coupling between the amino and carboxyl groups of two amino acids, and protection groups such as Boc and Fmoc are used for the alpha-amino protection to avoid side reactions (Wade, 2000). We gained insight from this solution-phase synthesis method and utilized this strategy in the present study. Here, an amide derivative was rapidly synthesized by conjugating the carboxyl group of Fmoc-protected PO with the C2-amino group of GlcN under the activation of phosphonium salts BOP (schematic synthesis is summarized in Figure 4.1). After purification and lyophilisation, the final product in acetate form (white powder) yielded $37.0 \pm 1.5\%$ with no detectable contamination signal using HPLC UV detector at 214 nm (Figure 4.2), and the identity of the glycopeptide was confirmed by MS/MS_n (Figure 4.3). In Figure 4.3A, the protonated glycopeptide $(M+H)^+$ showed a major peak at m/z of 390.19 and a small shoulder peak on its right side with m/z of 391.19 while the latter from the ^{13}C isotope form. Except for the major glycopeptide peaks, there were minimal contamination peaks. The MS/MS fragmentation pattern of these glycopeptide peaks are shown in Figure 4.3B. A fragment of Hyp-GlcN with a monoisotopic molecular mass of 292.13 Da was found as a pseudomolecular ion $(M+H)^+$ at m/z 293.13 and 294.13 from the precursor ions at m/z 390.19 and 391.19, respectively. The major fragment peak at m/z 372.18 was the dehydrated form of ion 390.19. The peaks at m/z 229.12 and 211.11 corresponded to Pro-Hyp fragment and its dehydrated form, respectively. GlcN fragment and its dehydrated form were found at m/z 180.09 and 162.08, respectively. The major peak at m/z 372.18 was further fragmented to obtain a pattern shown in Figure 4.3C. Interestingly, this pattern almost mirrors the one for intact glycopeptide presented in Figure 4.3B. No peak at m/z 293.13 was detected; however, the ion at m/z 275.12 was probably its dehydrated form. These two similar fragment patterns confirmed the Pro-Hyp-GlcN composition of the glycopeptide.

To further confirm the chemical bond between Hyp and GlcN, and purity of the glycopeptide, the ^{1}H and ^{13}C NMR spectroscopy was used to generate spectra (Figure 4.4). As the glycopeptide was in the acetate form, a peak occurred with the chemical shift of 1.88 ppm, which indicates the presence of acetic acid as shown in Figure 4.4 (^{1}H NMR). Only minor peaks from impurities present in the spectra indicated that the final glycopeptide had purity around 96%. GlcN usually exists in equilibrium with two anomers when dissolved in water, the α anomer and β anomer, at a ratio of 63:37 (Horton et al., 1966). In this study, the two peaks with chemical shifts of 5.20 and 4.77 ppm represent the H1 of α and β anomers of GlcN residue, respectively (Table 4.1); they gave a ratio of 64:36 upon the integration of their signal intensities. This shows that the GlcN anomers ratio was maintained in the glycopeptide form. Along with the ^{1}H spectra, the ^{13}C NMR spectra confirmed the amide bonds between Hyp and GlcN, and between Pro and Hyp, representing the carbonyl chemical shifts at 176.14 and 171.10 ppm, respectively. Other proton and carbon arrangements are summarized in Table 1 which are consistent with ^{1}H TOCSY, ^{1}H COSY, ^{1}H-^{13}C HSQC and ^{1}H-^{13}C HMBC 2-D NMR spectra (data not shown). The label and position of each hydrogen and carbon is indicated in the POGlcN structure in Figure 4.1. Taken all together, the glycopeptide was verified as an amide derivative Pro-Hyp-CONH-GlcN (POGlcN), which maintained the structure of both components. The synthesis and purification processes were effective to produce this very pure glycopeptide POGlcN with a molecular weight of 389.19 Da.
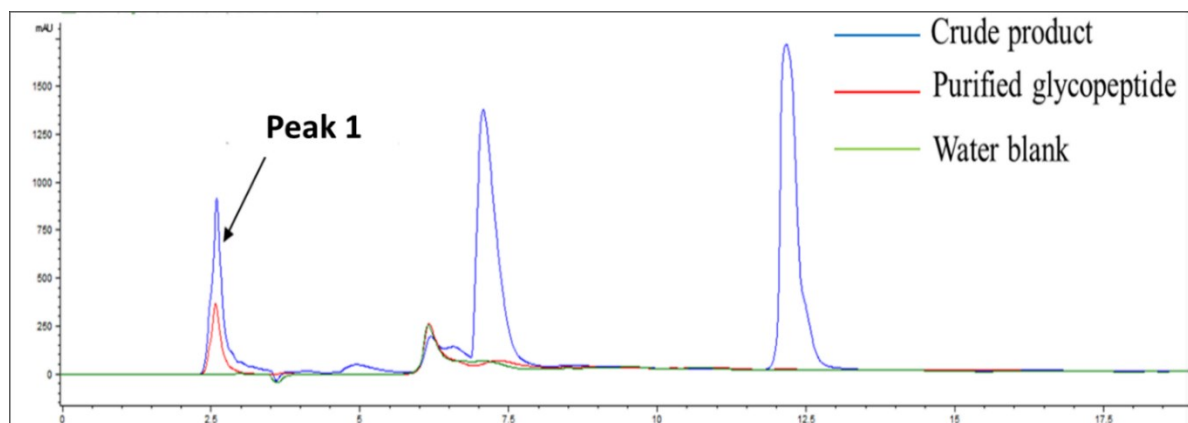
Figure 4.2. HPLC chromatographs of the synthesized glycopeptide before and after the HPLC purification. Peak 1 is identified by LC-MS/MS as the glycopeptide Pro-Hyp-CONH-GlcN.
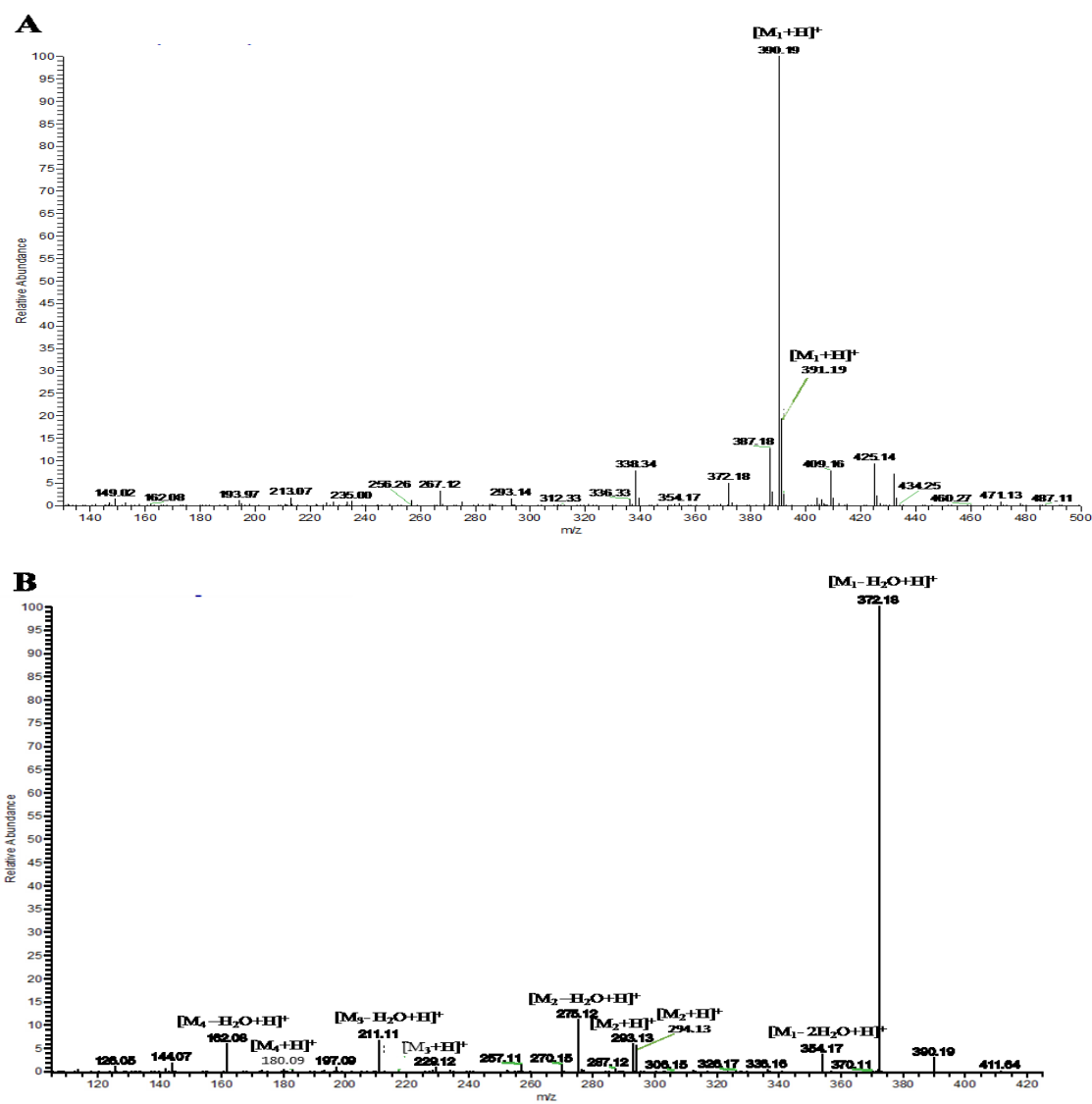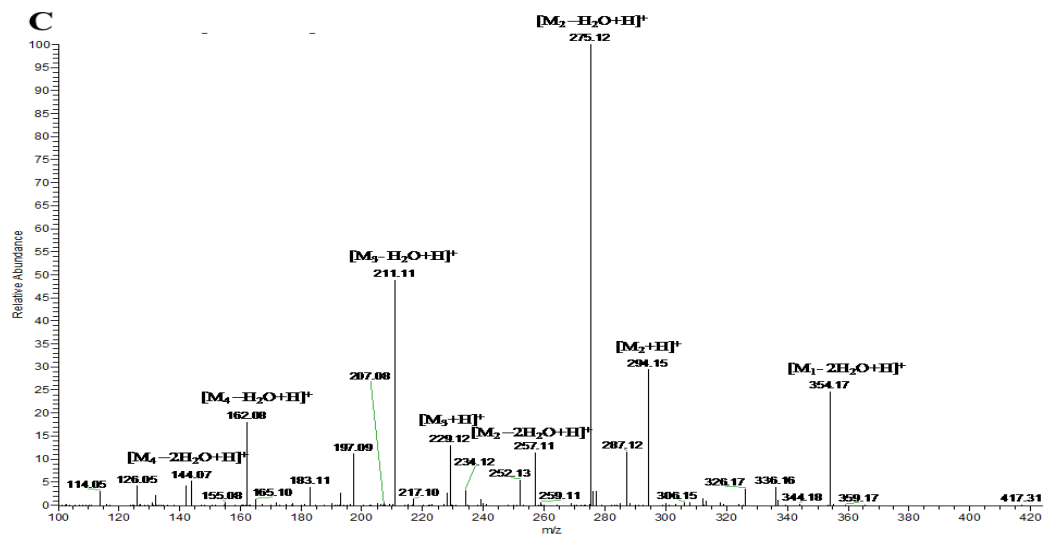
Figure 4.3. Mass spectrometry analysis of the synthesized glycopeptide Pro-Hyp-CONH-GlcN (POGlcN) after purification using HPLC. (A) Mass spectra of the glycopeptide; (B) MS/MS fragment pattern of the glycopeptide m/z at 390.19 and 391.19; (C) MS/MS/MS fragment pattern of the dehydrated glycopeptide m/z at 372.18, M_1 denotes the molecular weight of POGlcN (389.19), M_2 denotes the molecular weight of Hyp-GlcN (292.13 Da), M_3 denotes the molecular weight of Pro-Hyp (228.12 Da), M_4 denotes the molecular weight of GlcN (179.08 Da).

4.3.2. Stability of the POGlcN

Similar with a tripeptide, the amide bond between Hyp and GlcN can be digested either by the GI proteases or by the harsh acidic environment of the stomach. Therefore, the stability of this newly synthesized glycopeptide POGlcN was assessed under simulated gastric and intestinal fluid conditions. As Figure 4.5 shows, around 5% of POGlcN was digested in simulated gastric fluid while around 10% of POGlcN was digested in simulated intestine fluid. The newly synthetized glycopeptide is relatively stable in the simulated GI digestion, unlike the findings of Pandey et al. (2013) where etodolac-CONH-GlcN, a nonsteroidal anti-inflammatory prodrug against arthritis, was easily digested in simulated intestinal fluid. The good stability of this amide POGlcN implies the potential protective effect of the dipeptide PO as compared to the etodolic acid in etodolac-CONH-glucosamine. In the testing of control systems, the degradation of the POGlcN was

negligible in pancreatin-free intestinal juice and pepsin-free acidic gastric juice, indicating its good chemical stability. In summary, the results suggest POGlcN exerted satisfactory GI enzymatic and chemical stability for at least 2 h. This is consistent with the findings of Sontakke et al. (2016) about the good stability of tripeptide Gly-Pro-Hyp which shares a similar structure with the glycopeptide POGlcN.
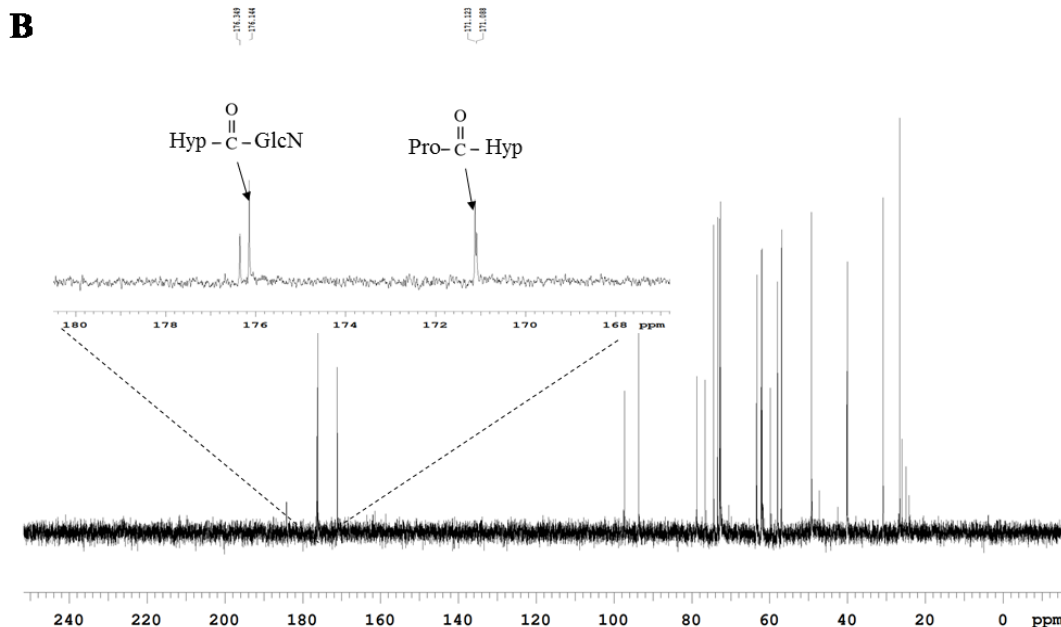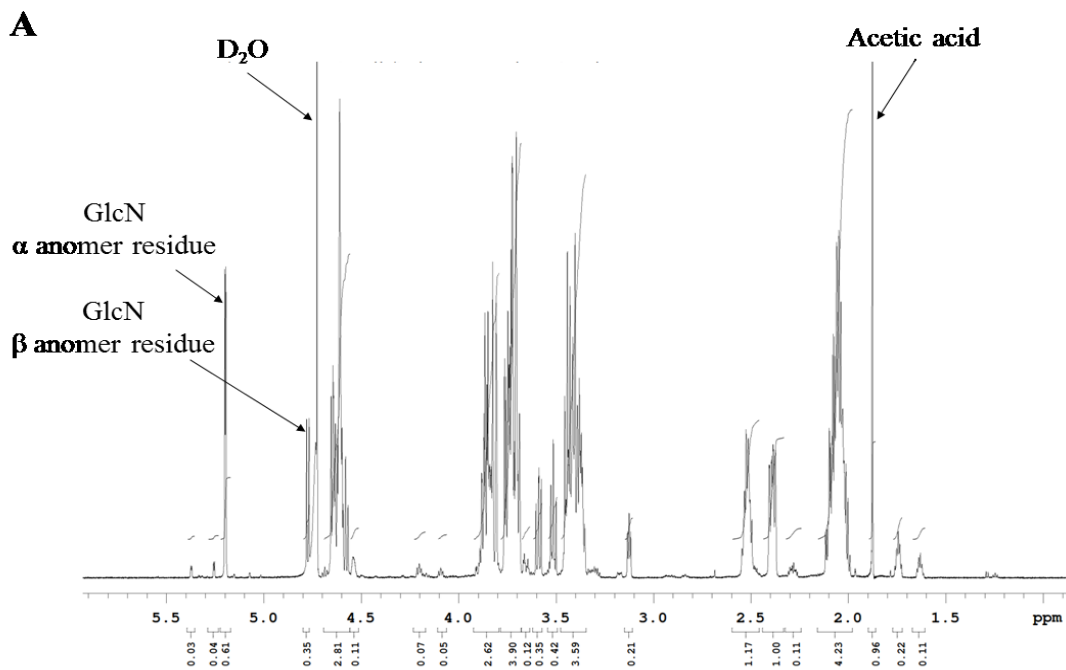
Figure 4.4. NMR spectra of the glycopeptide Pro-Hyp-CONH-GlcN (POGlcN) acetate. (A) ^{1}H NMR spectra; (B) ^{13}C NMR spectra.
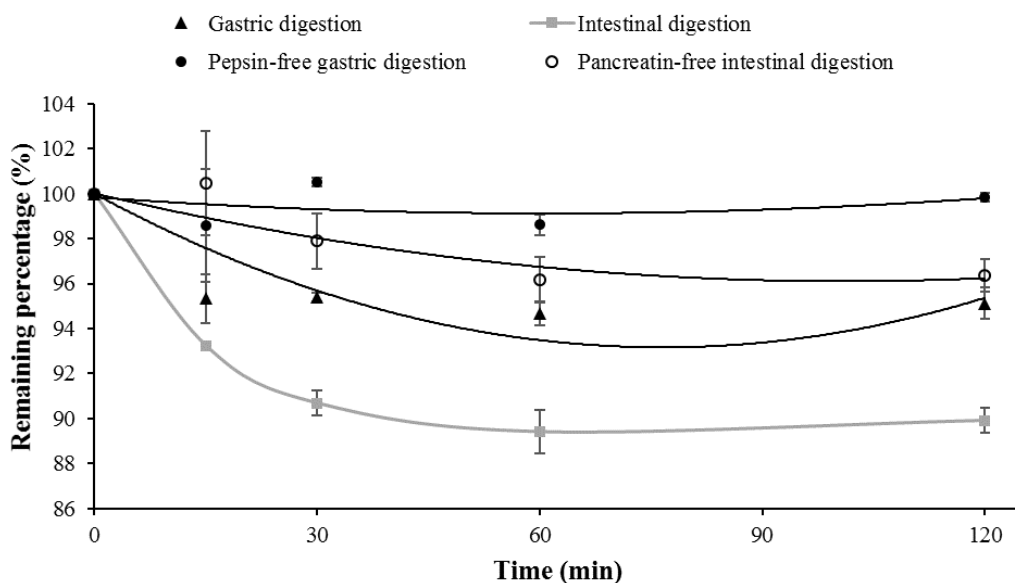
Figure 4.5. Remaining amount of Pro-Hyp-CONH-GlcN (POGlcN) over time in simulated gastric juice, intestinal juice, and corresponding enzyme-free juice controls, respectively. Bars represent standard deviation (n=3).

4.3.3. Permeability of the Glycopeptide POGlcN, PO, and GlcN Across the Caco-2 Cell Monolayer

Caco-2 cells are grown on a semi-permeable membrane which allows the nutrients, ions, and water to diffuse to both sides, and the cells can well differentiate into polarized epithelial monolayer to exhibit the typical morphological and functional characteristics of human intestine mucosa (Hidalgo et al., 1989). The permeability through this monolayer is used to predict the corresponding *in vivo* intestine transport especially for drugs which are absorbed paracellularly due to the good correlation (Artursson et al., 2012). This well characterized system has been a widely used *in vitro* model for studying the transport and metabolism of drugs and chemicals in the last three decades. As a small hydrophilic compound, Lucifer yellow normally crosses the

Caco-2 cell monolayer through the tight junctions among the cells (Artursson et al., 2012). In the

present study, Lucifer yellow was used as a reference compound to validate the suitability of the

Table 4.1. Proton and carbon assignments of the Pro-Hyp-CONH-GlcN (POGlcN) from ^{1}H NMR
and ^{13}C NMR

	Proton NMR				Carbon NMR	
Assignment	Chemical Shift (ppm)	Coupling constant (Hz)	Multicity	Assignment		Chemical Shift (ppm)
Pro Residue						
Hα	4.64	$J = 6.90$	dd	Cα		61.89
Hβ$_a$, Hβ$_b$	2.51, 2.04	$J = 8.30$	m	Cβ		31.05
Hγ	2.05	-[a]	m	Cγ		26.59
Hδ$_a$, Hδ$_b$	3.42, 3.39	-	m	Cδ		49.30
				C=O		171.10
Hyp Residue						
Hα	4.60	-	dd	Cα		62.10
Hβ$_a$, Hβ$_b$	2.38, 2.08	-	m	Cβ		40.08
Hγ	4.60	-	m	Cγ		72.60
Hδ$_a$, Hδ$_b$	3.75, 3.72	-	m	Cδ		58.06
				C=O		176.14
GlcN α Isomer Residue						
H1	5.20	$J = 3.50$	d	C1		93.61
H2	3.86	$J = 10.90$	dd	C2		57.08
H3	3.71	$J = 9.30$	dd	C3		73.41
H4	3.43	$J = 9.30$	dd	C4		72.83
H5	3.82	-	ddd	C5		74.36
H6$_a$, H6$_b$	3.81, 3.76	$J = 5.00, 12.10$	dd, dd	C6		63.28
GlcN β Isomer Residue						
H1	4.77	$J = 8.90$	d	C1		97.19
H2	3.58	$J = 10.10$	dd	C2		59.94
H3	3.51	$J = 8.80$	dd	C3		76.58
H4	3.39	$J = 9.80$	dd	C4		72.77
H5	3.43	$J = 1.40$	ddd	C5		78.66
H6$_a$, H6$_b$	3.86, 3.70	$J = 5.40, 12.10$	dd, dd	C6		63.58

[a] Data not available.

Caco-2 cell monolayer. We found that Lucifer yellow had a P_{app} = 3.05×10^{-7} cm/s with a permeability lower than 0.24% after 60 min, when TEER of the monolayers were above 450 $\Omega \bullet cm^2$. This performance of Lucifer yellow is comparable with previously reported screening standards, for the Lucifer yellow transport < 0.25% and P_{app} < 3×10^{-6} cm/s (Hidalgo et al., 1989; Nožinić et al., 2010). The Caco-2 cell model in this study was therefore reliable to predict the transepithelial transport of test compounds. Moreover, a concentration of one millimolar of POGlcN was justified as non-saturable condition in our model, since the apical to basolateral transport of newly synthesized PHG was linearly concentration dependant over the range of 0 to 2 mM (Figure 4.6).
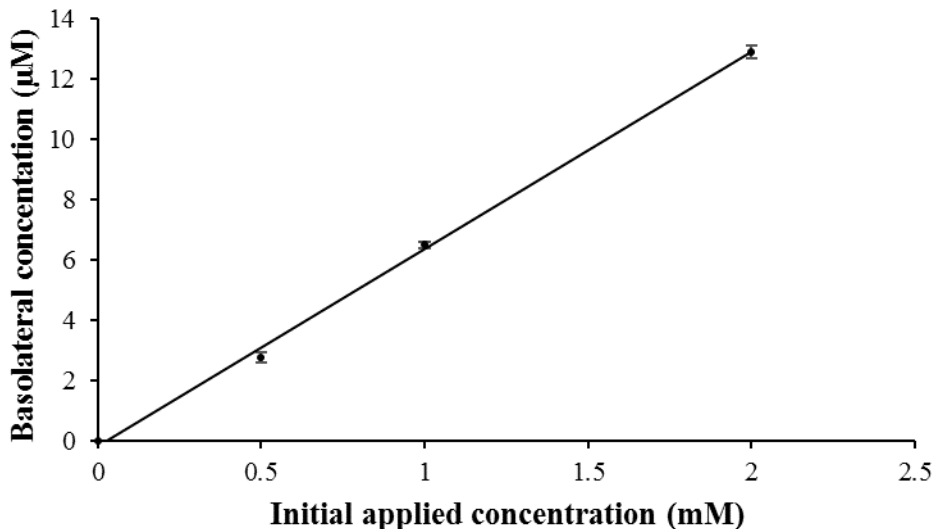
Figure 4.6. Concentration effect of Pro-Hyp-CONH-GlcN (POGlcN) on its apical to basolateral transport across Caco-2 cell monolayer. Error bars represent standard deviation (n≥3).

The chromatographic separation of derivatized POGlcN, PO, and GlcN is shown in Appendix D. The permeability of POGlcN, PO, and GlcN were compared in Figure 4.7A, which shows that the transported amount of all three compounds from apical to basolateral showed good linearity ($R^2 \geq 0.96$) over time in the range from 15 to 60 min. The incubation time axis intercept of each linear line indicates the lag time for each compound, i.e. 9.5 min for POGlcN, 16.3 min

for GlcN and 12.9 min for PO. The lag time is defined as the time needed for one compound to reach steady-state flux from which the P_{app} is calculated. It takes some time for the test compounds to partition into the absorption surface and well equilibrate, so these lag times are expected and typical (Tavelin et al., 2002). During the permeability assay, POGlcN exerted significantly greater P_{app} ((2.82 ±0.15) ×10^{-6} cm/s) than that of PO ((1.45 ± 0.17) ×10^{-6} cm/s) and GlcN ((1.87 ± 0.15) ×10^{-6} cm/s), respectively. These values are similar with those reported for bioactive oligopeptides such as QIGLF and RVPSL in other studies (Ding et al., 2014; Ding et al., 2015). The P_{app} of PO is much greater than that the 0.13×10^{-6} cm/s value as reported by Sontakke et al.,[20] while the P_{app} of POGlcN is comparable to that of Gly-Pro-Hyp (1.09×10^{-6} cm/s) in the same study. The difference is likely due to the different transport mechanism involved, variable culturing conditions and protocols, and different cell origins. However, the final transport percentage of the total applied amount at the basolateral side after 60 min incubation were 1.95%, 0.98%, and 1.13% for PHG, PH, and GlcN, respectively, which are in the same range (<2%) as that of tripeptide VPP, YPI, and tetrapeptide PFGK and GGYR reported in previous studies (Satake et al., 2002; Miguel et al., 2008; & Shimizu et al., 1997). The greater permeability of POGlcN implies the positive effect of conjugation on transepithelial transport, and this additive effect was derived from the sugar moiety, GlcN. Interestingly, when only POGlcN was applied apically, except for POGlcN, an increasing amount of dipeptide PO was also found in the basolateral side as the incubation time increased (Figure 4.7B). After 60 min, the accumulated PO was around 0.28% of the originally applied POGlcN and 12.5% of total transported peptides. The minor presence of PO in the receptor side can be explained by the action of peptidases from the brush border membrane and endocellular enzymes. However, no free Pro was detected, which further confirms that PO and POGlcN are resistant or at least not significantly hydrolyzed when subjected to transepithelial transport.
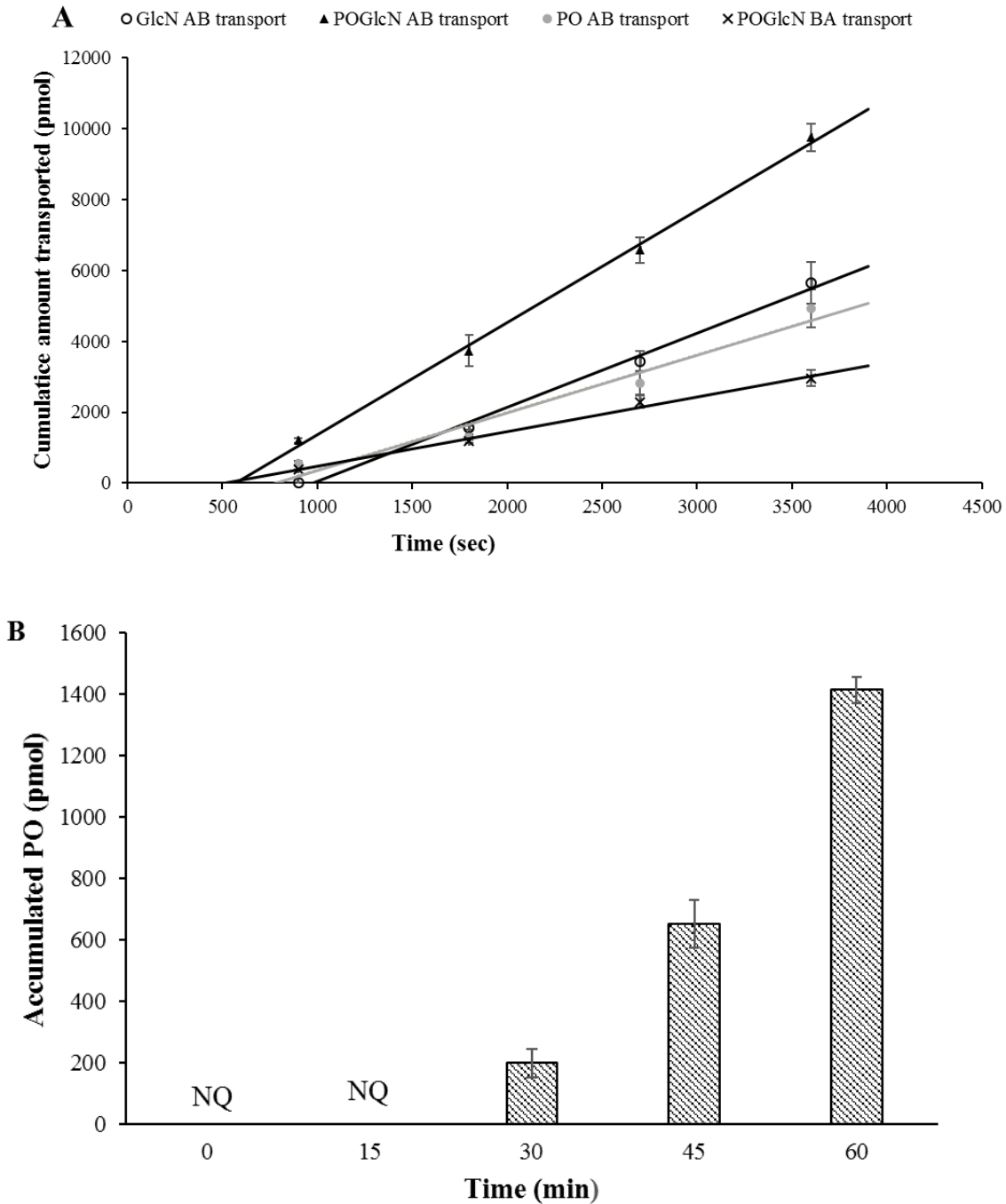
Figure 4.7. (A) Mean cumulative amount of Pro-Hyp-CONH-GlcN (POGlcN), Pro-Hyp (PO), and Glucosamine (GlcN) transported across the Caco-2 cell monolayer. "AB transport" refers that compounds were applied on the apical side, while "BA transport" refers that compounds were applied on the basolateral side. (B) Accumulated Pro-Hyp (PO) at the basolateral side over time when the POGlcN was applied at the apical side of the Caco-2 cell monolayer. NQ means PO

concentration is below the quantifiable linear range (<0.05 µg/mL). Bars represent standard deviation (n=3).

To have a more comprehensive understanding of the permeability of this novel glycopeptide, the POGlcN transport was done bi-directionally, i.e. apical to basolateral (AB transport) and vice versa (BA transport). As shown in Figure 4.7A, the AB transport of POGlcN was much faster than BA transport, with an uptake ratio ($P_{app,AB}/P_{app,BA}$) of 3.24. This asymmetrical permeation is a first indicator of active transport routes' involvement. Normally no clear difference of permeability between two directions appears if a compound is only passively transported.[22] The di- and tripeptide transporter PepT1 on the epithelial cells may actively shuttle the uptake of POGlcN because of its tripeptide-like structure. The lower uptake ratio of POGlcN than that of Gly-Sar (uptake ratio at 5) (Hubatsch et al., 2007), which is the substrate of PepT 1, suggests that the POGlcN may exert lower affinity to PepT1 transporter. However, the POGlcN uptake may also be the combined effect of passive and active pathways.

4.3.4. The Effects of Different Inhibitors/interrupters on the Transepithelial Transport of POGlcN

In general, di- and tripeptides uptake in intestinal epithelial cells largely depend on the proton-coupled transporter PepT1. In addition, peptides may also be absorbed through the passive diffusion across the lipid bilayer, endocytosis, and through paracellular channels of the tight junction (Artursson et al., 2012). The four hydroxyl groups and an imino group of POGlcN impart a significant hydrophilic nature, and thus is unlikely to passively merge into the cell membrane and be transported transcellularly (Shore et al., 1957). Instead, it is possible that POGlcN uses paracellular channels to access the serosal side. POGlcN could also be mediated via the previously mentioned carrier PepT1 due to its PO component which can be a substrate for PepT1 (Aito-Inoue

et al., 2007). On the other hand, as the NMR results indicated, POGlcN retained the structure of the sugar moiety GlcN; its exposed part shares a similar structure with glucose. In this respect, the chemical synthesis used in this study introduced the potential for this glycopeptide to be transported through a shuttle mechanism used by hexose, such as facilitated diffusion by GLUTs and active sodium-dependent transport by SGLTs (Augustin et al., 2010). Hence, inhibitors or interrupters for each potential transport pathway were used strategically to better understand the transport mechanism of POGlcN through the Caco-2 cell monolayers.

As shown in Figure 4.8A, after 60 min incubation, there was no significant effect of cytochalasin D and wortmannin on the accumulated amount of POGlcN and PO in the basolateral chamber compared to POGlcN and PO controls. Cytochalasin D is normally used to induce the

A

B
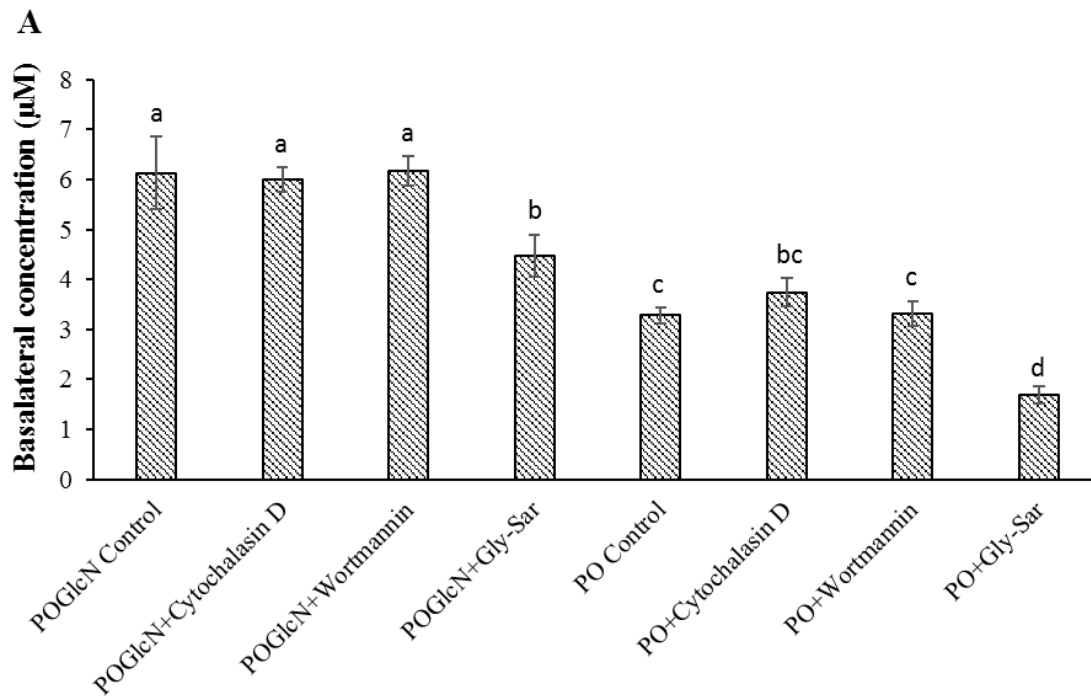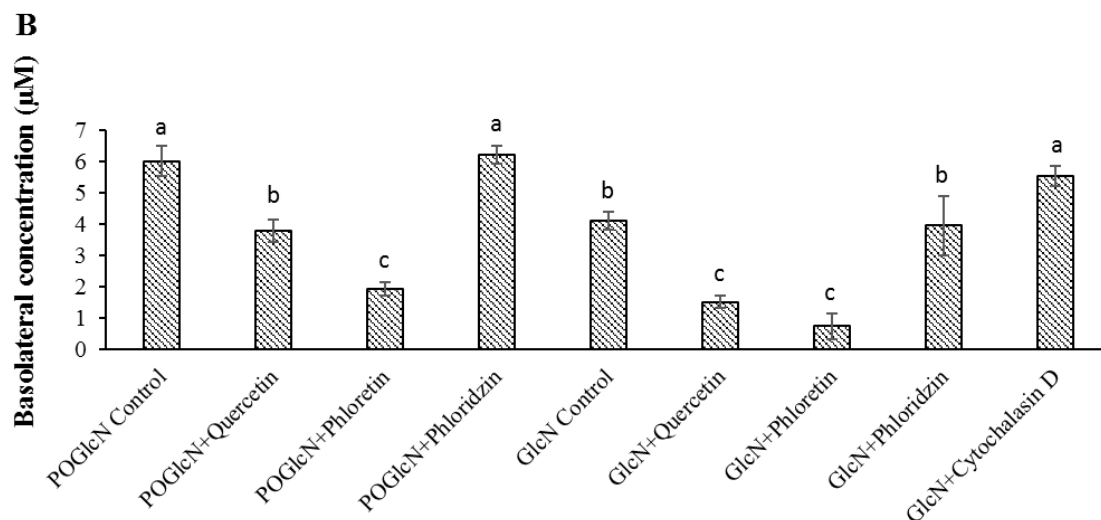
Figure 4.8. Transport mechanism experiment of Pro-Hyp-CONH-GlcN (POGlcN) on Caco-2 cell monolayer. (A) Basolateral concentration of POGlcN or Pro-Hyp (PO) in the presence/absence of different inhibitors/interrupters; (B) Basolateral concentration of POGlcN or glucosamine (GlcN) in the presence/absence of different inhibitors/interrupters. Bars represent standard deviation (n=3). Mean basolateral concentration followed by different letters indicates significant difference ($p \leq 0.05$).

structure change of the cytoskeleton and occluding junctions of epithelial cells, thus facilitating the movement of compounds across the tight junctions (Madara et al., 1986). Cytochalasin D slightly enhanced the permeability of PO; however, this was not statistically significant, so this paracellular pathway is not mainly involved. Despite some studies that emphasize the importance of paracellular route for the uptake of high molecular weight peptides (e.g. HLPLP) and peptide drugs (e.g. octreotide) (Quirós et al., 2008; Drewe et al., 1993), the cut off is usually <200 Da if acting as a major route (Fahmy et al., 2008), which likely explains the non-involvement of this pathway for the transport of PO and POGlcN. In contrast, the use of Gly-Sar, the typical substrate for PepT1, significantly reduced the absorption of both POGlcN (30% inhibition) and PO (50% inhibition), implying that PepT1 transporter significantly accounted for the transport of both peptides. This confirms the findings of Aito-Inoue et al. (2007) who revealed the involvement of

PepT1 in transporting PO. This is also consistent with Kohan et al. (2015) who proposed that a similar ester derivative Gly-Val-COO-GlcN was transported via PepT1. The lower inhibition efficiency of Gly-Sar for POGlcN as compared to PO may be due to the involvement of other transporters as previously hypothesized. Considering the peptide nature of POGlcN, in conjunction with the apical active uptake by PepT1, it may be discharged from the cells via the basolateral facilitative peptide transporter designated for small peptides (Terada et al., 1999).

Figure 4.8B parallels the transport mechanism of POGlcN with that of GlcN in the presence of inhibitors/interrupters to hexose-related pathways. POGlcN behaved similarly in the presence or absence of phloridzin, so did the GlcN. This was in accordance with the results from Tesoriere et al. (1972) who used everted intestine sacs to test the influence of phloridzin on GlcN transport and firstly proposed its sodium-independent transport mechanism. Since phloridzin exhibits variable efficacy as a competitive inhibitor on SGLTs, especially more on SGLT2 and 1 (Raja et al., 2015), its ineffectiveness on the permeability of POGlcN and GlcN suggests their lack of SGLTs-mediated pathways. SGLT cotransporters have a relatively strict specificity requiring the D-configuration and a free hydroxyl group at C2 position to recognize and bind (Kipp et al., 1997). Therefore, the amino group instead of hydroxyl group occupancy at the C2 position of both GlcN and POGlcN probably explains the non-involvement of SGLTs. In contrast, the accumulated basolateral concentration of POGlcN significantly decreased (67.9%) in the presence of phloretin, a competitive inhibitor especially for GLUT1 and GLUT2, and for GLUT 3 and GLUT 4 isoforms (Augustin, 2010). However, due to the absence of GLUT4 expression in Caco-2 cells (Mahraoui et al., 1994), the importance of GLUT1, 2, 3 isoforms should mainly explain the good permeability of POGlcN. This was further confirmed by the significant inhibitive effect on POGlcN (36.9% decrease) by quercetin, the inhibitor for GLUT1 and 2 transporters (Kwon et al., 2007; Vera et al.,

2001). Also, in a similar manner, phloretin and quercetin significantly reduced the permeability of GlcN by 82.1% and 63.3%, respectively, confirming that POGlcN used the same transport mechanism as GlcN. This can be explained due to the maintenance of an intact GlcN structure in the POGlcN molecule. In general, GLUT2 exhibits significant expression in Caco-2 cells after three weeks of growth (Takata, 1996), while the expression of both GLUT1 (in basolateral domain) and GLUT3 (in apical domain) decline rapidly during the differentiation (Mahraoui et al., 1994). Also, because GlcN has the greatest affinity to GLUT2 (Uldry et al., 2002), transporter GLUT 2 was probably the main isoform accounting for the transport of GlcN as well as POGlcN in the Caco-2 cell model. In addition, the transport of PO was not impaired in the presence of sugar-related transport inhibitors (quercetin, phloretin, and phloridzin), neither was GlcN in the presence of wortmannin and Gly-Sar (Appendix E), thus eliminating the interacting negative/positive effects of these pathway-specific inhibitors on other transport routes.

Unlike POGlcN and PO, the paracellular pathway contributed to the permeation of GlcN significantly (Figure 4.8B). It is consistent with Qian (2013) who used chitosan to increase the paracellular transport of GlcN. This extra pathway involvement can be explained by the greater charge-to-weight ratio of GlcN than that of POGlcN, and its positive charged form in solution which promotes a "cation selectivity" of the tight junction (Salamat-Miller). In general, the transport study using Caco-2 cell model clarified that the absorption of novel glycopeptide POGlcN was a combined effect of peptide-induced transport by the proton-coupled carrier PepT1, and GlcN-induced transport by facilitative GLUTs especially GLUT2. GLUT2 is conventionally found in the basolateral membrane of epithelial cells as an efflux transporter (Takata, 1996). However, recent studies also discovered GLUT2 translocated from basolateral membrane and expressed in the apical membrane, which emphasizes the importance of GLUT2 in glucose uptake

(Kwon et al., 2007; Kellett and Brot-Laroche, 2005). In this regard, the apically applied POGlcN could also induce the translocation of GLUT2 to apical membrane to facilitate its uptake, due to its inaccessibility to apical SGLT1 as indicated above. It is possible that POGlcN entered the epithelial cells primarily via PepT1, GLUT2, and much less so via GLUT3, then discharged mainly through GLUT2, partially through basolateral facilitative peptide transporter and GLUT1 to the outside of the cells. All these transporters cooperate in concert to facilitate good permeability of the glycopeptide POGlcN.

In summary, the present study suggests that the synthesized glycopeptide Pro-Hyp-CONH-GlcN is novel since it can utilize an extra transport pathway (i.e. the GLUTs transporter) without compromising the affinity to PepT1 transporter in a Caco-2 cell model. This is achieved by a well-maintained structure of each component, the PO and GlcN, through efficient chemical amidation. The superior transepithelial permeability of the intestinally-stable glycopeptide POGlcN compare to the parent peptide indicated the potential of the proposed synthesis method being used to improve the bioavailability of PO, and even some other small bioactive peptides. To the best of our knowledge, this is one of the first studies providing evidence that a glycopeptide can be transported through intestinal GLUT transporters. This approach, in which the glycopeptide relies on existing transporters for its transport through the intestinal cells, appears to be safer than the strategy of using permeation enhancers. Protecting the functional amino group of GlcN with a stable peptide may be a promising strategy, since it may stabilize the very reactive GlcN and thus avoid condensation and/or degradation during storage. However, the absorption efficiency of the glycopeptide, its subsequent metabolism in blood and liver, the functional form (i.e. intact or degraded form) and its potentially beneficial effects on skin and bone remain to be understood by more comprehensive *in vivo* experiments in future studies.

CHAPTER 5.

**A novel collagen-derived glycopeptide, Pro-Hyp-CONH-GlcN, stimulates cell proliferation
and hyaluronan production in cultured human dermal fibroblasts**

Abstract

Pro-Hyp-CONH-GlcN (POGlcN) is a glycopeptide synthesized from a typical bioavailable collagen peptide Pro-Hyp by conjugation with glucosamine. Since Pro-Hyp is a known stimulus for the growth of dermal fibroblasts and hyaluronan biosynthesis, this study investigated both the ability of POGlcN in retaining this property from its parental dipeptide and the underlying mechanism. The results suggest that the plasma digestion-resistant POGlcN stimulated the proliferation of cultured human dermal fibroblasts in a time- and concentration-dependent manner with optimal performance at 200nmol/mL and 6 days. Comparable to Pro-Hyp, POGlcN increased the cell number to 1.5-fold and HA production to 1.4-fold of control. Edu labeling-assisted cell cycle analysis revealed that POGlcN was a potential mitogen. Moreover, POGlcN up-regulated both hyaluronan synthase-2 and -3 gene transcriptions to 1.8-fold and 2.0-fold, respectively. The interim mitogenic and gene modulation property as indicated by time-lapse monitoring implied the potency of POGlcN for improving skin condition and regeneration safely.

Key words: Collagen peptide, Pro-Hyp-CONH-GlcN, Glycopeptide, Dermal fibroblast, Pro-Hyp.

5.1. Introduction

Beyond the conventional perception of skin as a barrier and sensory organ, now it has been appreciated an integral role in communicating with endocrine, immune, and nervous systems to modulate the homeostasis of the entire body (Chuong et al., 2002). The dermal extracellular matrix (ECM) of skin contributes to its structure and integrity and is occupied by the structural proteins, proteoglycans, glycosaminoglycans (mainly hyaluronan), growth factors, cytokines, etc. (Stern and Maibach, 2008), all of which are synthesized by resident fibroblasts. The fibrillar network is mainly composed of collagen and provides a scaffold to ECM. The stability and mechanical property is strengthened by interaction with the largely anionic hyaluronic acid (HA) to retain voluminous water of hydration (Mouw et al., 2014; Stern and Maibach, 2008). As skin ages, wrinkles, a rougher texture and drier appearance occurs with less elasticity; this is due to the increased deterioration and disorganization of the ECM components (e.g. collagen), and a reduction in fibroblasts and their tissue regenerative ability (Tobin, 2017). In this respect, increasing the synthesis of collagen may help to restore its homeostasis in skin. Moreover, by maintaining the ECM space and increasing the moisture content, an elevated HA level may facilitate cell detachment and migration, proliferation, as well as suppress cell differentiation (Kujawa and Tepperman, 1983; Pratt et al., 1975; Stern and Maibach, 2008). The skin conditions or its biological aging symptoms may therefore be controlled by affecting the efficacy on regeneration of skin collagen and HA.

Collagen and gelatin have been used as food sources or supplements for a long time. Recently, collagen hydrolysates and collagen-derived peptides are claimed to be active in improving skin conditions in some clinical trials. The ingestion of collagen hydrolysates (CH) can enhance the moisture content of skin stratum corneum, skin elasticity and smoothness in humans

(Matsumoto et al., 2006; Proksch et al., 2013). Animal studies suggest a protective effect of collagen-derived peptides against ultraviolet radiation-induced damage and photo-aging by controlling skin hydration and collagen content (Tanaka et al., 2009; Fujii et al., 2013). Upon oral administration, CH can be absorbed to some extent and distributed through the blood circulation system to various tissues among which skin is the final preferential and lasting site (up to 14 days) (Oesser et al., 1999; Kamiyama et al., 2010). Bioavailable CH found in plasma were either in free amino acid form, typically Hyp, or di- and tripeptide form, such as Pro-Hyp, Ala-Hyp, Gly-Pro-Hyp, Ala-Hyp-Gly, etc. (Ohara et al., 2007; Ichikawa et al., 2010). The amount and type of collagen-derived peptides found in plasma and skin may be variable depend on the source of ingested CH, yet the dipeptide Pro-Hyp (PO) was confirmed to be one of the most predominant (Yazaki et al., 2017). As a chemotactic stimulus (Postlethwaite et al., 1978), PO can stimulate the migration and proliferation of skin fibroblasts (Shigemura et al., 2009), and the production of HA by both synovium cells and fibroblasts (Ohara et al., 2010a; Ohara et al., 2010b). PO also shows a chondroprotective effect to mouse articular cartilage (Nakatani et al., 2009), as well as promoting the differentiation of osteoblastic cells (Kimira et al., 2014).

Glucosamine (GlcN), a naturally existing amino sugar, has long been used to treat osteoarthritis given its efficacy in relieving pain and delaying joint space narrowing (Reginster et al., 2012). During *in vitro* studies, GlcN also enhances the biosynthesis of HA by synovial cells and chondrocytes (Uitterlinden et al., 2008; Stoppoloni et al., 2015). Our previous research synthesized a novel collagen-derived glycopeptide Pro-Hyp-CONH-GlcN (POGlcN) by conjugating the typical dipeptide PO with GlcN (Feng and Betti, 2017b). This digestion-resistant glycopeptide has superior intestinal permeability to PO by passing the human intestinal Caco-2 cell monolayer using both PEPT1 peptide transporter and glucose transporters GLUTs as carriers.

Considering its structural similarity to the parent dipeptide PO, in the present study we hypothesized that the glycopeptide POGlcN may possess equal promoting effects on the growth of fibroblasts and their ability to secrete ECM ingredients; or in a better scenario, or a greater efficacy is introduced due to the promoting effects of GlcN on HA production. Therefore, our objective was to investigate cellular response to POGlcN in comparison with PO regarding the growth and biosynthesis of ECM components, and explore the possible mechanism with respect to cell cycle distribution and gene expression using cultured human dermal fibroblasts.

5.2. Materials and methods

5.2.1. Chemicals

The glycopeptide POGlcN was synthesized in our laboratory according to previous research[25]. Formaldehyde solution, Triton™ X-100, Tween-20, *2*-(*4*-Amidinophenyl)-6-indolecarbamidine dihydrochloride (DAPI), Cy5-azide, Copper(II) sulfate pentahydrate, bovine serum albumin (BSA), 3-Aminobutanoic acid, human plasma, Sodium ascorbate, 4-Bromoanisole were purchased from Sigma Aldrich (St. Louis, MO, USA). Hyaluronan Enzyme-Linked Immunosorbent Assay kit was purchased from Echelon Biosciences Inc. (Salt Lake City, UT, USA). TRI Reagent® RT for RNA isolation was from (Molecular Research Center, Inc., Cincinnati, OH, USA). FGF-Basic (AA 1-155) Recombinant Human Protein, UltraPure™ 1M Tris-HCI (pH 8.0), RIPA buffer and the gene expression related products including TaqMan® Fast Advanced Master Mix, Nuclease-Free Water (not DEPC-Treated), RNase-free Microfuge Tubes, and TaqMan Gene Expression assays for COL1A1 (Hs00164004_m1), HAS1 (Hs00758053_m1), HAS2(Hs00193435_m1), HAS3(Hs00193436_m1), and GAPDH (Hs99999905_m1) were the products from Thermo Fisher Scientific (Waltham, MA, USA). PrimeScript™ RT Reagent Kit (Perfect Real Time) was purchased from Takara (Takara Bio USA Inc. Mountain View, CA, USA).

The primary dermal fibroblast (normal, human, adult, ATCC®PCS-201-012) was obtained from American Type Culture Collection (ATCC, Manassas, VA, USA). 5-Ethynyl-2'-deoxyuridine (Edu) and WST-8 Cell Proliferation Assay kit were obtained from Cayman Chemical (Ann Arbor, MI, USA). Other cell culture supplies, such as phosphate buffered saline (PBS), Dulbecco's Modified Eagle Medium (DMEM), fetal bovine serum (FBS), Antibiotic-Antimycotic, N-2-hydroxyethylpiperazine-N-2-ethane sulfonic acid (HEPES), and Trypsin-EDTA were from Gibco (Thermo Fisher Scientific Inc., Waltham, MA, USA).

5.2.2. *In Vitro* Digestion of the Glycopeptide POGlcN in Plasma

The plasma stability for the compound of interest may imply its efficiency to be distributed via systemic circulation to the target tissue. To investigate the stability or potential degradation of the synthesized glycopeptide before reaching target cells, i.e. the human dermal fibroblasts in the present study, the POGlcN was digested *in vitro* within human plasma according to Di et al. (2005) with some modifications. In brief, the plasma was firstly diluted with PBS (pH 7.4) to 50% (v/v) before being used in the assay. Forty micromolar of POGlcN was digested with the assay plasma at 37°C in a shaking incubator (200 rpm). The reaction was terminated at 0, 15, 30, 60, and 120 min by adding TCA to make its final concentration at 20% (w/v) for protein precipitation. The plasma matrix blank without the glycopeptide addition was simultaneously incubated. The samples were then centrifuged at 10,000 rpm for 10 min at 4°C after sitting on the ice for 15 min. Aliquots of the supernatant was collected and neutralized with 2 M NaOH, followed by determination of the remaining POGlcN content by ultra-high pressure liquid chromatography (UHPLC) according to the method described previously (Feng and Betti, 2017b).

5.2.3. Cell Culturing of Human Dermal Fibroblasts (HDF)

The HDF were cultured by 10% DMEM with the addition of 10% FBS, 25 mM HEPES and 1% Antibiotic-Antimycotic. The cell culturing was conducted in a sterilized incubator (Heracell VIOS 160i, Thermo Fisher Scientific) which controls constant CO_2 and moisture content at 5% and 95%, respectively. To maintain the growth of the fibroblasts, the culturing media were changed every other day. The fibroblasts were passaged with 0.05% (w/v) trypsin-EDTA when around 80% confluence was reached in the flask. All the fibroblasts used in this study were between passages 3 and 8.

5.2.4. Effects of the Glycopetide POGlcN on HDF Growth

To investigate effect of the glycopeptide POGlcN on the growth of fibroblasts in relation to its concentration and incubation time, two single factor experiments were designed. The fibroblasts were seeded on 96-well plates at a density of 5×10^4 cells/mL (100 µL/well), pre-cultured with complete growth media for 24 hours, and starved for 16 hours with serum-free media. The cells were then cultured in 1% FBS-DMEM in the presence or absence of test compounds. For the time factor experiment, a fixed concentration of POGlcN (200 nmol/mL) was applied on the cells for 0, 24, 48, 96, or 144 hours. For the concentration factor experiment, POGlcN at a concentration of 0, 50, 100, 200, 400, or 800 nmol/mL was applied for 6 days.

The effect of the glycopeptide POGlcN on the proliferation of HDF was then compared with that of its parent dipeptide PO and GlcN under optimized experimental condition (time and concentration) determined from the single factor experiments. The basic fibroblast growth factor (bFGF) which regulates the growth of HDF was used as a positive control at 25 ng/mL. For all the experiments, a negative control which was not treated with any test compound was included simultaneously. The cell media was collected for the determination of collagen and hyaluronic acid in later experiments. The fibroblasts were subjected to cell number counting by WST-8

proliferation assay following the protocol from the manufacture (Cayman Chemical). The effects on HDF proliferation were expressed as ratio of the negative control regarding the cell numbers.

5.2.5. Effects of the Glycopetide POGlcN on the Biosynthesis of Collagen and Hyaluronic Acid (HA)

Collagen and HA content were estimated to investigate the effects of the glycopeptide on the production of extracellular components by HDF. As most of the hydroxyproline (Hyp) comes from collagen, its content can indicate the collagen level (Edwards and O'Brien, 1980). The cells were lysed by RIPA buffer for 5 min, briefly sonicated, and then centrifuged at 14,000×g for 15 min. The supernatant was collected and combined with the corresponding cell media collected before for the analysis. To evaluate the Hyp amount, aliquot of the sample was hydrolyzed by 6 M HCl at 110°C under nitrogen atmosphere for 24 hours. After being dried with flush nitrogen, it was redissolved in distilled water, and neutralized with 2 M NaOH. Finally, following the pre-column derivatization with Fmoc-Cl, the Hyp content was determined by UHPLC as described previously (Feng and Betti, 2017b).

The HA content was determined by a hyaluronan enzyme-linked immunosorbent assay according to the protocol from the manufacturer (Echelon Biosciences Inc.).

5.2.6. Cell Cycle Analysis by High Content Screening

Cell cycle distribution of HDF in response to the glycopeptide was determined after nuclei staining by DAPI accompanied with Edu labeling (to assess cell sub-population in S phase) according to Ranall et al. (2010) with some modifications. Following the culturing procedures from the previous section, the fibroblasts were plated on 96-well plates, pre-cultured, starved, and then treated with or without 200 nmol/mL of POGlcN, PO, or GlcN, using bFGF (25 ng/mL) as a positive control. After treatment for 2 days, 4 days, or 6 days, the cells were pulse-labelled with

10 μM Edu for 6 hours in the culturing incubator followed by gently washing with PBS (pH 7.4). The cells were then fixed with freshly prepared 3.7% (v/v) formaldehyde in PBS for 15 min, and rinsed with 3% BSA (w/v) in PBS. To facilitate the staining, Triton X-100 (0.5% in PBS, v/v) was used to permeabilize the cell membrane for 20 min. The fibroblasts were again washed with 3% BSA, and blocked with 0.1% (v/v) Tween-20 in 3% BSA (PBST-BSA). The washing media was removed to minimum volume before Cy5 staining. Staining reaction with the CuAAC mixture was performed for 30 min, and stopped by rinsing with PBS. The CuAAC cocktail, which is composed of 4mM CuSO4, 10μM Cy5-azide, 50mM sodium ascorbate in 100mM Tris-HCl (pH 8.0) should be used within 15 min considering its instability after the addition of sodium ascorbate. Excess Cy5-azide was then destained with PBST-BSA for 20 min. Finally, the cells were washed with PBS, counterstained by 0.5 μg/mL of DAPI for 40 min, and rinsed again with PBS. The final cell samples were stored in 70% (v/v) glycerol in PBS at 4°C in dark until later imaging analysis. All the reactions were performed in dark at room temperature if not specified.

The cell plates were scanned by the ImageXpress Micro XLS Widefield High-Content Analysis System (Molecular Devices, LLC., CA, USA) at 10× magnification, while the data acquisition and analysis were achieved by the MetaXpress High-Content Image Acquisition and Analysis Software version 6.1 (Molecular Devices). Data of the cell distribution histogram and scatterplots were obtained from 9 images per well which captured at least 1000 objects. The histograms were created by subdividing the range of DAPI total pixel intensity into 200 equal sized bins using Graphpad Prism 7 (GraphPad Software, Inc., CA, USA). The scatterplots were generated by SigmaPlot 13.0 (Systat Software Inc., CA, USA). The threshold (2×10^6) was set according to the nuclei signal intensity of cells that lack Cy5 fluorescence. Cell nuclei with Edu-Cy5 intensity higher than the threshold was considered as positive, i.e. active in DNA synthesis.

5.2.7. Quantitative Reverse Transcription Polymerase Chain Reaction (qRT-PCR)

To understand effects of the glycopeptide on gene expression of HDF, total RNA was extracted from the fibroblasts upon treatments, while specific genes were quantified by qRT-PCR. Briefly, the fibroblasts were seeded on 12-well plates at a density of 5×10^4 cells/mL (1mL/well) for pre-culturing 24 hours with complete growth media, starved with serum-free DMEM for 16 hours, and then treated in 1% FBS-DMEM with or without 200 nmol/mL of POGlcN, PO, or GlcN, using bFGF (25ng/mL) as a positive control. After treatment for 2 days, 4 days, or 6 days, the cells were lysed with 0.5 mL Trizol reagent and homogenized for 4 min at room temperature. The RNA isolation was conducted according to the protocol from the manufacture with some modifications (Molecular Research Center, Inc.). Briefly, the lysed cell suspension was phase separated by addition of 25 µL bromoanisole, and centrifuged at 12,000 ×g for 15 min. This phase separation step was repeated once again to minimize the potential DNA, protein and phenol contamination. The aqueous RNA layer was then carefully collected and precipitated with equal volume of isopropanol for 10 min. After centrifugation at 12,000 ×g for 10 min, the white RNA pellets were washed multiple times with 75% ethanol, centrifuged (7,500 ×g for 10 min), and air-dried. All the steps were performed in cold (2-8°C) if not specified. The final RNA was redissolved in nuclease-free water, stored at -80°C or subjected to cDNA synthesis. Purity and content was determined by NanoDrop 1000 (Thermo Fisher Scientific Inc.). Only RNA samples with A260/A280 ≥ 1.7 and A260/A230 ≥ 2.0 were selected for downstream applications.

Two hundred and fifty nanograms of the total RNA was used for the cDNA synthesis by PrimeScript™ RT reagent Kit (Perfect Real Time) following the protocol from the manufacturer (Takara Bio USA Inc.). The synthesis was conducted in a thermal cycler (ProFlex™ 96-well PCR System), which held the reverse transcription for 15 min at 37°C and inactivation of the reverse

transcriptase for 5 seconds at 85°C. The cDNA was stored at -20°C until PCR analysis using StepOnePlus™ system. Primers and Taqman probes for gene COL1A1, HAS1, HAS2, HAS3 and endogenous control GAPDH were designed by Applied Biosystems (Thermo Fisher Scientific). Real-time PCR reaction was performed in duplicates for each biological sample using the Taqman™ Fast Advanced Master Mix. The relative expression level of target genes was calculated following the $2^{-\Delta\Delta Ct}$ method and expressed as the fold change in comparison to the untreated control (Schmittgen and Livak, 2008). Instruments used in this qRT-PCR were from Thermo Fisher Scientific; the PCR amplifications were also conducted following suggestions from the manufacturer.

5.2.8. Statistical Analysis

Data from the cell cycle analysis and gene expression assays were analyzed by two-way analysis of variance (ANOVA), while data from other experiments were analyzed by one-way ANOVA using SAS 9.4 (Cary, NC, USA). Post hoc analysis was done with Tukey's test where $p < 0.05$ was considered significantly different, and $p < 0.01$ as very significantly different.

5.3. Results and Discussion

5.3.1. POGlcN Stability in Plasma

Plasma stability of a bioactive compound endows its *in vivo* beneficial performance which requires desirable concentration in intact form on target site. As clarified in a previous study (Feng and Betti, 2017b), the glycopeptide POGlcN is essentially an amide derivative. The amide bond formed between the carboxyl group of Hyp and amine group of GlcN is therefore a potential substrate for enzymatic hydrolysis of plasma peptidase and esterase. However, as shown in Figure 5.1, POGlcN was very resistant to the plasma digestion with around 95% remaining even after 2 hours' reaction. The digestion resistance of POGlcN is consistent with that of other small Hyp-

containing peptides, such as Gly-Pro-Hyp which shows <10% plasma degradation (Sontakke et al., 2016), and Pro-Hyp which is stable in plasma and partially excreted in intact form in urine (Weiss and Klein, 1969). The negligible plasma degradation of POGlcN, together with its improved transepithelial transport as indicated in our previous *in vitro* study, confer its possibility of distribution and accumulation in target tissues, such as skin, cartilage, and bone.
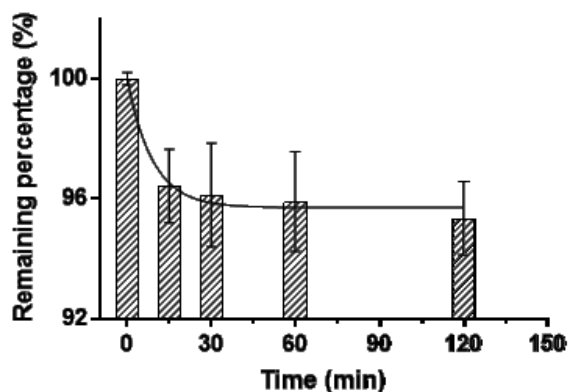
Figure 5.1. Remaining amount of the glycopeptide Pro-Hyp-CONH-GlcN over time in human plasma. Bars represent standard deviation (n=3).

5.3.2. Stimulation of HDF Proliferation by POGlcN was Time- and Dose-dependent

To study optimal performance of the glycopeptide on the growth of HDF, POGlcN was applied on the cells for various incubation times up to 6 days when cells grew close to confluence. Longer treatments were not conducted, as the fibroblasts may fall into stationary growth phase and undergo further differentiation, where the potential stimulation effect may be masked. Figure 5.2A shows that the stimulation of POGlcN on the fibroblast propagation became more obvious as incubation time prolongs. The cell number was not significantly greater than the control until 4 days of culturing (1.2-fold), maximal performance 1.4-fold of control was reached after 6 days. It suggests that the stimulation effect was accumulated along with time as POGlcN treated groups either exhibited bigger cardinal number of active proliferating cell, or shorter cell cycle duration.

To obtain the maximal performance, fibroblasts were incubated for 6 days in the later concentration factor experiment. Incremental cell numbers were observed as the dose of POGlcN increased up to 200 nmol/L (1.5-fold) (Figure 5.2B), while significance already appeared at 100 nmol/ml (1.2-fold) which is similar with the physiological level of Hyp-containing peptides in human plasma after oral ingestion of gelatin hydrolysate (Ichikawa et al., 2010). The cell number declined at a concentration of 400 nmol/mL (1.3-fold) or higher probably due to POGlcN-introduced toxicity which may have influenced both the cell number and the synthesis of DNA during cell division (Gibbs et al., 1982). Therefore, fibroblasts culturing with 200 nmol/mL of POGlcN for 6 days was determined to be the optimal experimental condition for treatments comparing dipeptide PO and sugar moiety GlcN.

Basic FGF is an important polypeptide growth factor secreted by diverse cell types such as dermal fibroblasts to modulate cell behavior and matrix homeostasis. Basic FGF was reported to stimulate the proliferation of skin fibroblasts dose-dependently from 0.5ng/mL to 50 ng/mL.[33] It was therefore used as a positive control to compare with the effects of our test compounds and explore the potential similarity in underlying mechanism. Even at the low concentration of 25ng/mL, bFGF behaved more efficiently than all other test compounds by inducing 2.4-fold increase in cell number (Figure 5.2C). Figure 5.2C also indicates that HDF response to glycopetide POGlcN (1.5-fold) was as large as that of the parent dipeptide PO (1.4-fold), while GlcN at this concentration did not trigger any difference compared to the control. The stimulation efficiency was consistent with the 1.5-fold increase generated by 200nmol/mL of PO as reported previously (Ohara et al., 2010b). POGlcN may function as a chemotactic stimulus like PO, since not only intact alpha chains of collagen, but also hydrolysis-generated collagen peptides or synthesized Hyp-containing peptides such as Gly-Hyp, Gly-Pro-Hyp, and Pro-Hyp, are chemoattractants for

fibroblasts (Postlethwaite et al., 1978). Although the responsible receptor on the cell surface was not identified, Hyp has been proposed to be an important recognition site despite itself, as a single amino acid, is not functional (Haratake et al., 2015; Postlethwaite et al., 1978). GlcN can slow down the doubling of chondrocytes and thus inhibiting the proliferation as exposure dose increase from 1mM to 15 mM (Varghese et al., 2007). The lack of GlcN effecton dermal fibroblasts in the present study could be the result of its low concentration or response variety by different cell lines. The results suggest that GlcN incorporation did not compromise the positive effects of the collagen-derived dipeptide PO on HDF growth.
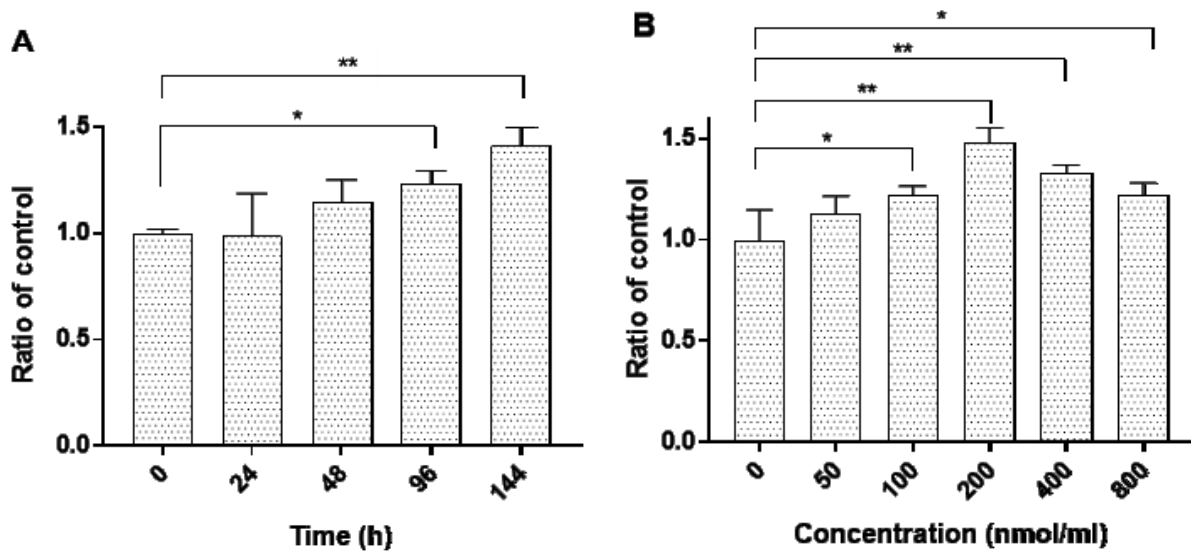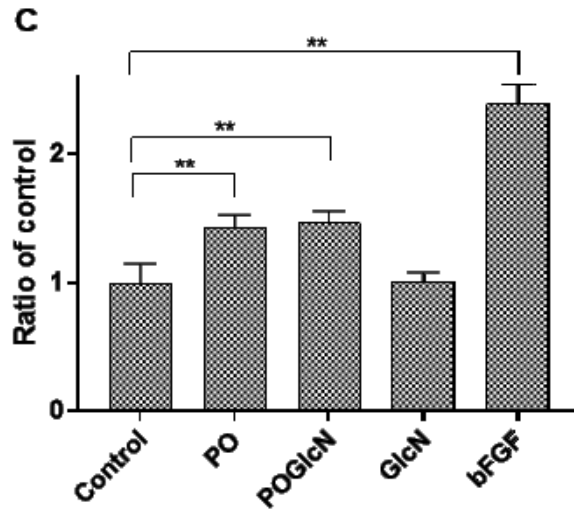
Figure 5.2. (A) Cell number of human dermal fibroblasts treated with 200 nmol/mL Pro-Hyp-CONH-GlcN (POGlcN) for different time periods; (B) Cell number of human dermal fibroblasts treated with different concentrations of POGlcN for 6 days; (C) Cell number of human dermal fibroblasts treated with or without test compound for 6 days, PO means collagen dipeptide Pro-Hyp, GlcN means the amino sugar glucosamine, bFGF means basic fibroblast growth factor, Control means a negative control which was not treated with any added test compound. The cell number was expressed as the relative ratio of control. Bars represent standard deviation (n=4). *$p < 0.05$; **$p < 0.01$.

5.3.3. POGlcN Improved the Production of HA by HDF

Collagen, proteoglycan, and HA are the primary macromolecules within ECM. These components are well organized and connected through proteins such as hyaladherin, laminins and fibronectin to form a structural network as well as to interact with resident cells via surface receptors; thus, mediating cell behavior (Mouw et al., 2014). As mentioned before, CH ingestion can alleviate skin aging symptoms by contributing to the skin hydration and elasticity (Matsumoto et al., 2006; Proksch et al., 2013). *In vivo* studies also reported that the oral administration of CH can enhance the diameter and density of collagen fibrils in pig skin (Matsuda et al., 2006).

However, Ohara et al. (2010b) found no effect for the treatment with predominant collagen-derived PO on the production of collagen by skin fibroblasts *in vitro*. This was also confirmed in our study as shown in Figure 5.3A. When cells were exposed to different test compounds, no significant change was observed for the accumulation of Hyp which reflects collagen content except the bFGF group. The difference in biological response to a single peptide PO and the CH mixture may suggest the potential synergistic effects among various collagen-derived peptides. Alternatively, PO may behave differently *in vitro* and *in vivo* considering the different microenvironment surrounding the cells. In general, bFGF triggers the proliferation of skin fibroblasts while suppressing collagen biosynthesis. In the present study, bFGF inhibited about 39% secretion of Hyp after exposure for 6 days, which was comparable to the 50-90% inhibition induced by 2.0-50 ng/mL bFGF on skin fibroblasts as described by Tan et al. (1993) This echoes the fact that bFGF also acts antagonistically to transforming growth factor-beta which stimulates collagen accumulation (Dolivo et al., 2017). GlcN is a chondroprotective agent that can alleviate osteoarthritis by stimulating the production of Type II collagen (Varghese et al., 2007) and preventing collagen degradation via suppressing related lipid peroxidation (Tiku et al., 2007) and the expression of cleavage metalloproteinases in chondrocytes (Derfoul et al., 2007). Research regarding GlcN effects on skin fibroblasts, however, is very limited. The unexpected response to GlcN seen in our study (Figure 5.3A) remains to be confirmed with more comprehensive studies.

In contrast to being ineffective on collagen accumulation, both the dipeptide PO and glycopeptide POGlcN can significantly promote the biosynthesis of HA; up to 1.3-fold and 1.4-fold of the control, respectively (Figure 5.3B). Though the slightly greater efficiency of POGlcN than PO was not significant, its performance was comparable to that of bFGF (25 ng/mL) which gave a 1.7-fold increase. The improving effects of PO and bFGF were also reported before at

similar levels (Ohara et al., 2010b). It is known that higher HA deposition correlates with cell mitosis (Brecht et al., 1986), while inhibition of HA results in reduced cell proliferation (Matuoka et al., 1987). The elevated HA level, conferring a more hydrated extracellular microenvironment to aid cell migration could probably explain at least in part of the enhanced proliferation of HDF in the peptides and bFGF group (Pratt et al., 1975). The unique mechanical properties of hyaluronan, such as maintaining skin hydration, viscosity and elasticity, endow its application in cosmetic medicine as a safe and simple procedure to improve skin appearance (Lupo, 2006). HA content also increases to serve multiple biological functions during inflammation, tissue injury and repairing, embryonic morphogenesis, and cell malignancy (Stern and Maibach, 2008). Therefore, the stimulation of HA synthesis induced by collagen-derived PO and POGlcN may have important implications in ameliorating skin conditions, facilitating tissue regeneration and wound healing.

D-glucosamine serves as a precursor for HA, and it can improve the biosynthesis of HA in cultured cells such as synovial cells and chondrocytes at an elevated dosage, i.e. 5mM and 1mM, respectively (Uitterlinden et al., 2008; Stoppoloni et al., 2015). This explains its efficacy in slowing down the joint space narrowing of osteoarthritis, since HA in this respect functions as space filler and lubricator by entrapping more water in cartilage. Figure 5.3B only shows a small increase of HA content as expose to a 200 nmol/mL of GlcN treatment (1.2-fold), suggesting that a greater dosage may be needed to express any effect comparable to that of glycopeptide POGlcN. Actually, GlcN *in vivo* is incorporated into HA in acetalized form of GlcN, N-acetyl-glucosamine, by a series of enzymes (Sacoman and Hollingsworth, 2011). Despite there is no report about GlcN effects on skin fibroblasts, its acetylated form was proven to increase the production of HA by cultured fibroblasts (Breborowicz et al., 1998), and to improve the skin moisture content upon oral administration (Kikuchi and Matahira, 2002).
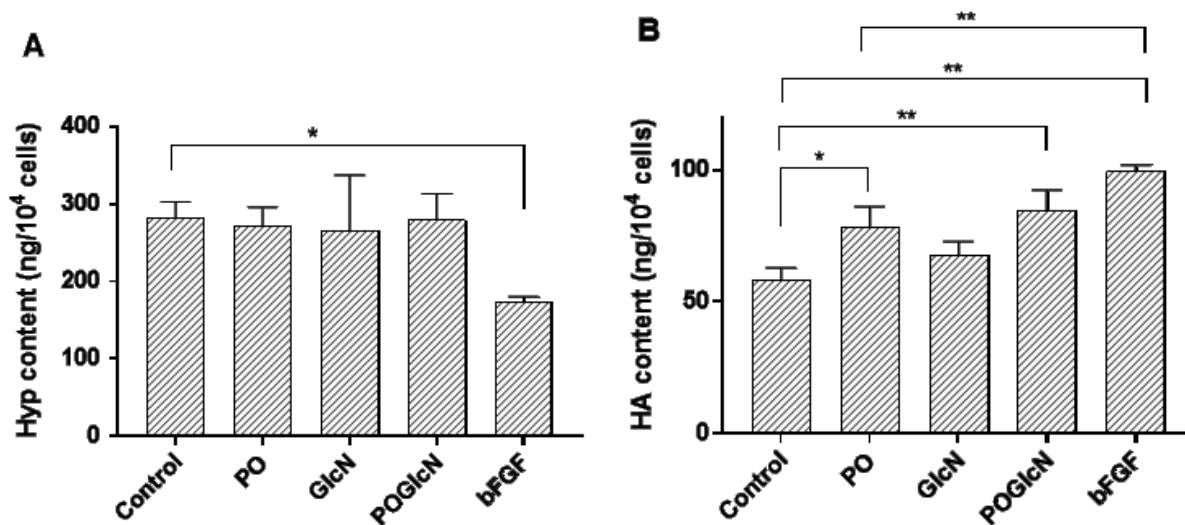
Figure 5.3. Amount of (A) collagen and (B) hyaluronic acid (HA) secreted by fibroblasts treated with or without test compound; abbreviations for treatments are the same with those in Figure 5.2. Bars represent standard deviation (n=3). *$p < 0.05$; **$p < 0.01$.

5.3.4. POGlcN was A Potential Mitogen for HDF

In most cases, the growth of live eukaryotic cells occurs continuously, the cell cycle of which can be divided into a short mitosis phase (M) followed by the interphase when cells orderly prepare for division. In general, the interphase consists of three discrete phases; G1, S, and G2 phases. Analyzing the cell stage of individual cells is possible since the DNA content of cells in different stages are distinguishable. For example, cells in G1 phase are diploid (refers to 2n DNA content), but range from 2n to 4n during which DNA of cells duplicate. DNA in the following G2 and M phase maintains its content at 4n. There are also cells which only replicate occasionally, such as some skin fibroblasts, as they temporally exit G1 phase to enter a quiescent G0 phase with 2n DNA (Cooper and Hausman, 2009). Cell cycle analysis confers critical information about the principles of test compounds in controlling cell behavior. Flow cytometry requires large number of cells and single cell dispersion which is challenging for adherent fibroblasts even after

trypsinization. Therefore, for our study an image-based high content screening method was used instead. This was achieved by a bivariable analysis via staining cell nuclei with both DAPI and Edu, the former of which determines total DNA content while the latter one labels cells that are active in S phase.

Figure 5.4A shows the representative DNA content distribution of cell populations after 4 days treatments. Two peaks in the histogram denote DNA content of cells in G0/G1 (2n) and G2/M (4n) phase, respectively, since cells in each of this phase should possess uniform chromosomes. The narrow shoulder of each peak probably came from variance in instrumental measuring and/or DAPI biological binding. The histograms show that the cultured HDF were mostly in G0/G1 phase, some in G2/M phase, and minimal numbers in S phase. Very few were in apoptosis with fragmented DNA (<2n). This identical distribution pattern among different groups suggests that none of those test compounds altered the cell cycle distribution of HDF abnormally. Similar distribution histograms are shown in Appendix F for 2 days and 6 days treatment durations. However, a difference was indeed generated. For example, the fraction of cells in S phase (Figure 5.4A) (i.e. the section between two peaks in the histogram), was more evident for cell populations from PO, POGlcN, and bFGF groups. To understand the kinetics of cell progression through the cycle and changes induced by the glycopeptide, the fibroblasts were treated for different times. Cells were firstly synchronized in G0 phase after serum deprivation for 16 hours before any treatment. The time-lapse data was summarized for each cell cycle phase in Figure 5.4B (G0/G1), Figure 5.4C (S), and Figure 5.4D (G2/M). In general, after 2 days and 4 days, dipeptide PO and glycopeptide POGlcN recruited significantly more cells in S phase and G2/M phase, leading to less number of cells in G0/G1 phase than control. To a larger degree, bFGF also induced this effect. No effect was observed for the two peptides and bFGF after 6 days, or for GlcN at any time. The

results revealed the mitogenic property of both PO and POGlcN, while no significant difference was manifested between them. It is interesting to notice that changes in frequency of cells in S phase was very dynamic among different treatments and along with time as shown in Figure 5.4C. Although after 2 days, the fraction of cells in S phase from bFGF group (9.5 ± 1.2%) was significantly greater than both the peptide PO (5.2 ± 0.3%) and POGlcN (6.7 ± 1.0%), after 4 days the POGlcN (11.3 ± 1.7%) but not PO (9.8 ± 0.8%) exhibited comparable capacity in arresting cells in S phase with bFGF (13.0 ± 1.1%). From a vertical perspective, the HDF distributed in S and G2/M phase increased with time till 4 days and then declined back to minimal after 6 days, which parallels the fluctuation in cell growth rate and potential of proliferation.
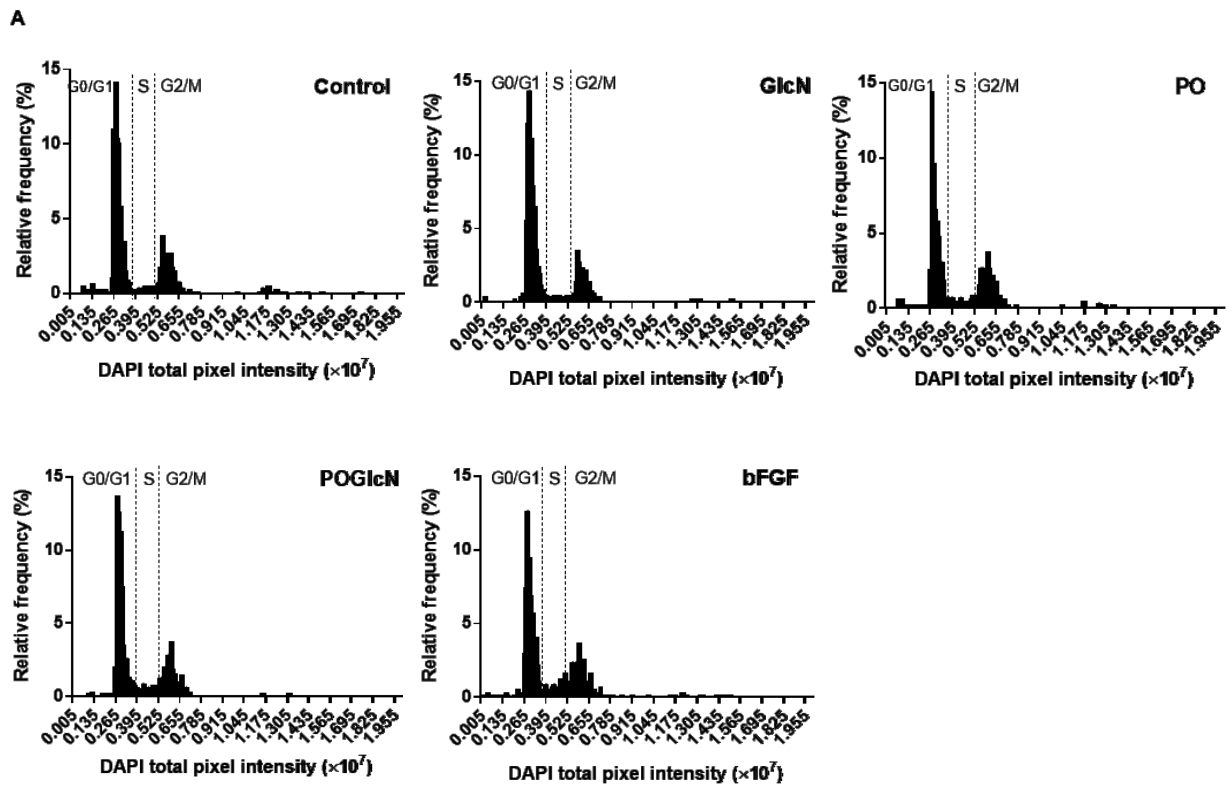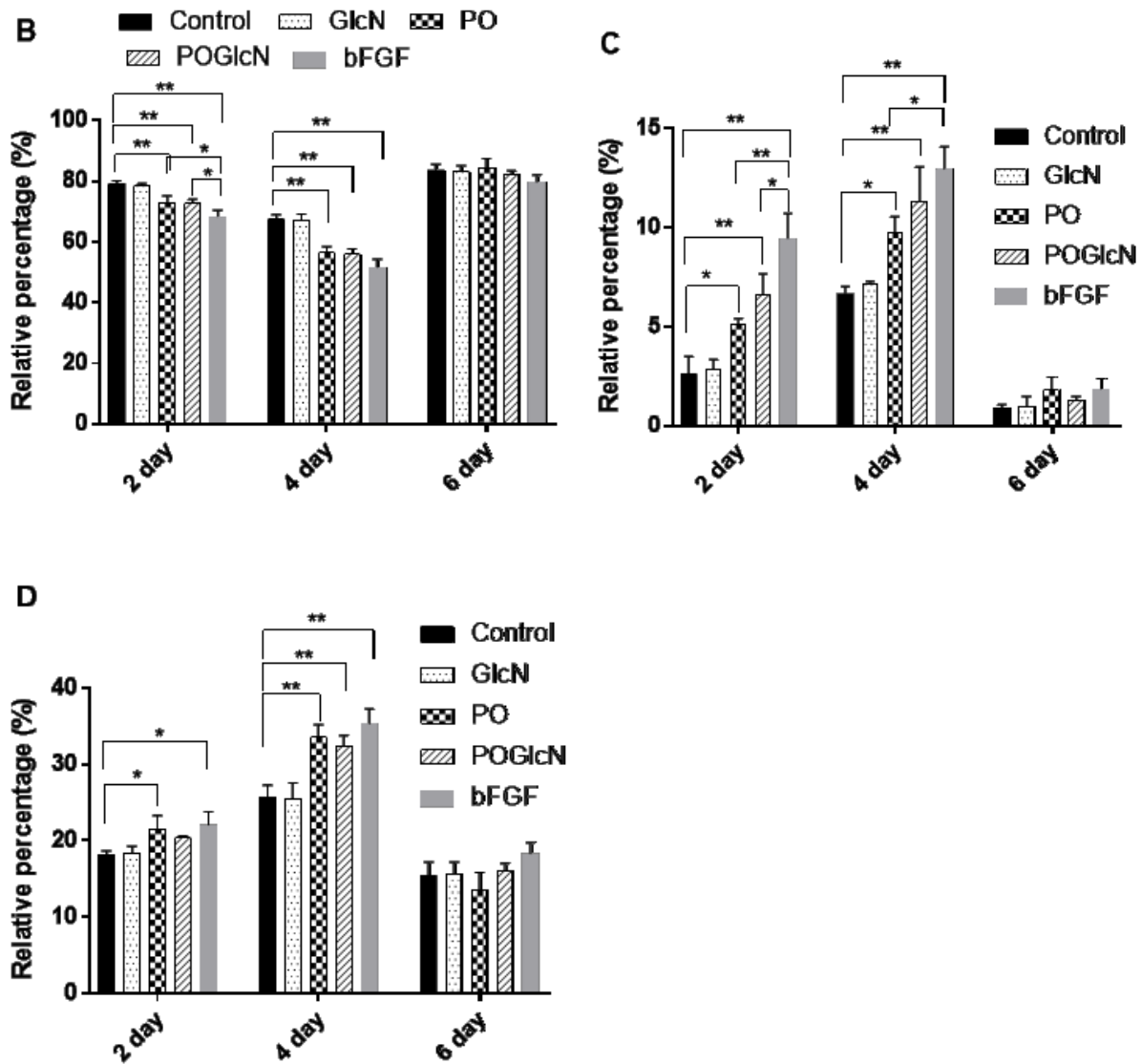
Figure 5.4. Cell cycle analysis by high content screening. (A) Representative cell cycle histograms generated from DAPI stained fibroblasts treated with or without test compound for 4 days; (B) Quantification of cells in G0/G1 phase (B), S phase (C), and G2/M phase (D) in human fibroblasts population treated with or without test compound for different time periods; abbreviations for treatments are the same with those in Figure 5.2. Bars represent standard deviation (n ≥ 3). *$p < 0.05$; **$p < 0.01$.

To have a comprehensive understanding of the stimulation mechanism of the glycopeptide, an extra labeling, Edu, was used to complement the cell cycle analysis to further estimate cells that

are active in DNA replication. As an analogue of thymidine nucleoside, Edu can be incorporated into DNA and quenched by the fluorescent Cy5-azide that is finally detected (Ranall et al., 2010). Figure 5.5A shows the representative images captured by the fluorescent microscope after 4 days' culturing, where blue dots stand for DAPI stained nuclei, pink ones denote Edu-Cy5 positive nuclei. The round and intact morphology of nuclei from all the treatments were comparable to untreated control, which confirmed the non-toxicity of these test compounds as shown in Figure 5.2C. A visually greater presence of Edu-Cy5 positive cells and greater density of cells can be observed in PO, POGlcN and bFGF group than GlcN and control group. This is also affirmed in the cell scoring scatterplots (Figure 5.5B) which combine all the 9 images per well containing a larger cell population. Scatterplots for 2 days and 6 days are displayed in Appendix G. Two stacked regions (e.g. indicated in Figure 5B POGlcN group) located below and above $5.0e^{+6}$ intensity, correspond to the 2n and 4n DNA peaks, respectively, as shown in Figure 5.4A. Cell spots above the threshold line were considered as Edu-Cy5 positive. The distribution of the scatterplots revealed that despite most positive cells had DNA content between 2n and 4n, a non-negligible portion of them were not. These cells with DNA content within 2n or 4n region were considered in G0/G1 or G2/M phase as calculated from in Figure 5.4, which demonstrates the potential underestimation of S phase cell subpopulation by the cell cycle analysis. This underestimation is manifested in Figure 5.5C which displays greater fraction of cells in S phase than those shown in Figure 5.4C, especially for cells treated for 2 days and 4 days. The greater sensitivity of Edu labeling method was also reported somewhere else (Massey, 2015). Interestingly, this method distinguished the greater capacity of POGlcN (15.3 ± 1.0%) than PO (9.4 ± 1.4%) in activating cells to synthesize DNA after 2 days, as well as the greater efficiency of bFGF (24.0 ± 0.3%) than POGlcN (19.8 ± 1.6%) after 4 days. However, after 4 days dipeptide PO (18.2 ± 2.2%) effect tied that of POGlcN,

suggesting that the HDF were more rapidly affected by glycopeptide POGlcN. After 6 days, only bFGF (2.7 ± 1.1%) still shows the stimulation effect compare to control (0.3 ± 0.1%), which can be attributed to the ability of bFGF in maintaining cell division and thus prolonging the proliferation (Cavanagh et al., 1997). In agreement with the cell cycle analysis, the growth rate of fibroblasts increased with time up to 4 days, while decreased to a minimal level after 6 days, suggesting that the cell culture was close to confluency after 6 days. Since DNA duplication is the prerequisite step for cell mitosis, an improved proportion of fibroblasts that were undergoing this process reflects their intriguing proliferative capacity. Therefore, the mitogenic property of glycopeptide POGlcN and PO also explains their stimulation effect on HDF proliferation.
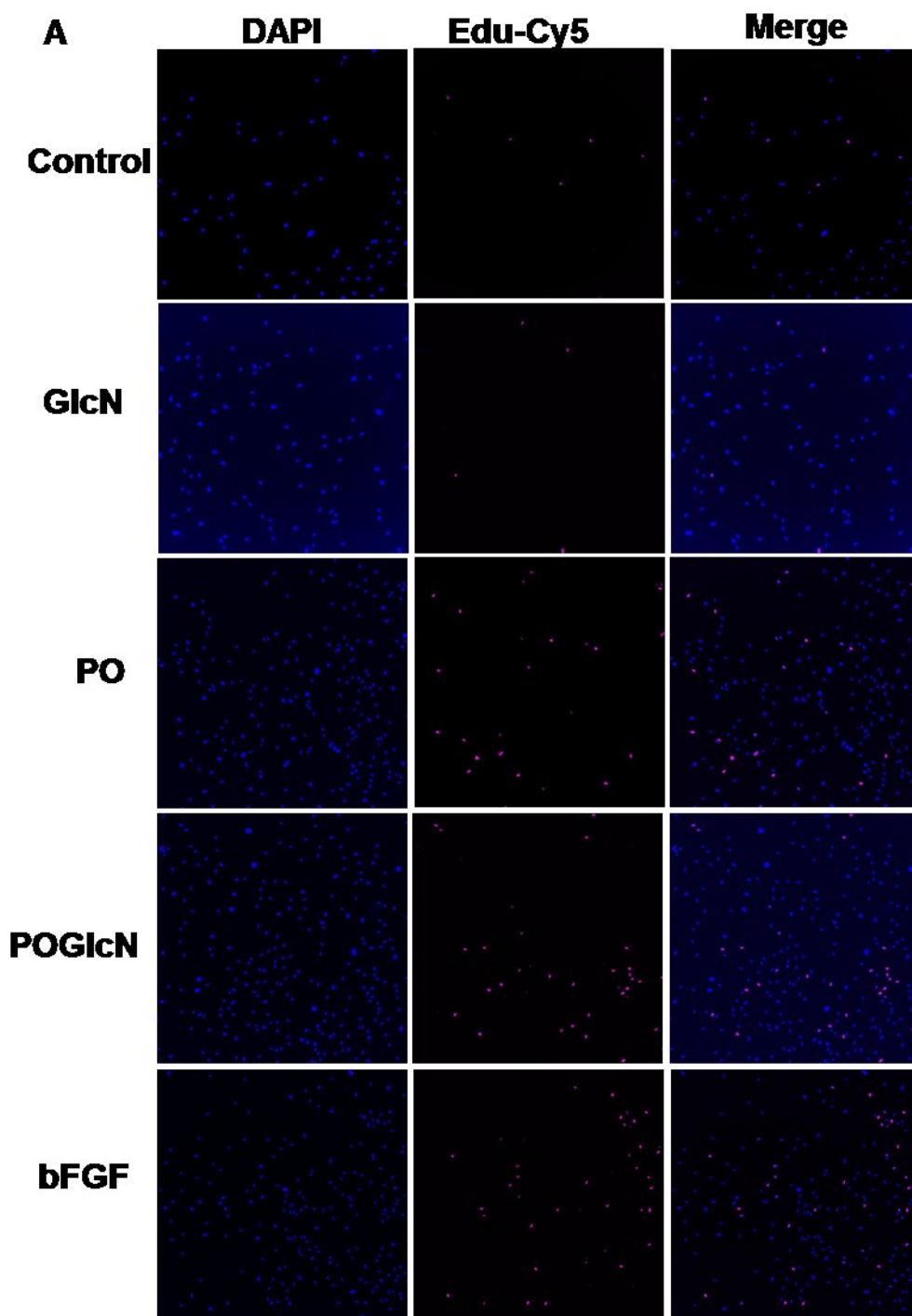
Figure 5.5. The incorporation of Edu by fibroblasts. (A) Representative images of DAPI and Cy5 stained fibroblasts treated with or without test compound for 4 days;
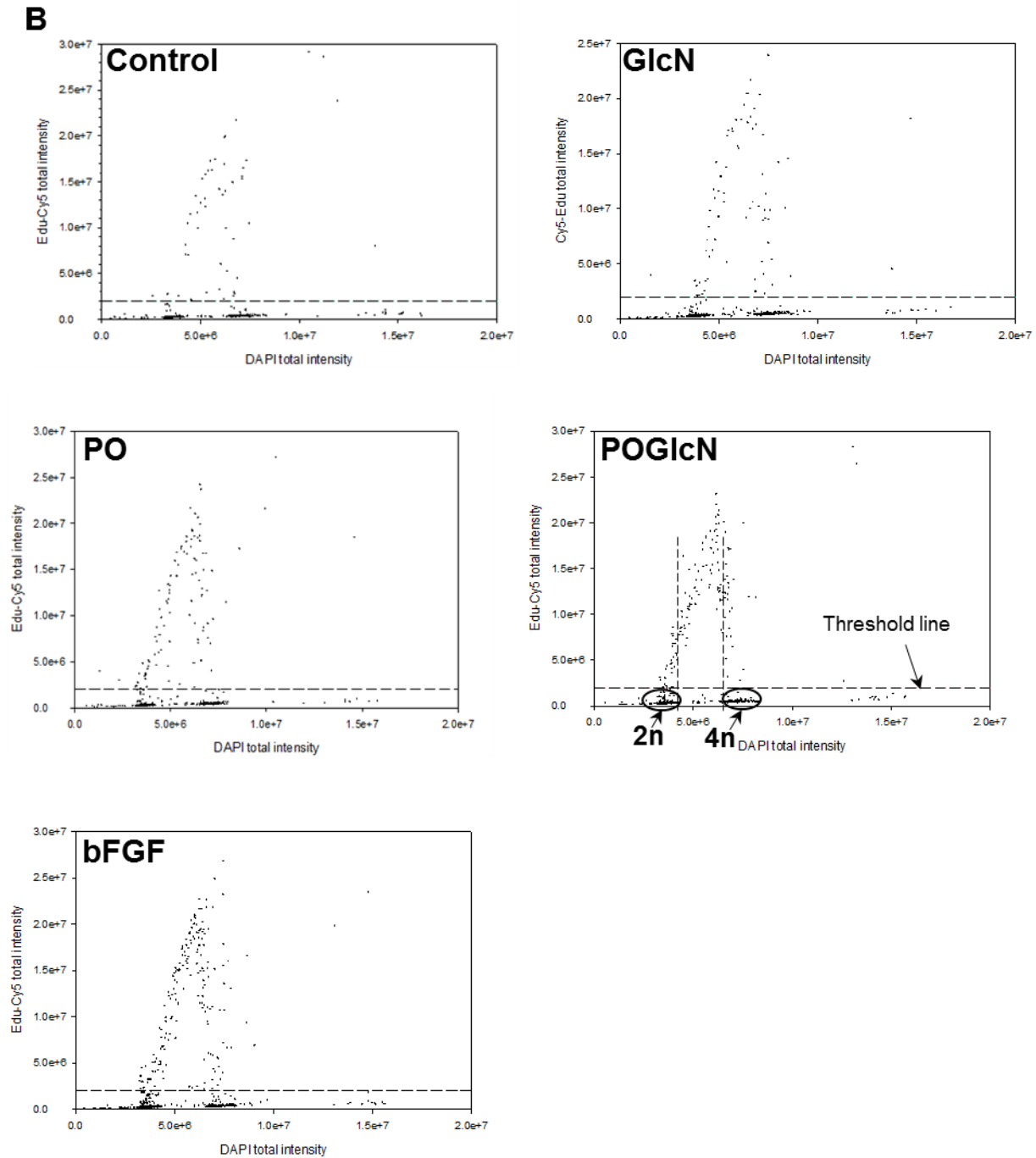
Figure 5.5. (B) Representative scatterplots of total Edu-Cy5 fluorescence intensity versus total DAPI intensity from fibroblasts treated with or without test compound for 4 days. A threshold line for Edu-Cy5 total pixel intensity ($> 2\times10^6$, dashed line) to define the fraction of total cell population in DNA synthesis phase
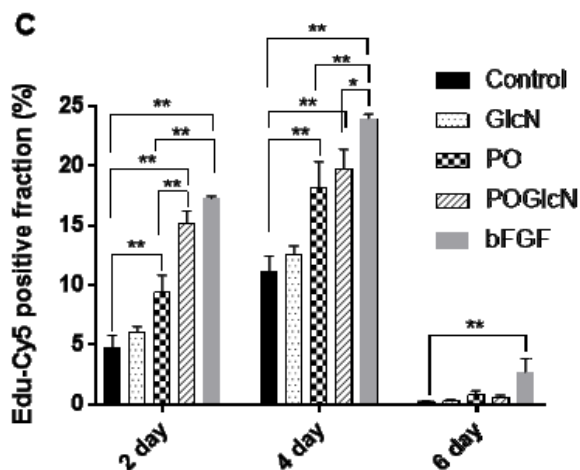
Figure 5.5. (C) Edu-Cy5 positive cell fractions of fibroblasts population treated with or without test compound for different time periods; abbreviations for treatments are the same with those in Figure 5.2. Bars represent standard deviation (n $\geqslant$ 3). *$p < 0.05$; **$p < 0.01$.

5.3.5. POGlcN Up-regulated the HAS2 and HAS3 Expression in HDF

Collagen production in ECM is the result of biosynthesis from type-specific gene expression. Type I collagen accounts for about 80% of collagen within dermal ECM, while type III accounts for about 15% (Tobin, 2017). Gene COL1A1 encodes pro-α1 chain of Type I collagen molecule which is consist of two identical alpha-1 chains and one alpha-2 chain. The expression level of COL1A1 can, therefore be an important biomarker for skin collagen production. On the other hand, the identified three isoforms of putative hyaluronan synthases responsible for the biosynthesis of HA are encoded by gene HAS1, HAS2, and HAS3. In this study, we extracted total RNA from fibroblasts and quantified the mRNA level of selected genes, COL1A1, and HAS1, HAS2, HAS3, to infer the production of collagen and HA, respectively. The response of each gene to the test compounds helped to clarify which gene was involved in the turnover of collagen/HA in cultured HDF. The amplification plot obtained from qRT-PCR shows a comparable high

expression level of COL1A1 to the endogenous control GAPDH, while relatively low level of HAS genes (Figure 5.6). It reflects the abundance of type I collagen in dermal skin and confirms the typical function of our cultured HDF. The greater expression level of HAS2 than HAS1 and HAS3 suggests that hyaluronan synthase-2 was probably the predominant isoform to control the production of HA by the HDF, which was also observed in the previous study (Kuroda et al., 2001). Some trials of the HAS3 expression level were so low that the fluorescence signal was not distinguishable from background, and thus not able to be quantified. The amplification efficiency of other tested genes including GAPDH, were similar at around 100% (99.3 ± 4.5%). PCR amplifications of later experimental samples which showed consistent expression of GAPDH were verified in the linear range. Therefore, it was reliable to quantify the relative expression level of COL1A1, HAS2 and HAS3 by comparative C_T method using GAPDH as the calibrator.
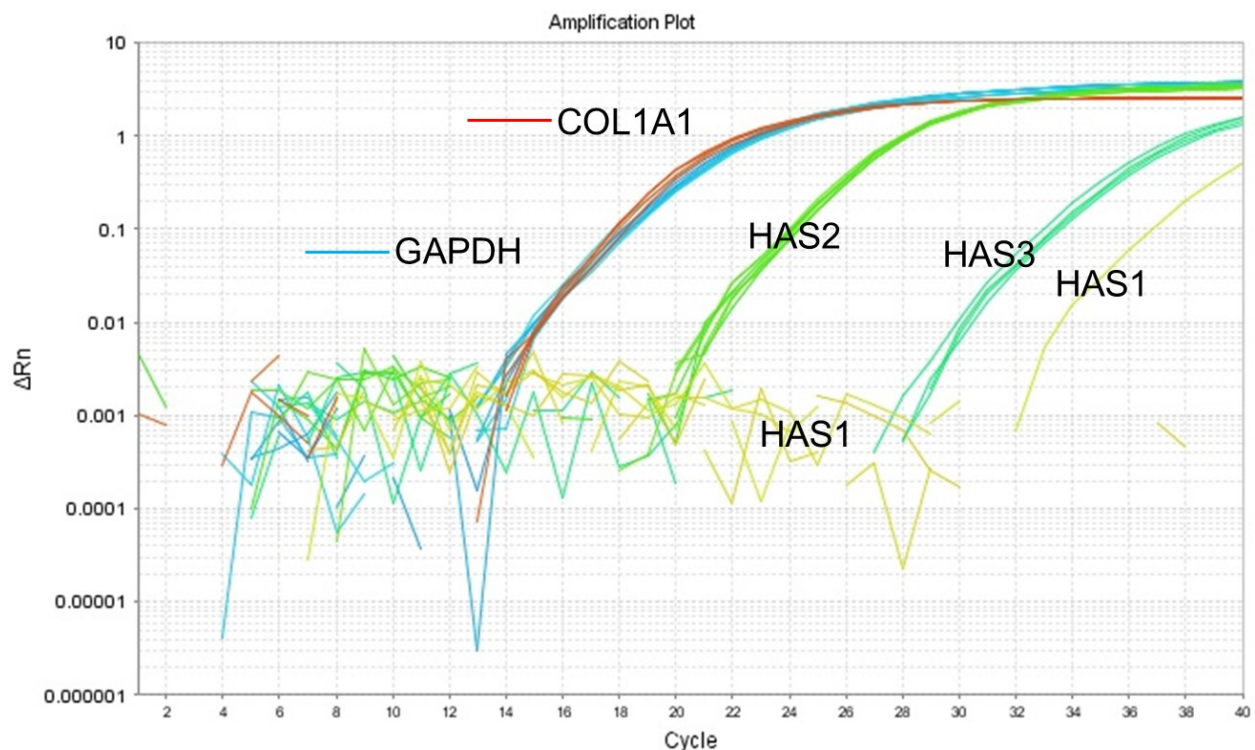

Figure 5.6. The representative amplification plot of gene COL1A1, HAS1, HAS2, HAS3, and GAPDH expressed by cultured fibroblasts.

Figure 5.7A shows the time-lapse of COL1A1 mRNA level change upon different treatments. No significant difference was observed compared to the control for all the treatments except bFGF. The ineffectiveness of these two peptides and GlcN on the expression of COL1A1 may explain the invariable collagen accumulation compared to control as indicated above (Figure 5.3A). The inhibition effect of bFGF on COL1A1 gene expression appeared after 2 days treatment (53.4%), and increased along with time up to 90.4% after 6 days, which was more acute than its inhibition on Hyp production. Basic FGF-induced down regulation of COL1A1 was observed in other studies (Tan et al., 1993). This supports its application to prevent fibrosis and wound healing cascade (Dolivo et al., 2017). In contrast, HAS genes seem to be more active in response to the external stimuli, dipeptide PO and glycopeptide POGlcN. After 2 days exposure, both significantly enhanced the mRNA levels of HAS2 to 1.8-fold of control, while only POGlcN up-regulated HAS3 expression at 2.0-fold. Despite GlcN stimulation on HAS3 expression was very modest (1.2-fold), HAS3 mRNA level of cells from POGlcN group was significantly greater than that from control and PO group (1.5-fold). This implies a synergistic effect may be involved when the two components are in the form of glycopeptide POGlcN. This effect was not manifested in HA production (Figure 3B) probably due to the less dominant expression of HAS3 and the slower synthesis rate of HAS3 synthase (Itano et al., 1999). As mentioned before, GlcN may function in acetalized form. However, in glycopeptide POGlcN molecule, the amino group of GlcN is already occupied. The higher efficiency of POGlcN than PO may imply that GlcN could also act as a signaling factor by itself considering its reserved structure in POGlcN, or it is released from POGlcN by some cellular enzymes before showing any function. Mammalian hyaluronan synthase isoforms exhibit different enzymatic properties regarding the duration of their activity, the rate in elongation of HA, and the molecular size of secreted HA products (Itano et al., 1999). HA extruded

by the membrane hyaluronan synthase-2 has a higher molecular weight ($>2\times10^6$ Da) than those secreted by synthase-1 and synthase-3 ($2\times10^5 \sim 2\times10^6$ Da). The molecular size of HA correlates with its mechanical property in retaining water of hydration and its effect in cell proliferation. Low-molecular-weight HA is angiogenic and favors cell growths (Stern and Maibach, 2008). In this respect, in comparison with PO, POGlcN stimulates the synthesis of a HA matrix with more diverse physical and biological properties, and greater potential in promoting tissue remodeling and regeneration.

As exposure time is prolonged, the up-regulation effect from both PO and POGlcN on HAS2 and/or HAS3 transcription decreased to insignificant after 4 days and 6 days (Figure 5.7B and Figure 5.7C). A decrease was also observed for the HAS2 transcripts of bFGF group from 5.40-fold after 2 days to 1.64-fold after 4 days, while the up-regulation remained significant. The bFGF effect on HAS2 gene seems to be more long-lasting. After 6 days treatment, however, it unexpectedly suppressed the expression of both the gene HAS2 (0.3-fold) and HAS3 (0.4-fold). The change in efficacy or even pattern of regulation at different time, reveals that the cell response to these stimuli was further complicated by the variation in growth rate, confluence level of the cell population, ability to secret ECM components, and other unknown properties during its growth. The expression of HAS genes has been reported to be lower in confluent cell cultures than subconfluent ones (Jacobson et al., 2000). The up-regulation of HAS genes by PO and POGlcN could be gradually masked as the cell cultures grew near to confluence when less transcripts were expressed after 4 days and 6 days. As the fibroblasts grew closer to confluence after 4 days in bFGF group than POGlcN group, the HAS3 transcript level of the former group (0.8-fold) was significantly less than the latter one (1.3-fold) due to the emerging suppressive effect of bFGF (Figure 5.7C). The down-regulation of HAS genes by bFGF on relatively confluent fibroblasts

after 6 days agrees with its antagonistic property to transforming growth factor-beta, which involves excess HA accumulation and myofibroblast transformation associated with fibrosis and hypertrophic scarring (Dolivo et al., 2017).
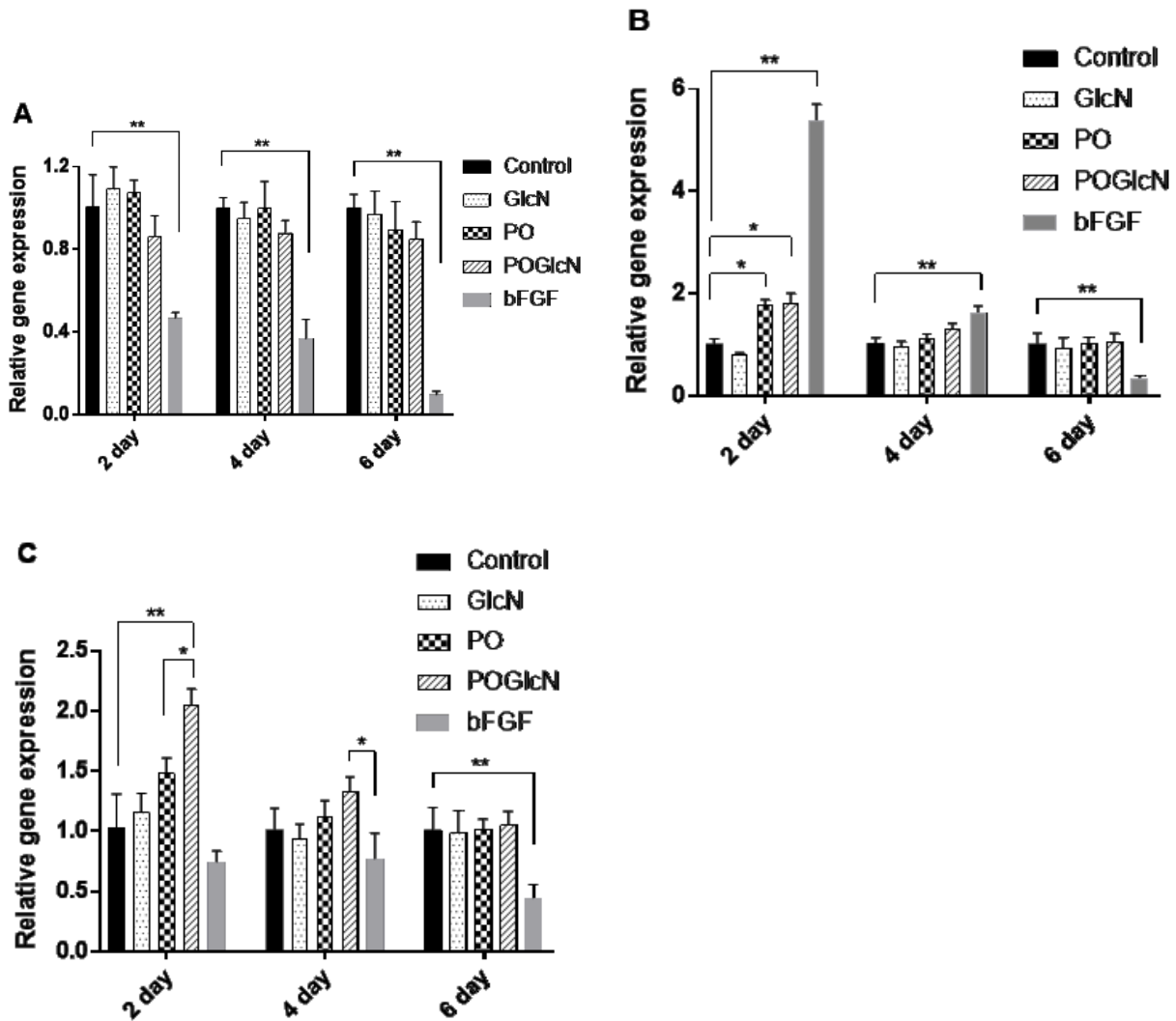
Figure 5.7. COL1A1 (A), HAS2 (B), and HAS3 (C) mRNA levels in cultured fibroblasts treated with or without test compound for various time periods. Abbreviations for treatments are the same with those in Figure 5.2. Bars represent standard deviation (n ≥ 3). *$p < 0.05$; **$p < 0.01$.

This study demonstrated that the novel collagen-derived glycopeptide Pro-Hyp-CONH-GlcN (POGlcN) can exhibit comparable effect to its parent dipeptide Pro-Hyp (PO) on promoting

the proliferation of cultured dermal fibroblasts and the production of matrix hyaluronan. In this respect, the incorporation of GlcN did not contribute to a better performance of POGlcN as hypothesized. However, as a potential mitogen, the glycopeptide POGlcN more rapidly affected cell cycle distribution of fibroblasts than PO by arresting more cells active in DNA synthesis and mitosis phases compared to the untreated control, which contributed to its enhanced proliferation capacity. Moreover, the incorporation of GlcN in POGlcN endowed it with the ability to up-regulate HAS3 gene expression, in addition to the up-regulation of HAS2 resulting from PO. The gradually decreased effect of POGlcN over time on controlling cell cycle and HAS expression suggested its non-aggressive promoting effect on cell growth and on HA deposition, respectively. This also implies its intriguing potential of being used to improve skin condition, treat wound healing, and facilitate tissue regeneration, without introducing risk factors for skin disease. In addition, the results suggest the practical meaning of extending the previously proposed synthesis method to other bioactive peptides to fortifying their effects. Further research about the mechanism of POGlcN action on dermal fibroblasts need to be conducted, such as the potential transporter, signaling receptor and related pathways, and *in vivo* performance efficacy.

CHAPTER 6.

Conclusions, implications, and future directions

From bovine hide to collagen hydrolysates (CH) to final functionalized collagen-derived peptides, this project represents the development of a system to improve CH accumulation in target sites in body, thus enhancing their biological efficiency. Key challenges were addressed, from very practical details of removing dirt and blood from the raw bovine hide, to relatively complicated and technical experiments devoted to overcoming the problematic intestinal absorption bottleneck of CH. Biological *in-vitro* models were then used to determine how successful CH were absorbed, and how the chemical modification affected cell responses and the gene expression. This production of CH was done using two different strategies - enzymatic hydrolysis and chemical modification - roughly dividing the project into two. The first part is depicted in chapter 3, while the second one is mainly in chapters 4 and 5. These studies contribute to advancing our understanding of CH and their absorption in the following ways:

1. Production of very low MW CH

At the beginning, this project developed an efficient, practical and easy method to extract collagen from an extremely tough bovine hide. Bovine hide is molecularly cross-linked at a greater level than material from other sources and represent a particular challenge. The combination of two affordable commercially available enzymes, Alcalase and Flavourzyme, was screened as the most effective treatment generating greater than 80% of very low MW (< 2 kDa) peptides. Bovine hide is considered as low-value by-product from beef industry, and the branding system used to mark the animal makes it less usable for leather industry. This study could help add value to the

bovine hide through enabling its bioconversion into collagen peptides that can be used for health benefits, and also used as functional ingredients in the food industry.

2. Transepithelial transport efficiency of CH

The *in vitro* gastrointestinal (GI) digestion and intestinal transport study revealed that CH with lower MW were more resistant to GI digestion, and exhibited greater transepithelial permeability. It provided solid evidence that the overall absorption of CH could be enhanced through reducing the MW of CH with intensive pre-digestion hydrolysis. Also, it justified the use of Alcalase and Flavourzyme in producing low MW CH that are more efficiently absorbed. The CH produced, especially from the Alcalase/Flavourzyme treatment, could be competitive alternatives to CH now commercially available due to an improved solubility, greater free amino acid content, and superior intestinal absorption.

3. Glycosylation with GlcN to improve intestinal absorption of collagen-derived peptides

The second part of this thesis is mainly focused on improving the intestinal absorption of collagen-derived peptides with structural chemical modification. Conjugation of a model collagen peptide, Pro-Hyp, with a simple amino sugar GlcN, generated a novel glycoeptide Pro-Hyp-CONH-GlcN that possessed improved intestinal permeation ability due to absorption by the GLUTs transport pathway. This approach did not compromise the affinity to the peptide transporter (PepT1) in common with the parent peptide. This suggests the potential of extending this method to modify other small bioactive peptides and therapeutic peptides accordingly. This study demonstrated the feasibility and effectiveness of glycosylation of peptides with GlcN to target glucose transporters.

4. Influence of peptide glycosylation and its biological effects on dermal fibroblasts

CH and some collagen-derived peptides have shown health benefits in many aspects (Proksch et al., 2014; Tanaka et al., 2009; Moskowitz, 2000). The last study used a specific *in vitro* human dermal fibroblast model to ask, "will the structural change by incorporating GlcN impact the biological effect of CH?" In this study, effects of the model peptide Pro-Hyp and its derivative Pro-Hyp-CONH-GlcN were compared, and this glycosylation strategy did not diminish either the ability of the parent peptide to stimulate the growth fibroblasts or the production of matrix HA. On the other hand, it did not improve the peptide efficiency of performance in HA biosynthesis as hypothesized either. However, the results clarified the mitogenic activity of both the peptides, and their role in the up-regulation of matrix-related genes. Compared to the parent peptide, the derived glycopeptide was shown to have potential as a promising agent to improve skin health; it was faster in controlling the fibroblast cell cycle and had a greater intestinal permeability. The glycopeptide treatment was shown to activate fibroblasts and stimulate the biosynthesis of HA, indicating its potential of being used to accelerate wound healing, and maintain the capacity of skin to regenerate and prevent premature skin aging. Nutricosmetics is an emerging area that arises from the convergence of cosmeceuticals and nutraceuticals; it refers to oral nutrient-supplements that target skin for beauty and health purposes. Skin fibroblast activity and the regulation of HA production are crucial contributors for skin regeneration, hydration and health. The positive findings in our study support the idea of developing collagen peptides and derived glycopeptides for nutricosmetic applications; these products are able be developed and evaluated scientifically to support claims in a systematic way.

For a broader application of chemical modification strategy, a few more representative collagen-derived peptides, such as Hyp-Gly, Pro-Hyp-Gly, may also be used as model peptides to evaluate the feasibility of GlcN incorporation for increasing its intestinal permeation. The

enzymatic stability of newly synthesized glycopeptides may vary depending on the structure of parent peptides. The biological effects of those collagen peptides and derived glycopeptides could be evaluated using *in vivo* models. Given the complex body digestion system where numerous enzymes are present, there is a greater chance that the glycopeptides with an amide functional group would be degraded or further modified. If that is the case, their half-life and final functional forms would need to be determined. If they survive digestion, the tissue distribution and preferential accumulation sites and therapeutic effects would need to be determined. Furthermore, glycosylation with GlcN applied to a fraction or a whole mixture of CH is worth investigating in a way that optimizes the reaction and purifies the final products. Any physiological function of the collagen-derived glycopeptides to improve skin conditions and prevent premature skin aging should be further verified with well-controlled clinical trials which include large size of subjects and undergo long-term monitoring. The effective doses and applicable people could therefore be suggested from those trials.

In addition, considering the beneficial effects of CH on other tissues, such as bone and joints, future studies could also focus on evaluating the effects of GlcN modified collagen peptides on chondrocytes and osteoblasts. There is a critical need to identify and understand the molecular signaling pathway and cell surface receptors involved, or simply any specific cell uptake transporter important in absorption of CH. It is also possible that these peptides affect cellular behavior by indirectly altering the cell-matrix interaction. Regardless of the findings, it would advance our understanding about the health benefits associated with collagen products.

In the foreseeable future of adding value to the gelatin industry and associated markets in CH nutricosmetics, a practical challenge will include the scale up of the extraction and hydrolysis methods, such as those proposed in the first part of this thesis. The Alcalase and Flavourzyme that

are needed in relatively small amounts (E/S: 1/50, w/w) are commercially available and could certainly be a feasible part of an industrial process. There are many potential technical obstacles though that will need to be addressed in extending the glycosylation strategy proposed in the second part. Although the food and cosmetic industries are well established, and they should have the capability to adapt to these very large opportunities, their success will be based on the sound research foundation created for CH production, bioavailability, biological efficacy and safety.

BIBLIOGRAPHY

Adam, M.; Spacek, P.; Hulejová, H.; Galiánová, A.; Blahos, J. Postmenopausal osteoporosis. Treatment with calcitonin and a diet rich in collagen proteins. *Cas. Lek. Cesk.* **1996**, 135(3), 74–78.

Adessi, C.; Soto, C. Converting a Peptide into a Drug: Strategies to Improve Stability and Bioavailability. *Curr. Med. Chem.* **2002**, *9* (9), 963–978.

Adler-Nissen, J. In *Enzymic Hydrolysis of Food Proteins*. Elsevier Applied Science Publishers Ltd: London, UK, **1986**, pp 116-124.

Agarwal, V., Reddy, I.K., Khan, M.A. Oral delivery of proteins: Effect of chicken and duck ovomucoid on the stability of insulin in the presence of α-chymotrypsin and trypsin. *Pharm Pharmacol Communications*, **2000**, *6* (5), 223-227.

Aito-Inoue, M; Lackeyram, D; Fan, MZ; Sato, K; Mine, Y. Transport of a tripeptide, Gly-Pro-Hyp, across the porcine intestinal brush-border membrane. *J Pept Sci.* **2007**, *13,* 468-474.

Alemán, A.; Giménez, B.; Pérez-Santin, E.; Gómez-Guillén, M. C.; Montero, P. Contribution of Leu and Hyp residues to antioxidant and ACE-inhibitory activities of peptide sequences isolated from squid gelatin hydrolysate. *Food Chem.* **2011**, *125* (2), 334–341.

Alemán, A.; Gómez-Guillén, M. C.; Montero, P. Identification of ACE-inhibitory peptides from squid skin collagen after *in vitro* gastrointestinal digestion. *Food Res. Int.* **2013**, *54* (1), 790–795.

Alemán & Martínez-Alvarez. Marine collagen as a source of bioactive molecules. A review. *The Nat. Prod. J.,* **2013**, *3,*105-114.

Alikhani, Z.; Alikhani, M.; Boyd, C. M.; Nagao, K.; Trackman, P. C.; Graves, D. T. Advanced glycation end products enhance expression of pro-apoptotic genes and stimulate fibroblast apoptosis through cytoplasmic and mitochondrial pathways. *J. Biol. Chem.* **2005**, *280,* 12087-12095.

Alzaid, F.; Cheung, HM.; Preedy, VR.; Sharp, PA. Regulation of Glucose transporter expression in human intestinal caco-2 cells following exposure to an anthocyanin-rich berry extract. *PLoS One.* **2013**, *8,* e78932. doi: 10.1371.

Anderberg, E. K.; Artursson, P. Epithelial transport of drugs in cell culture. VIII: effects of sodium dodecyl sulfate on cell membrane and tight junction permeability in human intestinal epithelial (Caco-2) cells. *J. Pharm. Sci.* **1993**, *82*(4), 392–398.

Artursson, P.; Palm, K.; Luthman, K. Caco-2 monolayers in experimental and theoretical predications of drug transport. *Adv. Drug Deliv. Rev.* **2012**, *64,* 280-289.

Asserin, J.; Lati, E.; Shioya, T.; Prawitt, J. The effect of oral collagen peptide supplementation on skin moisture and the dermal collagen network: Eevidence from an *ex vivo* model and randomized, placebo-controlled clinical trials. *J. Cosmet. Dermatol.* **2015**, *14* (4), 291–301.

Augustin, R. The protein family of glucose transport facilitators: It's not only about glucose after all. *IUBMB Life.* **2010**, *62,* 315-333.

Avery, N. C.; Bailey, A. J. The effects of the Maillard reaction on the physical properties and cell interactions of collagen. *Pathol. Biol.* (Paris) **2006**, *54*, 387-95, http://dx.doi.org/10.1016/j.patbio. 2006.07.005.

Avery, N. C.; Bailey, A. J. Restraining cross-links responsible for the mechanical properties of collagen fibers: natural and artificial. In *Collagen structure and mechanics,* ed. Fratzl, P. Springer Science+Business Media, LLC, New York, NY, USA, **2008;** pp. 91-95.

Baehaki, A.; Nopianti, R.; Anggraeni, S. Antioxidant activity of skin and bone collagen hydrolyzed from striped catfish (Pangasius pangasius) with papain enzyme. *J. Chem. Pharm. Res.* **2015**, *7* (11), 131–135.

Bailey, A. J.; Paul, R. G.; Knott, L. Mechanisms of maturation and ageing of collagen. *Mech. Ageing Dev.* **1998**, *106* (1–2), 1–56.

Balian, G. & Bowes, J. H. The structure and properties of collagen. In Ward, A. G. & Courts, A., The Science and Technology of Gelatin (page 21-23). **1977**, London: Academic Press Inc. Ltd.

Balimane, P.; Chong, S. Cell culture models for intestinal permeability: a critique. *Drug Discov. Today* **2005**, *10* (5), 335–343.

Banu, J. The Ovariectomized Mice and Rats. In *Osteoporosis Research*, G. Duque and K. Watanabe (eds.). Springer-Verlag Ltd., London, UK. **2011,** pp 101-114, DOI: 10.1007/978-0-85729-293-3_9

Bapst, J. P.; Calame, M.; Tanner, H.; Eberle, A. N. Glycosylated DOTA - α-Melanocyte-stimulating hormone analogues for melanoma targeting: Influence of the site of glycosylation on *in vivo* biodistribution. *Bioconjug. Chem.* **2009**, *20* (5), 984–993.

Beelen, M.; Koopman, R.; Gijsen, A. P. Protein coingestion stimulates muscle protein synthesis during resistance-type exercise. *Am. J. Physiol. Endocrinol. Metab.* **2008**, *295*, E70–E77.

Bello, A. E.; Oesser, S. Collagen hydrolysate for the treatment of osteoarthritis and other joint disorders: a review of the literature. *Curr. Med. Res. Opin.* **2006**, *22* (11), 2221–2232.

Benito-Ruiz, P.; Camacho-Zambrano, M. M.; Carrillo-Arcentales, J. N.; Mestanza-Peralta, M. A.; Vallejo-Flores, C. A.; Vargas-López, S. V.; Villacís-Tamayo, R. A.; Zurita-Gavilanes, L. A. A randomized controlled trial on the efficacy and safety of a food ingredient, collagen hydrolysate, for improving joint comfort. *Int. J. Food Sci. Nutr.* **2009**, *60* (sup2), 99–113.

Bernkop-Schnurch A. The use of inhibitory agents to overcome the enzymatic barrier to perorally administered therapeutic peptides and proteins. *J. Control. Release.* **1998**, *52* (1–2):1–16.

Bernkop-Schnurch, A.; Krajicek, ME. Mucoadhesive polymers as platforms for peroral peptide delivery and absorption: synthesis and evaluation of different chitosan-EDTA conjugates. *J. Control. Release.* **1998**, *50*(1–3), 215–223.

Biron, E.; Chatterjee, J.; Ovadia, O.; Langenegger, D.; Brueggen, J.; Hoyer, D.; Schmid, H.A.; Jelinek, R.; Gilon, C.; Hoffman, A.; Kessler, H. Improvingoral bioavailability of peptides by multiple N-methyla-tion: somatostatin analogues. *Angew Chem Int Ed Eng.* **2008**, *47*, 2595–2599.

Borumand, M.; Sibilla, S. Daily consumption of the collagen supplement Pure Gold Collagen reduces visible signs of aging. *Clin. Interv. Aging* **2014**, *9*, 1747–1758.

Borumand, M.; Sibilla, S. Effects of a nutritional supplement containing collagen peptides on skin elasticity, hydration and wrinkles. *J. Med. Nutr. Nutraceuticals* **2015**, *4* (1), 47.

Bourhis, J. M. Mariano, N. Zhao, Y. Harlos, K. Exposito, J. Jones, E. Y. Moali, C. Aghajari, N. and Hulmes, D. Structural basis of fibrillar collagen trimerization and related genetic disorders. *Nature Struct. Mol. Biol.* **2012**, *19*, 1031–1036.

Brandsch, M. Transport of L-proline, L-proline-containing peptides and related drugs at mammalian epithelial cell membranes. *Amino Acids* **2006**, *31* (2), 119–136.Ghosh, A. K. Collagen gene expression. *Exp. Biol. Med.* **2002**, *227* (5), 301–304.

Breborowicz, A.; Kuzlan-Pawlaczyk. M.; Wieczorowska-Tobis, K.; Wisniewska, J.; Tam, P.; French, I.; Wu, G.The effect of N-acetylglucosamine as a substrate for *in vitro* synthesis of glycosaminoglycans by human peritoneal mesothelial cells and fibroblasts. *Adv. Perit. Dial.* **1998**, *14*, 31-35.

Brecht, M.; Mayer, U.; Schlosser, E.; Prehm, P. Increased hyaluronate synthesis is required for fibroblast detachment and mitosis. *Biochem. J.* **1986**, *239* (2), 445–450.

Bröer, S. Amino acid transport across mammalian intestinal and renal epithelia. *Physiol Rev,* **2008**, *88,* 249–286.

Bruno, B. J.; Miller, G. D.; Lim, C. S. Basics and recent advances in peptide and protein drug delivery. *Ther. Deliv.* **2014**, *4* (11), 1443–1467.

Bruyère, O.; Zegels, B.; Leonori, L.; Rabenda, V.; Janssen, A.; Bourges, C.; Reginster, J. Y. Effect of collagen hydrolysate in articular pain: A 6-month randomized, double-blind, placebo controlled study. *Complement. Ther. Med.* **2012**, *20* (3), 124–130.

Calceti, P.; Salmaso, S.; Walker, G.; Bernkop-Schnürch, A. Development and *in vivo* evaluation of an oral insulin–PEG delivery system. *Eur. J. Pharm. Sci.* **2004**, 22, 315-323.

Carvalho, F.C.; Bruschi, M.L.; Evangelista, R.C.; Gremia, M.P.D. Mucoadhesive drug delivery systems. Braz. *J. Pharm. Sci.* **2010**, *46*(1), 1–17.

Cavanagh, J. F.; Mione, M. C.; Pappas, I. S.; Parnavelas, J. G. Basic fibroblast growth factor prolongs the proliferation of rat cortical progenitor cells *in vitro* without altering their cell cycle parameters. *Cereb. Cortex.* **1997**, *7* (4), 293–302.

Chalasani, K. B.; Russell-Jones, G. J. Yandrapu, S. K. Diwan, P.V.; Jain, S. K. A novel vitamin B12-nanosphere conjugate carrier system for peroral delivery of insulin. *J. Control. Release*. **2007**, *117*(3), 421–429.

Chan, J.M.; Valencia, P.M.; Zhang, L. Polymeric nanoparticles for drug delivery. *Methods Mol. Bio.* **2010**, 624, 163–175.

Chaturvedi, V.; Dye, D. E.; Kinnear, B. F.; Van Kuppevelt, T. H.; Grounds, M. D.; Coombe, D. R. Interactions between skeletal muscle myoblasts and their extracellular matrix revealed by a serum free culture system. *PLoS One* **2015**, *10* (6), 1–27.

Chen, M., and Li, B. The effect of molecular weights on the survivability of casein-derived antioxidant peptides after the simulated gastrointestinal digestion. *Innov Food Sci Emerg Technol,* **2012**, *16,* 341 – 348.

Chen, T.; Hou, H. Protective effect of gelatin polypeptides from Pacific cod (Gadus macrocephalus) against UV irradiation-induced damages by inhibiting inflammation and improving transforming growth factor-β/Smad signaling pathway. *J. Photochem. Photobiol. B Biol.* **2016**, *162*, 633–640.

Chi, C. F.; Cao, Z. H.; Wang, B.; Hu, F. Y.; Li, Z. R.; Zhang, B. Antioxidant and functional properties of collagen hydrolysates from Spanish mackerel skin as influenced by average molecular weight. *Molecules* **2014**, *19* (8), 11211–11230.

Chiquet, M.; Birk, D. E.; Bönnemann, C. G.; Koch, M. Collagen XII: Protecting bone and muscle integrity by organizing collagen fibrils. *Int. J. Biochem. Cell Biol.* **2014**, *53*, 51–54.

Cho, S.; Lee, M.J.; Kim, M.S.; Lee, S.; Kim, Y.K.; Lee, D.H.; Lee, C.W.; Cho, K.H.; Chung, J.H. Infrared plus visible light and heat from natural sunlight participate in the expression of MMPs and type I procollagen as well as infiltration of inflammatory cell in human skin *in vivo*. *J. Dermatol. Sci.* **2008**, *50* (2), 123 – 133.

Choi, S. Y.; Ko, E. J.; Lee, Y. H.; Kim, B. G.; Shin, H. J.; Seo, D. B.; Lee, S. J.; Kim, B. J.; Kim, M. N. Effects of collagen tripeptide supplement on skin properties: A prospective, randomized, controlled study. *J. Cosmet. Laser Ther.* **2014**, *16* (3), 132–137.

Chun, J.-Y.; Min, S.-G.; Jo, Y.-J. Production of low molecular collagen peptides-loaded liposomes using different charged lipids. *Chem. Phys. Lipids* **2017**, *209* (April), 1–8.

Chuong, C.; Nickoloff, B.; Elias, P.; Goldsmith, L.; Macher, E.; Maderson, P.; Sundberg, J.; Tagami, H.; Plonka, P. M.; K, T.-P. Section Editor: Ralf Paus, Hamburg What is the "true" function of skin? *Exp. Dermatol.* **2002**, *11*, 159–187.

Church, F. C., H. E. Swaisgood, D. H. Porter, and G. L. Catignani. Spectrophotometric assay using o-phthaldialdehyde for determination of proteolysis in milk and isolated milk proteins. *J. Dairy Sci.,* **1983**, *66,* 1219–1227.

Cinq-Mars, C. D., Hu, C., Kitts, D. D., & Li-Chan, C. Y. Investigations into inhibitor type and mode, simulated gastrointestinal digestion, and cell transport of the angiotensin I-converting enzyme-inhibitory peptides in pacific hake (Merluccius productus) fillet hydrolysate. *J. Agric. Food Chem.,* **2008***, 56,* 410 – 419.

Contet-Audonneau, J. L.; Jeanmaire, C.; Pauly, G. A histological study of human wrinkle structures: comparison between sun- exposed areas the face, with or without wrinkles and sun-protected areas. *Br J Dermatol.* **1999**, *140*, 1038–1047.

Cooper, G. M.; Hausman, R. E. The cell cycle. In *The cell a molecular approach*. 5th ed.; ASM Press: Washington, D.C., **2009**; pp 653-655.

Cowieson, A. J. & Adeola, O. Carbohydrases, protease, and phytase have an additive beneficial effect in nutritionally marginal diets for broiler chicks. *Poult Sci.* **2005***, 84,* 1860–1867.

Craik, D. J.; Fairlie, D. P.; Liras, S.; Price, D. The future of peptide-based drugs. *Chem. Biol. Drug Des.* **2013**, *81*(1), 136–147.

Cuthbertson, D. J. Anabolic signaling and protein synthesis in human skeletal muscle after dynamic shortening or lengthening exercise. *Am. J. Physiol. Endocrinol. Metab.* **2006**, *290* (4), E731–E738.

Cúneo, F.; Costa-Paiva, L.; Pinto-Neto, A. M.; Morais, S. S.; Amaya-Farfan, J. Effect of dietary supplementation with collagen hydrolysates on bone metabolism of postmenopausal women with low mineral density. *Maturitas* **2010**, *65* (3), 253–257.

Daniel, L. U.S. Patent No. 3,894,132. **1975**, Washington, DC: U.S. Patent and Trademark Office.

Davis, S.S.; Illum, L. Absorption enhancers for nasal drug delivery. *Clin. Pharmacokinet.* **2003**, *42*(13), 1107–1128.

Deibert, P.; Solleder, F.; Konig, D. Soy protein based supplementation supports metabolic effects of resistance training in previously untrained middle-aged males. *Aging Male* **2011**, *14*, 273–279.

Derfoul, A.; Miyoshi, A. D.; Freeman, D. E.; Tuan, R. S. Glucosamine promotes chondrogenic phenotype in both chondrocytes and mesenchymal stem cells and inhibits MMP-13 expression and matrix degradation. *Osteoarthr. Cartil.* **2007**, *15* (6), 646–655.

Doren, V. S. R. Matrix metalloproteinase interactions with collagen and elastin. *Matrix Biol.* **2015**, *44–46* (i), 224–231.Danby, F. W. Nutrition and aging skin: Sugar and glycation. *Clin. Dermatol.* **2010**, *28* (4), 409–411.

Di, L.; Kerns, E. H.; Hong, Y.; Chen, H. Development and application of high throughput plasma stability assay for drug discovery. *Int. J. Pharm.* **2005**, *297* (1–2), 110–119.

Ding, L.; Zhang, Y.; Jiang, Y.; Wang, L.; Liu, B.; Liu, J. Transport of egg white ACE-inhibitory peptide, Gln-Ile-Gly-Leu-Phe, in human intestinal Caco-2 cell monolayers with cytoprotective effect. *J Agric. Food Chem.* **2014**, *62,* 3177-3182.

Ding, L.; Wang, L.; Zhang, Y.; Liu, J. Transport of antihypertensive peptide RVPSL, ovotransferrin 328-332, in human intestinal Caco-2 cell monolayers. *J Agric. Food Chem.* **2015**, *63,* 8143-8150.

Dolivo, D. M.; Larson, S. A.; Dominko, T. Fibroblast growth factor 2 as an anti fibrotic: antagonism of myofibroblast differentiation and suppression of pro-fibrotic gene expression. *Cytokine Growth Factor Rev.* **2017**, http://dx.doi.org/10.1016/j.cytogfr.2017.09.003.

Dolphin, J. M., & Russell, J. D. U.S. Patent No. 7,897,728 B2. **2011**, Washington, DC: U.S. Patent and Trademark Office.

Dong, S., Zeng, M., Wang, D., Liu, Z., Zao, Y. & Yang, H. Antioxidant and biochemical properties of protein hydrolysates prepared from silver carp (*Hypophthalmichthys molitrix*). *Food Chem.,* **2008***, 107,* 1485–1493.

Drewe, J.; Fricker, G.; Vonderscher, J.; Beglinger, C. Enteral absorption of octreotide: absorption enhancement by polyoxyethylene-24-cholesterol ether. *Br. J. Pharmacol.* **1993***,108,* 298–303.

Driskell, R. R.; Watt, F. M. Understanding fibroblast heterogeneity in the skin. *Trends Cell Biol.* **2015**, *25* (2), 92–99.

Du, L., Khiari, Z., Pietrasik, Z. and Betti, M. Physicochemical and functional properties of gelatins extracted from turkey and chicken heads. *Poult Sci.,* **2013***, 92*, 2463–2474.

Dupont, E.; Gomez, J.; Bilodeau, D. Beyond UV radiation: A skin under challenge. *Int. J. Cosmet. Sci.* **2013**, *35* (3), 224–232.

Edward, L.; Sutton, S. C. *In vitro* models for selection of development candidates. Permeability studies to define mechanisms of absorption enhancement. *Adv. Drug Deliv. Rev.* **1997**, *23* (1–3), 163–183.

Edwards, C. A., and W. D. Jr. O'Brien. Modified assay for determination of hydroxyl-proline in a tissue hydrolyzate. *Clinica Chimica Acta,* **1980,** *104,* 161–167.

Evans, W. J. Protein nutrition, exercise and aging. *J Am Coll Nutr.* **2004**, *23*, 601S–609S.

Fahmy, R.; Danielson, D.; Martinez, M. Formulation and design of veterinary tablets. In *Pharmaceutical Dosage Forms – Tablets*, 3rd; Augsburger, L.L.; Hoag, S.W., Eds.; CRC Press: Boca Raton, Florida, **2008**; pp 383-431.

Farrar, M. D. Advanced glycation end products in skin ageing and photoageing: what are the implications for epidermal function? *Exp. Dermatol.* **2016**, *25* (12), 947–948.

Feng, M.; Betti, M. Transepithelial transport efficiency of bovine collagen hydrolysates in a human Caco-2 cell line model. *Food Chem.* **2017a**, *224,* 242–250.

Feng, M.; Betti, M. Both PepT1 and GLUT Intestinal transporters are utilized by a novel glycopeptide Pro-Hyp-CONH-GlcN. *J. Agric. Food Chem.* **2017b**, *65* (16), 3295–3304.

Fink, B.; Braun, L. Treatment of extensive gluteus muscle tears with transosseous fixation and a nonresorbable collagen patch. *J. Arthroplasty* **2017**, 1–5.

Fligiel, S. E.; Varani, J.; Datta, S. C. Collagen degradation in aged/photodamaged skin *in vivo* and after exposure to matrix metalloproteinase-1 *in vitro*. *J Invest Dermatol.* **2003,** *120*, 842–848.

Fujii, T.; Okuda, T.; Yasui, N.; Wakaizumi, M.; Ikami, T.; Ikeda, K. Effects of amla extract and collagen peptide on UVB-induced photoaging in hairless mice. *J. Funct. Foods* **2013**, *5* (1), 451–459.

Fukuda, M.; Takahashi, K.; Ohkawa, C.; Sasaki, Y.; Hasegawa, Y. Identification of a resistant protein from scallop shell extract and its bile acid-binding activity. *Fish. Sci.* **2013**, *79* (6), 1017–1025.

Fukuta, M.; Okada, H.; Iinuma, S.; Yanai, S.; Toguchi, H. Insulin fragments as a carrier for peptide delivery across the blood-brain barrier. *Pharm. Res.***1994**, *11* (12), 1681-1688.

Ganopathy, V., Gupta, N., & Martindale, R. G. Protein digestion and absorption. In L. R. Johnson, Physiology of the gastrointestinal tract. **2006,** San Diego: Elsevier Academic Press. pp. 1667-1670.

Gibbs, J. H.; Potts, R. C.; Brown, R. A.; Robertson, A. J.; Beck, J. S. Mechanisms of phytohaemagglutinin (PHA) stimulation of normal human lymphocytes: 'trigger', 'push' or both? *Cell Prolif.* **1982**, *15* (2), 131–137.

Gibson, T.; Kenedi, R. M.; Craik, J. E. The mobile micro-architecture of dermal collagen: a bio-engineering study. *Brit J Surg.* **1965**, *52,* 764–770.

Gillies, A. R.; Lieber, R. L. Structure and function of the skeletal muscle extracellular matrix. *Muscle nerve,* **2011**, *44* (3), 318–331.

Gkogkolou, P.; Böhm, M. Advanced glycation end products. *Dermato-endocrinol.* **2012**, *4* (3), 259–270.

Gross, J.; Schmitt, F.O. The structure of human skin collagen as studied with the electron microscope. *J. Exp. Med.*, **1948**, *88*, 555-568.

Grove, G. L. Physiologic changes in older skin. *Clin Geriatr Med.* **1989**, *5*, 115–125.

Gupta, A.; Al-Aubaidy, H. A.; Mohammed, B. I. Glucose dependent insulinotropic polypeptide and dipeptidyl peptidase inhibitors: Their roles in management of type 2 diabetes mellitus. *Diabetes Metab. Syndr.* **2016**, *10* (2), S170–S175.

Guillerminet, F.; Beaupied, H.; Fabien-Soulé, V.; Tomé, D.; Benhamou, C.; Roux, C.; Blais, A. Hydrolyzed collagen improves bone metabolism and biomechanical parameters in ovariectomized mice: An *in vitro* and *in vivo* study. Bone, **2010**, *46*, 827−834.

Hanani. Z. N. Gelatin. In *Reference Module in Food Science*. Elsevier Inc. Amsterdam, Netherlands, **2015**; pp 191-195.

Haratake, A.; Watase, D.; Fujita, T.; Setoguchi, S.; Matsunaga, K.; Takata, J. Effects of oral administration of collagen peptides on skin collagen content and its underlying mechanism using a newly developed low collagen skin mice model. *J. Funct. Foods* **2015**, *16*, 174–182.

Hausch, F., Shan, L., & Santiago, N. A. Intestinal digestive resistance of immunodominant gliadin peptides. *Am J Physiol Gastrointest Liver Physiol,* **2002***, 283,* 996 – 1003.

Herregods, G.; Van Camp, J.; Morel, N.; Ghesquière, B.; Gevaert, K.; Vercruysse, L.; Dierckx, S.; Quanten, E.; Smagghe, G. Angiotensin I-converting enzyme inhibitory activity of gelatin hydrolysates and identification of bioactive peptides. *J. Agric. Food Chem.* **2011**, *59* (2), 552–558.

Herrera-Ruiz, D.; Knipp, G. T. Current perspectives on established and putative mammalian oligopeptide transporters. *J. Pharm. Sci.* **2003**, *92* (4), 691–714.

Heu, M. S.; Lee, J. H.; Kim, H. J.; Jee, S. J.; Lee, J. S.; Jeon, Y. J.; Shahidi, F.; Kim, J. S. Characterization of acid- and pepsin-soluble collagens from flatfish skin. *Food Sci. Biotechnol.* **2010**, *19* (1), 27–33.

Hidalgo, I.J.; Raub, T.J.; Borchardt, R.T. Characterization of the human colon carcinoma cell line (Caco-2) as a model system for intestinal epithelial permeability. *Gastroenterol.* **1989**, *96,* 736-749.

Hong, H.; Chaplot, S.; Chalamaiah, M.; Roy, B. C.; Bruce, H. L.; Wu, J. Removing Cross-Linked Telopeptides Enhances the Production of Low-Molecular-Weight Collagen Peptides from Spent Hens. *J. Agric. Food Chem.* **2017**, *65* (34), 7491–7499.

Horton, D.; Jewell, J. S., Philips, K. D. Anomeric equilibria in derivatives of amino sugars. Some 2-Amino-2-deoxy-D-hexose Derivatives. *J Organic Chem.* **1966**, *31,* 4022-4025.

Horowitz, W. Official Methods of Analysis of AOAC International (18 ed.). **2000**, Gaithersburg, AOAC International.

Hou, H.; Li, B.; Zhao, X.; Zhuang, Y.; Ren, G.; Yan, M.; Cai, Y.; Zhang, X.; Chen, L. The effect of pacific cod (Gadus macrocephalus) skin gelatin polypeptides on UV radiation-induced skin photoaging in ICR mice. *Food Chem.* **2009**, *115* (3), 945–950.

Hrynets, Y.; Ndagijimana, M.; Betti, M. Studies on the Formation of Maillard and Caramelization Products from Glucosamine Incubated at 37°C. *J. Agric. Food Chem.* **2015**, *63* (27), 6249–6261.

Hubatsch, I1; Ragnarsson, EG; Artursson, P. Determination of drug permeability and prediction of drug absorption in Caco-2 monolayers. *Nat. Protoc.* **2007**, *2,* 2111-2119.

Hulmes, D. J. S. Collagen diversity, synthesis and assembly. In *Collagen Structure and Mechanics* ed. Fratzl, Springer Science+Business Media, LLC, New York, NY, USA, **2008;** pp 15–47.

Hulmes, D. J. S. Building collagen molecules, fibrils, and suprafibrillar structures. *J. Struct. Biol.* **2002**, *137*, 2–10.

Huang, S. L.; Hung, C. C.; Jao, C. L.; Tung, Y. S.; Hsu, K. C. Porcine skin gelatin hydrolysate as a dipeptidyl peptidase IV inhibitor improves glycemic control in streptozotocin-induced diabetic rats. *J. Funct. Foods* **2014**, *11* (C), 235–242.

Huertas, A. C.; Schmelzer, C. E. H.; Hoehenwarter, W.; Heyroth, F.; Heinz, A. Molecular-level insights into aging processes of skin elastin. *Biochimie* **2016**, *128–129*, 163–173.

Hüls, A.; Vierkötter, A.; Gao, W.; Krämer, U.; Yang, Y.; Ding, A.; Stolz, S.; Matsui, M.; Kan, H.; Wang, S.; Jin, L.; Krutmann, J.; Schikowski, T. Traffic-related air pollution contributes to development of facial lentigines: further epidemiological evidence from Caucasians and Asians. *J. Invest. Dermatol.* **2016**, *136* (5), 1053–1056.

Hüls, A.; Schikowski, T.; Krämer, U.; Sugiri, D.; Stolz, S.; Vierkoetter, A.; Krutmann, J. Ozone exposure and extrinsic skin aging: results from the SALIA cohort, *J. Invest. Dermatol.* **2015**, *135* 286 (S49, Abstract).

Ichikawa, S.; Morifuji, M.; Ohara, H.; Matsumoto, H.; Takeuchi, Y.; Sato, K. Hydroxyproline-containing dipeptides and tripeptides quantified at high concentration in human blood after oral administration of gelatin hydrolysate. *Int. J. Food Sci. Nutr.* **2010**, *61* (1), 52–60.

Ibrahim, A.; Jamali, F. Improved sensitive high performance liquid chromatography assay for glucosamine in human and rat biological samples with fluorescence detection. *J. Pharm. Sci.* **2010**, *13,* 128-135.

Ibrahim, A; Gilzad-kohan, MH; Aghazadeh-Habashi, A; Jamali, F. Absorption and bioavailability of glucosamine in the rat. *J. Pharm. Sci.* **2012**, *101,* 2574-2583.

Ichikawa, S.; Morifuji, M.; Ohara, H.; Matsumoto, H.; Takeuchi, Y.; Sato, K. Hydroxyproline-containing dipeptides and tripeptides quantified at high concentration in human blood after oral administration of gelatin hydrolysate. *Int. J. Food Sci. Nutr.* **2010**, *61* (1), 52–60.

Itano, N.; Sawai, T.; Yoshida, M.; Lenas, P.; Yamada, Y.; Imagawa, M.; Shinomura, T.; Hamaguchi, M.; Yoshida, Y.; Miyauchi, S.; Spicer, A. P.; et al. Three isoforms of mammalian hyaluronan synthases have distinct enzymatic properties. *J. Biol. Chem.* **1999**, *274* (35), 25085–25092.

Iwai, K., Hasegawa, T.; Taguchi, Y.; Morimatsu, F.; Sato, K.; Nakamura, Y.; Higashi, A.; Kido, Y.; Nakabo, Y.; Ohtsuki, K. Identification of food-derived collagen peptides in human blood after oral ingestion of gelatin hydrolysates. *J Agric. Food Chem.* **2005**, *53,* 6531-6536.

Iwami, K., K. Sakakibara, and F. Ibuki. Involvement of pot-digestion "hydrophobic" peptides in plasma cholesterol-lowering effect of dietary plant proteins. *Agric. Biol. Chem.* **1986.** 50:1217–1222.

Iwanaga K, Ono S, Narioka K, et al. Application of surface-coated liposomes for oral delivery of peptide: effects of coating the liposome's surface on the GI transit of insulin. *J. Pharm. Sci.* **1999**, *88*(2), 248–252.

Jacobson, A.; Brinck, J.; Briskin, M. J.; Spicer, A. P.; Heldin, P. Expression of human hyaluronan synthases in response to external stimuli. *Biochem. J.* **2000**, *348 Pt 1* (Pt 1), 29–35.

Jin, Y.; Yan, J.; Yu, Y.; Qi, Y. Screening and identification of DPP-IV inhibitory peptides from deer skin hydrolysates by an integrated approach of LC-MS/MS and in silico analysis. *J. Funct. Foods* **2015**, *18*, 344–357.

Johnston-Banks, F. A. Gelatine. In P. Harris, Food Gels, **1990**, London and New York: Elsevier Applied Science. pp. 234-237

Jridi, M.; Lassoued, I.; Nasri, R.; Ayedi Mohamed, A.; Nasri, M.; Souissi, N. Characterization and potential use of cuttlefish skin gelatin hydrolysates prepared by different microbial proteases. *BioMed Res. Int.* **2014**, doi:10.1155/2014/461728.

Kanis, J. A.; McCloskey, E. V.; Johansson, H.; Oden, A.; Melton, L. J.; Khaltaev, N. A reference standard for the description of osteoporosis. *Bone,* **2008**, *42* (3), 467–475.

Kent K. Miyamoto, Susan A. McSherry, Simon P. Robins, Jeffrey M. Besterman, James L. Mohler. Collagen Cross-Link Metabolites in Urine as Markers of Bone Metastases in Prostatic Carcinoma. *J. Urol.* **1994**, *151* (4), 909-913.

Kim, H.K.; Kim, M.G.; Leem, K.H. Osteogenic activity of collagen peptide via ERK/ MAPK pathway mediated boosting of collagen synthesis and its therapeutic efficacy in osteoporotic bone by back-scattered electron imaging and microarchitecture analysis, *Molecules,* **2013**, *18,* 15474–15489.

Kimira, Y.; Ogura, K.; Taniuchi, Y.; Kataoka, A.; Inoue, N.; Sugihara, F.; Nakatani, S.; Shimizu, J.; Wada, M.; Mano, H. Collagen-derived dipeptide prolyl-hydroxyproline differentiation of MC3T3-E1 osteoblastic cells. *Biochem. Biophys. Res. Commun.* **2014**, *453* (3), 498–501.

Kamiyama, M. W.; Shimizu, M.; Kamiyama, S.; Taguchi, Y.; Sone, H.; Morimatsu, F.; Shirakawa, H.; Furukawa, Y.; Komai, M. Absorption and effectiveness of orally administered low molecular weight collagen hydrolysate in rats. *J. Agric. Food Chem.* **2010**, *58* (2), 835–841.

Keil-Dlouhá, V., N. Zylber, N. T. Tong, and B. Keil. Cleavage of glucagon by α- and β-trypsin. *FEBS Letters.* **1971**, *16,* 287–290.

Kellett, G.L.; Brot-Laroche, E. Apical GLUT2: a major pathway of intestinal sugar absorption. *Diabetes.* **2005**, *54,* 3056-3062.

Khiari, Z., Ndagijimana, M., & Betti, M. Low molecular weight bioactive peptides derived from the enzymatic hydrolysis of collagen after isoelectric solubilization/precipitation process of turkey by-product. *Poult.Sci.,* **2014**, *93*, 2347–2362.

Kikuchi, K.; Matahira, Y. Oral N-acetylglucosamine supplementation improves skin conditions of female volunteers: Clinical evaluation by a microscopic three-dimensional skin surface analyzer. *J. Appl. Cosmetol.* **2002**, *20* (2), 143–152.

Kim, S., Kim, Y., Byun, H., Park, P., & Ito, H. Purification and characterization of antioxidative peptides from bovine skin. *J. Biochem. and Mol. Biol.,* **2001a,** *34*, 219-224.

Kim, S., Byun, H., Park, P., & Shahidi, F. Angiotensin I-converting enzyme inhibitory peptides purified from bovine skin gelatin hydrolysate. *J. Agric. Food Chem.* **2001b**, *49,* 2992-2997.

Kimira, Y.; Ogura, K.; Taniuchi, Y.; Kataoka, A.; Inoue, N.; Sugihara, F.; Nakatani, S.; Shimizu, J.; Wada, M.; Mano, H. Collagen-derived dipeptide prolyl-hydroxyproline promotes differentiation of MC3T3-E1 osteoblastic cells. *Biochem. Biophys. Res. Commun.* **2014**, *453,* 498-501.

Kipp, H.; Kinne-Saffran, E.; Bevan, C.; Kinne, R.K. Characteristics of renal Na+-D-glucose cotransport in the skate (*Raja erinacea*) and shark (*Squalus acanthias*). *Am J Physiol.* **1997**, 273, R134-142.

Kjaer, M. Role of Extracellular Matrix in Adaptation of Tendon and Skeletal Muscle to Mechanical Loading. *Physiol. Rev.* **2004**, *84* (2), 649–698.

Ko, S.-C.; Jang, J.; Ye, B.-R.; Kim, M.-S.; Choi, I.-W.; Park, W.-S.; Heo, S.-J.; Jung, W.-K. Purification and molecular docking study of angiotensin I-converting enzyme (ACE) inhibitory peptides from hydrolysates of marine sponge Stylotella aurantium. *Process Biochem.* **2016**, *54*, 1–8.

Kohan, H.G.; Kaur, K.; Jamali, F. Synthesis and characterization of a new peptide prodrug of glucosamine with enhanced gut permeability. *PLoS One.* **2015**, *10,* e0126786.

Koyama, Y.; Hirota, A.; Mori, H.; Takahara, H.; Kuwaba, K.; Kusubata, M.; Matsubara, Y.; Kasugai, S.; Itoh, M.; Irie, S. J NutrSci Vitaminol, 47, 84-86, 2001. *J. Nutr. Sci. Vitaminol.* **2001**, *47*, 84–86.

Krutmann, J.; Bouloc, A.; Sore, G.; Bernard, B. A.; Passeron, T. The skin aging exposome. *J. Dermatol. Sci.* **2017**, *85* (3), 152–161.

Kujawa, M.J.; Tepperman, K. Culturing chick muscle cells on glycosaminoglycan substrates: attachment and differentiation. *Dev. Biol.* **1983**, *99,* 277-286.

Kuroda, K.; Utani, a; Hamasaki, Y.; Shinkai, H. Up-regulation of putative hyaluronan synthase mRNA by basic fibroblast growth factor and insulin-like growth factor-1 in human skin fibroblasts. *J. Dermatol. Sci.* **2001**, *26* (2), 156–160.

Kwon, O.; Eck, P.; Chen, S.; Corpe, C.P.; Lee, J.; Kruhlak, M.; Levine, M. Inhibition of the intestinal glucose transporter GLUT2 by flavonoids. *FASEB J.* **2007**, *21,* 366-377.

Langton, A. K.; Halai, P.; Griffiths, C. E. M.; Sherratt, M. J.; Watson, R. E. B. The impact of intrinsic ageing on the protein composition of the dermal-epidermal junction. *Mech. Ageing Dev.* **2016**, *156*, 14–16.

Lawson, M. A.; Purslow, P. P. Differentiation of myoblast in serum-free media: effects of modified media are cell line specific. *Cell Tissue Organs,* **2000**, *167,* 130–137.

Liebel, F.; Kaur, S.; Ruvolo, E.; Kollias, N.; Southall, M.D. Irradiation of skin with visible light induces reactive oxygen species and matrix-degrading enzymes, *J. Invest. Dermatol.* **2012,** *132* (7), 1901–1907.

Lin, L.; Lv, S.; Li, B. Angiotensin-I-converting enzyme (ACE)-inhibitory and antihypertensive properties of squid skin gelatin hydrolysates. *Food Chem.* **2012**, *131* (1), 225–230.

Lindley, D. J.; Carl, S. M.; Herrera-Ruiz, D., Pan, L.; Karpes L. B.; Goole J.; Gudmundsson, P.; and Knipp G. T. Drug transporters and their role in absorption oadn disposition of peptides and peptide-based pharmaceuticals. In *Oral bioavailability: basic principles, advanced concepts, and applications.* John Wiley & Sons, Inc., Hoboken, New Jersey, USA. **2011**; pp 291-303.

Listrat, A.; Pissavy, A. L.; Micol, D.; Jurie, C.; Lethias, C.; Pethick, D. W.; Hocquette, J. F. Collagens XII and XIV: Two collagen types both associated with bovine muscle and intramuscular lipid metabolism. *Livest. Sci.* **2016**, *187*, 80–86.

Liu, J.; Zhang, B.; Song, S. Bovine collagen peptides compounds promote the proliferation and differentiation of MC3T3-E1 pre-osteoblasts. *PLoS One* **2014**, 9, e99920.

Liu, D.; Nikoo, M.; Boran, G.; Zhou, P.; Regenstein, J. M. Collagen and Gelatin. *Annu. Rev. Food Sci. Technol.* **2015**, *6* (1), 527–557.

Lupo, M.P. Hyaluronic acid fillers in facial rejuvenation. *Semin. Cutan. Med. Surg.* **2006**, *25*(3), 122–126.

Machado, E. C. F. A.; Ambrosano, L.; Lage, R.; Abdalla, B. M. Z.; Costa, A. Nutraceuticals for

healthy skin aging. In *Nutrition and functional foods for healthy aging*, 1st ed. London: Academic Press **2017**, pp. 273-281.

Madara, J.L.; Barenberg, D.; Carlson, S. Effects of cytochalasin D on occluding junctions of intestinal absorptive cells: further evidence that the cytoskeleton may influence paracellular permeability and junctional charge selectivity. *J Cell Biol.* **1986**, *106,* 2125-2136.

Maher, S.; Mrsny, R. J.; Brayden, D. J. Intestinal permeation enhancers for oral peptide delivery. *Adv. Drug Deliv. Rev.* **2016**, *106*, 277–319.

Mahraoui, L.; Rodolosse, A.; Barbat, A.; Dussaulx, E.; Zweibaum, A.; Rousset, M.; Brou-Laroche, E. Presence and differential expression of SGLT1, GLUT1, GLUT2, GLUT3 and GLUT5 hexose-transporter mRNAs in Caco-2 cell clones in relation to cell growth and glucose consumption. *Biochem. J.* **1994**, *298,* 629-633.

Makino, T.; Jinnin, M.; Muchemwa, F. C.; Fukushima, S.; Kogushi-Nishi, H.; Moriya, C.; Igata, T.; Fujisawa, A.; Johno, T.; Ihn, H. Basic fibroblast growth factor stimulates the proliferation of human dermal fibroblasts via the ERK1/2 and JNK pathways. *Br. J. Dermatol.* **2010**, *162* (4), 717–723.

Makrantonaki, E.; Zouboulis, C. C. Characteristics and pathomechanisms of endogenously aged skin. *Dermatology,* **2007**, *214*, 352e60.

Mari, W. K.; Muneshige, S.; Shin, K.; Yasuki, T.; Hideyuki, S.; Fumiki, M.; Hitoshi, S.; Yuji, F.; Michio, K. Absorption and effectiveness of orally administered low molecular weight collagen hydrolysate in rats. *J. Agric. Food Chem.* **2010**, *58* (2), 835–841.

Massey, A. J. Multiparametric cell cycle analysis using the operetta high-content imager and harmony software with PhenoLOGIC. *PLoS One* **2015**, *10* (7), 1–16.

Matsuda, N.; Koyama, Y.; Hosaka, Y.; Ueda, H.; Watanabe, T.; Araya, T.; Irie, S.; Takehana, K. Effects of ingestion of collagen peptide on collagen fibrils and glycosaminoglycans in the Dermis. *J Nutr. Sci. Vitaminol.* **2006,** *52* , 211–215.

Matsumoto, H.; Ohara, H.; Itoh, K.; Nakamura, Y.; Takahashi, S. Clinical effect of fish type I collagen hydrolysate on skin properties. *ITE Lett.* **2006**, *7*, 386–390.

Matuoka, K.; Namba, M.; Mitsui, Y. Hyaluronate synthetase inhibition by normal and transformed human fibroblasts during growth reduction. *J. Cell Biol.* **1987**, *104* (4), 1105–1115.

McAlindon, T. E.; Nuite, M.; Krishnan, N.; Ruthazer, R.; Price, L. L.; Burstein, D.; Griffith, J.; Flechsenhar, K. Change in knee osteoarthritis cartilage detected by delayed gadolinium enhanced magnetic resonance imaging following treatment with collagen hydrolysate: A pilot randomized controlled trial. *Osteoarthr. Cartil.* **2011**, *19* (4), 399–405.

McCormick, R. J. Collagen. In *Applied Muscle Biology and Meat Science*. M. Du and R. J. McCormick, ed. CRC Press: London, UK, **2009**; pp 129–148

McEwan, P. A.; Scott, P. G.; Bishop, P. N.; Bella, J. Structural correlations in the family of small leucine rich repeat proteins and proteoglycans. *J. Struct. Biol.* **2006,** *155*, 294–305.

McLaren, A. M.; Hordon, L. D.; Bird, H. A.; Robins, S. P. Urinary excretion of pyridinium crosslinks of collagen correlated with joint damage in arthritis. *Ann. Rheum. Dis.* **1992***, S1*, 648-651

Mendis, E.; Rajapakse, N.; Kim, S. K. Antioxidant properties of a radical-scavenging peptide purified from enzymatically prepared fish skin gelatin hydrolysate. *J. Agric. Food Chem.* **2005**, *53* (3), 581–587.

Meyer, L.J.; Stern, R.; Age-dependent changes of hyaluronan in human skin. *J. Invest. Dermatol.* **1994**, *102*, 385–389.

Miguel, M; Dávalos, A; Manso, MA; de la Peña G; Lasunción, MA; López-Fandiño, R. Transepithelial transport across Caco-2 cell monolayers of antihypertensive egg-derived peptides. PepT1-mediated flux of Tyr-Pro-Ile. *Mol. Nutr. Food Res.* **2008**, *52,* 1507-1573.

Miller, B. F.; Olesen, J. L.; Hansen, M.; Døssing, S.; Crameri, R. M.; Welling, R. J.; Langberg, H.; Flyvbjerg, A.; Kjaer, M.; Babraj, J. A.; et al. Coordinated collagen and muscle protein synthesis in human patella tendon and quadriceps muscle after exercise. *J. Physiol.* **2005**, *567* (3), 1021–1033.

Miller, E. J. Collagen chemistry. In *Extracellular Matrix Biochemistry.* Piez, KA.; Reddi, AH., editors. Elsevier; **1984;** pp. 41-78.

Miyamura, Y.; Coelho, S.G.; Schlenz, K. The deceptive nature of UVA tanning versus the modest protective effects of UVB tanning on human skin. *Pigment. Cell. Melanoma. Res.* **2011**, *24*, 136–147.

Moradi, S. V.; Hussein, W. M.; Varamini, P.; Simerska, P.; Toth, I. Glycosylation, an effective synthetic strategy to improve the bioavailability of therapeutic peptides. *Chem. Sci.* **2016**, *7* (4), 2492–2500.

Moskowitz, R. W. Role of collagen hydrolysate in bone and joint disease. *Semin. Arthritis. Rheum.* **2000***, 30*, 87-99.

Mouw, J. K.; Ou, G.; Weaver, V. M. Extracellular matrix assembly: a multiscale deconstruction. *Nat. Rev. Mol. Cell Biol.* **2014**, *15* (12), 771–785.

Nakatani, S.; Mano, H.; Sampei, C.; Shimizu, J.; Wada, M. Chondroprotective effect of the bioactive peptide prolyl-hydroxyproline in mouse articular cartilage *in vitro* and *in vivo*. *Osteoarthr. Cartil.* **2009**, *17* (12), 1620–1627.

Nasri, R.; Chataigné, G.; Bougatef, A.; Chaâbouni, M. K.; Dhulster, P.; Nasri, M.; Nedjar-Arroume, N. Novel angiotensin I-converting enzyme inhibitory peptides from enzymatic hydrolysates of goby (*Zosterisessor ophiocephalus*) muscle proteins. *J. Proteomics.* **2013**, *91*, 444–452.

Neves, A. C.; Harnedy, P. A.; O'Keeffe, M. B.; Alashi, M. A.; Aluko, R. E.; FitzGerald, R. J. Peptide identification in a salmon gelatin hydrolysate with antihypertensive, dipeptidyl peptidase IV inhibitory and antioxidant activities. *Food Res. Int.* **2017**, *100* (June), 112–120.

Ngo, D.-H.; Vo, T.-S.; Ryu, B.; Kim, S.-K. Angiotensin- I- converting enzyme (ACE) inhibitory peptides from Pacific cod skin gelatin using ultrafiltration membranes. *Process Biochem.* **2016**, *51* (10), 1622-1628.

Ngo, D. H.; Kang, K. H.; Ryu, B.; Vo, T. S.; Jung, W. K.; Byun, H. G.; Kim, S. K. Angiotensin-I converting enzyme inhibitory peptides from antihypertensive skate (Okamejei kenojei) skin gelatin hydrolysate in spontaneously hypertensive rats. *Food Chem.* **2015**, *174*, 37–43.1622–1628.

Noguchi, S.; Ogawa, M.; Malicdan, M. C.; Nonaka, I.; Nishino, I. Muscle Weakness and Fibrosis Due to Cell Autonomous and Non-cell Autonomous Events in Collagen VI Deficient Congenital Muscular Dystrophy. *EBioMedicine* **2017**, *15*, 193–202.

Nojima, Y.; Suzuki, Y.; Iguchi, K.; Shiga, T.; Iwata, A.; Fujimoto, T.; Yoshida, K.; Shimizu, H.; Takeuchi, T.; Sato, A. Development of poly (ethylene glycol) conjugated lactoferrin for oral administration. *Bioconjug. Chem.* **2008**, *19*, 2253-2259.

Nomura, Y.; Oohashi, K.; Watanabe, M.; Kasugai, S. Increase in bone mineral density through oral administration of shark gelatin to ovariectomized rats. *Nutrition,* **2005**, *21* (11–12), 1120–1126.

Nožinić, D.; Milić, A.; Mikac, L.; Ralić, J.; Padovan, J.; Antolović, R. Assessment of macrolide transport using PAMPA, Caco-2 and MDCKII-hMDR1 assays. *Croat. Chem. Acta.* **2010**, *83,* 323-331.

Oesser, S.; Adam, M.; Babel, W.; Seifert, J. Oral administration of ^{14}C labeled gelatin hydrolysate leads to an accumulation of radioactivity in cartilage of mice (C57/BL). *J. Nutr.* **1999**, *129* (10), 1891–1895.

Oesser, S.; Raabe, A.; Schunck, M. Orally administered collagen hydrolysate halts the progression of osteoarthritis in STR/ort mice. *Osteoarthr. Cartil.* **2007**, 15 (Suppl C), 94-95.

Oesser, S.; Seifert, J. Stimulation of type II collagen biosynthesis and secretion in bovine chondrocytes cultured with degraded collagen. *Cell Tissue Res.* **2003**, *311* (3), 393–399.

Oh, J.H.; Kim, Y.K.; Jung, J.Y.; Shin, J.E.; Kim, K.H.; Cho, K.H. Intrinsic aging- and photoaging-dependent level changes of glycosaminoglycans and their correlationwithwatercontent inhumanskin. *J. Dermatol. Sci.* **2011**, *62*, 192–201.

Ohara, H.; Matsumoto, H.; Ito, K.; Iwai, K.; Sato, K. Comparison of quantity and structures of hydroxyproline-containing peptides in human blood after oral ingestion of gelatin hydrolysates from different sources. *J Agric. Food Chem.* **2007**, *55,* 1532-1535.

Ohara, H; Ichikawa, S; Matsumoto, H; Akiyama, M; Fujimoto, N; Kobayashi, T; Tajima, S. Collagen-derived dipeptide, proline-hydroxyproline, stimulates cell proliferation and hyaluronic acid synthesis in cultured human dermal fibroblasts. *J Dermatol.* **2010**, *37,* 330-338.

Ohara, H.; Iida, H.; Ito, K.; Takeuchi, Y.; Nomura, Y. Effects of Pro-Hyp, a Collagen Hydrolysate-Derived Peptide, on Hyaluronic Acid Synthesis Using *in Vitro* Cultured Synovium Cells and Oral Ingestion of Collagen Hydrolysates in a Guinea Pig Model of Osteoarthritis. *Biosci. Biotechnol. Biochem.* **2010**, *74* (10), 2096–2099.

O'Keeffe, M. B.; Norris, R.; Alashi, M. A.; Aluko, R. E.; FitzGerald, R. J. Peptide identification in a porcine gelatin prolyl endoproteinase hydrolysate with angiotensin converting enzyme (ACE) inhibitory and hypotensive activity. *J. Funct. Foods* **2017**, *34*, 77–88.

Paddon-Jones, D.; Short, K.R.; Campbell, W. W. Role of dietary protein in the sarcopenia of aging. *Am. J. Clin. Nutr.* **2008**, *87,* 1562S–1566S.

Pandey, P.; Pandey, S.; Dubey, A. Mutual Amide Prodrug of Etodolac-glucosamine: Synthesis, Characterization and Pharmacological Screening. *Indian J. Pharm. Sci.* **2013**, *75,* 406-412.

Panwar, P.; Butler, G. S.; Jamroz, A.; Azizi, P.; Overall, C. M.; Brömme, D. Aging-associated modifications of collagen affect its degradation by matrix metalloproteinases. *Matrix Biol.* **2017**. http://dx.doi.org/10.1016/j.matbio.2017.06.004

Postlethwaite, a E.; Seyer, J. M.; Kang, a H. Chemotactic attraction of human fibroblasts to type I, II, and III collagens and collagen-derived peptides. *Proc. Natl. Acad. Sci. U. S. A.* **1978**, *75* (2), 871–875.

Patel, D.; McKinley, B. D.; Davis, T. P.; Porreca, F.; Yamamura, H. I.; Hruby, V. J. Peptide targeting and delivery across the blood-brain barrier utilizing synthetic triglyceride esters: Design, synthesis, and bioactivity. *Bioconjug. Chem.* **1997**, *8* (3), 434–441.

Perazella, M. Renin-angiotensin-aldosterone system: Fundamental aspects and clinical implications in renal and cardiovascular disorders. *J. Nucl. Cardiol.* **2003**, *10* (2), 184–196.

Pratt, R. M.; Larsen, M.A.; Johnston, M. C. Migration of cranial neural crest cells in a cell-free hyaluronate-rich matrix. *Dev. Biol.* **1975**, *44,* 298-305.

Proksch, E.; Segger, D.; Degwert, J.; Schunck, M.; Zague, V.; Oesser, S. Oral supplementation of specific collagen peptides has beneficial effects on human skin physiology: A double-blind, placebo-controlled study. *Skin Pharmacol. Physiol.* **2013**, *27* (1), 47–55.

Qian, S.; Zhang, Q.; Wang, Y.; Lee, B.; Betageri, G.V.; Chow, M.; Huang, M.; Zuo, Z. Bioavailability enhancement of glucosamine hydrochloride by chitosan. *Int. J Pharm.* **2013**, *455,* 365– 373.

Quirós, A.; Dávalos, A.; Lasunción, MA.; Ramos, M. Recio, I. Bioavailability of the antihypertensive peptide LHLPLP: Transepithelial flux of HLPLP. *Int. Dairy J.* **2008**, *18,* 279-286.

Rahmati, M.; Nalesso, G.; Mobasheri, A.; Mozafari, M. Aging and Osteoarthritis: Central Role of the Extracellular Matrix. *Ageing Res. Rev.* **2017**, *40*, 20–30.

Raja, M.; Kinne, R. Identification of phlorizin binding domains in sodium-glucose cotransporter family: SGLT1 as a unique model system. *Biochimie.* **2015**, *115,* 187-193.

Ranall, M. V.; Gabrielli, B. G.; Gonda, T. J. Adaptation and validation of DNA synthesis detection by fluorescent dye derivatization for high-throughput screening. *Biotechniques,* **2010**, *48* (5), 379–386.

Rao, B. M.; Kamal, T. T.; Vafaye, J.; Taylor, L. Surgical repair of hip abductors. A new technique using Graft Jacket allograft acellular human dermal matrix. *Int. Orthop.* **2012**, *36*, 2049-2053.

Rao, SV.; Agarwal, P.; Shao, J. Self-nanoemulsifying drug delivery systems (SNEDDS) for oral delivery of protein drugs: II. *In vitro* transport study. *Int. J. Pharm.* **2008**, *362* (1–2), 10–15.

Regenstein, J. M.; Chaudry, M. M.; Regenstein, C. E. The kosher and halal food laws. *Comp. Rev. Food Sci.* **2003,** *F2*, 111–117.

Reginster, J. Y.; Neuprez, A.; Lecart, M. P.; Sarlet, N.; Bruyere, O. Role of glucosamine in the treatment for osteoarthritis. *Rheumatol. Int.* **2012**, *32* (10), 2959–2967.

Renukuntla, J.; Vadlapudi, A. D.; Patel, A.; Boddu, S. H.S.; Mitra, A. K. Approaches for enhancing oral bioavailability of peptides and proteins. *Int. J. Pharm.* **2013**, *447,* 75-93.

Richelle, M., Sabatier, M., Steiling, H., & Williamson, G. Skin bioavailability of dietary vitamin E, carotenoids, polyphenols, vitamin C, zinc and selenium. *Br. J. Nutr.,* **2006**, *96,* 227 – 238.

Rittie´, L.; Fisher, G. J. UV-light-induced signal cascades and skin aging. *Ageing Res. Rev.* **2002**, 1, 705e20.

Rose, P. I. Gelatine. In Mark, H. F. & Kroschwitz, J. I., Encyclopedia of polymer science and engineering, **1987**, New York: John Wiley & Sons, Inc. pp 488-513.

Sacoman, J. L.; Hollingsworth, R. I. Synthesis and evaluation of an N-acetylglucosamine biosynthesis inhibitor. *Carbohydr. Res.* **2011**, *346* (14), 2294–2299.

Sakata, K.; Yamashita, T.; Maeda, M.; Moriyama, Y.; Shimada, S.; Tohyama, M. Cloning of a lymphatic peptide/histidine transporter. *Biochem. J.* **2001**, *356* (Pt 1), 53–60.

Salamat-Miller, N.; Johnston, T.P. Current strategies used to enhance the paracellular transport of therapeutic polypeptides across the intestinal epithelium. *Int. J Pharm.* **2005**, *294,* 201–216.

Sánchez-Rivera, L., Martínez-Maqueda, D., Cruz-Huerta, E., Miralles, B. & Recio, I. Peptidomics for discovery, bioavailability and monitoring of dairy bioactive peptides. *Food Research International,* **2014***, 63,* 170 – 181.

Shimizu, J.; Asami, N.; Kataoka, A.; Sugihara, F.; Inoue, N.; Kimira, Y.; Wada, M.; Mano, H. Oral collagen-derived dipeptides, prolyl-hydroxyproline and hydroxyprolyl-glycine, ameliorate skin barrier dysfunction and alter gene expression profiles in the skin. *Biochem. Biophys. Res. Commun.* **2015**, *456* (2), 626–630.

Schipper, N.G.; Varum, K. M.; Artursson, P. Chitosans as absorption enhancers for poorly absorbable drugs. 1: Influence of molecular weight and degree of acetylation on drug transport across human intestinal epithelial (Caco-2) cells. *Pharm. Res.* **1996**, *13*(11), 1686–1692.

Schmittgen, T. D.; Livak, K. J. Analyzing real-time PCR data by the comparative CT method. *Nat. Protoc.* **2008**, *3* (6), 1101–1108.

Schneider, M.R.; Schmidt-Ullrich, R.; Paus, R. The hair follicle as a dynamic mini organ. *Curr. Biol.* **2009**, *19*, R132–R142.

Schönherr, E.; Beavan, L.A.; Hausser, H.; Kresse, H.; Culp, L.A. Differences in decorin expression by papillary and reticular fibroblasts *in vivo* and *in vitro*. *Biochem. J.* **1993**. *290* (Pt 3), 893–899.

Schrieber, R., and Gareis. H. The role of collagen hydrolysates in the prophylaxis of osteoarthritis and osteoporosis. In *Gelatine Handbook: Theory and Industrial Practice*, 1st. Wiley-VCH GmbH & Co: Weinheim, Germany, **2007**; pp 301-309.

Schroeder, P.; Lademann, J.; Darvin, M.E.; Stege, H.; Marks, C.; Bruhnke, S.; Krutmann, J. Infrared radiation-induced matrix metalloproteinase in human skin: implications for protection, *J. Invest. Dermatol.* **2008**, *128* (10), 2491–2497.

Schwartz, S. R.; Park, J. Ingestion of BioCell Collagen®, a novel hydrolyzed chicken sternal cartilage extract; enhanced blood microcirculation and reduced facial aging signs. *Clin. Interv. Aging* **2012**, *7*, 267–273.

Setters, B.; Holmes, H. M. Hypertension in the Older Adult. *Prim. Care - Clin. Off. Pract.* **2017**, *44* (3), 529–539.

Shah, P.; Bhalodia, D.; Shelat, P. Nanoemulsion: a pharmaceutical review. *Syst. Rev. Pharm.* **2010**, *1*, 24–32.

Sharom, F. J.; DiDiodato, G.; Yu, X.; Ashbourne, K. J. D. Interaction of the P-glycoprotein multidrug transporter with peptides and ionophores. *J. Biol. Chem.* **1995**, pp 10334–10341.

Shigemura, Y.; Akaba, S.; Kawashima, E.; Park, E. Y.; Nakamura, Y.; Sato, K. Identification of a novel food-derived collagen peptide, hydroxyprolyl-glycine, in human peripheral blood by pre-column derivatisation with phenyl isothiocyanate. *Food Chem.* **2011**, *129* (3), 1019–1024.

Shigemura, Y.; Iwai, K.; Morimatsu, F.; Iwamoto, T.; Mori, T.; Oda, C.; Taira, T.; Park, E. Y.; Nakamura, Y.; Sato, K. Effect of prolyl-hydroxyproline (Pro-Hyp), a food-derived collagen peptide in human blood, on growth of fibroblasts from mouse skin. *J. Agric. Food Chem.* **2009**, *57* (2), 444–449.

Shigemura, Y.; Kubomura, D.; Sato, Y.; Sato, K. Dose-dependent changes in the levels of free and peptide forms of hydroxyproline in human plasma after collagen hydrolysate ingestion. *Food Chem.* **2014**, *159*, 328–332.

Shimizu, J.; Asami, N.; Kataoka, A.; Sugihara, F.; Inoue, N.; Kimira, Y.; Wada, M.; Mano, H. Oral collagen-derived dipeptides, prolyl-hydroxyproline and hydroxyproline-glycine, ameliorate

skin barrier dysfunction and alter gene expression profiles in the skin. *Biochem. Biophys. Res. Commun.* **2015**, *456,* 626-630.

Shinkai, H.; Yonemasu, K. Hydroxylysine-linked glycosides of human complement subcomponent C1q and various collagens. *Biochem. J.* **1979**, *177*, 847–852.

Shore, P.A.; Brodie, B.B.; Hogben, C.A. The gastric secretion of drugs: a pH partition hypothesis. *J. Pharm. Exp. Ther.* **1957**, *119,* 361–369.

Sibilla, S.; Godfrey1 M.; Brewer, S.; Budh-Raja, A.; Genovese1, L. An overview of the beneficial effects of hydrolysed collagen as a nutraceutical on skin properties: scientific background and clinical studies. *Open Nutraceuticals J.* **2015**, *8,* 29-42.

Silva, T. H.; Moreira-Silva, J.; Marques, A. L. P.; Domingues, A.; Bayon, Y.; Reis, R. L. Marine origin collagens and its potential applications. *Mar. Drugs* **2014**, *12* (12), 5881–5901.

Singh, P.; Carraher, C.; Schwarzbauer, J. E. Assembly of fibronectin extracellular matrix. *Annu. Rev. Cell Dev. Biol.* **2010**, *26*, 397–419.

Solá, R. J.; Griebenow, K. Glycosylation of Therapeutic Proteins: An Effective Strategy to Optimiza Efficacy. *BioDrugs* **2011**, *24* (1), 9–21.

Sontakke, S.B.; Jung, J.; Piao, Z.; Chung, H.J. Orally available collagen tripeptide: enzymatic stability, intestinal permeability, and absorption of Gly-Pro-Hyp and Pro-Hyp. *J Agric. Food Chem.* **2016**, *64,* 7127-7133.

Sorrell, J.M.; Caplan, A.I. Fibroblast heterogeneity: more than skin deep. *J. Cell Sci.* **2004**, *117*, 667–675.

Sorrell, J.M.; Baber, M.A.; Caplan, A.I. Site-matched papillary and reticular human dermal fibroblasts differ in their release of specific growth factors/cytokines and in their interaction with keratinocytes. *J. Cell. Physiol.* **2004**, *200,* 134–145.

Sriram, G.; Bigliardi, P. L.; Bigliardi-Qi, M. Fibroblast heterogeneity and its implications for engineering organotypic skin models *in vitro*. *Eur. J. Cell Biol.* **2015**, *94* (11), 483–512.

Stern, R.; Maibach, H. I. Hyaluronan in skin: aspects of aging and its pharmacologic modulation. *Clin. Dermatol.* **2008**, *26* (2), 106–122.

Stoll, G.; Bendszus, M. Inflammation and atherosclerosis: Novel insights into plaque formation and destabilization. *Stroke* **2006**, *37* (7), 1923–1932.

Stoppoloni, D.; Politi, L.; Leopizzi, M.; Gaetani, S.; Guazzo, R.; Basciani, S.; Moreschini, O.; De Santi, M.; Scandurra, R.; Scotto d'Abusco, A. Effect of glucosamine and its peptidyl-derivative on the production of extracellular matrix components by human primary chondrocytes. *Osteoarthr. Cartil.* **2015**, *23* (1), 103–113.

Sudel, K. M.; Venzke, K.; Mielke, H.; Breitenbach, U.; Mundt, C.; Jaspers, S.; Koop, U. Novel aspects of intrinsic and extrinsic aging of human skin: beneficial effects of soy extract. *Photochem Photobiol.* **2005**, *81*, 581–587.

Sun, L.; Zhang, Y.; Zhuang, Y. Antiphotoaging effect and purification of an antioxidant peptide from tilapia (Oreochromis niloticus) gelatin peptides. *J. Funct. Foods* **2013**, *5* (1), 154–162.

Svobodová, A.R.; Galandáková, A.; Sianská, J.; Dolezal, D.; Lichnovská, R.; Ulrichová, J.; Vostálová, J. DNA damage after acute exposure of mice skin to physiological doses of UVB and UVA light. *Arch. Dermatol. Res.* **2012**, *304*, 407–412.

Tabor, A.; Blair, R. M. Introduction. In Nutritional Cosmetics. William Andrew. Oxford, UK. **2009**, pp. xxxi–xxxiv.

Taga, Y.; Kusubata, M.; Ogawa-Goto, K.; Hattori, S. Identification of Collagen-Derived Hydroxyproline (Hyp)-Containing Cyclic Dipeptides with High Oral Bioavailability: Efficient Formation of Cyclo(X-Hyp) from X-Hyp-Gly-Type Tripeptides by Heating. *J. Agric. Food Chem.* **2017**, acs. jafc.7b03714.

Tagliavini, F.; Pellegrini, C.; Sardone, F.; Squarzoni, S.; Paulsson, M.; Wagener, R.; Gualandi, F.; Trabanelli, C.; Ferlini, A.; Merlini, L.; et al. Defective collagen VI α6 chain expression in the skeletal muscle of patients with collagen VI-related myopathies. *Biochim. Biophys. Acta - Mol. Basis Dis.* **2014**, *1842* (9), 1604–1612.

Tajima, S.; Pinnell, S.R. Collagen synthesis by human skin fibroblasts inculture: studies of fibroblasts explanted from papillary and reticular dermis. *J. Invest. Dermatol.* **1981**. *77*, 410–412.

Takata, K. Glucose transporters in the transepithelial transport of glucose. *J Electron Microsc.* **1996**, *45,* 275-284.

Tan, E. M. L.; Rouda, S.; Greenbaum, S. S.; Moore, J. H.; Iv, J. W. F.; Sollbergt, S. Acidic and basic fibroblast growth factors down-regulate collagen gene expression in keloid fibroblasts. *Am. J. Pathol.* **1993**, *142* (2), 463–470.

Tanaka, M.; Koyama, Y.; Nomura, Y. Effects of collagen peptide ingestion on UV-B-induced skin damage. *Biosci. Biotechnol. Biochem.* **2009**, *73*(4), 930-932.

Tavelin, S.; Gråsjö, J.; Taipalensuu, J.; Ocklind, G.; Artursson, P. Applications of epithelial cell culture in studies of drug transport. In *Epithelial Cell Culture Protocols*, 1st; Wise, C., Ed.; Human Press Inc.: Totowa, New Jersey, **2002**; pp 233-272.

Terada, T.; Sawada, K.; Saito, H.; Hashimoto, Y.; Inui, K. Functional characteristics of basolateral peptide transporter in the human intestinal cell line Caco-2. *Am. J. Physiol.* **1999**, *276,* G1435-G1441.

Tesoriere, G.; Dones, F.; Magistro, D.; Castagnetta, L. Intestinal absorption of glucosamine and N-acetylglucosamine. *Experientia.* **1972**, *28,* 770-771.

Tiku, M. L.; Narla, H.; Jain, M.; Yalamanchili, P. Glucosamine prevents *in vitro* collagen degradation in chondrocytes by inhibiting advanced lipoxidation reactions and protein oxidation. *Arthritis Res. Ther.* **2007**, *9* (4), R76, doi:10.1186/ar2274.

Timpl, R.; Brown, J. C. The laminins. *Matrix Biol.* **1994**, *14*, 275–281.

Tobin, D. J. Introduction to skin aging. *J. Tissue Viability.* **2017**, *26* (1), 37–46. Tokudome, Y.; Nakamura, K.; Kage, M.; Todo, H.; Sugibayashi, K.; Hashimoto, F. Effects of soybean peptide and collagen peptide on collagen synthesis in normal human dermal fibroblasts. *Int. J. Food Sci. Nutr.* **2012**, *63* (6), 689–695.

Toutfaire, M.; Bauwens, E.; Debacq-Chainiaux, F. The impact of cellular senescence in skin ageing: A notion of mosaic and therapeutic strategies. *Biochem. Pharmacol.* **2017**, *142*, 1–12.

Tozaki, H., Emi, Y., Horisaka, E., Fujita, T., Yamamoto, A., Muranishi, S. Degradation of insulin and calcitonin and their protection by various protease inhibitors in rat caecal contents: implications in peptide delivery to the colon. *J. Pharm. Pharmacol.* **1997**, 49 (2), 164–168.

Turco, L., & Angelis, I. D. Caco-2 cell as a model for intestinal absorption. *Current Protocols in Toxicology,* **2011**, 20.6.1 – 20.6.15.

Uldry, M.; Ibberson, M.; Hosokawa, M.; Thorens, B. GLUT2 is a high affinity glucosamine transporter. *FEBS Lett.* **2002**, *524*, 199-203.

Uitterlinden, E.; Koevoet, J.; Verkoelen, C.; Bierma-Zeinstra, S.; Jahr, H.; Weinans, H.; Verhaar, J.; van Osch, G. Glucosamine increases hyaluronic acid production in human osteoarthritic synovium explants. *BMC Musculoskelet. Disord.* **2008**, *9* (1), 120.

Upadhyay, J.; Polyzos, S. A.; Perakakis, N.; Thakkar, B.; Paschou, S. A.; Katsiki, N.; Underwood, P.; Park, K.-H.; Seufert, J.; Kang, E. S.; et al. Pharmacotherapy of Type 2 Diabetes: An Update. *Metabolism* **2017**, *78*, 13–42.

Uzawa, K. Yeowell, H. N. Yamamoto, K, Mochida, Y. Tanzawa, H. Yamauchi, M. Lysine hydroxylation of collagen in a fibroblast cell culture system. *Biochem. Biophys. Res. Commun.* **2003**, *305*, 484–487.

Varghese, S.; Theprungsirikul, P.; Sahani, S.; Hwang, N.; Yarema, K. J.; Elisseeff, J. H. Glucosamine modulates chondrocyte proliferation, matrix synthesis, and gene expression. *Osteoarthr. Cartil.* **2007**, *15* (1), 59–68.

Vera, J.C.; Reyes, A.M.; Velásquez, F.V.; Rivas, C.I.; Zhang, R.H.; Strobel, P.; Slebe, J.C.; Núñez-Alarcón, J.; Golde, D.W. Direct inhibition of the hexose transporter GLUT1 by tyrosine kinase inhibitors. *Biochemistry.* **2001**, *40,* 777-790.

Voet, D. & Voet, J. G. Three-dimensional structure of proteins. In *Biochemistry*. 2nd ed. J. Wiley & Sons: New York, **1995**; pp 158.

Wade, JD. Amino acids: alpha-amino protecting groups. In *Solid-Phase Synthesis: A Practical Guide*, 1st; Kates, S.A.; Albericio, F., Eds.; Marcel Dekker: New York, **2000**, pp 103-128.

Watanabe, K.; Shimizu, M.; Kamiyama, S.; Taguchi, Y.; Sone, H.; Morimatsu, F.; Hitoshi, S.; Yuji, F.; Michio, K. Absorption and effectiveness of orally administered low molecular weight collagen hydrolysate in rats. *J. Agric. Food Chem.* **2010**, *58* (2), 835–841.

Wang, J.; Chow, D.; Heiati, H.; Shen, W. C. Reversible lipidization for the oral delivery of salmon calcitonin. *J. Control. Release.* **2003**, *88*(3), 369–380.

Wang, T. Y.; Hsieh, C. H.; Hung, C. C.; Jao, C. L.; Chen, M. C.; Hsu, K. C. Fish skin gelatin hydrolysates as dipeptidyl peptidase IV inhibitors and glucagon-like peptide-1 stimulators improve glycaemic control in diabetic rats: A comparison between warm- and cold-water fish. *J. Funct. Foods.* **2015**, *19*, 330–340.

Watanabe-Kamiyama, M.; Shimizu, M.; Kamiyama, S.; Taguchi, Y.; Sone, H.; Morimatsu, F.; Shirakawa, H.; Furukawa, Y.; Komai, M. Absorption and effectiveness of orally administered low molecular weight collagen hydrolysate in rats. *J. Agric. Food. Chem.* **2010**, *58* (2), 835–841.

Weiss, P. H.; Klein, L. The quantitative relationship of urinary peptide hydroxyproline excretion to collagen degradation. *J. Clin. Invest.* **1969**, *48* (1), 1–10.

Wu, J., Fujioka, M., Sugimoto, K., Mu, G., & Ishimi, Y. Assessment of effectiveness of oral administration of collagen peptide on bone metabolism in growing and mature rats. *J. Bone Miner. Res.,* **2004**, *22,* 547 – 553.

Yamamoto, T.T., Rikyuu, K., Tsuji, T., Fujita, T., Murakami, M. Effects of various protease inhibitors on the intestinal absorption and degradation of insulin in rats. *Pharm. Res.* **1994**, *11*(10), 1496–1500.

Yamauchi, M.; Sricholpech, M. Lysine post-translational modifications of collagen. *Essays Biochem.* **2012**, *52*, 113–133.

Yang, C.-M. J. & Russell, J. B. Resistance of proline-containing peptides to ruminal degradation in *vitro*. *Appl. Environ. Microbiol.* **1992***, 58,* 3954-3958.

Yoon, H.S.; Kim, Y.K.; Matsui, M.; Chung, J.H. Possible role of infrared or heat in sun-induced changes of dermis of human skin *in vivo*. *J. Dermatol. Sci.* **2012**, *66* (1), 76–78.

Yazaki, M.; Ito, Y.; Yamada, M.; Goulas, S.; Teramoto, S.; Nakaya, M. aki; Ohno, S.; Yamaguchi, K. Oral Ingestion of Collagen Hydrolysate Leads to the Transportation of Highly Concentrated Gly-Pro-Hyp and Its Hydrolyzed Form of Pro-Hyp into the Bloodstream and Skin. *J. Agric. Food Chem.* **2017**, *65* (11), 2315–2322.

Zague, V., Freitas, V., Costa Rosa, M., Castro, G. A., Jaeger, R. G., Machado-Santelli, G. M. Collagen hydrolysate intake increases skin collagen expression and suppresses matrix metalloproteinase 2 activity. *J. Med. Food*, **2011,** *14*(6), 618–624.

Zdzieblik, D.; Oesser, S.; Baumstark, M. W.; Gollhofer, A.; König, D. Collagen peptide supplementation in combination with resistance training improves body composition and increases muscle strength in elderly sarcopenic men: a randomised controlled trial. *Br. J. Nutr.* **2015**, *114* (8), 1237–1245.

Zhang, Y.; Kouguchi, T.; Shimizu, K.; Sato, M.; Takahata, Y.; Morimatsu, F. Chicken collagen hydrolysate reduces proinflammatory cytokine production in C57BL/6.KOR-ApoEshl mice. *J. Nutr. Sci. Vitaminol. (Tokyo)*. **2010**, *56* (3), 208–210.

Zhang, Y.; Ma, L.; Cai, L.; Liu, Y.; Li, J. Effect of combined ultrasonic and alkali pretreatment on enzymatic preparation of angiotensin converting enzyme (ACE) inhibitory peptides from native collagenous materials. *Ultrason. Sonochem.* **2017**, *36*, 88–94.

Zhang, Y., Olsen, K., Grossi, A., & Otte, J. Effect of pretreatment on enzymatic hydrolysis of bovine collagen and formation of ACE-inhibitory peptides, *Food Chem.,* **2013***, 141,* 2343–2354.

APPENDIX A

Tryptophan content determination in purified collagen. The detection range is 0.03~0.1 mg/g. The content of tryptophan is too low to be quantified, as shown in "Replicate 3" and "Replicate 2" in the figure.
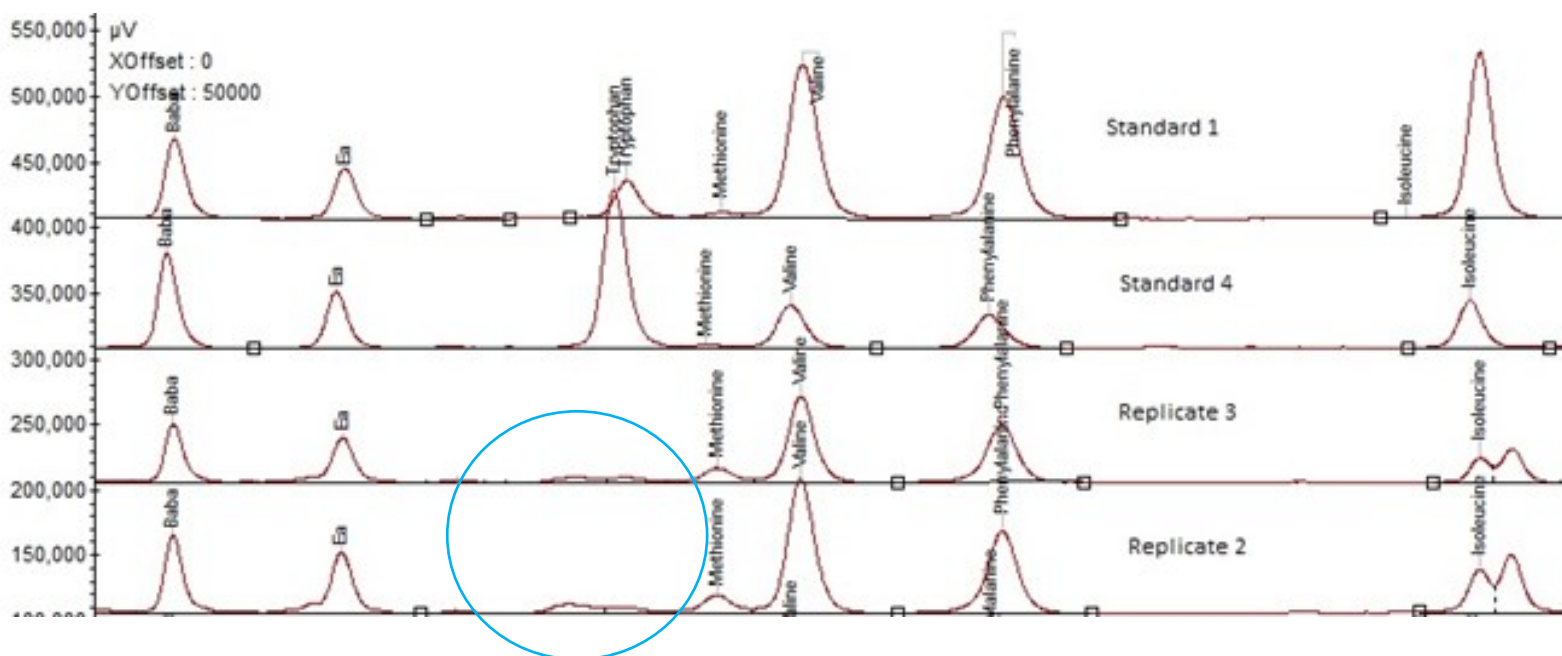
APPENDIX B

Chromatograph of peptide standards: Cytochrome c (12384 Da) and Aprotinin (6511.4 Da) were purchased from Sigma-Aldrich (St. Louis, MO). Peptide 1(GNNRPVUIPRPPHPRL, 2108.5 Da), peptide 2 (PRGDGETGE, 916.9 Da) and peptide 3 (Pro-Hyp-Gly, 285.3 Da) were obtained from GenScript (Piscataway, NJ, USA).
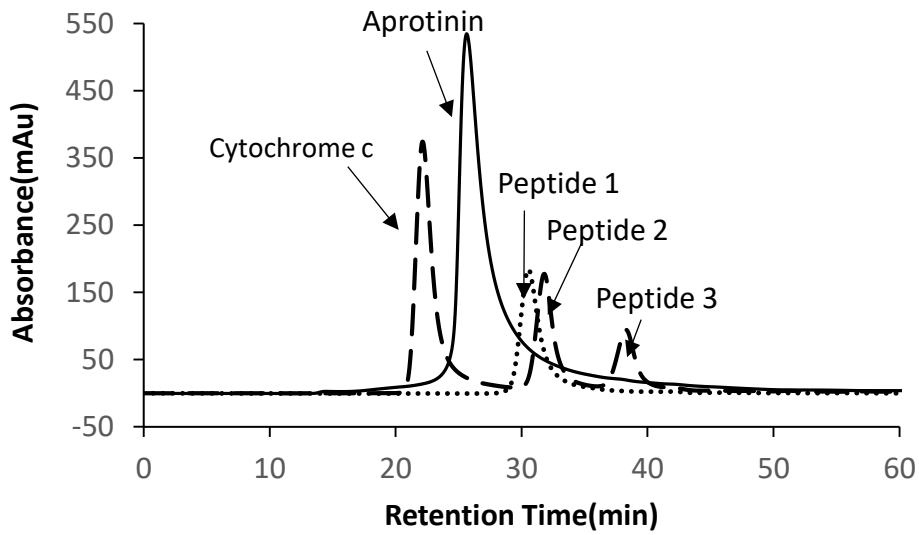
APPENDIX C

MS molecular weight distribution of collagen hydrolysates (from Alcalase/Flavourzyme treatment) transported through Caco-2 cell membrane. Compounds pass through the Caco-2 cell monolayer were mostly below 600 Da.
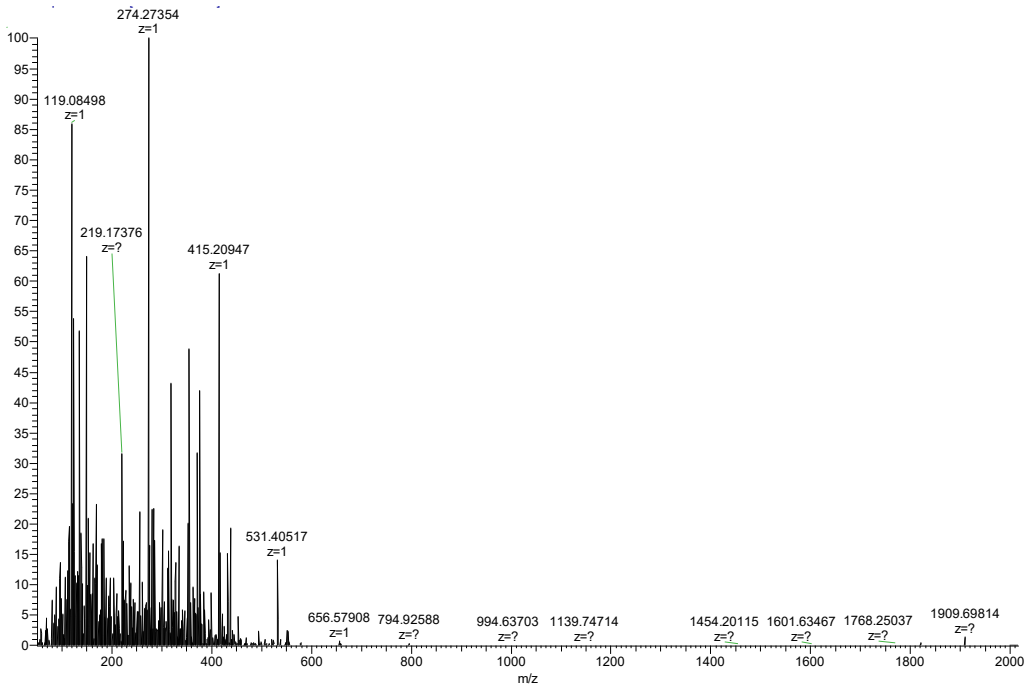
APPENDIX D.

Representative chromatographs of glucosamine (GlcN), Pro-Hyp-CONH-GlcN (POGlcN), and Pro-Hyp (PO) standard determination using UHPLC and detection at excitation/emission 265/315 nm. As shown in the figure, derivatized GlcN had a retention time at around 4.3 min, POGlcN at around 9.5 min, and PO at around 18.7 min.
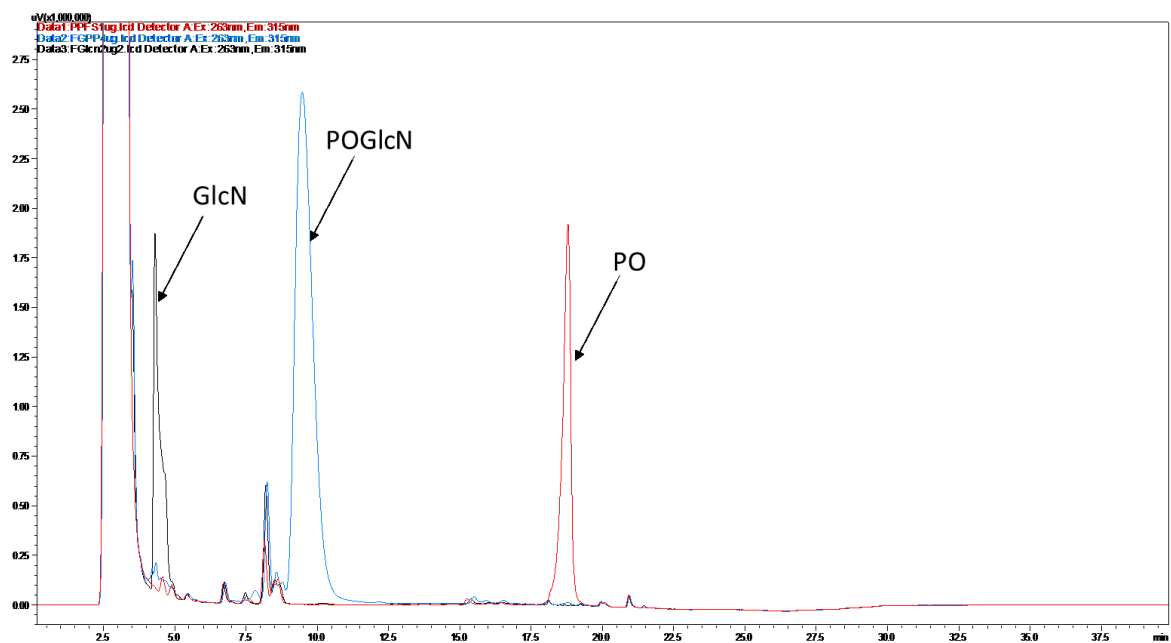
Transport of (A) Pro-Hyp (PH) and (B) Glucosamine (GlcN) in the presence of different inhibitors.
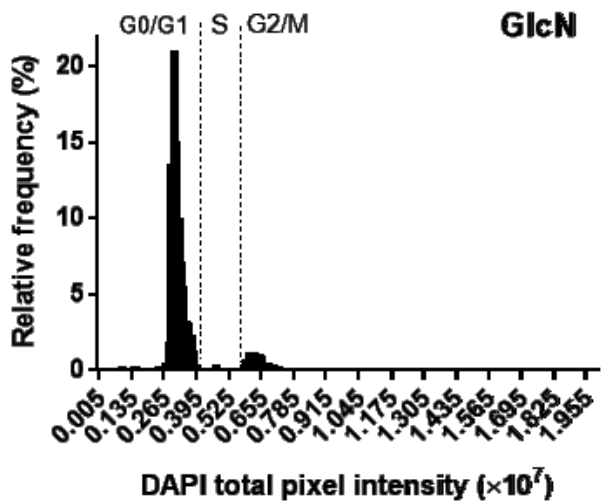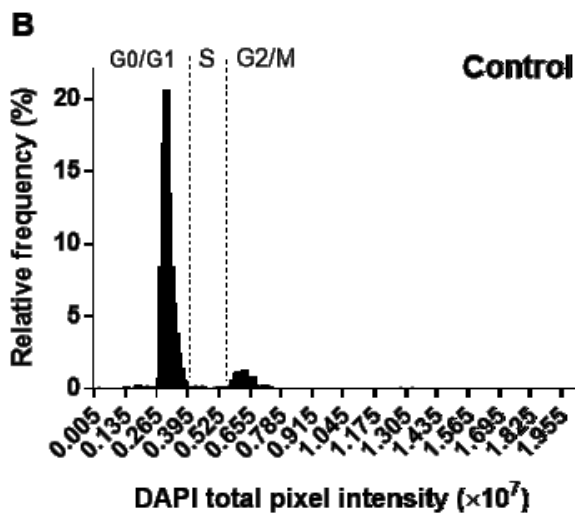
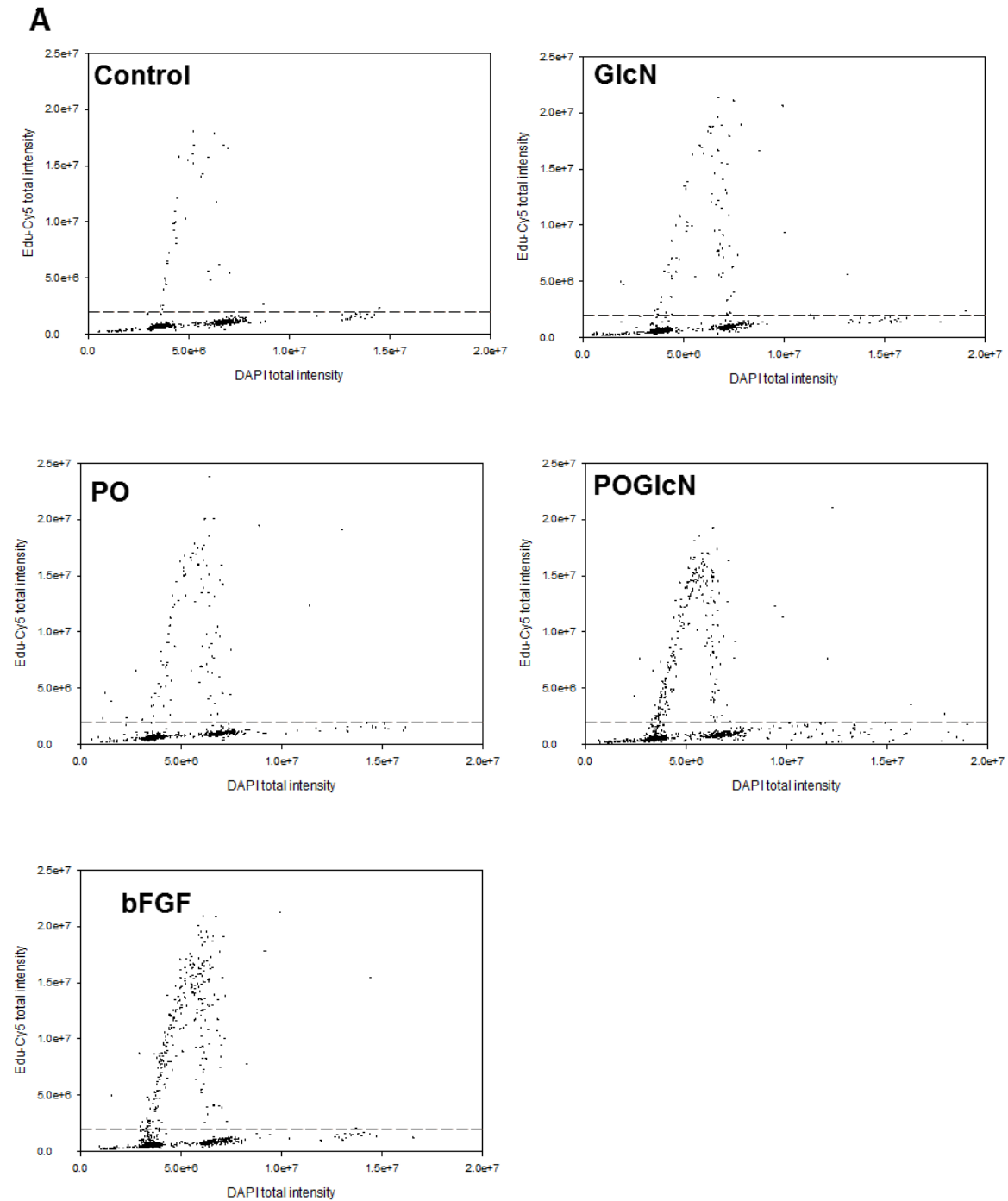Error bars represent standard deviation (n≥2).
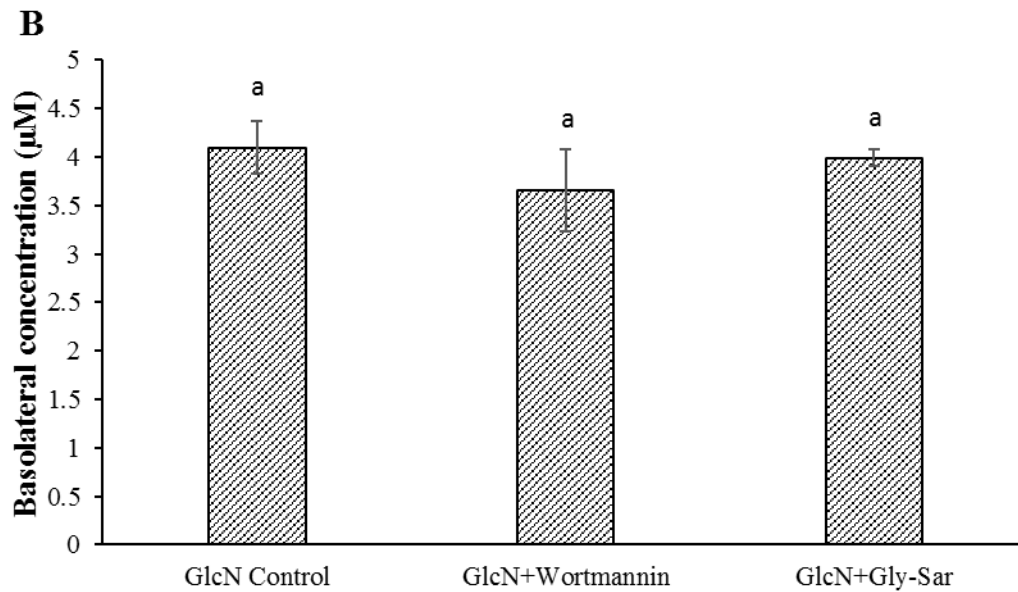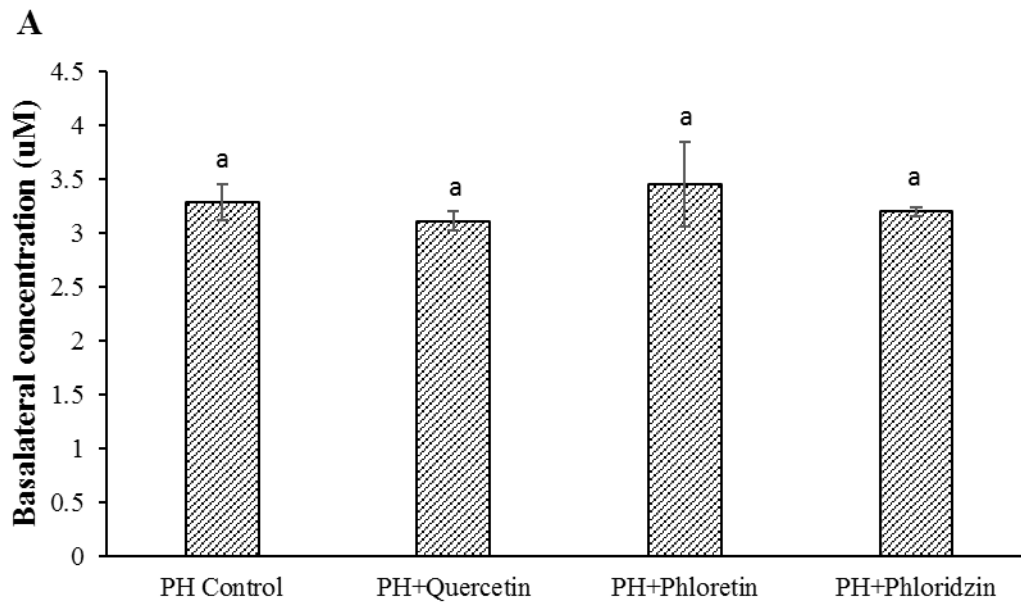
APPENDIX F

Cell cycle analysis by high content screening. Representative cell cycle histograms generated from DAPI stained fibroblasts treated with or without test compound for 2 days (A) or 6 days (B).

B

Control

GlcN

PO

POGlcN

bFGF

180
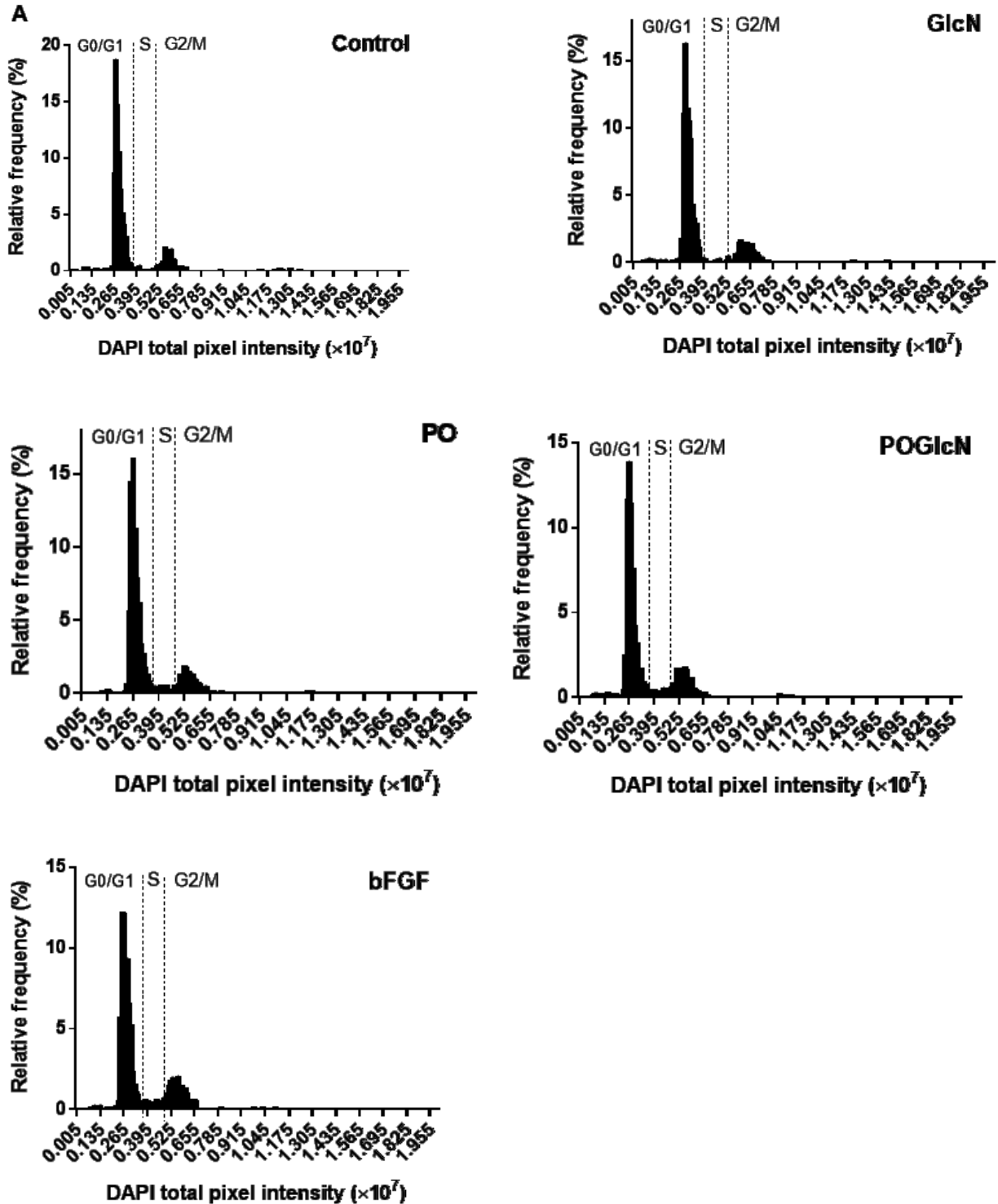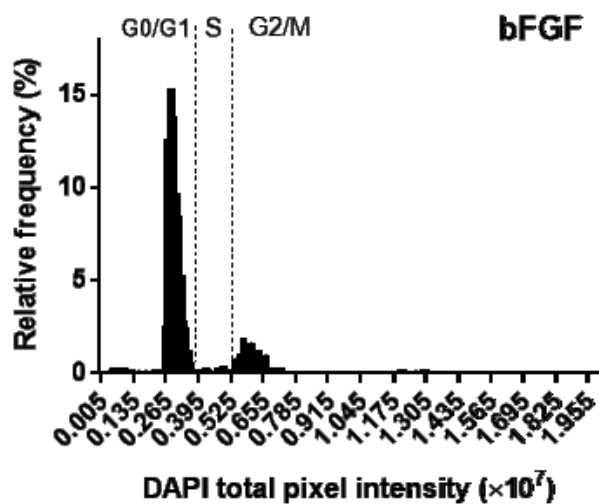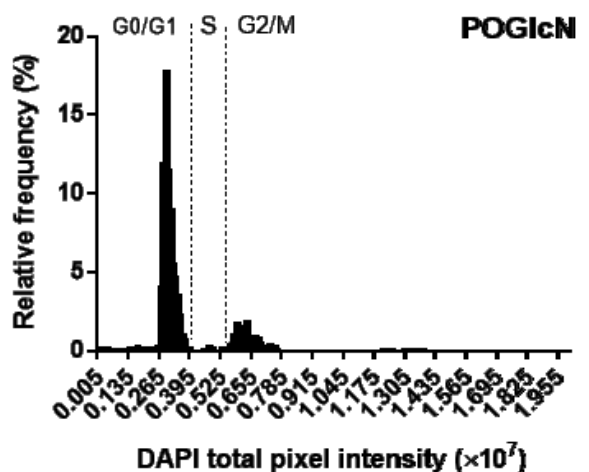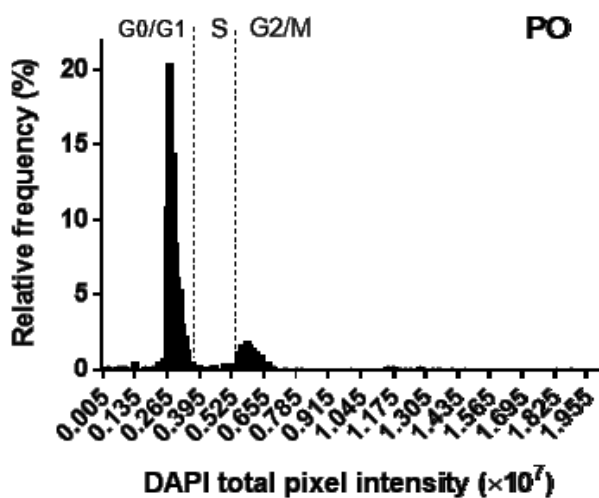
APPENDIX G.

The incorporation of Edu by fibroblasts. Representative scatterplots of total Edu-Cy5 fluorescence intensity versus total DAPI intensity from fibroblasts treated with or without test compound for 2 days (A) or 6 days (B).

B

182